# Ctrl-*atl*-delete:

# Re-thinking the mechanisms of biofilm formation by staphylococci

**A thesis submitted to the National University of Ireland Galway**

**for the Degree of Doctor of Philosophy**

**by**


## Hannah E. McCarthy, B.Sc.

**Microbiology, School of Natural Sciences,**

**National University of Ireland Galway**



**January 2015**

**Supervisor and Head of Microbiology**

**Prof James P. O'Gara**

**Table of Contents**

**Summary of contents**

Biofilm formation by staphylococci on implanted medical devices represents a major virulence mechanism and a serious threat to hospital patients. *Staphylococcus aureus* strains including, methicillin-resistant *S. aureus* (MRSA), produce biofilms dependent on the major autolysin Atl. Antibodies to the amidase (AM) and glucosaminidase (GL) domains of Atl inhibited *in vitro* Atl-dependent biofilm formation and Atl was required for the normal expression of cytolytic toxins. However, an *atl* mutant was not significantly attenuated in a mouse model of catheter-related infections. Consistent with this finding, Atl and a number of previously characterised biofilm factors were subsequently shown to be redundant for biofilm formation on surfaces coated with human plasma. In contrast, coagulase activity, and specifically coagulase-mediated conversion of fibrinogen to fibrin, was critical for biofilm formation under these physiologically relevant conditions. These findings identify a novel third mechanism of *S. aureus* biofilm development, the other two being mediated by the extracellular polysaccharide poly-*N*-acetylglucosamine (PNAG) or a combination of cell surface proteins (including Atl) and extracellular DNA (eDNA).

A correlation between upregulated autolytic activity and high-level homogeneous methicillin resistance or growth in sub-MIC oxacillin was demonstrated in MRSA. This observation appears to be related to altered cell wall architecture and, when combined with previous observations showing the impact of high level antibiotic resistance on biofilm and virulence, further shows the pleiotrophic effects of antibiotic resistance on the physiology of *S. aureus*.

Extension of the studies on PNAG-independent mechanisms of biofilm formation revealed that the *Staphylococcus epidermidis* Atl homologue protein, AtlE, and the accumulation associated protein, Aap, contribute to *S. epidermidis* PNAG-independent biofilm formation in a strain-dependent manner. The role for autolytic activity in biofilm formation differed between strains and proteolytic cleavage of surface proteins was identified as having a significant influence on PNAG-independent biofilm formation.

**Declaration**

I declare that the work embodied within this thesis is my own and that no part of this thesis has previously been submitted in part fulfilment of a degree to the National University of Ireland, Galway or to any other University. National University of Ireland, Galway library may lend or copy this thesis upon request.

_____

Hannah E. McCarthy

**Publications list**

1. Ctrl-*atl*-delete; Re-thinking the mechanisms of *Staphylococcus aureus* biofilm formation. McCarthy H., Waters E.M., Schaeffer C.R., Bose J.L., Rudkin J.K., Foster S., Bayles K.W., Fey P.D., O'Neill E., O'Gara J.P. Manuscript in preparation. Contribution: Lead author.

2. Early *Staphylococcus aureus* colonisation of human plasma coated biomaterials is characterised coagulase-dependent, drug-susceptible biofilm accumulation. Zapotoczna M., McCarthy H., Rudkin J.K., O'Gara J.P., O'Neill E. Submitted. Contribution: Bioflux images, Figures 2C and 3A.

3. Methicillin resistance and the biofilm phenotype in *Staphylococcus aureus*. McCarthy H., Rudkin J.K., Black N.S., Gallagher L., O'Neill E., O'Gara J.P. Front. Cell. Infect. Microbiol. 2015. Contribution: Lead author.

4. Role for the A domain of unprocessed accumulation-associated protein (Aap) in the attachment phase of the *Staphylococcus epidermidis* biofilm phenotype. Conlon B.P., Geoghegan J.A., Waters E.M., McCarthy H., Rowe S.E., Davies J.R., Schaeffer C.R., Foster T.J., Fey P.D., O'Gara J.P. J Bacteriol. 2014. Contribution: Figure 3.

5. Fibronectin-binding proteins are required for biofilm formation by community-associated methicillin-resistant *Staphylococcus aureus* strain LAC. McCourt J., O'Halloran D.P., McCarthy H., O'Gara J.P., Geoghegan J.A., FEMS Microbiol Lett. 2014. Contribution: Figure 5.

6. Rapid quantitative and qualitative analysis of biofilm production by *Staphylococcus epidermidis* under static growth conditions. Waters E.M., McCarthy H., Hogan S., Zapotoczna M., O'Neill E., O'Gara J.P., Methods Mol Biol. 2014. Contribution: Co-author.

## Acknowledgements

There are many people who supported me throughout this PhD and I am extremely grateful to you all.

My first thanks go to my supervisor, Prof Jim O'Gara. You have been a remarkable support for me throughout the ups and downs of the research and your enthusiasm and passion for the work kept me going. Thank you for your patience and for helping me through the more difficult times. It has been a pleasure working with you and I am glad I could be a part of the transition from UCD to NUIG. Congratulations on the achievements you've had in the past four years. It's been an exciting time to be a part of the JOG lab.

Thank you to my co-supervisor, Dr Eoghan O'Neill. Thank you for your help and valuable input at various meetings between Dublin and Galway. It has been a pleasure working with you. Thank you to Prof Paul Fey for facilitating two visits to your lab. My thanks to Prof Ken Bayles and Dr Jeffery Bose for the gift of strains. Thank you to Dr Joan Geoghegan and Prof Timothy Foster for facilitating visits to your lab and our continued collaborations. Thanks to Dr Marta Zapotoczna who has been a wonderful collaborator. Thank you also to Prof Simon Foster for the gift of antibodies which were so important for this project. Twice the project took me to Prof Fey's lab in UNMC and I want to express my gratitude to Paul and all of the staff and students at the Staphylococcal Research Centre for their terrific assistance during the animal work. To Paul, Carolyn, Jill, Austin, Cortney, Katie, Roxanne, Trammy, Ken, Jeff, Jennifer, Todd, VJ, Vinai and Sujata, thank you for being so welcoming and always willing to lend a hand and ease the workload on me and Elaine. If it weren't for your help I'm pretty sure we'd both still be in Omaha counting plates today!

This project has brought me from Dublin to Galway (with a few trips to Nebraska squeezed in between!) and I am lucky to have been part of two great faculties in UCD and NUIG. To all the staff at the Ardmore Annex and Science Centre West in UCD, thank you for helping me get settled during the early days of the project. To Maurice, Ann, Mike, Katrina, Caroline and Seamus and all of the academic staff of the Department of Microbiology at NUIG, thank you for making me feel welcome in the department and for making the transition from UCD to NUIG that bit easier.

I am lucky to have had two JOG labs throughout my project! To my first JOG lab; Elaine, Siobhan, and Aly thank you so much for all the wonderful times we had in Science West. I have such fond memories of working with you and I'm so lucky to have you for friends. Elaine, you have been an incredible support. Thank you for your constant encouragement and faith in my abilities. Thank you for the calmness you brought to moments of panic and for all the valuable help and advice you gave me in the early days (and still are giving me!). You were so helpful during both trips to UNMC and with the thesis. Siobhan, thank you for all the great times, the little surprises and for your support. You've been a great friend. Aly, thank you for being there for me and for all of the laughs we shared. It was so much fun working with you. We were lucky to share our old JOG lab in UCD with an amazing bunch of people. Aisling, you were such a bright spark in the lab. Thank you for being you and making the lab a nicer place to work in. Eimear, thank you for being such

a great friend. I'm so excited for the arrival of Baby Casey and all the future holds for you and Will. Doreen, it was so lovely working with you. Thank you for all the fun memories of our time together in UCD. To all the other members of the Science West Infection Biology lab, thank you for creating a wonderful working environment.

To my new JOG lab; Juss, Laura, Nikki, and Colm, thank you for being my new lab buddies. Thank you for helping to make Galway my second home. Juss, thanks for everything, for all the help in the lab and for proof-reading the thesis. Your guidance has been invaluable. Laura, thank you for all the help and for getting me settled into life in and outside the lab in Galway. A sincere thank you to you both for all the non-science related chats. Your friendship helped me through the tougher days. Thanks Nikki and Colm for all of your valuable help too. Thanks for all the laughs we shared and the fond memories I have of the new JOG lab. I wish all of you the best with your future careers. Best of luck to the newest members Chris and Andrea too! Thanks to my Spice Girls; Sporty, Scary, Posh, Ginger, and the newest edition, Aussie Spice! Thanks girls for being there, for the girlie nights in and out and for being my Galway family. To the rest of the Micro gang at NUIG, thank you for welcoming me into the department (despite my dodgy background being from Dublin!).

To all my non-science friends, especially Rachel, thank you for being there for me. To my extended family in Ireland and England, especially my Nan, thank you all for your constant support. To June, Derry, John and Hilary, thank you all for the love and support you've shown me over the last four years.

My Granny Sheila has been such an important help in getting me through the write-up. Thank you Sheila for giving me a warm, peaceful space to write in and for keeping me stocked up with tea and freshly baked scones daily! Most importantly, thank you for your continuing love and care over the years. Thank you for always having your door open to me and my studies and for facilitating so many hours of work over the years. I owe a lot of my success at college to you.

I couldn't have gotten through this project without my family. Mum, Dad, Ellie and Cormie, thank you for being a rock of support. Thank you for your patience, understanding and love. I am so grateful for all you've done and sacrificed for me. Mum, thank you so much for proof-reading the thesis. Thank you all for the encouraging chats, the constant support and for always making home a refuge for me.

Finally, thank you to Will for everything. You have been phenomenal. Thank you for being so patient over the last four years. Thank you for your positivity, for always knowing what to do to lift my spirits, for all the trips to Galway and for waiting patiently for me while I got through the work (even though I'd have promised I'd be finished hours ago!). Thank you for always being there for me, even when you were the other side of the country or on an entirely different continent! Your love carried me through the hard times and I am so grateful for all you have done for me. I hope that when you need me I can step up to the mark as you've done for me.

*To my support network:*

*Will, Mum, Dad, Ellen, Cormac and Sheila*

# Chapter 1:
# Introduction

## 1.1 Staphylococci and their medical significance

Staphylococci are Gram positive coccoid bacteria which belong to the family *Micrococcaceae*. Staphylococci are characterised based on production of a coagulase enzyme with coagulase positive *Staphylococcus aureus* and coagulase negative *Staphylococcus epidermidis* being two medically important species. Both are common commensal bacteria which are part of the normal skin flora. *S. aureus* asymptomatically colonises the anterior nares and the epithelial and mucosal surfaces of 20% of people, while 60% are transiently colonised and 20% are rarely or never colonised (2, 3). Colonisation is a known risk factor for infection by staphylococci (4, 5). *S. aureus* and *S. epidermidis* are opportunistic pathogens that commonly cause infections in immunocompromised people when the epithelial barrier is breached. The species share a core genome of 1,681 open reading frames with genome islands in non-syntenic regions the main basis of variation in virulence between the two species (6). The *S. aureus* genome contains genomic islands which encode for a variety of pathogenicity factors, most of which are absent in the closely related *S. epidermidis* and brand *S. aureus* the more virulent species. These pathogenicity factors encode for a variety of toxins that enable *S. aureus* to successfully evade factors of the host immune response and destroy tissue, for example enterotoxins, exotoxins, leukotoxins, leukocidins and toxic shock syndrome toxin (6-8). These toxins and other secreted and cell surface-associated factors enable *S. aureus* to cause a variety of acute and life-threatening conditions, including sepsis, food poisoning, endocarditis and toxic shock and scalded skin syndromes (9). It has been estimated that in the U.S.A., infections caused by *S. aureus* are responsible for the same number of deaths as those caused by AIDS, tuberculosis and viral hepatitis combined, highlighting the importance of this opportunistic pathogen within the healthcare setting (10). The emergence of antibiotic resistance and community-associated strains of *S. aureus* which cause infections in people with no predisposing risk factors are a cause for concern for public health. Methicillin resistance, which is common in *S. aureus* and *S. epidermidis*, is a significant medical problem. Methicillin resistance almost certainly originated in coagulase negative staphylococci (CoNS) with transfer of the mobile genetic elements from

these CoNS to *S. aureus*, most commonly from *S. epidermidis*, giving rise to methicillin resistant *S. aureus* (MRSA) strains (11). This rise in MRSA and methicillin resistant *S. epidermidis* (MRSE) strains has complicated the issue of nosocomial staphylococcal infections with many resistant strains now characterised as multidrug resistant (12). In contrast to *S. aureus*, the production of harmful molecules by *S. epidermidis* is very low and biofilm formation is a key virulence factor on which *S. epidermidis* relies for establishing successful infections (13). *S. epidermidis*, which for a long time was regarded as innocuous, does produce exopolymers and proteins that aid in immune evasion and are cytolytic, but their most important contribution to *S. epidermidis* pathogenesis is through aiding biofilm formation (13). A strong correlation between the pathogenicity of *S. epidermidis* and biofilm formation has been reported (14). Both *S. aureus* and *S. epidermidis* are important nosocomial pathogens and are frequently associated with infections of indwelling medical devices, made possible by their abilities to form biofilms. Biofilms are communities of sessile bacteria that are encased in a self-produced extracellular polymeric substance in which sophisticated quorum sensing between bacteria regulates growth and development of the biofilm community. Biofilms formed by staphylococci are a significant cause of morbidity and mortality and pose a great threat to healthcare patients.

### 1.2 Biofilm-associated infections caused by staphylococci

Biofilm formation by staphylococci is associated with a range of chronic and life-threatening conditions including urethritis, gingivitis, conjunctivitis, osteomyelitis and lung infections in cystic fibrosis patients (15, 16). Biofilms are associated with more than 80% of all microbial infections, with *S. aureus* and *S. epidermidis* two of the leading causative agents of biofilm-associated infections (15, 17). Staphylococci have the ability to colonise damaged host tissue such as damaged heart valves and the damaged skin of post-operative wounds and burn victims which can lead to the establishment of serious skin and soft tissue infections and conditions such as endocarditis and sepsis (18-20). Staphylococci are a leading cause of device-related infections (DRIs) and are capable of colonising implanted medical devices

ranging from contact lenses to cerebrospinal fluid shunts, cardiac pacemakers, joint replacements and central venous and urinary catheters (21-23). The increasing use of implanted medical devices for monitoring and treatment purposes is exacerbating the problem of DRIs. Patients that have indwelling medical devices are at an elevated risk of developing a biofilm-associated infection, with intense levels of antibiotic usage within hospitals aggravating the problem of DRIs (24, 25). Cells encased in a biofilm matrix are protected from factors of the host's immune system and the actions of antibiotics, rendering DRIs extremely difficult to treat (17). There are multiple ways in which biofilms render staphylococci resistant to therapeutics. Biofilms promote staphylococci cells to enter into a dormant state in which metabolic and growth rates are reduced. These persister cells have been identified as the main factor contributing to the drug resistance and chronic nature of DRIs caused by staphylococci (26). Persister cells within a biofilm are physiologically different from free-floating planktonic cells which are more susceptible to the action of antibiotics. For instance, a 600-fold increase in concentration of sodium hypochlorite is required to kill *S. aureus* cells in a biofilm compared to planktonic cells (27). The persister state renders staphylococci within a biofilm resistant to antibiotics that specifically target fast growing cells (28, 29). Furthermore, the biofilm matrix itself may prevent some drugs from diffusing across the biofilm barrier or the structure of the biofilm itself can physically prevent interaction between antibiotics and encased cells (15). Due to the resistant nature of biofilms, surgical removal of the infected device is often the treatment course required for DRIs, resulting in increased financial costs.

Biofilm formation by staphylococci occurs in three stages as outlined in figure 1.1. Initial attachment of staphylococci to the implanted medical device is the first stage of biofilm formation and the establishment of DRIs. Initial attachment is mediated by the microbial surface component recognising adhesive matrix molecules (MSCRAMMs) which interact with specific host proteins (30). Non-specific interactions between staphylococci cells and uncoated biomaterial also contribute to the initial stages of biofilm formation with cell surface hydrophobicity a contributory factor (31). The second stage of biofilm formation is the establishment of the mature biofilm

and sophisticated fluid-filled channels that facilitate the transport of waste and nutrients throughout the biofilm matrix (32). Finally, individual cells or clusters of cells from the biofilm matrix detach and disseminate to secondary sites of infection within the host (16). This detachment and dissemination aids in the development of systemic infections like bacteraemia and sepsis, with staphylococci infections regarded as the primary cause of nosocomial bloodstream infections (16). Consequently, biofilm-associated infections are not only a significant threat to patients but are also a source of increased economic burden on our healthcare systems. Research to understand the mechanisms of staphylococcal biofilm formation is vital for the development of novel therapeutics to combat this important healthcare issue.

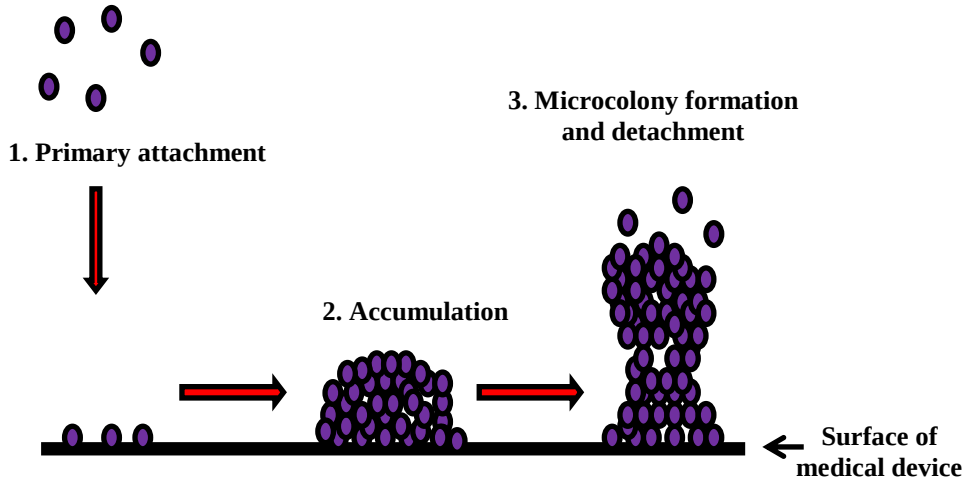


**Fig. 1.1. The stages of biofilm formation by staphylococci.** 1) The first stage of biofilm formation begins with the interactions between planktonic cells and either uncoated surfaces or biomaterial coated with host extracellular matrix proteins. Planktonic, free-floating cells attach to a surface. 2) More sessile bacteria accumulate and grow to form a biofilm on the medical device in which fluid-filled channels develop. 3) The mature microcolony tower develops and from this individual cells or clusters of cells detach and can disseminate to other parts of the host.

## 1.3 The initial stages of biofilm formation

Initial attachment of staphylococci can occur on biotic or abiotic surfaces and is mediated by both specific and non-specific interactions. Non-specific interactions aid in the attachment of cells to abiotic surfaces such as the surface of uncoated medical devices (16). These non-specific interactions depend on the physiochemical characteristics of both the device or surface and the cells. Non-specific interactions that initiate biofilm formation involve cell surface hydrophobic interactions, polarity and van der Waal's forces (33). However, specific cell surface-associated proteins can mediate the interaction between cells and abiotic surfaces (34-36). The major autolysin is an example of a surface-associated protein reported to mediate attachment of both *S. aureus* and *S. epidermidis* to uncoated polystyrene (37, 38). Specific receptor-mediated interactions also occur between staphylococci and biotic surfaces such as damaged human tissue and implanted medical devices coated with host extracellular matrix proteins (39-41). Implanted medical devices are rapidly coated with host extracellular matrix proteins such as fibronectin, fibrinogen, collagen and vitronecin and the MSCRAMMs interact with these proteins to mediate primary attachment of staphylococci to the coated medical device or damaged host tissue (42). The factors contributing to the primary attachment stage of staphylococcal biofilm formation are described below.

### 1.3.1 The major autolysin Atl/AtlE

The major autolysin (Atl) was first implicated in the primary attachment stage of biofilm formation by *S. epidermidis* and has since been implicated in the primary attachment stage of *S. aureus* biofilm formation (37, 38). There is 61% amino acid identity between the major autolysins of *S. aureus* (Atl) and *S. epidermidis* (AtlE) and in both species the *atl* gene is flanked by the same genes (37, 43). Beyond its role in initiating biofilm formation, the major autolysin also functions as a bifunctional peptidoglycan hydrolase involved in daughter cell separation and is required for penicillin-induced autolysis (44, 45). The Atl and AtlE pro-proteins share similar domain organisation as highlighted in figure 1.2. The *atl* gene of *S. aureus* encodes for a 137.5 kDa pro-protein which is proteolytically processed to yield a 3.1kDa signal sequence at the N-terminus, a 17.6 kDa propeptide and two enzymatically active domains; a 63.3 kDa *N*-acetylmuramyl-L-alanine amidase enzyme (AM) and a C-terminally located 53.6 kDa endo-β-*N*-acetylglucosaminidase enzyme (GL; Fig. 1.2) (46). The AtlE of *S. epidermidis* is 148 kDa in size and consists of a 3 kDa signal peptide, followed by a 30 kDa pro-peptide, a 60 kDa AM domain and a C-terminally located 52 kDa GL domain (Fig. 1.2) (37). Atl was first identified in *S. aureus* by T. Oshida, *et al*. (46) and subsequently identified in *S. epidermidis* by C. Heilmann, *et al*. (37). Mutants in *atl* have a number of striking characteristics. Deletion of *atl* does not impair growth but results in unregulated cell division and clumps of cells of *atl* mutants can be viewed microscopically (45-47). An *atl* mutation also has pleiotropic effects on the cell's surface with impaired cell wall turnover resulting in a rough outer cell wall (45). Non-covalently cell wall bound proteins are less abundant in an *atl* mutant and mutants are more sensitive to penicillin-induced lysis (45). All of these characteristics support a role for Atl in cell division, peptidoglycan turnover and penicillin-induced cell lysis. It has been proposed that in the absence of *atl*, other murein hydrolases can partially compensate for the loss of Atl activity, including Sle1, LytN and LytM (48-50). In addition, more than 15 proteins with putative AM and GL activity

have been described in *S. aureus* that could possibly compensate for an *atl* defect (49, 51).

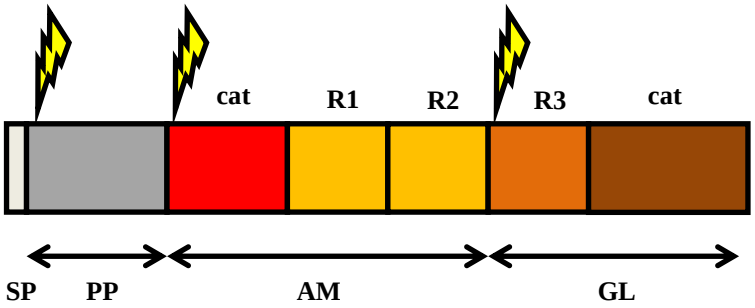


**Fig. 1.2. Domain arrangement of the bifunctional Atl/AtlE precursor protein.** Schematic diagram of the 137.5kDa Atl / 148kDa AtlE pro-protein illustrating the amidase (AM) and glucosaminidase (GL) domains, the signal peptide (sp), pro-peptide (pp), three repeat regions (R1-3) containing GW-dipeptide motifs, catalytic domains (cat) and cleavage sites (arrows). Image adapted from S. Zoll, *et al*. (1).

The Atl protein is proteolytically processed via an as yet uncharacterised mechanism. Proteolytic processing of the Atl pro-protein yields an AM protein containing two repeat regions located at its C-terminus which are responsible for localisation and targeting of AM to the substrate during cell wall turnover (Fig. 1.2) (47, 52). The AM enzyme cleaves the amide bond between N-acetyl muramic acid and L-alanine during peptidoglycan turnover with catalytic activity confined to the N-terminus of the enzyme (Fig. 1.2) (47). The GL protein has the opposite organisation to the AM protein and contains only one repeat region in the N-terminus and a catalytically active region in the C-terminus (Fig. 1.2) (46). After proteolytic processing of pro-Atl, the GL enzyme hydrolyses the bond between N-acetyl-b-D-glucosamine and N-acetyl muramic acid for efficient peptidoglycan hydrolysis (46). The three repeat regions of Atl (R1, R2 and R3; Fig. 1.2) are vital for targeting of the pro-protein to the equatorial ring on the cell surface to aid daughter cell division (52). Wall teichoic acids (WTA) aid correct targeting of the AM and GL enzymes to the cross-wall region for sites of cell division and mediate this targeting through an exclusion strategy (53). WTA prevents unregulated Atl-mediated cell lysis

and targets Atl enzymes to the old cell wall for completing daughter cell separation where WTA is not fully polymerised and concentrations are lowest (53). The repeat regions of Atl also contain GW-dipeptide motifs. The GW repeats of the AM region are responsible for mediating internalisation of *S. aureus* and *S. epidermidis* by non-professional phagocytes and specifically interact with the heat shock cognate protein Hsc70 on host cells (54). This interaction between the GW repeats of the amidase region and the Hsc70 cell receptor may act as a back-up mechanism of internalisation for *S. aureus* but may be the only mechanism by which *S. epidermidis* is internalised and persists within the host (54). A similar mechanism of internalisation is employed by the amidase Ami of *Listeria monocytogenes* and contributes to adherence to eukaryotic cells and virulence *in vivo* (55, 56). When the phenotypes of enzymatically inactive mutants of the *S. aureus* AM and GL regions were compared, it was found that the AM domain and not GL is predominantly responsible for the clumping phenotype associated with *atl* mutations (57). Similarly, the AM domain was found to be more important for Triton X-100 induced autolytic activity and *S. aureus* cell walls were found to be more susceptible to AM-mediated lysis than GL (57). It remains elusive why *S. aureus* cells have greater sensitivity to AM than GL.

As mentioned, the major autolysins of *S. aureus* and *S. epidermidis* mediate primary attachment during *in vitro* biofilm formation. There are several ways that Atl mediates primary attachment. Firstly, Atl can initiate primary attachment of both *S. epidermidis* and *S. aureus* directly through hydrophobic interactions with uncoated surfaces (37, 38, 47). Secondly, Atl can trigger primary attachment through direct interactions with host extracellular matrix proteins. The AtlE protein is known to interact with vitronectin and Atl of *S. aureus* can bind to fibrinogen, fibronectin, vitronectin and endothelial cells and, as mentioned earlier, binding is confined to the GW repeats of the AM regions which interact with the Hsc70 receptor (37, 54). Finally, the major autolysins of *S. aureus* and *S. epidermidis* can also mediate primary attachment indirectly through cell lysis and the release of extracellular DNA (eDNA) (38, 57-59). Several studies have reported an important role for tightly regulated autolysis and

the release of eDNA for staphylococcal biofilm formation (38, 57, 59-62). In other bacterial species, eDNA has been identified as an important component of the biofilm matrix and a possible therapeutic target. For example, cystic fibrosis patients suffering from *Pseudomonas aeruginosa* biofilm-associated infections have been treated successfully with a combination of antibiotics and DNaseI (63). The role for autolytic activity and the release of eDNA for staphylococcal biofilm formation has been demonstrated through biofilm dispersal experiments conducted with DNA degrading enzyme DNaseI and polyanethole sodium sulfanate (PAS) which inhibits autolytic activity without affecting growth (38, 58, 64). Likewise, the secreted thermostable nuclease enzyme, Nuc has been shown to negatively impact on biofilm formation, further revealing eDNA as a vital component of the biofilm matrix (59). Deletion of the Atl and AtlE genes dramatically reduces the amount of eDNA produced through impaired cell lysis (38, 53, 57, 58). Upon cell lysis and release, eDNA becomes an important matrix, aiding cells in attachment during biofilm formation. Furthermore, enzymatically inactive AM and GL mutants have been shown to be impaired in biofilm formation, demonstrating the importance of the catalytic activity of both domains for sufficient eDNA release and biofilm formation (38, 57). The biofilm negative phenotype of the enzymatically inactive GL mutant reported by J. L. Bose, *et al*. (57) highlights the important role for eDNA in the biofilm matrix of *S. aureus*. The GL domain, unlike AM, has no binding affinity for fibrinogen, fibronectin, or vitronectin, thus its sole contribution to biofilm formation appears to be through mediating autolysis and eDNA release (54). Recently, cytoplasmic proteins have been shown to be part of the biofilm matrix of *S. aureus* HG003 which may be a consequence of autolysis and appears to be in response to decreasing pH, which can be triggered by the addition of excess glucose to the growth media (65). Interestingly, addition of glucose to growth media is often the growth condition of choice to promote Atl/protein-mediated MRSA biofilm formation (38). In addition, research from our laboratory has implicated a transcriptional repressor of *atl*, the *atlR* gene, in Atl-mediated biofilm formation by the clinical MRSA strain BH1CC (38). The *atlR* gene (designated *SA0904* in *S. aureus* N315)

encodes a predicted 139-amino acid MarR-type transcriptional regulator that is found adjacent to *atl* on the chromosome and encodes for a protein that exhibits specific interactions with Atl (38). It has been demonstrated that AtlR acts as a repressor of Atl-mediated biofilm formation by BH1CC in a process influenced by temperature (38).

Several studies have assessed the impact of autolysins on virulence. The AtlE protein of *S. epidermidis* has been shown to contribute to biofilm formation and virulence *in vivo* in a rat model of central venous catheter infection (66). The importance of AtlE for *S. epidermidis* virulence has been further demonstrated by assessment of the serum from infected patients. People infected with *S. epidermidis* demonstrate a high IgG titre against the pro-protein, the cleaved amidase domain and the repeat sequences of AtlE (67). Vaccination of mice with recombinant AtlE was found to be effective at stimulating an immune response sufficient for opsonisation of *S. epidermidis* (67). Autolysis has been found to contribute to *S. aureus* virulence in an infective endocarditis model and for the virulence of other bacterial species (68-70). However, J. Takahashi, *et al*. (45) demonstrated that *S. aureus* Atl did not contribute to the development of acute infection in a mouse sepsis model, suggesting that Atl may not be vital *in vivo* in infections that do not involve biofilms. Part of the research presented in this thesis investigates the contribution of the major autolysin of *S. aureus* and the AM and GL regions of Atl to virulence using a mouse model of DRIs.

### 1.3.2 Teichoic acids

Teichoic acids (TA's) of *S. aureus* and *S. epidermidis* have important functions in multiple cellular processes and their roles can be classified into three categories as described by G. Xia, *et al*. (71). The three major themes for TA functionality are 1) protection from antimicrobial peptides and antibiotics and aiding survival in unfavourable environmental conditions, 2) regulating cationic exchange across the cell envelope and enzymatic activity during cell wall turnover and peptidoglycan synthesis and 3) acting as binding receptors to mediate host colonisation, biofilm formation, horizontal gene transfer and interference with the host immune response (71-73).

Staphylococci possess two types of TA's; peptidoglycan-bound wall teichoic acid (WTA), mainly composed of ribitol phosphate groups, and membrane-anchored lipoteichoic acid (LTA) containing glycerol phosphate groups (74, 75).

There are several ways TA's contribute to the initial stages of *S. aureus* and *S. epidermidis* biofilm formation. TA's display zwitterionic properties due to negatively charged phosphate groups and positively charged D-alanine residues incorporated onto the repeating units by the activity of the *dltABCD* operon (71). The net charge of *S. aureus* TAs has been shown to be an important factor controlling attachment to and subsequent biofilm formation on inert surfaces. A mutation in the *dltABCD* operon of *S. aureus* led to a net negative charge on the cell surface that is associated with the loss of D-alanine residues on the TA's. This increases the strength of repulsive forces which impair attachment to and biofilm formation on inert surfaces (76). A later study found a direct correlation between LTA biosynthesis and biofilm formation by *S. aureus* (77). An LTA mutant demonstrated significant changes in cell surface hydrophobicity which are essential for physiochemical interactions with hydrophobic surfaces and initiating primary attachment and biofilm formation by *S. aureus*. Furthermore, autolytic activity was reduced in an LTA mutant and, as described in an earlier section, the autolytic activity of Atl is another factor mediating primary attachment and biofilm formation. The work of M. Vergara-Irigaray, *et al.* (78) shows that TA's mediate *S. aureus* biofilm formation in a manner independent from production of the exopolysaccharide PIA/PNAG. The *tagO* gene encodes an enzyme that is required for the first step in WTA biosynthesis and mutation of *S. aureus tagO* impairs biofilm formation but does not impact on PIA production. Conversely, a *tagO* mutation in *S. epidermidis* which impaired biofilm formation is associated with reduced PIA expression due to upregulation of the negative regulator of the *ica* operon, *icaR* (79). The biofilm defect of a *S. epidermidis tagO* mutant is also due to increased cell surface hydrophobicity which impairs primary attachment (79).

### 1.3.3. Microbial surface component recognising adhesive matrix molecules

After a patient receives an implanted medical device, the device rapidly becomes coated with host extracellular matrix proteins, including fibronectin, fibrinogen, vitronectin, collagen and elastin (30). *S. aureus* and *S. epidermidis* express an array of cell wall anchored proteins that can interact with these host extracellular matrix proteins and mediate different stages of biofilm formation on implanted medical devices. Some of these proteins are classified as microbial surface component recognising adhesive matrix molecules or MSCRAMMs (42). Some MSCRAMMs are implicated in the initial attachment stage of staphylococcal biofilm formation (80-86), whereas others function in intercellular accumulation and the later stages of biofilm formation (80, 87-91).

The term MSCRAMM was initially used to describe proteins based on functional similarities, namely the ability to bind to host extracellular matrix proteins (42). However, recent work has demonstrated that many MSCRAMMs have roles in staphylococcal virulence that go beyond binding to host ligands. Many MSCRAMMs are multifunctional proteins and also have roles in immune evasion, cell invasion, iron acquisition and asymptomatic colonisation (92). The term MSCRAMM is now used to describe a family of proteins based on structural rather than functional similarity. Thus, MSCRAMMs are now defined as proteins which have a common mechanism for ligand binding mediated by at least two adjacent subdomains containing IgG-like folds in the N-terminal A region of the proteins (92, 93).

#### 1.3.3.1 Sortase anchored surface proteins

*S. epidermidis* and *S. aureus* both express an extracellular transpeptidase sortase gene, *srtA* which covalently anchors surface proteins containing a conserved C-terminal Leu-Pro-X-Thr-Gly (LPXTG) motif to the cell wall. The *srtA* gene was first described in *S. aureus* (94). Twenty one of the 28 surface proteins of *S. aureus* contain LPXTG motifs that covalently anchor them to the cell wall surface (95, 96) while *S. epidermidis* has only 11

described such proteins (97). Proteins recognised by SrtA share a similar structure with a C-terminal LPXTG sorting signal, a hydrophobic domain and a tail of positively charged residues (98, 99). Recognition of the LPXTG motif by SrtA is facilitated by the hydrophobic domain and the charged tail which keep the proteins temporarily in a secretory pathway (99). Sortase-anchored proteins are translocated through the cytoplasmic membrane, a process mediated by their N-terminal signal peptide (94, 100). After translocation, SrtA recognises the C-terminal LPXTG-motif and specifically cleaves the precursor polypeptide at the threonine and glycine residues (101-103). Cleavage by SrtA yields a threonine carboxyl residue that is amide linked to the free amino group of the pentaglycine crossbridge of peptidoglycan, thereby covalently linking the proteins to the cell wall (96, 101, 104, 105).

*S. aureus* expresses a second sortase gene, *srtB* which cleaves proteins with an NPQTN motif (106). The *srtB* gene is encoded on the *isd* locus which is involved in the transport of heme-iron across the cell envelope (106). The *isd* locus encodes for the surface proteins IsdA, IsdB and IsdC, the SrtB protein, as well as lipoprotein ATPase and membrane permease (106). Unlike SrtA which is constitutively expressed, the locus is only upregulated under iron-limiting conditions by the ferric uptake repressor, Fur (106, 107). Upon upregulation by Fur, SrtB anchors the IsdC protein via recognition of and cleavage of its NPQTN motif (106).

SrtA has been shown to be vital for *S. aureus* virulence in numerous animal models, including a murine model of septic arthritis, a murine acute lethal infection, a murine kidney infection model and a rat model of endocarditis (108-111). In contrast, SrtB is not essential for *S. aureus* virulence and has only been described as having a contributory role towards pathogenesis (108, 110).The fact that an *srtA* mutant is impaired in virulence in such a variety of animal models highlights the array of surface proteins that SrtA anchors to the cell wall. Some *srtA*-anchored proteins are characterised as MSCRAMMs and interact with host extracellular matrix proteins to initiate primary attachment during biofilm formation, whereas others are implicated in the latter stages and mediate intercellular accumulation, such as Aap of *S.*

*epidermidis*, SasG and the fibronectin binding proteins of *S. aureus* (112-114). Indeed, mutation of *srtA* in both *S. epidermidis* and *S. aureus* impairs biofilm formation (90, 115). As well as proteins involved in biofilm formation, SrtA also anchors surface proteins involved in immune evasion, such as protein A (100).

#### 1.3.3.2 The fibrinogen binding proteins: ClfA and B and SdrG

As mentioned, *S. aureus* and *S. epidermidis* express a variety of cell-anchored proteins that can mediate binding to and the initial stages of biofilm formation on host extracellular matrix proteins. One such host ligand is fibrinogen (Fg), a 340 kDa glycoprotein involved in the formation of blood clots (116). Thrombin-catalysed cleavage of Fg creates fibrin monomers that spontaneously polymerise and form clots (116). Beyond their role in clot formation and regulating blood loss, Fg cleavage products have roles in regulating cell adhesion and spreading and act as chemoattractants and mitogens for multiple cell types (116). Manipulation of Fg by cell-anchored proteins is an important virulence factor for staphylococci.

The Fg binding proteins of *S. aureus* are clumping factors A and B (ClfA and ClfB) (85, 117). *S. epidermidis* mediates Fg binding through the serine-aspartate repeat-containing protein G (SdrG). These Fg binding proteins are classic MSCRAMMs that bind Fg using variations of the dock, lock and latch (DLL) mechanism and share structural similarities (92). The N-terminal A domains contain three subdomains, N1, N2 and N3 with the IgG-like folds that are characteristic of all MSCRAMMS present in the N2 and N3 regions (92, 93, 118). The IgG-like folds mediate binding to Fg via the DLL mechanism. Linking the N-terminal A region to the C-terminal region is a serine-aspartate rich repeat region known as the SD region. The C-terminal region consists of a cell wall spanning region with an LPXTG motif for covalent anchorage to the cell wall peptidoglycan and a sorting signal (92).

The DLL mechanism of ligand binding was originally described for SdrG-mediated binding of *S. epidermidis* to Fg (118), but a similar mechanism is

employed by ClfA and ClfB of *S. aureus* (119, 120). A trench for ligand docking is created by the IgG-like folds within the N2 and N3 subdomains. After docking, an extension of the N3 domain is redirected for interaction between residues of N3 with Fg which locks the ligand in place. The structure is finally stabilised by latching of the C-terminal residues of the N3 domain into a trench within the N2 subdomain. There are variations in the DLL mechanism of ligand binding between the *S. aureus* and *S. epidermidis* proteins that involve side chain interactions within the binding trench (92). Hydrophobic pockets within the SdrG binding trench interact with hydrophobic residues of the Fg ligand. SdrG interaction with Fg blocks the thrombin cleavage site of Fg and inhibits fibrin clotting (81). ClfA and ClfB vary from SdrG in their DLL mechanism inasmuch as ligand binding requires parallel β-sheet complementation (93, 121). This is in contrast to the antiparallel β-sheet complementation characteristic of SdrG ligand binding and results in inversion of the Fg ligand within the binding trench of the ClfA and ClfB proteins (92). Additionally, ClfA differs from ClfB and SdrG as it can bind to both the closed and open forms of Fg whereas ClfB and SdrG can only bind the apo form of the protein. ClfA is capable of binding to the γ-chain of Fg via residues on the γ-chain that can breach the lock region of the closed ClfA protein (92, 117). Binding of ClfA to the γ-chain of Fg blocks interaction between Fg and the platelet $\alpha_{IIb}\beta_3$ integrin receptor and prevents platelet aggregation during clot formation (117, 122).

Binding of these MSCRAMMs to Fg mediates the initial stages of biofilm formation. ClfB is known to mediate *S. aureus* biofilm formation in low calcium conditions (123). Calcium chelating agents are commonly used in catheter locking solutions (23) and while this can inhibit biofilm formation by some *S. aureus* strains, it has been shown that $Ca^{2+}$ depletion can augment biofilms in other strains in a ClfB-dependent manner (123, 124). This has important implications for the use of such catheter locking solutions. Multiple animal models have demonstrated a role for ClfA in biofilm-associated infections. ClfA has been shown to contribute to biofilm formation in a rabbit model of infective endocarditis (IE) through binding to platelets (125, 126). A *clfA* mutant was attenuated in virulence in a rat model of IE, a phenotype that was complemented by reintroduction of the

*clfA* gene to the mutant (19). Additionally, constitutive expression of *clfA* by the non-pathogenic *Lactococcus lactis* significantly decreased the inoculum level required to establish infection (127). The affinity of SdrG for Fg has been exploited to enable successful delivery of vancomycin to the *S. epidermidis* biofilm (128). Vancomycin was covalently bound to a synthetic Fg-based peptide called β6-20. The peptide/antibiotic combination was then successfully incorporated and retained within the *S. epidermidis* biofilm matrix via the mechanism by which SdrG interacts with Fg. This exciting study is a promising step towards developing targeted novel treatments against staphylococcal DRIs that can manipulate specific interactions between host ligands and MSCRAMMs.

#### 1.3.3.3 Secretable expanded repertoire molecules (SERAMs)

Beyond the LPXTG-anchored MSCRAMMs, a collection of non-covalently anchored surface proteins and secreted proteins can also mediate primary attachment to host ligands and biofilm formation by *S. aureus* and *S. epidermidis*. These proteins that were originally identified based on their shared ability to bind to host extracellular matrix proteins do not share significant homology between their protein structures. None-the-less, they can all be classified as SERAM proteins or "secretable expanded repertoire adhesive molecules" (129). In addition to their shared abilities to bind to host ligands, the SERAM proteins are multifunctional and have a common role in modulating the host immune response through their interactions with host ligands (129) . Some of the most prominent of the *S. aureus* SERAM proteins to contribute to biofilm formation and virulence are the extracellular adherence protein (Eap) and the extracellular matrix binding protein (Emp). A non-covalently anchored surface protein of *S. epidermidis* that has an important role in biofilm formation and pathogenesis is the extracellular matrix binding protein (Embp) which has a role in biofilm accumulation (130) and will be discussed at a later stage.

### 1.3.3.4 The extracellular adherence protein (Eap)

The extracellular adherence protein Eap is a 60-70 kDa non-covalently linked surface protein that has a role in *S. aureus* biofilm formation. The Eap protein is found in various sizes in more than 96% of clinical *S. aureus* isolates screened (131). No homologues of this protein have been found in *S. epidermidis* (131). During the 1990s, a number of research groups isolated and characterised a number of proteins that shared similar binding properties to extracellular matrix glycoproteins and were of a similar size (132-135). The term Eap was first applied to the 60kDa protein identified by M. K. Bodén and J. I. Flock (133) and M. H. McGavin, *et al*. (134) that had a high binding affinity to a variety of host ligands including bone sialoprotein, fibronectin and fibrinogen (136). A subsequent study in 2001 found that all of the proteins identified during the 90's exhibited extensive homology and were in fact the same protein, namely Eap (131).

Secreted Eap mediates biofilm formation by binding with high affinity to epithelial, fibroblast and endothelial cells (137) and multiple host ligands including fibrinogen, fibronectin and serum proteins (136, 138, 139). Another mechanism by which Eap contributes to DRIs and biofilm formation is through direct interactions between secreted Eap proteins which can mediate intercellular aggregation and attachment to uncoated polystyrene (136, 140). Eap also contributes to biofilm formation under iron-limited conditions (141).

Eap has a role in uptake by nonprofessional phagocytes including endothelial cells and keratinocytes. Eap represents an additional mechanism for internalisation for these cells that is required when the fibronectin binding proteins are expressed at low levels, for example in the *S. aureus* strain Newman (129, 142, 143). Furthermore, Eap can contribute to modulation of the host response by binding to intercellular adhesin molecule-1 (ICAM-1) on endothelial cells and blocking the interaction between leukocytes and ICAM-1 (137, 144). Through this interaction, subsequent extravasation of leukocytes to the site of tissue damage is prevented (144). In a mouse renal abscess model an *eap* mutant was attenuated in persistent and chronic infections and antibodies against Eap

afforded a significant level of protection to the animals against disease progression (145). Recently, Eap has been identified as having inhibitory activity towards neutrophil serine proteases which further promotes the pathogenicity of *S. aureus in vivo* (146).

#### 1.3.3.5 Extracellular matrix binding protein (Emp)

The extracellular matrix binding protein (Emp) was identified in 2001 by the broad spectrum recognition it exhibited for multiple host ligands, including fibronectin, fibrinogen, collagen, and vitronectin (147). Although studied in less detail than Eap, Emp is known to contribute to biofilm formation and pathogenesis. The Emp protein is approximately 40 kDa in size and is found in clinical isolates of *S. aureus* but not in any *S. epidermidis* isolates screened to date (147). Secreted Emp contributes to biofilm formation and endovascular disease through its high affinity for multiple host ligands (129, 147). Emp also contributes to biofilm formation when cells are grown under iron-restricted conditions (141). In a mouse model of renal abscess, an *emp* mutant was found to be unaffected in establishing infections early on (145). However, mutation of *emp* significantly reduced the number of abscesses, indicating that beyond its role in biofilm formation, Emp also has a role in chronic infections and abscess formation. Antibodies to Emp only generated limited protective immunity to infections in the animals as Emp was found to be located within staphylococcal biofilms *in vivo* (145).

## 1.4 Accumulation of biofilms

After primary attachment of cells to a medical device or damaged host tissue, other factors begin to play a role in supporting intercellular accumulation. These factors include the exopolysaccharide PIA/PNAG (Fig. 1.3), LPXTG and non-LPXTG anchored surface proteins and extracellular DNA. Once sufficient intercellular accumulation is achieved the mature microcolony is formed, in which fluid-filled channels aid the transport of nutrients and waste around the biofilm. The cells encased in the mature biofilm communicate and regulate detachment from the established biofilm through the Agr quorum sensing system which responds to cell density

(148). The multiple factors that *S. aureus* and *S. epidermidis* utilise for the accumulation phase of biofilm formation are strain and environment dependent and are discussed below.

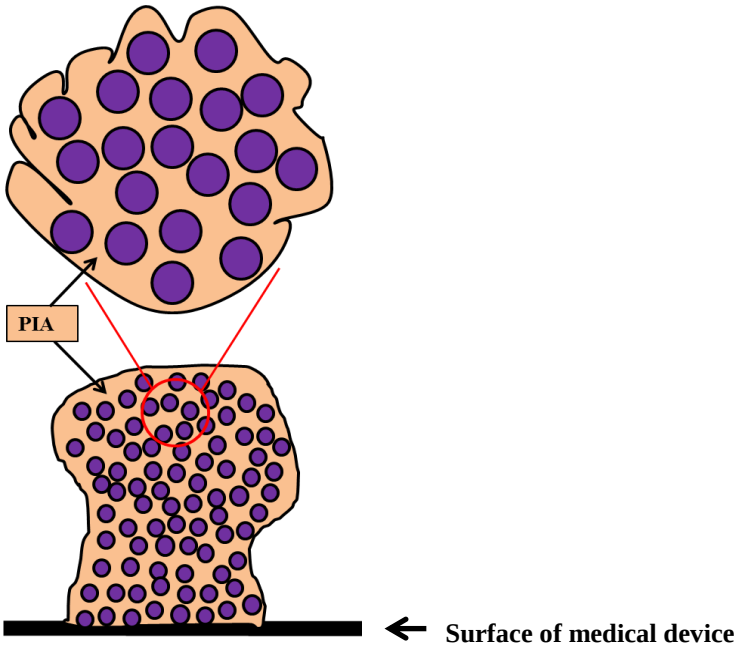


**Fig. 1.3: Illustration of PIA-dependent biofilm formation.** Intercellular accumulation mediated by PIA is dependent on the *icaADBC* operon. The PIA glycan acts as a glue-like substance that promotes cellular aggregation of negatively charged staphylococcal cells via the positive charge on the glycan.

### 1.4.1 *icaADBC*-dependent biofilm

The first characterised mechanism of staphylococcal biofilm formation was found to be dependent on production of an exopolysaccharide called polysaccharide intercellular adhesin (PIA), encoded for on the *icaADBC* (intercellular adhesin) operon (Fig 1.3). This sticky glycan is composed of β-1,6-linked 2-acetamido-2-deoxy-D-glucopyranosyl residues which essentially glue staphylococcal cells together within a biofilm matrix (149). The PIA glycan has a net positive charge which promotes intercellular aggregation between the negatively charged staphylococcal cells and mediates attachment of cells to inert surfaces (Fig. 1.3) (149). A contribution for PIA to intercellular accumulation was first described in *S. epidermidis* (150-153) and subsequently for *S. aureus* (154-156). There is high sequence homology between the *ica* operons of *S. aureus* and *S.*

*epidermidis* with 78% identity at the amino acid level (154). The *ica* operon consists of four biosynthesis genes, *icaA*, *icaD*, *icaB* and *icaC* and a divergently transcribed repressor, *icaR* (32, 157). PIA synthesis begins with upregulation of the *icaA* gene which encodes for a membrane located protein with N-acetylglucosaminyltransferase activity (158, 159). IcaA synthesises a partially deacetylated β 1–6 linked N-acetylglucosamine homopolymer, the activity of which is increased 20-fold when co-expressed with the *icaD* (32, 158, 159). IcaD acts as a chaperone that optimises the N-acetylglucosaminyl-transferase activity of IcaA and leads to the production of N-acetylglucosamine oligomers which reach a maximal length of 20 residues (32, 158). When the IcaC protein is co-expressed with IcaA and IcaD longer chains of N-acetylglucosamine oligomers are produced (32, 158). It is proposed that IcaC plays a role in translocation of the polysaccharide chain through the cytoplasmic membrane and elongation of the growing polysaccharide (32). IcaB facilitates partial de-acetylation of the N-acetylglucosamine residues which gives the polysaccharide chain a cationic charge deemed important for PIA-mediated intercellular accumulation and attachment of cells to surfaces (160). The *icaADBC* operon is regulated by the divergently transcribed *icaR* repressor, a member of the *tetR* family of transcriptional regulators which is located directly upstream of the operon (157). IcaR tightly regulates expression of the *icaADBC* locus in response to environmental stimuli, including temperature changes and the addition of ethanol and salt to growth medium, and has been shown to influence PIA-dependent biofilm formation (157, 161-163).

PIA-dependent biofilm formation has been shown to be important for both *S. epidermidis* and *S. aureus in vivo* biofilm formation. Slime production, as PIA production is often referred to, has long been known to contribute to *S. epidermidis* virulence (164, 165). Using a mouse model of device-related infections, a direct correlation between PIA production and virulence was later demonstrated for *S. epidermidis* DRIs (160). Subsequent studies using animal models of DRIs further implicated PIA production as an important virulence factor for *S. epidermidis* biofilm-associated infections (66, 166). PIA-dependent biofilm formation has also been shown to contribute to *S. aureus* virulence in a rat model of endocarditis (167). Several groups have

reported a strong association between virulence of *S. epidermidis* and *S. aureus* and the presence of *ica* and production of PIA (17, 168-172). Promising studies have also described how PIA may be a suitable vaccine candidate against *S. epidermidis* and *S. aureus* DRIs (156, 167, 173-175). However, despite all of these advances, PIA-independent mechanisms of biofilm formation have been described for both *S. epidermidis* and *S. aureus*. P. Francois, *et al*. (176) used a tissue cage guinea pig model to assess the contribution of PIA production to *S. epidermidis* and *S. aureus* DRIs and found no significant differences in virulence between the *ica* mutants and parent strains. The authors proposed that the lack of difference in colonisation may be due to the design of the model which allowed for the animals to recover from implantation of the tissue cage for three weeks prior to infection with *S. epidermidis* and *S. aureus*. It was suggested that this enabled the cages to become coated with host matrix proteins and that the surface proteins of *S. epidermidis* and *S. aureus* could mediate biofilm formation in the absence of a functioning *ica* operon. One of the first studies to identify a mechanism of PIA-independent biofilm formation was the description of the biofilm associated protein (*bap*) gene which contributes to biofilm formation in bovine mastitis isolates of *S. aureus* (177, 178). Mutation of the *ica* operon in a *bap*-positive strain of *S. aureus* did not impair its biofilm forming capacity. However, the importance of *bap* for human infections was put into doubt when the gene was found to be absent among a collection of 75 human isolates (177). A separate investigation by K. E. Beenken, *et al*. (28) found that mutation in *ica* did not impair *in vitro* or *in vivo* biofilm formation by the *S. aureus* strain UAMS-1. Furthermore, PIA-independent mechanisms of biofilm formation were shown to be significantly more important for virulence of the *S. aureus* strain 132 which is capable of switching from a PIA-dependent to a PIA-independent biofilm (179).

### 1.4.2 PIA-independent mechanisms of biofilm formation

Both *S. epidermidis* and *S. aureus* have the ability to form biofilms independent of PIA production. PIA-independent mechanisms of biofilm formation involve both sortase-anchored and non-covalently anchored surface proteins (Fig 1.4). The release of eDNA upon regulated autolysis also contributes to primary attachment and intercellular accumulation as discussed previously (Fig. 1.4). Intense research has been undertaken to characterise these mechanisms of biofilm formation and they are described below.

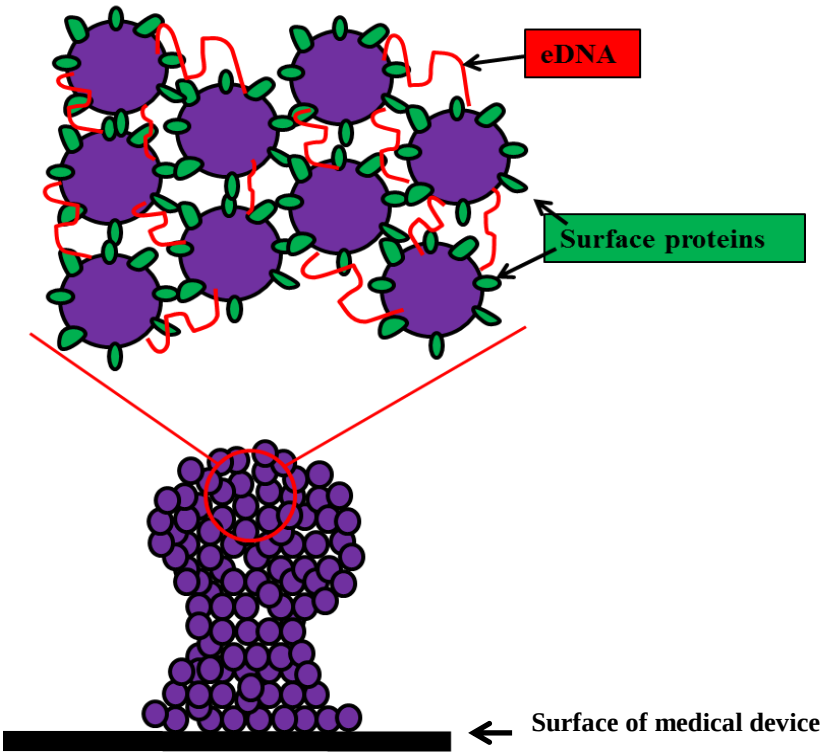


**Fig. 1.4: Illustration of PIA-independent mechanisms of biofilm formation.** Biofilm accumulation independent of PIA production requires LPXTG and non-LPXTG-anchored surface proteins, Atl-mediated cell lysis and eDNA release to mediate intercellular aggregation during biofilm formation.

### 1.4.2.1 Accumulation associated protein/*S. aureus* surface protein G

The accumulation associated protein (Aap) of *S. epidermidis* and the *S. aureus* surface protein G (SasG) are two structurally similar, typical LPXTG-anchored multidomain surface proteins that have roles in the accumulation phase of PIA-independent biofilm formation. The role for Aap in *S. epidermidis* biofilm accumulation was first described by M. Hussain, *et al*. (87) who described a mutant that was deficient in biofilm accumulation on glass and polystyrene surfaces. This biofilm defect was attributed to a 140 kDa protein and antibodies raised against this protein could inhibit *S. epidermidis* biofilm accumulation by 98%. The protein was identified as processed Aap and was found to have no role in primary attachment of cells to glass or polystyrene. Ten years after the identification of Aap, R. M. Corrigan, *et al*. (180) described the homologue protein in *S. aureus*, SasG, which, like Aap, contributed to biofilm accumulation in a PIA-independent manner.

There is 54% identity between the Aap and SasG proteins (180). The proteins consist of an N-terminal signal peptide that is removed during secretion across the cytoplasmic membrane followed by an A-domain that is composed of related amino acid sequences. These sequences are predicted to fold into an all β-structure that enables adhesion to desquamated epithelial cells and promotes colonisation of the skin and nares via interaction with an unidentified receptor (180-182). The B regions of Aap and SasG are 64% identical and are followed by a C-terminal LPXTG motif that covalently anchors the proteins to the cell wall (89). The B domains consist of tandemly arrayed glycine G5 domains interspersed with approximately 50 residue enzymatic domains (E) (183). The B domain of Aap consists of repeats of 3-12 G5-E domains of 128 amino acids, followed by a single G5 repeat. The SasG B domain has seven 128-residue repeats and one partial repeat. Biofilm formation is mediated by the B regions of Aap and SasG upon cleavage from the A domain (89, 113). This cleavage occurs through an as yet uncharacterised mechanism (113). It has been proposed that processing of SasG may occur spontaneously at labile peptide bonds (89). The importance of cleavage of Aap for *S. epidermidis* biofilm

accumulation was demonstrated through biofilm inhibition assays with addition of alpha (2)-macroglobulin to the growth media (113). Furthermore, biofilm formation could be induced through expression of the truncated protein and not the full length Aap in an *aap* and biofilm negative *S. epidermidis* strain (113). It has been proposed that cleavage of SasG, which occurs at a different site to Aap is required for *S. aureus* biofilm formation, however, the inability to inhibit cleavage of the protein has prevented conclusive evidence of this to date (89). Despite this, J. A. Geoghegan, *et al*. (89) could demonstrate that the cleaved B domain and not the A domain of SasG contributes to *S. aureus* biofilm accumulation.

After cleavage of the A domain, the B domain mediates biofilm accumulation through a "zinc-zipper mechanism" which is dependent on the G5 repeats. Homophilic interactions between the B domains of cells results in dimer formation and cellular aggregation that is dependent on a physiologically relevant concentration of $Zn^{2+}$ (89, 184, 185). This results in the formation of extended fibrils consisting of Aap and SasG on the cell surface that can promote cell to cell adhesion and biofilm accumulation (180, 183, 185, 186). Chelation of $Zn^{2+}$ from growth media inhibits both *S. epidermidis* and *S. aureus* biofilm formation, demonstrating the importance for this "zinc-zipper mechanism" for biofilm accumulation (89, 184). Purified recombinant B regions of Aap and SasG can also inhibit *S. epidermidis* and *S. aureus* biofilm formation respectively (89, 113). Additionally, biofilm accumulation independent of the "zinc zipper mechanism" mediated by the B domain of SasG has been described (185). Structures of E-G5 and G5-E-G5 within the B domain of SasG form monomeric structures in which the E sequences fold and interlock with the G5 domains in a head-to-tail fashion, resulting in the formation of fibrils on the cell surface that mediate accumulation within a biofilm.

### 1.4.2.2 The fibronectin binding proteins

Research from our laboratory has identified a role for the fibronectin binding proteins (FnBPs) in the accumulation phase of *S. aureus* PIA-independent biofilm formation (90). These MSCRAMM proteins, namely FnBPA and FnBPB, are structurally similar cell wall-associated proteins. Both are composed of a N-terminal signal sequence, an A region with fibrinogen and elastin binding A domains (N1, N2 and N3), a region of fibronectin binding motifs (11 in FnBPA and 10 in FnBPB), a wall/membrane spanning region and a C-terminally located LPXTG motif for covalent anchorage to the cell wall (114, 187) . The proteins are capable of binding to the host extracellular matrix proteins fibronectin, fibrinogen and elastin (114, 187-190). Fibronectin binding is mediated by the C-terminally located tandemly repeated motifs and occurs by a tandem β-zipper interaction mechanism (191). Binding to elastin and fibrinogen is mediated through a dock, lock and latch mechanism with the proteins recognising the same binding site of fibrinogen as ClfA, the extreme C-terminus of the γ-chain (189, 192-194). Peptides are docked within a hydrophobic trench located between the N-terminally located N2 and N3 subdomains. This docking induces redirection of the flexible N3 subdomain over the trench which locks the peptide in place. Latching then occurs when the remainder of the C-terminally located extension interacts with subdomain N2 via β-strand complementation (118, 120). Internalisation of *S. aureus* into fibroblasts, epithelial and endothelial cells is promoted through formation of a fibronectin bridge to the α5β1 integrin upon interaction of the FnBPs with fibronectin, highlighting an important role for these MSCRAMMs in invasive staphylococcal diseases (195, 196). There is a strong association between carriage of the *fnbps* and invasive staphylococcal diseases, with *S. aureus* isolates from invasive diseases such as endocarditis, osteomyelitis and septic arthritis more likely to carry both genes (197). Ninety-seven percent of a collection of nosocomial pneumonia and cystic fibrosis *S. aureus* isolates were found to possess both *fnbp* genes (198). People suffering from invasive *S. aureus* infections were found to have a significantly higher level of anti-FnBPA antibody in their sera when

compared to sera from healthy volunteers (199). Promisingly, antibodies to the FnPBs could elicit protection against dissemination and the development of endocarditis in a rat model of local joint infection (200).

As mentioned, the FnBPs have a crucial role for the accumulation phase of PIA-independent biofilm formation of both healthcare and community-associated MRSA with each individual FnBP protein capable of complementing the biofilm defect of a double *fnbpAB* mutant (90, 201). Supporting a role for the FnBPs in PIA-independent biofilm formation was the finding that the FnBPs are constitutively expressed throughout the growth cycle of a HA-MRSA producing biofilm independent of PIA, whereas they were found to be expressed only in the exponential growth phase of an MSSA strain expressing a PIA-based biofilm (194). The region of the FnBPs involved in biofilm formation has been identified within the A domain N-terminal region of FnBPA and is localised to residues 166 to 498 comprising the N2 and N3 subdomains (90, 194). Biofilm formation mediated by this region is dependent on a physiological concentration of $Zn^{2+}$ (194). The *in vivo* relevance of FnBP-mediated biofilm formation has been shown using a mouse foreign body infection model (179). In this study an *fnbpAB* double mutant was found to be significantly less virulent than the wild type strain or its isogenic *ica* mutant. An interesting study comparing isolates from infected cardiovascular devices (CDI isolates) to isolates from non-infected devices and asymptomatic carries found an important role for FnBPA polymorphisms in the pathogenesis of the CDI isolates (202). CDI isolates were identified as having three specific single amino acid polymorphisms within FnBPA that enabled the protein to bind with higher affinity to fibronectin (202). This *in vivo* selection for mutations in FnPBA which result in greater binding affinity to fibronectin further highlights the important contribution of the FnBP-mediated biofilm for DRIs.

### 1.4.2.3. Protein A

The LPXTG-anchored staphylococcal protein A (Spa) was the first LPXTG-anchored surface protein of *S. aureus* to be described (100, 203, 204). The Spa protein consists of a S domain with a signal peptide, A-E domains which are required for immunoglobulin binding, short octapeptide repeat sequences encoded for by $X_r$, and a $X_c$ encoded LPXTG anchoring domain in the C-terminal region (205, 206). Spa is well known for its role in facilitating immune evasion and aiding *S. aureus* in evading phagocytosis through binding to the constant region of immunoglobulin G (IgG) in the opposite orientation (206, 207). Consequently *S. aureus* cells become coated with IgG in the wrong alignment that cannot be recognised by the neutrophil complement binding (Fc) receptor, thereby enabling cells to evade phagocytosis (207, 208). Beyond its role in inhibiting opsonophagocytic killing by polymorphonuclear leukocytes, Spa also interacts with von Willebrand factor (209), platelets (210), B lymphocytes (211), tumor necrosis factor receptor 1 (212) and the epidermal growth factor receptor (213) which are all important interactions for initiating colonisation of damaged host tissue and inflammation in diseases such as infective endocarditis and pneumonia (214).The importance of Spa for *S. aureus* virulence has been demonstrated in multiple animal models. Spa contributes to a range of diseases including pneumonia (215), septic arthritis (216) and skin and soft tissue infections (217).

Spa has been characterised as an important mediator of *S. aureus* biofilm formation that promotes intercellular accumulation (91). N. Merino, *et al*. (91) described *spa* mutants that were biofilm negative *in vitro* and showed that the protein does not need to be anchored to the cell wall to function in biofilm accumulation as exogenous Spa could promote biofilm formation. A murine model of subcutaneous foreign body infection was employed during this study and coinfection of the animals with the parent and *spa* mutant strains revealed that Spa significantly contributes to DRIs.

As well as roles in immune evasion and biofilm formation, Spa is also important for nasal colonisation. Comparison of the exoproteome of *S. aureus* from nasal carriers to strains from non-carriers revealed that Spa was

present at significantly higher levels in the exoproteome of a strain from carriers than from non-carriers, suggesting a direct role for Spa in colonisation (218). A very recent publication demonstrated that the biofilm matrix exoproteome of *S. aureus* can elicit a protective immune response in mice against *S. aureus* biofilm-related infection (219). Immunisation of mice with the biofilm matrix exoproteome resulted in reduced levels of colonisation and persistence in the mice upon infection. Different strains of *S. aureus* were used in this study to the strain assessed in the colonisation study carried out by G. Muthukrishnan, *et al*. (218). However, Gil *et al*. reported that 85% of the exoproteins encompassed in the biofilm matrix exoproteome of the *S. aureus* strain which elicited protective immunity in the mice were identical to the components of the exoprotein of the colonising strain described by Muthukrishnan *et al*. It is interesting to note that in both studies, Spa was reported to be present in both exoproteomes.

#### 1.4.2.3 The extracellular matrix binding protein (Embp)

*S. epidermidis* can mediate biofilm accumulation through the extracellular matrix binding protein (Embp) in a PIA and Aap-independent manner (130). Embp is a giant protein, non-covalently anchored to the cell wall of 1 MDa in size and was first identified by its high binding affinity for fibronectin (88). Embp can bind to other host extracellular matrix proteins with less affinity than fibronectin, including heparin, hyaluronate, and plasminogen (88). Binding of Embp to fibronectin and other matrix proteins can mediate primary attachment of *S. epidermidis* to surfaces coated with these proteins (130). Embp also mediates intercellular accumulation during the later stages of biofilm formation (130). The regions of the Embp protein that mediate binding to host ligands are also required for mediating intercellular accumulation, specifically the FIVAR (found in various architecture) and the GA (protein G-related albumin) domains (130). Furthermore, *embp* gene and protein expression is upregulated under high osmotic conditions, conditions that are often encountered by skin colonising bacteria (220). This work shows that beyond its role in biofilm formation and intercellular accumulation, Embp may also serve as a mechanism of skin colonisation and cell wall stabilisation during osmotic stress conditions (220).

Embp is recognised as an important virulence factor of *S. epidermidis*. *S. epidermidis* strain 1585 only expresses Embp in the presence of serum which indicates the *in vivo* relevance of this mechanism of biofilm formation for *S. epidermidis* (130). Moreover, *embp* carriage is associated with invasive strains of *S. epidermidis* and has been identified in invasive isolates from blood cultures (221), prosthetic joint infections (222) and intraocular infections (223), highlighting the *in vivo* relevance of Embp for *S. epidermidis* DRIs.

## 1.5 Global virulence gene regulators and biofilm formation

To establish a successful infection staphylococci require a sophisticated and intricate regulatory network of virulence regulators that can respond to changing environments and the host response. Tightly regulated coordination of these virulence factors by global regulators is key to surviving within the host and the contribution of these global regulators to virulence and biofilm formation by staphylococci is discussed below.

### 1.5.1 The accessory gene regulator (Agr) quorum sensing system

The Agr system is by far the best understood quorum sensing system of *S. epidermidis* and *S. aureus*. Encoded for on the *agr* locus are two divergent transcripts, RNAII and RNAIII, expression of which is driven by the neighbouring but non-overlapping P2 and P3 promoters respectively (224). Quorum sensing, mediated by the *agr* system, is responsive to levels of the post-translationally modified autoinducing peptide, AIP (225). The AIP pheromone is produced as part of the cell density-sensing system of staphylococci. Once threshold levels of AIP are reached, regulation of virulence factors is activated by *agr*. The active *agr* system represses extracellular protease production and upregulates toxin secretion (226).

The RNAII transcript of the *agr* locus encodes for an operon of four genes, *agrBDCA*, which coordinate synthesis of AIP. AIP synthesis begins with transcription of *agrD* which encodes for the AIP precursor protein AgrD (227, 228). AgrD is posttranslationally modified by AgrB which functions as a protease that cleaves AIP to approximately eight amino acids in length

(229, 230). AgrB has also been proposed to function in secretion of the mature AIP (231, 232). AgrC and AgrA act as a two component signal transduction pathway that respond to AIP levels (231). AgrC is a sensor kinase that has a binding site for AIP. Upon binding with AgrC, the response regulator AgrA becomes activated and initiates transcription of RNAII and RNAIII (228). RNAIII is the effector molecule of the *agr* system and encodes for the phenol soluble modulin (PSM) δ-toxin. The Agr system also regulates expression of the *psm* operons encoding, for example, for the expression of *psmα* and *psmβ* molecules through direct binding of AgrA to the promoters (233).

Recent studies have shown that the Agr system is an important regulator of multiple stages of staphylococcal biofilm formation (234). It is likely that the downregulation of extracellular proteases and surfactant-like PSMs associated with the low level of *agr* activity during the planktonic state contribute to initiating biofilm formation in both *S. aureus* and *S. epidermidis* (234-236). The down regulation of *agr*-regulated proteases upregulates adhesins on the cell surface that can initiate primary attachment and mediate physio-chemical interactions with implanted biomaterial (236). Agr-regulation of AtlE expression has been implicated in the primary attachment stage of *S. epidermidis* biofilm formation (235). Agr is a negative regulator of AtlE and when Agr is expressed at low levels during the early stages of biofilm formation, AtlE is capable of initiating biofilm formation as described earlier. In contrast, Agr does not directly regulate Atl of *S. aureus* (236). Agr also has a well-documented role in detachment of cells from established biofilms (61, 148, 234, 237-239). The upregulation of extracellular proteases by *agr* transcription is one mechanism by which the Agr system mediates dispersal from biofilms. The second mechanism is through upregulation of PSM molecules. The β-PSMs of *S. epidermidis* and all classes of PSMs of *S. aureus* (α-PSM, β-PSM and δ-PSM) have been implicated in biofilm structuring and dispersal (234). It is believed that PSMs contribute to biofilm channel structuring and dispersal through disrupting non-covalent (electrostatic or hydrophobic) interactions between macromolecules of an established biofilm (16). Agr-positive *S. aureus* strains are capable of forming a film of amphipathic surfactant δ-toxin

molecules expressed at the biofilm/fluid interface. This δ-toxin film inhibits the hydrophobic interactions between bacterial cell surfaces, thus lowering surface tension and causing cell detachment from the biofilm matrix (240). Upregulated Agr activity and dispersal from established biofilms is important for acute infections (241, 242) whereas reduced Agr activity and *psm* expression have been implicated in the development of thick and dense biofilms (243). Thus, reduced *agr* expression favours the formation of localised chronic biofilm-associated infections (244) and indeed *agr*-negative strains of *S. aureus* and *S. epidermidis* are frequently isolated from such infections (240, 245).

### 1.5.2 The staphylococcal accessory regulator, SarA

The SarA gene was first identified in *S. aureus* and is known to regulate the expression of over 100 genes (246, 247). The SarA proteins of *S. aureus* and *S. epidermidis* share 84% homology (248). SarA is a DNA binding protein that is preferentially transcribed during the early log phase of growth. It is a key global regulator of *S. aureus* and *S. epidermidis* virulence, upregulating synthesis of a variety of cell wall and extracellular proteins and down regulating expression of proteases. SarA can control virulence gene regulation through *agr*-dependent and *agr*-independent mechanisms (249). The *sarA* locus encodes for the SarA protein and consists of three overlapping transcripts driven by three distinct promoters, P1, P2 and P3. SarA can directly regulate expression of virulence genes by binding to target gene promoters or indirectly via downstream effects on other regulators such as *agr* or by stabilising mRNA during the log phase of growth (250).

SarA is a known regulator of *ica*-dependent and *ica*-independent biofilm formation by *S. aureus* and *S. epidermidis*. SarA regulates *ica*-dependent biofilm formation in a manner independent of the Agr system (251, 252) and the icaR regulator (253). SarA binds with high affinity to the IcaA promoter, thereby upregulating transcription of the *icaADBC* locus and promoting biofilm formation. SarA also promotes *ica*-independent biofilm formation by downregulating extracellular protease production and promoting expression of surface adhesins to mediate primary attachment and intercellular accumulation (28, 254). In a *sarA* mutant the expression of

the extracellular proteases aureolysin, SspA, SspB, and ScpA is upregulated and surface adhesin expression is impaired (255, 256). The upregulation of proteases, and subsequent degradation of putative protein adhesins, has been shown to negatively impact on *ica*-independent biofilm formation and elimination of the production of all proteases fully restores virulence and biofilm formation by a *S. aureus sarA* mutant (256, 257). SarA has been shown to be required for *S. aureus* virulence in murine models of implant-associated biofilm infection and of *S. aureus* bacteraemia through upregulated protease activity and decreased production of virulence factors such as ClfA, ClfB and Hla in the absence of SarA (258). Moreover, mutation of *sarA* renders *S. aureus* biofilms more susceptible to daptomcyin treatment in a murine model of catheter-associated infection (259) and SarA has been shown to be required for attenuating the host's inflammatory response during staphylococcal biofilm infection of the central nervous system, although the exact mechanism remains to be determined (260).

### 1.5.3 Sigma B

The alternative sigma factors sigma B ($\sigma^B$) of *S. aureus* and *S. epidermidis* function as stress response regulators. $\sigma^B$ controls a large regulon that is involved in a number of cellular processes including protein secretion, oxidative stress response, signalling pathways, cell wall biosynthesis and turnover and biofilm formation (261, 262). $\sigma^B$ is an important modulator of virulence gene expression, controlling expression of over 250 genes of *S. aureus*, and acts conversely to the Agr system (261). The $\sigma^B$ operon consists of four genes *rsbUVW* and *sigB* (263). RsbW is an anti-sigma factor that represses transcription of $\sigma^B$ in the absence of a stress condition. When an environmental stress is encountered, the phosphatase RsbU dephosphorylates the anti-anti-sigma factor RsbV which subsequently binds to RsbW and enables disassociation of $\sigma^B$ from the RsbW protein. $\sigma^B$ is then free to interact with RNA polymerase and initiate a stress response.

As mentioned, $\sigma^B$ has a role in both *S. aureus* and *S. epidermidis* biofilm formation. $\sigma^B$ regulates *ica*-dependent biofilm formation by *S. epidermidis* in response to osmotic stress and anaerobic conditions (264, 265). $\sigma^B$-regulation of *S. epidermidis* biofilm formation occurs through indirect

repression of the negative regulator *icaR*. $\sigma^B$ was first implicated in *S. aureus* biofilm formation in 2000 (266). This study showed that a $\sigma^B$ mutation impaired osmotic stress-induced biofilm formation by *S. aureus*, which are the conditions used to trigger *ica*-dependent biofilm formation. $\sigma^B$ is a positive regulator of *icaR* transcription in *S. aureus* (267). However, $\sigma^B$ also has a role in regulating *ica*-independent biofilm formation by *S. aureus* and does so indirectly through regulation of *agr* and extracellular protease levels (239). Mutation of $\sigma^B$ upregulates *agr*-regulated expression of proteases which degrades putative protein adhesins required for *ica*-independent biofilm formation.

### 1.5.4 Biofilm formation under iron-limited conditions, the global regulators Fur and Sae

Iron depletion is a common stress that is encountered by staphylococci during infection. The ferric uptake regulator, Fur, is a global regulator of expression of virulence genes in low iron conditions in *S. epidermidis* and *S. aureus* (268). Originally, Fur was identified as an iron-dependent repressor of genes involved in iron acquisition during infection (269). However, Fur also has roles in regulation of virulence genes under high and low iron conditions (107, 268). Fur regulates *S. aureus* biofilm formation in an *ica*-independent manner (270) through upregulation of the secreted proteins Eap and Emp during iron-limited conditions (141). Interestingly, iron-dependent repression of Eap and Emp is Fur-independent. It has not been fully revealed exactly how Fur activates transcription under low iron. M. Johnson, *et al*. (271) propose several possible mechanisms for Fur-regulated transcription. It is possible that Fur mediates transcription through direct binding to target promoters although no Fur box consensus sequences have been identified to date in any of the positively regulated Fur-regulated promoters. Another possibility is that Fur is indirectly regulating transcription by repression of another protein regulator or is involved in post-transcriptional regulation, possibly mediated by small, non-coding regulatory RNAs.

Fur is involved in a complex regulatory network under iron-depleted conditions and is required for full expression of the *S. aureus* exoprotein

expression (Sae) two component system (TCS) (271). Sae, along with Fur, is required for full induction of Eap and Emp to aid *S. aureus* biofilm formation under iron depleted conditions (141). When induced under low iron conditions, Sae and Fur act cooperatively to induce not just biofilm formation but also expression of multiple exoproteins including hemolysins, lipases, nucleases and the surface IgG-binding protein SBI (271). The Sae TCS is involved in the regulation of not just biofilm formation under iron-limited conditions but also in the expression of toxins and immune evasion proteins, and is required during oxidative stress conditions (271). The *sae* operon is autoregulated and consists of four open reading frames, *saeP*, *saeQ*, and *saeR* and *saeS* which encode for the response regulator (SaeR) and the receptor kinase (SaeS) of the two component system (272). The Sae TCS regulates biofilm-associated infections in a protease-dependent manner (273) and acts synergistically with SarA to regulate extracellular protease production (274). Sae-regulated protease activity and production of key virulence factors can reverse the attenuation of *sarA* mutants in a murine model of catheter-associated infection (275). The SaeRS TCS also partially regulates biofilm formation through direct regulation of nuclease (275, 276).

The role for the Sae TCS is *S. epidermidis* biofilm formation differs from that of *S. aureus* Sae-dependent biofilm formation. A *saeRS* deletion mutant displayed increased levels of biofilm formation in the *S. epidermidis* strain 1457 which was mediated by increased expression of the AAP protein and the autolysins AtlE and Aae (277). This increase in autolysins and autolytic activity correlated with increased concentrations of eDNA in the biofilm matrix. The Sae TCS was shown to have no impact on *icaA* expression, revealing that *saeRS* is regulating *S. epidermidis* biofilm formation in an *ica*-independent manner.

## 1.6 Methicillin resistance

Methicillin resistance is one of the most challenging problems facing staphylococcal researchers. Methicillin-resistant *S. aureus* (MRSA) was first isolated in 1961, just two years after methicillin was first introduced into clinical practice (278). Since the 1970s, methicillin resistance has become a worldwide epidemic and hospital-acquired and community-associated strains of MRSA (HA-MRSA and CA-MRSA) have been characterised. HA-MRSA are confined to the hospital environment where they are associated with infections in immunocompromised individuals and carry resistance to multiple antibiotics (279). In contrast, CA-MRSA have enhanced virulence compared to HA-MRSA and can cause infections in healthy people that have no contact with the hospital environment (279). Additionally, methicillin resistance rates among *S. epidermidis* strains associated with hospital-acquired infections are extremely high and often exceed those of MRSA (280). Incidents of methicillin-resistant *S. epidermidis* (MRSE) do not prompt the same level of infection control measures as incidents of MRSA infections (281). However, recent studies have highlighted the importance of controlling and preventing MRSE infection rates as a measure for controlling MRSA outbreaks. There is strong evidence that MRSE is a reservoir for drug resistance elements acquired by methicillin-sensitive *S. aureus* (MSSA) and that MRSE populations facilitate ongoing evolution of novel SCC*mec* elements (282-285).

Methicillin resistance is mediated by acquisition of the *mecA* gene encoded for on the unique molecular vector called the staphylococcal chromosome cassette (SCC*mec*) (286). SCC*mec* elements share similar structural homology. Each element consists of inverted repeats, direct repeats (DR), joining regions (J1, J2 and J3), the *mecA* gene and the cassette chromosome recombinase (*ccr*) gene complex (287). The *ccr* complex encodes for one or two recombinases that are responsible for site- and orientation-specific excision and integration of SCC*mec* into a site close to the origin of replication called open reading frame X (*orfX*) (286). The DRs flank either side of the SCC*mec* element and contain integration site sequences that are

recognised by the *ccr*-complex to mediate correct integration of the SCC*mec* element into the chromosome. The joining regions consist of apparently useless pseudogenes and truncated copies of transposons and insertion sequences. These regions are used for subtyping SCC*mec* elements.

The *mecA* gene encodes for a foreign penicillin-binding protein called PBP2a. PBP2a is characterised by a low affinity for β-lactam antibiotics (288). β-lactam antibiotics such as methicillin and oxacillin, the clinically used derivative of methicillin, bind to the transpeptidase domain of native PBPs and prevent peptide cross-linking at the last stage of peptidoglycan synthesis (289). Cell death then occurs as autolytic enzymes puncture the cell wall while normal cell division continues in the presence of β-lactams (290, 291). PBP2a can maintain its transpeptidase action and facilitate normal cell wall turnover in the presence of β-lactams. However, PBP2a is a poor transpeptidase and requires the transglycosylase activity of native PBPs to confer resistance (292). There are two distinct sets of regulatory genes that control transcription of *mecA*, *mecRI-mecI* and *blaRI-blaI* (293). The *mecRI-mecI* regulatory element is located upstream and is divergently transcribed from *mecA*. The *blaRI-blaI* regulatory element is responsible for production of the β-lactamase *blaZ*. MecI and BlaI are repressors capable of repressing *mecA* as well as *blaZ* transcription (293). Activation of *mecA* and *blaZ* transcription occurs when the transmembrane receptors MecRI and BlaRI are activated by binding of an inducer to their extracellular domain which triggers metalloprotease cleavage of the repressors (294, 295). Resistance levels to β-lactams are affected by each regulatory system. The *mecRI-mecI* regulatory element has a much slower rate of induction in the presence of β-lactams than the *blaRI-blaI* regulatory element (296, 297).

To date, there are eleven identified SCC*mec* types but more are expected to be discovered (298). Classification of SCC*mec* types is based on the combination of *ccr*-gene complex and the class of *mec*-gene complex encoded for on the cassette (287). HA and CA-MRSA differ in their SCC*mec* types. The older and larger SCC*mec* types I-III are associated with HA-MRSA strains (299). These elements carry resistance to multiple

antibiotics and incur a fitness cost upon the strains. In contrast, the smaller SCC*mec* types IV and V are found in CA-MRSA strains (300-302). These new elements typically only carry the *mec*-gene complex and no other resistance genes, rendering less of a fitness burden on CA-MRSA than the larger SCC*mec* types of HA-MRSA (303, 304). These new elements are widely distributed among MRSE strains, further implicating *S. epidermidis* as a reservoir for horizontal gene transfer of resistance genes to *S. aureus* (283, 287).

### 1.6.1 Heterogeneous and homogeneous methicillin resistance

Heterogeneity is a feature of *S. aureus* resistance to methicillin (305-307). Heterogeneous resistance (HeR) occurs when the majority of a population (≥99.9%) of cells are susceptible to low levels of β-lactams and express an MIC from 1-10 μg/ml (307). Within this HeR population a subpopulation of cells (≥1%) express homogeneous resistance (HoR) that facilitates growth at high concentrations of β-lactams (307). Clinical MRSA strains often express HeR resistance and selection of HoR resistant strains in the laboratory is achieved by growth on high levels of oxacillin (≥100 μg/ml oxacillin), osmotic stress and growth at 30$^{o}$C or in the presence of sucrose (308).

The mechanisms governing the transition from a HeR to a HoR phenotype of resistance is not yet completely understood and levels of resistance do not necessarily correlate with the amount of PBP2a expressed (309). Mutations in the chromosome of MRSA and not within the *SCCmec* element are associated with the transition from HeR to HoR resistance (309). HoR resistance arises from numerous different mechanisms and includes mutations in regulatory factors, genes involved in cell wall turnover and peptidoglycan synthesis and mutations in housekeeping genes such as the *fem* genes (factor essential for methicillin resistance) and the *aux* genes (auxiliary genes) (288, 310-315). Recently, the HoR phenotype has also been associated with non-synonymous single nucleotide polymorphisms (SNPs) in *gdpP* (316). The *gdpP* gene encodes a c-di-AMP phosphodiesterase implicating c-di-AMP with increased resistance to beta-lactam antibiotics (317, 318). Further implicating a role for *gdpP* in the phenotype of HoR strains was the finding that mutation of *dacA*, the

diadenylate cyclase gene which reduces c-di-AMP levels, resulted in the conversion of a HoR to a heterogeneously resistant (HeR) strain (319).

### 1.6.2 Methicillin resistance and biofilm formation

Over the last decade, research in our laboratory has established a relationship between methicillin resistance and biofilm phenotypes (38, 90, 254, 320). MSSA strains were commonly found to produce biofilm dependent on PIA production (Fig. 1.3) whereas MRSA strains formed biofilms independent of PIA as illustrated in figure 1.4 (254). An initial study characterising *ica*-independent biofilm formation in four clinical MRSA isolates (320) was followed up with a larger study on a collection of 32 intensive care unit isolates (15 MSSA and 17 MRSA strains) which provided further evidence for *ica*-independent biofilm formation by MRSA (321). Finally, a comprehensive study of 212 clinical isolates (114 MRSA and 98 MSSA) representing five clonal complexes (CC5, CC8, CC22, CC30 and CC45) provided compelling evidence for *ica*-dependent biofilm formation by MSSA and *ica*-independent biofilm formation by MRSA (254). MSSA strains form biofilms induced by the addition of salt to the growth media, a known inducer of the *ica* operon. The biofilms formed by MSSA are susceptible to degradation by sodium metaperiodate (SM), which oxidises polysaccharide bonds, but are resistant to degradation by proteinase K, DNaseI and polyanethole sodium sulfanate (PAS), which inhibits autolytic activity without impairing growth (Fig. 1.3). In contrast, SM has no effect on glucose-induced MRSA biofilms whereas these biofilms are readily degraded by proteinase K, DNaseI and PAS, implicating roles for protein adhesins, autolysis and eDNA in the MRSA biofilm matrix (Fig. 1.4).

How methicillin resistance alters the biofilm phenotype of *S. aureus* is still under investigation but recent work from our laboratory has given insights into some of the mechanisms behind this phenomenon (316). Construction of a homogeneous (HoR), high level resistant MRSA from the laboratory MSSA strain 8325-4 implicated *mecA* in the switch in biofilm phenotype from a polysaccharide type to a proteinaceous type. Acquisition of the *mecA* gene was directly associated with a >300-fold repression of the *ica* operon.

High level expression of PBP2a was shown to be important for the proteinaceous biofilm of MRSA strains as a mutant expressing a catalytically inactive *mecA* was impaired in biofilm formation. Moreover, antibodies to PBP2a could inhibit MRSA biofilm formation. Further implicating a direct role for PBP2a in the HoR biofilm phenotype was the unexpected finding that *atl*, *srtA* and *fnbpAB* mutations had no effect on the HoR biofilm formation. Repression of *agr* was associated with high levels of PBP2a expression and this downregulation of *agr* is a contributory factor for promoting the proteinaceous biofilm formed by HoR MRSA strains (226, 316).

The switch in biofilm formation from a PIA-based to a proteinaceous type did not impair the ability of *S. aureus* to colonise implanted catheters in a mouse model of device-related infection (316). However, the switch from methicillin-sensitive to highly methicillin-resistant did impair overall virulence of the HoR strain. The HoR strain disseminated at significantly lower levels to organs than the parent MSSA strain and didn't induce as strong a pro-inflammatory response as the parent strain. This attenuation in virulence of an MRSA strain has been reported in other publications (226, 322, 323) and is supported by clinical reports that MSSA are significantly more associated with higher rates of endocarditis and higher illness severity scores than MRSA strains (324, 325). Based on the findings of C. Pozzi, *et al*. (316) and J. K. Rudkin, *et al*. (226) the attenuation in virulence of MRSA strains can be attributed to the reduction in *agr* activity via PBP2a expression.

Another mechanism for attenuated virulence in MRSA strains and downregulation in *agr* has recently been attributed to carriage of the *psm-mec* locus which is found on type II SCC*mec* elements commonly carried by highly resistant HA-MRSA (326-329). The *psm-mec* locus is located adjacent to the *mec* locus on type II elements. Transcription of this locus supresses expression of the cytolytic phenol-soluble modulin α (PSMα) via downregulation of *agrA*, a positive transcription factor for PSMα. Carriage of the *psm-mec* locus attenuates virulence of HA-MRSA in murine infection models (327-329) and promotes biofilm formation, indicating the relevance of biofilm formation for HA-MRSA (326, 329). The *psm-mec* locus has

been implicated as a source of differences in virulence between HA and CA-MRSA as carriage of the locus is absent on the smaller SCC*mec* elements of CA-MRSA and mutation or deletion of the locus was found to increase the virulence of HA-MRSA in murine skin and systemic infection models (326). Therefore, both carriage of the *psm-mec* locus and high level expression of PBP2a can be directly correlated with attenuated virulence of HA-MRSA compared to their MSSA counterparts or CA-MRSA.

Recent research from our laboratory has investigated a way of exploiting this attenuation in virulence for therapeutic potential. The work by J. K. Rudkin, *et al*. (330) has demonstrated that by increasing PBP2a expression with oxacillin pressure, CA-MRSA exhibit reduced expression of *agr* and secretion of the cytolytic PSMα. Although counterintuitive, treating MRSA with β-lactams to attenuate virulence may improve prognoses for patients and increase the efficacy of other antibiotics such as glycoproteins, the last resort antibiotics used to treat MRSA infection, for which there is now rising resistance. Despite this promising work further investigations are required as oxacillin pressure increased expression of alpha toxin and Panton-Valentine leukocidin (330) and, given the role of PBP2a in promoting biofilm formation, this too may be problematic for using β-lactams to treat MRSA infections.

### 1.7 Animal models of DRIs

Despite advances in the designs of flow cell models for studying *in vitro* biofilm formation and DRIs, the use of animal models of DRIs remains an invaluable tool for elucidating the relevant mechanisms of staphylococcal biofilm formation and for the discovery of novel therapeutics to treat DRIs. A variety of models have been designed that mimic human DRIs. Some of the commonly used models of DRIs are discussed below.

One of the earliest models designed for studying staphylococcal DRIs was the tissue cage guinea pig model which was designed by W. Zimmerli, *et al*. (331). This model has since been adapted for use in mice (176, 332) and is a useful tool for examining the mechanisms of staphylococcal biofilm, the inflammatory response to DRIs and for assessing the efficacy of antibiotics

and novel therapeutics against staphylococcal DRIs (176, 333, 334). The model involves the implantation of the tissue cage into the subcutaneous space of the flank of the animals. Rigid polymethacrylate and polytetrafluoroethylene tubes perforated with approximately 250 holes, each 1 mm in diameter are used as the cages. Perforations in the cage allow for an influx of inflammatory cells into the tissue cage fluid, particularly polymorphonuclear neutrophils and monocytes. After implantation of the tissue cage, the animals are allowed to recover and heal fully for several weeks after which infections are established by injecting a pre-determined inoculum of bacteria into the tissue cages within the subcutaneous space. Tissue cage fluid can then be assessed for colony forming units as well as inflammatory markers.

The mouse peritoneal cavity model is used to mimic DRIs associated with continuous ambulatory peritoneal dialysis (CAPD) and was designed by B. Gallimore, *et al*. (335). To ensure the development of confluent catheter-associated infections, catheter segments are incubated in a defined inoculum of bacteria for 72 hours, followed by multiple washes with sterile medium prior to implantation. Infected catheter segments are implanted intraperitoneally and secured to the lateral abdominal wall. After the infection course the animals are sacrificed and assessment of the DRI is carried out by peritoneal washing. This involves retracting the abdominal skin of the mice and gently injecting and withdrawing a volume of MEM (Eagle's modified, containing 10% heat-inactivated foetal calf serum and 20 mM HEPES buffer) into the peritoneal cavity. Total cell counts of the peritoneal washing can then be assessed, along with total cell counts from the parietal peritoneum, the surrounding peri-catheter tissue, the spleen and the catheter segment. Several studies have proved the effectiveness of this model for investigating staphylococcal DRIs and novel treatments associated with CAPD infections (335-337).

The mouse foreign body infection model is the *in vivo* model used for studies conducted as part of this thesis. This model is designed to mimic the subcutaneous space of humans and has been utilised previously for studying *S. epidermidis* and *S. aureus* DRIs (164, 166, 316, 338, 339). Segments of biomaterial, usually catheters, are aseptically implanted into the

subcutaneous space on the flank of the mouse. A pre-determined inoculum of bacterial is then injected into the lumen of the biomaterial once the wound is sealed or alternatively the biomaterial is immersed in a culture of bacteria prior to surgical implantation. After mice are sacrificed, the biomaterial is harvested along with the surrounding tissue and assessed for colonisation by plating and counting colony forming units (CFUs). Dissemination from the site of infection can also be assessed by harvesting organs and blood from the mice, including the peri-catheter tissue, kidneys, liver, heart and spleen. The immune response of the animals can be assessed by ELISA assays on the harvested organs. BALB/c mice are one species of mice commonly used but they produce a T-helper 2 (Th2) immune response to *S. aureus* infections. Th2 immunity is characterised as "humoral immunity" and involves the upregulation of antibody production upon infection (340).Th2 immunity is quite an effective mechanism for clearing *S. aureus* infections and can lead to spontaneous clearance of infection during experiments conducted with BALB/c mice (341, 342). An alternative strain of mice used is C57BL/6 mice which predominantly produce a T-helper 1 (Th1) immune response to *S. aureus* infection. The Th1 response characteristic of these mice is more likely to lead to development of chronic infection commonly associated with DRIs (341, 342). Th1 immunity is characterised as "cellular immunity" (340) and C57BL/6 mice are the strain of choice for this study.

The rat CVC model is an alternative model for investigating staphylococcal DRIs. This model was designed by M. E. Rupp, *et al*. (343) and is more complicated to set up compared to the mouse foreign body infection model. The model requires a surgeon to implant the central venous catheter into the rats via the jugular vein and advance it to the superior vena cava. However, the model has advantages over the mouse foreign body infection model inasmuch as the rat CVC model incorporates the contribution of blood flow, blood products and humoral immunity to staphylococcal infections (344). After surgery the CVC is left in place for 24 hours prior to infection set-up and restraint jackets are used to secure the catheters and prevent disruption of the surgical site by the animals. Bacterial strains are injected directly into the catheter and infections are allowed to establish. After the animals are

sacrificed, the catheter can be harvested along with blood from the catheter and tissue surrounding the catheter. As with the mouse foreign body infection model, the heart, lungs, liver, and kidneys can be harvested for examining metastatic infection. This model has been successfully utilised to assess the molecular factors contributing to staphylococcal DRIs and is ideal for studying the efficacy of novel catheter antilock solutions (66, 345, 346).

### 1.8 The Nebraska transposon mutant library

In 2012, the team at the Nebraska Centre for Staphylococcal Research developed a sequence-defined transposon mutant library of 1,952 strains (347). The library was created in the USA300 genetic background, an epidemic CA-MRSA isolate. Most non-essential genes in the USA300 genome were mutated to create the 1,952 strains. The *mariner*-based transposon *bursa aurealis*, which is known to create random transposon mutations in *S. aureus*, was utilised to create the library (348-350). To assess the value of the library for phenotypic screening purposes, the authors screened the collection for haemolysis activity, protease production, pigmentation and mannitol utilization. This method validated the use of the library for such purposes and helped to identify previously undiscovered genes related to these phenotypes. Construction of the library identified 579 open reading frames that are vital for *S. aureus* viability. Thus this library should prove important for the discovery of novel antibacterial drugs. This library is an invaluable tool for the staphylococcal research community and strains from the NTML have been used for screening experiments and research which are presented in this thesis.

### 1.9 Aims of this thesis

2. To expand on previous research from our laboratory and investigate further the contribution of Atl to biofilm formation by both MRSA and MSSA and the contribution of Atl to MRSA cytotoxin production under *in vitro* conditions.

3. To assess the potential of Atl as a novel therapeutic target against *S. aureus* DRIs.

4. To assess the contribution of Atl to *S. aureus* pathogenesis *in vivo* using a mouse foreign body infection model.

5. To investigate the effect of oxacillin growth pressure and heterogeneous and homogeneous methicillin resistance phenotypes on Atl-dependent phenotypes.

6. To expand on previous research from our laboratory investigating PIA-independent mechanisms of biofilm formation by *S. epidermidis* mediated by AtlE and Aap.

# Chapter 2:
# Materials and Methods

## 2.1 *S. aureus* strains

In collaboration with Dr. Jeffrey Bose and Professor Kenneth Bayles of the University of Nebraska Medical Centre (UNMC), two strains each carrying a point mutation in one of the two enzymatic regions of Atl were generated, namely strains KB4057 ($AM_{H265A}$) and KB4056 ($GL_{E1128A}$). Strain KB4057 was generated by mutating the histidine at amino acid 256 to alanine rendering the amidase region enzymatically inactive and strain KB4056 was generated by mutating the glutamic acid at amino acid 1128 to alanine rendering the glucosaminidase region enzymatically inactive. These point mutations rendered both the AM and GL regions enzymatically inactive as confirmed by zymograph analysis at UNMC with expression of the Atl protein unaffected by both mutations (zymograph image presented in Fig. 3.6).

The Nebraska Transposon Mutant Library (NTML) was purchased from the Network on Antimicrobial Resistance in *Staphylococcus aureus* (NARSA) and strains from this collection were utilised for screening experiments during the course of this project. This library was created at UNMC in the USA300-derivative strain JE2 and contains a collection of 1,952 mutants of most non-essential genes in *S. aureus*. The *mariner*-based transposon (Tn) *bursa aurealis* was used to generate random Tn insertion mutations in *S. aureus* as described by P. D. Fey, *et al*. (347).

The *S. aureus* strains used in this study are listed in Table 2.1, *S. epidermidis* strains used in this study are listed in Table 2.2 and plasmids used in this study are listed in table 2.3.

**Table 2.1 Bacterial strains used in this study**

| Strain | Relevant details | Reference or source |
|---|---|---|
| 8325-4 | 8325 derivative cured of known prophages with 11-bp deletion in *rsb*U. MSSA. | (262) |
| 8325-4 Δ*icaADBC*::Tc$^r$ | Isogenic 8325-4 Δ*icaADBC*::Tc$^r$ mutant. | (38) |
| 8325-4 Δ*atl*::Cm$^r$ | Isogenic 8325-4Δ*atl*::Cm$^r$ mutant. | (38) |
| 8325-4 *pmecA* HeR | 8325-4 carrying p*mecA* expressing heterogeneous resistance to oxacillin. | (226) |
| 8325-4 *pmecA* HoR | 8325-4 carrying p*mecA* expressing homogeneous resistance to oxacillin. | (316) |
| RN4220 | Restriction-deficient derivative of 8325-4. MSSA. | (351) |
| JT1392 | Isogenic RN4220 Δ*atl*::Cm$^r$ mutant. | (45) |
| RN4220 Δ*icaADBC*::Tc$^r$ | Isogenic RN4220 Δ*icaADBC*::Tc$^r$ mutant. | (320) |
| SH1000 | Functional *rsb*U derivative of 8325-4. *rsb*U$^+$. MSSA. | (262) |
| SH1000 Δ*atl*:cm$^r$ | Isogenic SH1000 Δ*atl*:cm$^r$ mutant. | This study. |
| SH1000 Δ*atl*:: em$^r$ | Isogenic SH1000 Δ*atl*:: em$^r$ mutant. | (352) |
| SH1000 Δ*icaADBC*::Tc$^r$ | Isogenic SH1000 Δ*icaADBC*::Tc$^r$ mutant. | This study. |
| BH1CC | HA-MRSA. Biofilm positive. SCC*mec* type II. MLST type 8. CC8. | (254) |
| BH1CC Δ*atl*::Cm$^r$ | Isogenic BH1CC Δ*atl*::Cm$^r$ mutant. | (38) |

| | | |
|---|---|---|
| BH1CC Δ*atlR*::Tc$^r$ | Isogenic BH1CC Δ*atlR*::Tc$^r$ mutant. | (38) |
| BH1CC Δ*fnbpAB*::Tc$^r$ | Isogenic BH1CCΔ *fnbpAB*::Tc$^r$ mutant. | (90) |
| BH1CC Δ*SCCmec* | Isogenic BH1CC ΔSCC*mec* mutant | (323) |
| BH1CC Δ*mecA*:: Tc$^r$ | Isogenic BH1CC Δ*mecA* mutant | (226) |
| USA300 JE2 | USA300 LAC derivative cured of plasmids p01 and p03. CA-MRSA, SCC*mec* type IV. Parent strain of NTML. | (347) |
| USA3000 JE2 Δ*atl*::φNΣ | Strain NE460 from NTML. *bursa aurealis atl* mutation. Erm$^r$. CA-MRSA isogenic USA3000 JE2. | (347) |
| USA3000 JE2 Δ*atlR*::φNΣ | Strain NE1066 from NTML. *bursa aurealis atlR* mutation. Erm$^r$. CA-MRS isogenic USA3000 JE2. | (347) |
| USA3000 JE2 ΔAM | Strain KB4057 ($AM_{H265A}$). CA-MRSA USA300 isogenic JE2 with an active site mutation in the amidase of Atl. | This study (gift from Dr Jeffery Bose) |
| USA3000 JE2 ΔGL | Strain KB4056 ($GL_{E1128A}$). CA-MRSA isogenic USA300 JE2 strain with an active site mutation in the glucosaminidase of Atl. | This study (gift from Dr Jeffery Bose) |
| USA3000 JE2 Δ*icaA*::φNΣ | Strain NE37 from NTML. *bursa aurealis icaA* mutation. Erm$^r$. CA-MRSA isogenic USA3000 JE2. | (347) |
| USA3000 JE2 Δ*fnbpA*::φNΣ | Strain NE186 from NTML. *bursa aurealis fnbpA* mutation. Erm$^r$. CA-MRSA isogenic USA3000 JE2. | (347) |
| USA3000 JE2 Δ*fnbpB*::φNΣ | Strain NE728 from NTML. *bursa aurealis fnbpB* mutation. Erm$^r$. CA- | (347) |

| | | |
|---|---|---|
| | MRSA isogenic USA3000 JE2. | |
| USA3000 JE2 Δ*clfA*::φNΣ | Strain NE543 from NTML. *bursa aurealis clfA* mutation. Erm$^r$. CA-MRSA isogenic USA3000 JE2. | (347) |
| USA3000 JE2 Δ*clfB*::φNΣ | Strain NE391 from NTML. *bursa aurealis clfB* mutation. Erm$^r$. CA-MRSA isogenic USA3000 JE2. | (347) |
| USA3000 JE2 Δ*eap*::φNΣ | Strain NE111 from NTML. *bursa aurealis eap* mutation. Erm$^r$. CA-MRSA isogenic USA3000 JE2. | (347) |
| USA3000 JE2 Δ*emp*::φNΣ | Strain NE1558 from NTML. *bursa aurealis emp* mutation. Erm$^r$. CA-MRSA isogenic USA3000 JE2. | (347) |
| USA3000 JE2 Δ*srtA*::φNΣ | Strain NE1787 from NTML. *bursa aurealis srtA* mutation. Erm$^r$. CA-MRSA isogenic USA3000 JE2. | (347) |
| USA3000 JE2 Δ*srtB*::φNΣ | Strain NE1363 from NTML. *bursa aurealis srtB* mutation. Erm$^r$. CA-MRSA isogenic USA3000 JE2. | (347) |
| USA3000 JE2 Δ*spa*::φNΣ | Strain NE286 from NTML. *bursa aurealis spa* mutation. Erm$^r$. CA-MRSA isogenic USA3000 JE2. | (347) |
| USA3000 JE2 Δ*nuc*::φNΣ | Strain NE1241 from NTML. *bursa aurealis nuc* mutation. Erm$^r$. CA-MRSA isogenic USA3000 JE2. | (347) |
| USA3000 JE2 Δ*sarA*::φNΣ | Strain NE1193 from NTML. *bursa aurealis sarA* mutation. Erm$^r$. CA-MRSA isogenic USA3000 JE2. | (347) |
| USA3000 JE2 Δ*fur*::φNΣ | Strain NE723 from NTML. *bursa aurealis fur* mutation. Erm$^r$. CA-MRSA isogenic USA3000 JE2. | (347) |

| | | |
|---|---|---|
| USA3000 JE2 Δ*saeS*::φNΣ | Strain NE1296 from NTML. *bursa aurealis saeS* mutation. Erm$^r$. CA-MRSA isogenic USA3000 JE2. | (347) |
| USA3000 JE2 Δ*agrC*::φNΣ | Strain NE873 from NTML. *bursa aurealis agrC* mutation. Erm$^r$. CA-MRSA isogenic USA3000 JE2. | (347) |
| USA3000 JE2 Δ*vwbp*::φNΣ | Strain NE1181 from NTML. *bursa aurealis vwbp* mutation. Erm$^r$. CA-MRSA isogenic USA3000 JE2. | (347) |
| USA3000 JE2 Δ*coa*::φNΣ | Strain NE26 from NTML. *bursa aurealis coa* mutation. Erm$^r$. CA-MRSA isogenic USA3000 JE2. | (347) |
| USA3000 JE2 Δ*atl*::Cm$^r$ Δ*srtA*::Tc$^r$ | Double Δ*atl*::Cm$^r$ Δ*srtA*::Tc$^r$ CA-MRSA isogenic USA3000 JE2 mutant. | This study. |
| USA300 LAC | Erm$^s$. CA-MRSA expressing heterogeneous resistance to oxacillin. | (239) |
| USA300 LAC HoR | Erm$^s$. CA-MRSA expressing homogeneous resistance to oxacillin. | (316) |
| USA300 *ΔsaePQRS* | Isogenic *saePQRS* CA-MRSA USA300 mutant. | (353) |
| MW2 | CA-MRSA, USA400 SCC*mec* type IV. | (354) |
| MW2 *ΔsaeQRS::spc* | Isogenic *saeQRS* MW2 mutant. | (354) |
| MW2 *ΔsaeQRS::spc* pRB473*saeRS* | Isogenic *saeQRS* MW2 mutant complemented with pRB473*saeRS*. | (354) |
| UAMS-1 | Low-passage methicillin-susceptible USA200 strain isolated from an osteomyelitis infection. MSSA. | (355) |

| | | |
|---|---|---|
| UAMS-1 *ΔsaeRS* | Isogenic UAMS-1 *saeRS* mutant. | (274) |

**Table 2.2. *S. epidermidis* strains used in this study**

| Strain | Relevant details | Reference |
|---|---|---|
| CSF 41498 | Biofilm positive, cerebrospinal fluid isolate from Beaumont Hospital, Dublin. *ica*$^+$, *aap*$^+$. | (356) |
| 1457 | Biofilm positive central venous catheter infection isolate. *ica*$^+$, *aap*$^+$. | (357) |
| RP62A | Biofilm positive blood culture isolate. *ica*$^+$, *aap*$^+$. | (358) |
| CSF41498 Δ*aap*::Tc$^r$ | CSF41498 derivative, Δ*aap*::Tc$^r$. | (115) |
| 1457 Δ*aap*::Tc$^r$ | 1457 derivative, Δ*aap*::Tc$^r$ | (346) |
| 1457 Δ*icaADBC*::Tmp$^r$ | 1457 derivative, Δ*icaADBC*::Tmp$^r$ | (359) |
| CSF414898 Δ*icaC::*IS*256*Δ*tnp* | CSF41498 derivative, Δ*icaC::*IS*256*Δ*tnp* | (360) |

**Table 2.3 Plasmids used in this study**

| Plasmid | Relevant details | Reference |
|---|---|---|
| pLI50-*tet* | 2,413-bp XbaI-HindIII fragment containing the *tetA* gene from pBlue-*tet* cloned into XbaI-HindIII-digested pLI50 | (38) |
| p*atl* | 4,330-bp EcoRI fragment containing the *atl* gene from p*atl*TOPO cloned into the EcoRI site of pLI50-*tet* | (38) |
| p*atl*H265A | p*atl* with an amidase H265A mutation | (38) |
| pLI50 | *E. coli-Staphylococcus* shuttle vector; $Amp^r$ (*E. coli*), $Cm^r$ (*Staphylococcus*) | (361) |
| pLI50*atlR* | 985-bp EcoRI fragment containing the *atlR* gene from p*atlR*TOPO cloned into the EcoRI site of pLI50 | (38) |

## 2.2 Sterilisation techniques

All agar and broth solutions were autoclaved at 121$^o$C and 1 bar of pressure for 20 minutes before use. Sucrose solutions for electroporations were autoclaved separately at the same conditions. NaCl and glucose solutions were made up to a 20% w/v concentration, filter sterilized using 0.22 µm filters (Millipore) and stored at 4$^o$C. After autoclaving, agar and broth media were cooled to 50°C and room temperature, respectively, prior to the addition of sucrose, glucose, NaCl or antibiotics.

## 2.3 Media and Growth Conditions

Bacterial strains were grown at 37$^o$C on either brain heart infusion (BHI) (Oxoid) or tryptic soy agar (TSA) (Sigma) with chloramphenicol (5-10 µg/ml), tetracycline (5-10 µg/ml) or erythromycin (5-10 µg/ml) where indicated. Strains were grown where indicated in liquid media in either BHI broth (Oxoid), tryptic soy broth (TSB) or RPMI-1640 (Gibco) (362) medium with vigorous shaking (200 rpm). Where indicated, BHI broth, TSB

and RPMI-1640 broth were supplemented with chloramphenicol (5-10 µg/ml), tetracycline (5-10 µg/ml) or erythromycin (5-10 µg/ml).

### 2.4 Genetic Techniques

Genomic and plasmid DNA were prepared using Wizard genomic DNA and plasmid purification kits (Promega). Prior to DNA extraction, cells were pre-treated with 2 µl of 1 mg/ml lysostaphin (Ambi Products, New York) to facilitate subsequent lysis. Restriction enzymes (Roche, UK and New England Biolabs, MA) were used according to the manufacturer's instructions. The enzyme buffers were supplied in a 10X concentration and used at a final 1X concentration. Restriction digests were performed at a volume ranging from 20 µl – 50 µl. Oligonucleotide primers used for PCR were supplied by Sigma and are listed in Table 2.4. Primers were supplied in a dried form and the volume of DNase-free water in which to resuspend the primers was indicated. Once resuspended, primers were diluted to a working concentration of 25 pmol/µl. 0.5 µl of this working concentration solution was added to a 25 µl PCR reaction to give a final concentration of 0.5 pmol/µl per reaction. PCR analysis was carried out using GoTaq DNA polymerase (Promega) by following the manufacturer's instructions. PCR reactions were carried out with 1 µl of DNA per reaction using the following programme:

1. Initial denaturation at 98$^{o}$C for 30sec,
2. 30 cycles of –
    - Denaturation at 98$^{o}$C for 30 seconds,
    - Annealing for 30 seconds,
    - Extension at 72$^{o}$C for 1 min per kb of pcr product.
3. Final extension at 72$^{o}$C for 10 minutes.

**Table 2.4. PCR primers used in this study**

| Target gene | Primer Name | Primer Sequence (5'-3') |
|---|---|---|
| *atl* | Atl_Big_Fwd | AAGCAGCTGAGACGACACAA |
| | Atl_Big_Rev | GTGTCCCAACCAGCTTGTTT |
| *atlR* | AtlR_Fwd | TCGCGAAATAACCAGATATAAACA |
| | AtlR_Rev | AGATGGAATCCTGCACATCC |
| *fnbpA* | FnBPA_USA300_Fwd | TGGCGACAGGTGAAGTTTTA |
| | FnBPA_USA300_Rev | ATAGCGAAGCAGGTCACGTT |
| *fnbpB* | FnBPB_USA300_Fwd | TGGTCAAGTTATGGCGACAG |
| | FnBPB_USA300_Rev | GTGCAGAAGGTCATGCAGAA |
| *icaADBC* | icaAB_USA300_Fwd | TGTTGGATGTTGGTTCCAGA |
| | icaAB_USA300_Rev | GAAACTATGGGCATTTTCGC |
| *srtA* | srtAerm_USA300_Fwd | TGACAATGCCTGCAACTAGC |
| | srtAerm_USA300_Rev | TGCTGTCGCTCCAAGTAATG |
| *esp* | EspFor1 | TGGCTAATGGTTTGTCACCA |
| | EspRev1 | CATTCCTCACTTGGCACAGA |
| *esp* | EspFor2 | TGGCTAATGGTTTGTCACCA |
| | EspRev2 | GGCAAATTTGTGGGTCAAGA |

## 2.6 RNA extraction

Bacteria cells were grown to the desired density, washed in RNA Later (Ambion), pelleted and immediately stored at –20°C to ensure maintenance of RNA integrity prior to purification. RNA extraction was carried out using the RNeasy Mini Kit (Qiagen) by following the manufacturer's instructions with the following adaptions. Cells in RNA Later were washed in Tris buffer at pH 8.5 after thawing. Cells were lysed in 50 mM EDTA with 4 µl of 1 mg/ml lysostaphin at 37°C for 20 minutes. Purified RNA was eluted in 50 µl of RNA Secure (Ambion). Twenty microliters of RNA was treated with Turbo DNaseI (Ambion) for 20 minutes at 37°C. After deactivation of DNaseI, 2 µl purified RNA was run on a 1% agarose gel to assess efficiency of the prep. Purified RNA was converted to cDNA using the Transcriptor First Strand cDNA Synthesis Kit (Roche) following the manufacturer's instructions.

## 2.5 RT-PCR

RT-PCR was performed using the LightCycler 480 instrument (Roche) and the LightCycler 480 Sybr Green Kit (Roche) following the manufacturer's instructions. The following programme was used for each RT-PCR reaction: denaturation was conducted at 95$^{o}$C for 5 minutes and followed by 45 cycles of 95$^{o}$C for 10 seconds, 58$^{o}$C for 20 seconds and 72 $^{o}$C for 20 seconds at which point the readings were taken. Melt curve analysis was conducted at 95$^{o}$C for 5 seconds followed by 65$^{o}$C for one minute up to 97$^{o}$C at a ramp rate of 0.11c/sec with five readings taken for every degree of temperature increase. The *gyrB* gene was used as an internal standard for all reactions. Each experiment was performed three times and average data and standard deviations are presented. The RT-PCR primers used in this study are listed in table 2.5.

**Table 2.5. RT-PCR primers used in this study**

| Target gene | Primer Name | Primer Sequence (5'-3') |
|---|---|---|
| *atl* | Atl_Fwd | AATGGTGTCGCACAAATCAA |
| | Atl_Rev | CCACATCGCCTTCTTTAACC |
| *hla* | Hla_Fwd | TGGCCTTCAGCATTTAAGGT |
| | Hla_Rev | CAATCAAACCGCCAATTTTT |
| *fmt* | Fmt_Fwd | AATGTCGGTACGATGCATGA |
| | Fmt_Rev | ACTGGCCATGGTGATAATCC |
| *lytS* | LytS_Fwd | TGCATTTGTTGGGAGAAACA |
| | LytS_Rev | AAAAGTGGTACCGCTCGATG |
| *lytR* | LytR_Fwd | ACTGCACATGACCAATACGC |
| | LytR_Rev | CGCACGCACTTTATTGACTG |
| *murZ* | MurZ_Fwd | GGGTTACCGCAAATCTCTGA |
| | MurZ_Rev | ATCCTCCCGGTAAACCAATC |
| *walK* | WalK_Fwd | AGCGTCGTGAATTTGTTGCC |
| | WalK_Rev | TCGTTCTGTTTCTTCACGGGT |
| *walR* | WalR_Fwd | AGTATGTCGTGAAGTGCGCA |
| | WalR_Rev | CAGTGTCTTGTGCTGGTTGTG |
| *gyrB* | GyrB_Fwd | CCAGGTAAATTAGCCGATTGC |
| | GyrB_Rev | AAATCGCCTGCGTTCTAGAG |

## 2.6 Bacteriophage transduction

Phage 80α was used during all bacterial phage transductions carried out in this study. Transductions were carried out in three stages.

Propagation: For the propagation of phage in their corresponding propagating strain, 1 ml of tryptic soya broth with TSB 5 X $10^{-3}$ M $CaCl_2$ was used to resuspend propagating strains grown for 24 hours at 37ºC on a BHI agar slant. Phage 80α solution was diluted to $10^{-9}$ in TSB 5 X $10^{-3}$ M $CaCl_2$ broth. Selected dilutions of phage were then added to 50 µl of resuspended propagating cells and 10 ml of cooled 0.5% agar was added to the cells and phage solution. This was inverted three times and poured onto a TSB 5 X $10^{-3}$ M $CaCl_2$ agar plate. Plates were incubated at 37ºC and were examined for plaque forming units (PFU) after 24 hours. Propagation was continued until a desired PFU/ml of $10^{10}$ or higher was achieved to ensure efficient transductions.

Harvest: After each propagation, phage with the desired mutation were harvested from the 0.5% agar. Soft agar harvested from the plates was resuspended in either 2 ml of TSB 5 X $10^{-3}$ M $CaCl_2$ broth or lysate solution already containing the desired mutation from a previous propagation and vortexed vigorously. The agar was then centrifuged and the lysate solution produced was filter sterilised with 0.22 µm filters (Millipore) and stored at -4°C until use.

Transduction: Recipient cells were grown for 24 hours at 37ºC on a BHI agar slant and resuspended in 1ml of TSB 5 X $10^{-3}$ M $CaCl_2$ broth. Resuspended cells were then divided between a 'transduction' microcentrifuge tube and a 'control' microcentrifuge tube. In the 'transduction' tube, 1 ml of TSB 5 X $10^{-3}$ M $CaCl_2$ broth, 0.5 ml of cells and 0.5 ml of phage lysate was added. The 'control' tube received 0.75 ml of TSB 5 X $10^{-3}$ M $CaCl_2$ and 0.25 ml of cells and no lysate solution. The two tubes were incubated for 20 minutes at 37ºC and 200rpm. After this period, 1 ml of solution from the 'transduction' tube was transferred to a second microcentrifuge tube marked 'transduction two'. One millilitre of ice-cold 0.02 M sodium citrate solution was added to the 'control' tube and each 'transduction' tube. Tubes were centrifuged for 1 minute at 14,000 rpm

and the supernatants discarded. The pellets were resuspended in 1 ml of ice-cold 0.02 M sodium citrate and plated onto TSB agar plates containing 0.5 g/L sodium citrate and 5-10 µg/ml of the relevant antibiotic. The plates were left for 24-48 hours at 37ºC and any candidates that grew were confirmed by PCR analysis.

### 2.7 Bacterial transformation

Transformation of *S. aureus* strains was carried out by electroporation with the MicroPulser (BioRad, CA). Twenty millilitre cultures of *S. aureus* were grown at 37ºC and 200 rpm to approximatey $A_{600}$ = 0.2. The cultures were centrifuged for 10 minutes and washed twice in 10 ml of ice-cold sterile water. The resulting pellets were then resuspended in 100 µl of plasmid DNA and the mixture was subjected to one pulse of 1.8 kV for 2.5 msec on the MicroPulser (BioRad, CA). The electroporation mixture was then resuspended in 1 ml of BHI 0.5 M sucrose solution and incubated at 37ºC shaking at 200 rpm for 2-4 hours. Transformed cells were plated out on BHI agar plates containing 0.5 M sucrose and supplemented with inhibitory concentrations of the desired antibiotic (5–10 µg/ml). Plates were left at 37ºC for 24-48 hours and colonies that grew were selected for plasmid prep and restriction digest analysis.

### 2.9 Static biofilm assays

Static biofilm assays were carried out based on the procedure described by G. D. Christensen, *et al*. (363) with the following modifications described by E. Waters, *et al*. (364). Ninety-six-well tissue culture treated plates (Nunc$\Delta^{TM}$, Denmark) and 96-well untreated polystyrene plates (Sarstedt, USA) were used for the semi-quantitative determinations of biofilm formation under static conditions. Cultures of bacteria were grown for 24 hours in 5 ml of BHI broth at 37ºC. These overnight cultures were diluted 1:200 into freshly prepared media (BHI, BHI 4% NaCl or BHI 1% glucose). The samples were vortexed for five seconds and each well of a 96-well plate was inoculated with 100 µl of this solution. Microtitre plates were incubated at 37ºC for 24 hours. After 24 hours plates were dunk washed three times in water and left at 65ºC for one hour to allow any remaining

biofilms to fix to the bottom of the wells. Plates were then stained with 0.4% crystal violet for five minutes and plates were washed three times in water to remove any unbound crystal violet. Crystal violet stained biofilms were solubilised with 5% acetic acid and absorbance values were read at $A_{490}$ using the Multiskan plate reader (Flow Laboratories, UK). Each experiment was carried out in triplicate and at least eight wells were inoculated per strain during each experiment. Average absorbance values and standard deviations for each experiment were calculated using Microsoft Excel (2010). Strains were regarded as biofilm positive if they had an average $A_{490}$ of more than 0.17.

### 2.8 Biofilm inhibition and dispersal assays

To examine the components of biofilm matrices biofilm assays were set up as described previously and BHI, BHI 4% NaCl and BHI 1% glucose were supplemented, where indicated, with Deoxyribonuclease I (DNaseI; Sigma) at 0.5 mg/ml, proteinase K (ProK; Sigma) at 0.1 mg/ml and polyanethole sodium sulfanate (PAS; Sigma) at 0.5 mg/ml. Components of mature biofilms (24 hours old) were examined by removal of the growth media from the wells of the microtitre plate and replaced where indicated with 100 µl of DNaseI at 0.5 mg/ml, 100 µl of ProK at 0.1 mg/ml and 100 µl of 10 mM sodium metaperiodate (SM; Fluka). Treatments of biofilms were performed at 37$^{o}$C for 2 hours. After incubation, plates were washed and stained as described above. Biofilm inhibition assays were carried out with polyclonal Atl antibodies, a kind gift from Prof Simon Foster. Antibodies were added as indicated to BHI, BHI 4% NaCl or BHI 1% glucose at a concentration of 1:100 with cells diluted 1:200 in the media. After set-up on the microtitre plate as described above, plates were incubated for one hour at 4$^{o}$C prior to incubation at 37$^{o}$C for 24 hours. After incubation plates were washed and stained as described above.

## 2.9 Preparation of platelet-poor plasma (PPP)

Platelet-poor plasma (PPP) was prepared by drawing human blood into a syringe containing heparin at 16 I.E. per ml. PPP was obtained by centrifugation of the whole blood at 500 × *g* (ca. 2000 rpm) for 10 minutes. The resulting supernatant was designated PPP, which was immediately transferred into clean polypropylene tubes using a Pasteur pipette and maintained at 2-8°C while handling. If the PPP was not used immediately it was aliquoted and stored at –20°C, avoiding freeze-thaw cycles. Thawing was performed in a water bath at 37ºC. Any clots that formed during the thawing process were removed by filter-sterilising the plasma with a 0.22 µm filter (Millipore) before use.

## 2.10 Plasma-coated biofilm assays

Plasma (PPP)-coated biofilm assays were performed as described above with the following modifications. Prior to inoculation with bacterial solutions, the wells of microtitre plates were coated for 2 hours at 37˚C with100 µl of 20% human PPP (v/v) diluted in 50 mM carbonate buffer, pH 9.6. After incubation, excess plasma was removed before inoculating the wells with bacterial suspensions. To form biofilm in RPMI-1640, overnight cultures of *S. aureus* grown in RPMI-1640 were diluted 1:1 (v/v) in fresh RPMI-1640 and inoculated in microtitre wells at 100 µl per well allowing attachment for 1 hour at 37ºC. Unattached bacteria were then removed and replaced with 100 µl of fresh RPMI-1640 per well. To form biofilm in rich media, overnight cultures of *S. aureus* were diluted 1:200 into either TSB or BHI and inoculated into wells pre-coated with human plasma. Bacteria were incubated in the wells for 1 hour at 37ºC allowing attachment. Excess bacteria were then replaced with 100 µl of fresh media per well. All biofilms were grown for 24 hours at 37ºC and washed and stained as described above. For all experiments, control wells with plasma coating and no bacterial solutions were set up and the absorbance values for these wells were subtracted from the absorbance values for the wells with bacterial samples.

## 2.11 Biofilm formation under shear-flow conditions in the BioFlux 1000Z


**Fig. 2.1. Photograph and illustration of the 48-well plate used in the BioFlux 1000Z microfluidic system.** Illustration demonstrates the input (left side, labelled "I") and output (right side, labelled "O") wells in each of the columns with the microfluidic channels (labelled 1-24) connecting the input and output wells. Images adapted from the BioFlux website http://fluxionbio.com/bioflux/.

The BioFlux 1000z microfluidic system (Fluxion Biosciences Inc., San Francisco, CA) was used to assess biofilm formation under shear flow conditions using a modification of the protocol of D. Moormeier and K. Bayles (365). To grow biofilms in the BioFlux system, 200 µl of BHI 1% glucose was added to the output wells of a 48-well plate and the channels were primed for 5 minutes at 5.0 dynes/cm$^2$. After priming, the media was aspirated from the output wells and replaced with a 50 µl BHI 1% glucose suspension of cells grown to early exponential growth phase and adjusted to an $A_{600}$ = 0.8. A further 50 µl of BHI 1% glucose was added to the input wells and the channels were seeded by pumping from the output wells to the

input wells for 3-5 seconds at a speed of 3 dynes/cm$^2$. Bacterial cells were allowed to attach to the surface of the plate for 1 hour at 37°C. Excess inoculum solution was aspirated from the output wells and a further 1.2 ml of BHI 1% glucose was added to the input wells. The flow rate was set where indicated at 0.6 dyne/cm$^2$ for 18 hours (equivalent to 64 µl/hour) or at 0.4 dyne/cm$^2$ for 24 hours (equivalent to 42 µl/hour). Brightfield images were captured every 5 minutes at 10X magnification. A total of 217 images were captured over 18 hours and 289 images were captured over 24 hours. The gain and exposure settings remained constant over the 18/24 hour period for all images.

### 2.12 Biofilm formation on human plasma under shear-flow conditions using the BioFlux 1000Z

The BioFlux 1000z microfluidic system (Fluxion Biosciences Inc., San Francisco, CA) was used to assess biofilm formation under shear flow conditions. Each channel of a 48-well plate was coated from the output well with 50 µl of platelet-poor human plasma for 30 minutes at 37ºC. Inoculation was repeated once for a total of one hour of coating at 37ºC. Overnight cultures of *S. aureus* grown in RPMI-1640 were diluted 1:1 in fresh RPMI-1640. Excess plasma was removed from the output and input wells of the plate after coating. RPMI-1640 was used to prime the plasma-coated channels by adding 200 µl of media to the output wells and priming for 5 minutes at 5.0 dynes/cm$^2$ at 37ºC. Excess priming media was aspirated from the output wells and replaced with 50 µl of *S. aureus* diluted 1:1 in fresh RPMI-1640. A further 50 µl of fresh RPMI-1640 was added to the input wells and the channels were seeded with bacteria by pumping from the output wells to the input wells for 3-5 seconds at a speed of 3 dynes/cm$^2$. Bacterial cells were allowed to attach to the plasma-coated surface of the plate for one hour at 37°C. Excess inoculum solution was aspirated from the output wells and 1.2 ml of fresh RPMI-1640 was added to the input wells. The flow rate was set at 0.6 dynes/cm$^2$ for 18 hours (64 µl/hour) and brightfield images were captured every 5 minutes at 10X magnification. A total of 217 images were captured and the gain and exposure settings remained constant over the 18 hour period for all images.

## 2.13 Protein purification and Western blot analysis

Western blot analysis was carried out with monoclonal mouse *Staphylococcus* alpha haemolysin (Hla) antibody (Sunny Labs), polyclonal anti-AM serum or anti-GL serum (kind gift from Prof Simon Foster). Cells were prepared for Western blot analysis by the following procedure. Cultures were centrifuged for 10 minutes at 7,800 rpm. Pellets obtained were resuspended in the same volume of PBS and samples were centrifuged again. Pellets were resuspended in 1ml of PBS, the $A_{600}$ was measured and cultures were readjusted in PBS to an $A_{600}$ = 10. Readjusted cultures were centrifuged at 14,000 rpm for 1 minute. Different extraction buffers were used for covalently and non-covalently bound proteins.

Covalently bound proteins were prepared with the following method: Pellets were resuspended in 200 µl of an extraction buffer containing 30% raffinose with 200 µl of Tris/MgCl2 stock solution/ml, 50 µl of protease inhibitor (Roche) and 10 µl of 10 mg/ml lysostaphin. Pellets were incubated in 200 µl of this solution for 10 mins at 37$^{o}$C with occasional mixing.

Non-covalently bound proteins were prepared with the following method: Pellets were resuspended in 200 µl of a 1% SDS extraction buffer solution. Samples were incubated at 95$^{o}$C for 5mins and 50 µl of protease inhibitor per ml (Roche) was added to each sample.

After addition of the appropriate extraction buffer and incubation, samples were centrifuged again for 10 minutes at 14,000 rpm and 50 µl of the supernatant was transferred to a clean microcentrifuge tube.

Total protein samples were prepared by pelleting cultures and resuspending pellets in 500 µl of distilled water with 1 µl of DNaseI, 5 µl of lysostaphin and 50 µl of 10% SDS and incubating at 37$^{o}$C for 30 minutes. After incubation, samples were centrifuged at maximum speed for 15 minutes and the resulting supernatant was retained for Western blot analysis.

Secreted proteins were purified by trichloroacetic acid (TCA; Sigma) purification. One millilitre of supernatant was filter sterilised and incubated at 4$^{o}$C in TCA at a ratio of 1:4 to supernatant for 24 hours. After this period,

cells were centrifuged at maximum speed for 10 minutes and pellets were washed three times in ice-cold acetone. Pellets were dried at 50$^{o}$C for 15 minutes and resuspended in 5 µl of Tris-HCl at pH 8.8 to which 35 µl of 2X SDS-loading buffer was added.

After preparation of samples, protein concentration was assessed using the BCA protein assay kit (Pierce; Thermo) and by following the manufacturer's instructions. Once protein concentration was quantified, adjusted volumes of protein solution were added to 2X loading buffer (Fisher Scientific) at a 1:1 ratio and boiled at 95$^{o}$C for 5 minutes. Protein samples were then centrifuged briefly before loading onto a 10% SDS gel (Amersham). Gels were run for one hour at 60 v. Transfer was done using the XCell Sure Lock semi-dry transfer tank (Invitrogen) or the TE 70 semi-dry transfer unit (Amersham) and nitrocellulose membranes (Thermo Scientific). Transfer was carried out at 20 v or 400 mA for one hour. Membranes were then blocked in 10% skimmed milk (Marvel) for one hour at room temperature or overnight at 4$^{o}$C. After blocking, membranes were washed three times in phosphate buffer saline (PBS) and incubated at room temperature for an hour or overnight at 4$^{o}$C with primary antibody in PBS solution with 100 µl of 10% tween-20 (Sigma) at 1:1500 concentration for Atl antibodies and 1:500 for Hla antibody. Membranes were washed three times for 10 minutes in PBS and membranes were incubated with the secondary antibody, horse-radish peroxidase-conjugated protein A peroxidase diluted 1:200 in PBS with 100 µl of 10% tween-20 at room temperature for half an hour. Membranes were washed a further three times with PBS and developed using Lumi-Light Western Blotting developer solution (Roche) and imaged on either the Fluro Chem® FC2 imager (Alpha Innotech) or the Gbox imager (Syngene, Mason Technology).

## 2.14 Triton X-100 induced autolytic assay

Triton X-100 induced autolytic assays were performed essentially as described previously with the following modifications (57, 366). Cultures of *S. aureus* were subcultured into 20 ml of fresh BHI broth and incubated at 37ºC and 200 rpm until an approximate $A_{600}$ of one was obtained. Cultures were centrifuged for ten minutes at maximum speed. Pellets were washed in the same volume of PBS and centrifuged for a further ten minutes. Pellets were then resuspended in 1 ml of fresh PBS and the $A_{600}$ was adjusted to one in 1 ml of PBS containing 0.1% Triton X-100 (Sigma) in a cuvette. Cuvettes were covered in parafilm and samples were vortexed for ten seconds and the $A_{600}$ of the culture at time zero was recorded. Cultures were then incubated at 37ºC and 200 rpm for four hours and the $A_{600}$ was measured every fifteen minutes. Triton X-100 induced autolysis was presented as a percentage of the initial $A_{600}$ at time zero. Each experiment was repeated three times.

## 2.15 Bacteriolytic assay

Assessment of lytic activity of culture supernatants were performed essentially as described previously (367) with the following modifications. Cultures of *S. aureus* were subcultured into 10 ml of fresh BHI broth and incubated at 37ºC and 200 rpm until an approximate $A_{600}$ of one was obtained. Cultures were filter-sterilised after incubation with a 0.22 µm filter (Millipore). Nine hundred microlitres of filter-sterilised supernatant was added to a cuvette. To this, 100 µl of heat-killed RN4220 cells were added to give an approximate $A_{600}$ of one. Initial $A_{600}$ of the samples was recorded and samples were incubated for four hours at 30ºC and 200 rpm and $A_{600}$ values were recorded every 30 minutes. Filter-sterilised BHI broth was used as a control. Bacteriolytic activity is expressed as % lysis relative to initial $A_{600}$ ($A_{600}i$), where lysis at time $t$ = [$A_{600}i$ – $A_{600}$ at time $t$)/ $A_{600}i$]. Each experiment was repeated three times.

## 2.16 Skimmed milk agar

Protease activity of cultures was assessed by growth on 2% skimmed milk agar plates. Skimmed milk agar was made by autoclaving skimmed milk solutions (Sigma) separately to BHI agar and then mixing to a final concentration of 2% once cooled to 50ºC. The $A_{600}$ of cell suspensions was normalised prior to inoculation of plates. Plates were incubated for 24 hours at 37ºC and protease activity was assessed by zones of proteolysis on the agar. Each experiment was repeated three times.

## 2.17 Blood agar

Haemolysis activity was assessed by growth of cultures on either horse or sheep blood agar. Blood agar was prepared by autoclaving BHI agar and adding either sheep or horse blood to a final concentration of 5% once the agar was cooled to 40ºC. Sheep blood was utilised to assess beta haemolysis and plates were incubated overnight at 37ºC and then for a further 24 hours at 4ºC. Alpha haemolysis was assessed using horse blood agar incubated at 37ºC for 24 hours and delta haemolysis was assessed by growing cells on a lawn of heat-killed RN4200 cells spread on a sheep blood agar plate and incubated at 37ºC for 24 hours. Haemolysis activity was assessed by zones of haemolysis on the agar. Each experiment was repeated three times.

## 2.18 Haemolysis assay

Haemolysis activity of culture supernatants was assessed by using a 1% horse or sheep's blood solution. Cultures were grown for 20 hours, one ml of cells was pelleted by centrifugation and 250 µl of supernatant was added to 250 µl of PBS and 500 µl of 1% blood in a sterile microcentrifuge tube. Mixtures were incubated statically at 37ºC for two hours, after which samples were centrifuged gently at 450 rpm and 4ºC for 20 minutes. Resulting supernatants were transferred to cuvettes and the $A_{450}$ was recorded. A solution of 450 µl PBS, 50 µl 10% SDS and 500 µl of 1% blood was used as a positive control and a solution of 500 µl PBS and 500 µl 1% blood served as a negative control. Each experiment was repeated three times.

## 2.19 Growth rate assay

A 100 ml solution of BHI was inoculated with 100 µl of overnight culture. Flasks were incubated at 37ºC and 200 rpm for 11 hours. The $A_{600}$ of growing cultures was recorded every 60 minutes and each experiment was performed in duplicate.

## 2.20 Ethics statement

Animal experiments were carried out in strict accordance with the recommendations in the Guide for the Care and Use of Laboratory Animals of the National Institutes of Health. All protocols were reviewed and approved by the Institutional Animal Care and Use Committee at the University of Nebraska Medical Centre. All mandatory training prior to experimental set-up was undertaken. All surgery was performed under anaesthesia and all efforts were made to minimise suffering.

## 2.21 Murine model of device-related infection

A murine model of device-related infections was used to assess the contribution of *atl* to virulence as described previously (164, 166, 316, 344). The flanks of anaesthetised 6-week old male C57BL/6 mice were shaved, and the skin sterilised with povidone-iodine. Using aseptic technique, a one cm segment of 14-gauge polyethylene intravenous catheter was implanted into the subcutaneous space and closed with Vetbond (3M, Minneapolis, MN). Once the wound was sealed, $5x10^5$ *S. aureus* were injected into the catheter lumen. A minimum of eight mice were used per strain of *S. aureus* being tested. Experimental time course ranged from three to seven days. Animals were monitored daily and their weights were recorded as an indication of health status and any animals that showed excessive loss of body weight (i.e. 20% or more) were euthanized immediately. Other indices for evaluating whether a moribund state had been achieved and euthanasia was required before experimental completion included: extreme lethargy, failure to demonstrate typical avoidance behaviour when handled, ulceration of the infection site through the skin and/or laboured breathing. Animals were euthanized at the end of the experiment time course or before (if

required) by carbon dioxide inhalation followed by cervical dislocation. The catheters, surrounding peri-catheter tissue, kidney, liver and spleen were all retrieved from the animals for assessment. Catheters were aseptically removed, placed in sterile microcentrifuge tubes with 1 ml of PBS and protease inhibitor, vortexed for one minute, sonicated in a water bath at approximately 33$^{o}$C, sonicated for a further ten seconds on ice with a probe and quantitatively cultured on TSA. All organs were aseptically harvested and weighed in pre-weighed polyethylene tubes. After recording weights, one ml of PBS and protease inhibitor solution was added to each organ which was homogenised and sonicated in a water bath at approximately 33$^{o}$C. Organ solutions were then quantitatively cultured on TSA. Results were presented as colony forming units (CFU) per one cm catheter segment or per gram of tissue/organ.

### 2.22 Cytokine analysis

Cytokine analysis of the peri-catheter tissue from the seven day infection course experiment was conducted on samples from the wild type strain JE2 and the isogenic *atl* mutant. The Proteome Profiler™ Array Mouse Cytokine Array Panel A (R&D Systems) was used to assess cytokine response in the tissue by following the manufacturer's instructions with concentrations of tissue samples normalised prior to experimental set-up.

### 2.23 Statistical analysis

Two-tailed, two-sample equal variance Student's t-Tests (Microsoft Excel 2010) were used to determine statistically significant differences in assays performed during this study. Statistical significance is denoted as NS for $P > 0.05$, as * for $P \leq 0.05$, as ** for $P \leq 0.01$ and as *** for $P \leq 0.001$. For the animal experiments descriptive statistic values (including mean and standard deviation) were calculated for each strain at each location i.e. the catheter, peri-catheter tissue, liver, kidney and spleen. Log10 transformation of CFU data from catheters and organs was used to ensure normal distribution. One-way ANOVA analysis was used to compare CFU from the catheters and organs of all strains and statistically significant differences relative to CFUs of the parent JE2 strain are reported.

# Chapter 3:

# Contribution of Atl to *S. aureus in vitro* and *in vivo* biofilm formation and virulence

## 3.1 Introduction

Previous research in our laboratory has revealed an important role for the major autolysin, Atl, for both MRSA and MSSA *in vitro* biofilm formation (38). As described in chapter one, MSSA strains commonly produce a biofilm dependent on PIA production whereas MRSA strains produce biofilm independent of PIA (254). MRSA strains require Atl to mediate primary attachment to hydrophilic and hydrophobic polystyrene and the LPXTG-anchored FnBPs to promote the accumulation phase of biofilm formation (38, 90, 201). While MSSA strains predominantly require PIA for biofilm formation, it was found that surface hydrophobicity can influence the biofilm phenotype of the MSSA strain 8325-4 (38). When grown in NaCl-supplemented growth medium on hydrophilic polystyrene 8325-4 requires the *ica* operon for biofilm formation and forms biofilm independent of Atl (38). In contrast, when grown in BHI 1% glucose media and on a hydrophobic polystyrene surface, 8325-4 produces a biofilm dependent on both PIA and Atl. Therefore, Atl appears to have a role in both MRSA and MSSA biofilm formation that is influenced by surface hydrophobicity. In this chapter work was undertaken to further define the role for Atl in MSSA biofilm formation. Experiments were also undertaken to investigate the therapeutic potential of antiserum to Atl in the inhibition of Atl-dependent biofilm formation by MRSA and MSSA.

Other factors beyond surface hydrophobicity influence Atl-mediated biofilm formation and previous work from our laboratory has revealed a role for the negative regulator AtlR in Atl-mediated biofilm formation by the HA-MRSA strain BH1CC (38). Here experiments were carried out to further elucidate the role of AtlR in Atl-dependent biofilm formation and virulence of clinically relevant MRSA strains.

Atl mediates biofilm formation through tightly regulated autolysis and the release of eDNA which forms a major component of the biofilm matrix (38, 57). Atl consists of two catalytically active proteins which serve different roles in peptidoglycan synthesis. The amidase (AM) and glucosaminidase (GL) regions of Atl become enzymatically activated after proteolytic cleavage of the pro-protein (Fig. 1.2). It has been shown that both regions

need to be enzymatically active for biofilm formation by the clinical MSSA isolate UAMS-1 (57). In this chapter, investigations were undertaken to assess the contribution of the AM and GL regions of Atl to MRSA lytic activity and Atl-dependent biofilm formation.

Beyond contributing to biofilm formation, Atl is also required for the regulated extracellular release of cytoplasmic proteins including some virulence factors such as the alpha toxin, Hla (368). To this end, the contribution of Atl and the AM and GL enzymes to virulence and toxin production of clinically relevant MRSA strains was assessed. A *S. epidermidis* Δ*atlE* mutant was attenuated in a rat central venous catheter model (66), and here we investigated if Atl and, specifically, the AM and GL regions contribute to *S. aureus* virulence in a mouse model of device-related infection.

## 3.2 Results

### 3.2.1 Comparison of the influence of surface hydrophobicity on MRSA and MSSA biofilm formation

The MSSA strain 8325-4 switches from producing a PIA-dependent biofilm on hydrophilic polystyrene to a PIA and Atl-dependent biofilm when grown on hydrophobic polystyrene (38). Biofilm formation by RN4220 and its isogenic *atl* and *icaADBC* mutants was assessed on both hydrophilic and hydrophobic polystyrene. As controls, biofilm formation by strains 8325-4 and BH1CC and their isogenic *atl* and *icaADBC* mutants were assessed in the same experiments. In agreement with the findings of Houston *et al* (2011) (38), the biofilm phenotype exhibited by RN4220, a chemically mutagenized, restriction-deficient derivate of 8325-4, is similar to that produced by the 8325-4 (Fig. 3.1). RN4220 produced a glucose-induced biofilm on hydrophobic polystyrene that requires expression of both the *ica* operon and Atl (Fig. 3.1B). Similar to 8325-4, RN4220 produces a PIA-dependent biofilm on hydrophilic polystyrene in which Atl plays a less important role (Fig. 3.1A). BH1CC produced an Atl-dependent biofilm on both hydrophilic and hydrophobic as observed previously (Fig. 3.1). These data support the idea that Atl can mediate both MRSA and MSSA biofilm formation in a manner dependent on surface hydrophobicity.

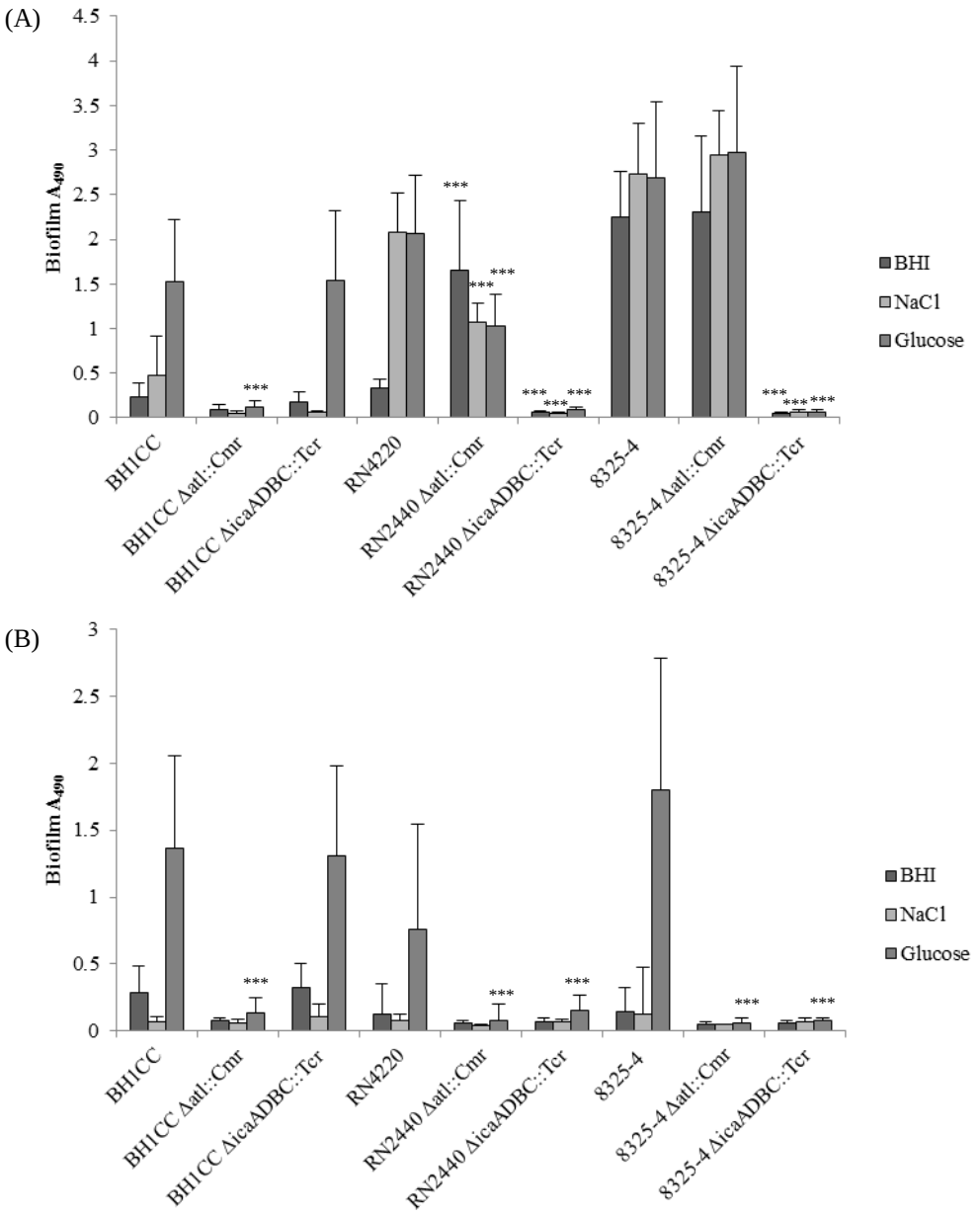


**Fig. 3.1. Contribution of Atl to MRSA and MSSA biofilm formation.** Biofilm phenotypes of strains BH1CC, BH1CC Δ*atl*::Cm$^r$, BH1CC Δ*icaADBC*::Tc$^r$, RN4220, RN4220 Δ*atl*::Cm$^r$, RN4220 Δ*icaADBC*::Tc$^r$, 8325-4, 8325-4 Δ*atl*::Cm$^r$ and 8325-4 Δ*icaADBC*::Tc$^r$ grown for 24 hrs at 37°C in BHI, BHI 4% NaCl and BHI 1% glucose on (A) hydrophilic 96-well polystyrene plates and (B) hydrophobic 96-well polystyrene plates. Results of at least three independent experiments are shown. Comparisons made between wild type strains and isogenic *atl* and *icaADBC* mutants. Standard deviations are indicated. Statistical significance denoted as NS for $P > 0.05$, as * for $P \leq 0.05$, as ** for $P \leq 0.01$ and as *** for $P \leq 0.001$.

### 3.2.2 Contribution of Atl to MSSA biofilm formation and lytic activity

SigB has been shown to influence Atl-mediated primary attachment in the MRSA strain BH1CC in part through reduced *atl* transcription (38). Therefore, to further investigate the contribution of Atl to MSSA biofilm formation on hydrophobic polystyrene, SH1000 and its isogenic *atl* mutant were assessed for biofilm formation under the same conditions employed for the experiments in figure 3.1. SH1000 is an *rsbU* repaired derivative of 8325-4 (262). SH1000 exhibited a similar biofilm phenotype to that of 8325-4 and RN4220 (Fig. 3.1 and 3.2). SH1000 did not produce biofilm dependent on Atl when grown in BHI 1% glucose on hydrophilic plates but did require Atl for optimal glucose-induced biofilm formation on hydrophobic plates ($P \leq 0.001$, Fig. 3.2). The biofilm defect of SH1000 Δ*atl* carrying the empty pLI50-*tet* vector was complemented by introducing pLI50-*tet* expressing the *atl* gene (p*atl*) into SH1000 Δ*atl* (Fig. 3.2B).

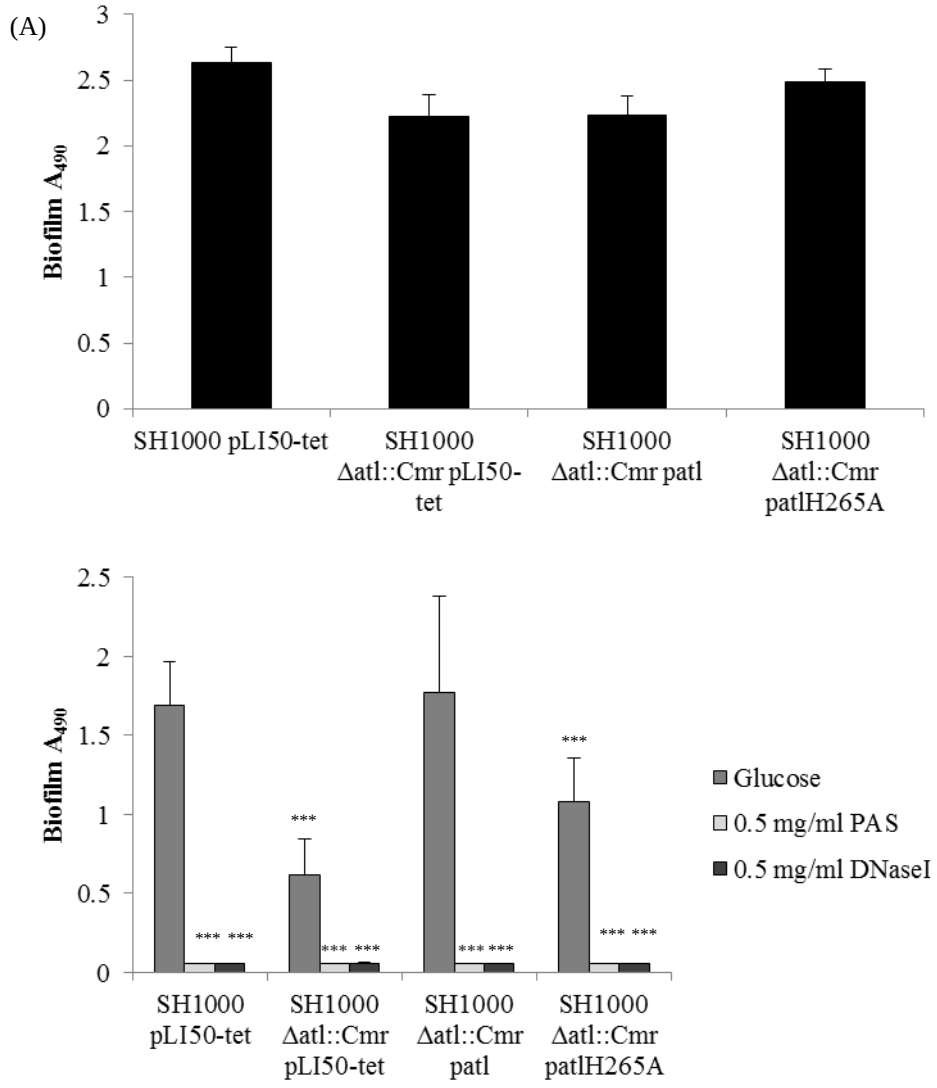


**Fig. 3.2. Contribution of Atl to SH1000 biofilm formation.** Biofilm phenotypes of strains SH1000 pLI50-*tet*, SH1000 Δ*atl*::em$^r$ pLI50-*tet*, SH1000 Δ*atl*::em$^r$ p*atl*, , SH1000 p*atl* H265A grown for 24 hrs at 37°C in (A) BHI 1% glucose on hydrophilic 96-well polystyrene plates and (B) on hydrophobic 96-well polystyrene plates in BHI 1% glucose, BHI 1% glucose supplemented with 0.5 mg/ml PAS and BHI 1% glucose supplemented with 0.5 mg/ml DNaseI. Results of at least three independent experiments are shown. Comparisons made between: 1) SH1000 pLI50-*tet* and untreated controls and 2) untreated controls and treatments. Standard deviations are indicated. Statistical significance denoted as NS for $P > 0.05$, as * for $P \leq 0.05$, as ** for $P \leq 0.01$ and as *** for $P \leq 0.001$.

To confirm a role for Atl-mediated lytic activity and eDNA release in the SH1000 biofilm phenotype, SH1000 glucose-induced biofilms grown on hydrophobic plates were treated with PAS and DNaseI as described in chapter 2. Both PAS, which inhibits autolytic activity without impairing growth, and DNaseI, which degrades eDNA, impaired SH1000 biofilm formation on hydrophobic polystyrene ($P \leq 0.001$) (Fig. 3.2B). To determine if the activity of the AM region was required for MSSA biofilm

formation the plasmid p*atl*H265A was introduced into the SH1000 Δ*atl* mutant and the biofilm forming capacity of this strain was assessed. The histidine residue at position 256 is located within the active site of the AM region of Atl and coordinates zinc ions to the active site for efficient activity (38). The SH1000 Δ*atl* mutant carrying the plasmid expressing the inactive AM enzyme exhibited significantly reduced glucose-induced biofilm levels on hydrophobic surfaces ($P \leq 0.001$) (Fig. 3.2B). In contrast, the active site mutation in the AM region of Atl did not contribute to glucose-induced biofilm formation by SH1000 on hydrophilic polystyrene, further demonstrating that this biofilm phenotype does not require Atl-dependent activity (Fig. 3.2A). While levels of biofilm formed by SH1000 Δ*atl* p*atl*H265A on hydrophobic polystyrene were significantly lower than the wild type (WT) strain, the levels remained higher than those formed by SH1000 Δ*atl* (Fig. 3.2B). This slight increase in biofilm formation compared to SH1000 Δ*atl* may indicate a compensatory role for the GL domain of Atl in the absence of the active AM region. Indeed, subsequent to this work Bose *et al*., reported a significant role for the enzymatic activity of both the AM and GL regions in biofilm formation by the MSSA osteomyelitis isolate UAMS-1 (57).

Previous work from our laboratory revealed that a mutation in Atl significantly impaired HA-MRSA autolysis which correlated with impaired biofilm formation (38). Triton X-100 induced autolysis was reduced by 50% in the SH1000 Δ*atl* mutant and over 25% activity was restored by complementing the *atl* mutant with p*atl* (Fig. 3.3). However, only 10% of lytic activity was restored in the *atl* mutant when complimented with p*atl*H265A, indicating an important contribution for the AM region in SH1000 autolysis (Fig 3.3). This result correlates with results observed for the HA-MRSA strain BH1CC in which the p*atl*H265A plasmid failed to complement the autolytic defect of the *atl* mutant (38). The inability of the active site mutation in the AM region of Atl to restore autolytic activity in SH1000 also correlates with the biofilm defect observed on hydrophobic polystyrene (Fig. 3.2B) and further confirms a role for Atl-mediated autolysis in the biofilm phenotype of SH1000.

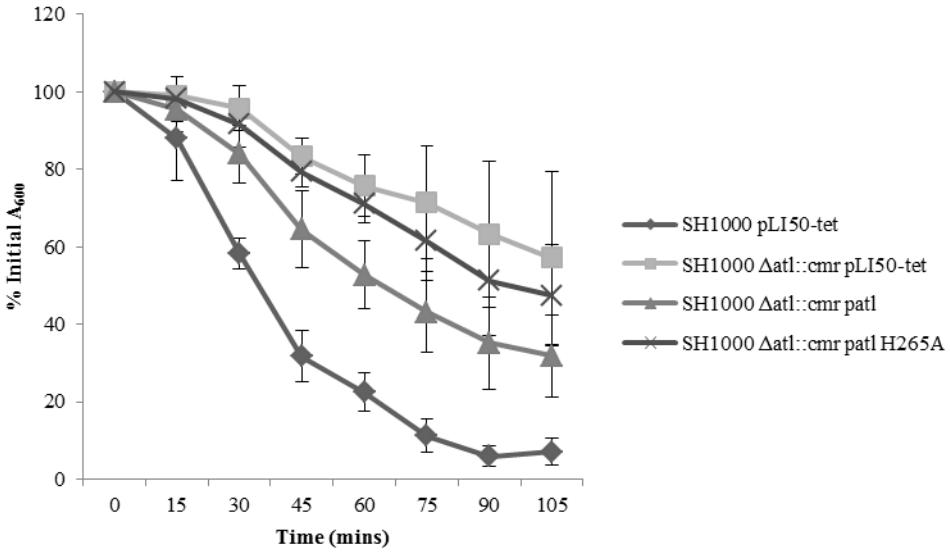


**Fig. 3.3. Contribution of Atl to SH1000 autolytic activity.** Comparison of Triton X-100-induced autolysis of SH1000 pLI50-*tet*, SH1000 Δ*atl*::Cm$^r$ pLI50-*tet*, SH1000 Δ*atl*::Cm$^r$ p*atl* and SH1000 Δ*atl*::Cm$^r$ p*atl*H265A. Cells were grown to early exponential phase in BHI at 37°C and washed in PBS and adjusted to $A_{600}$= 1.0 in 0.01% TRX-100. $A_{600}$ was measured at 15 min intervals with shaking incubation at 37°C. Autolytic activity was expressed as a percentage of the initial $A_{600}$. Results are representative of three independent experiments.

Experiments were undertaken to determine if antibodies raised against the AM and GL regions of Atl could inhibit MSSA biofilm formation. Polyclonal antibodies to AM and GL were donated as a gift by Prof Simon Foster of Sheffield University. SH1000 was incubated with a 1:100 concentration of either antibody for AM or GL or with a 1:100 combination of both AM and GL antibodies during set-up for semi-quantitative biofilm assays as described in chapter 2. SH1000 was also incubated with 1:100 anti-IgG to determine that any biofilm inhibition achieved was not due to non-specific interactions. Given the prominent role for PIA in MSSA biofilm formation on both hydrophilic and hydrophobic polystyrene (Fig. 3.1), anti-PIA antibody was also tested for its ability to inhibit SH1000 biofilm formation on hydrophobic plates. Only antibodies to Atl AM and GL regions significantly inhibited SH1000 glucose-induced biofilm formation on hydrophobic polystyrene ($P \leq 0.001$, Fig. 3.4). PIA antibody reduced SH1000 biofilm formation by 19% but this was not a statistically significant decrease compared to the IgG control (Fig. 3.4). In contrast, antibodies to AM and GL reduced SH1000 biofilm levels by 88% and 86% respectively and when used in combination the antibodies inhibited SH1000

biofilm formation by 90%, similar to levels exhibited by the *atl* mutant ($P \leq 0.001$, Fig. 3.4). This data indicates therapeutic potential in device-related infections (DRIs) caused by strains exhibiting an Atl-dependent biofilm phenotype. The inability of anti-PIA antibodies to significantly impair SH1000 biofilm formation on hydrophobic polystyrene indicates that the Atl-mediated biofilm phenotype is more important for SH1000 biofilm formation on hydrophobic surfaces.

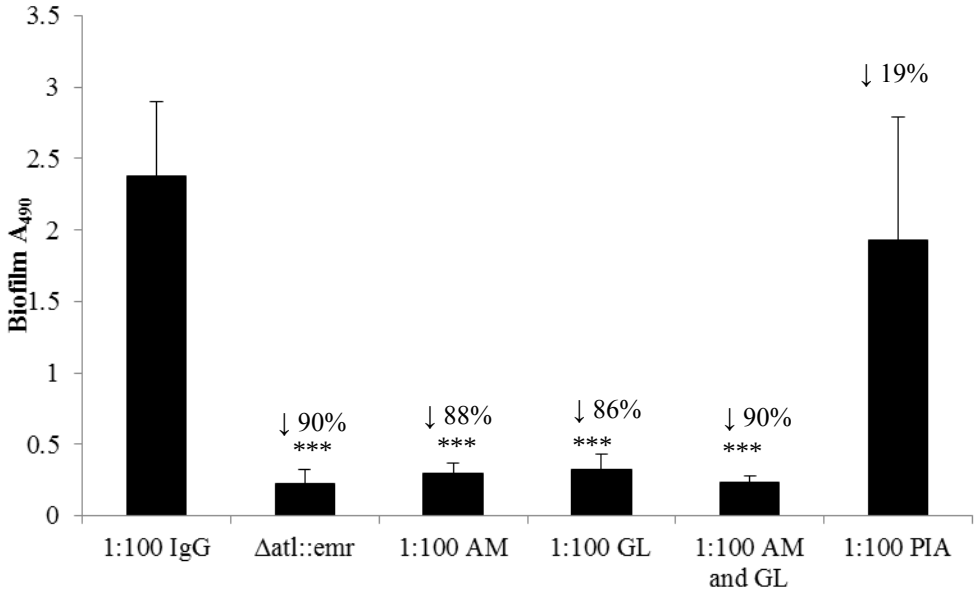


**Fig. 3.4. Inhibition of SH1000 biofilm formation by Atl and PIA antibodies.** Biofilm phenotypes of strains SH1000 treated with 1:100 anti-IgG antibody, SH1000 Δ*atl*::em$^r$, SH1000 treated with 1:100 anti-AM antibody, SH1000 treated with 1:100 anti-GL antibody, SH1000 treated with a combination of 1:100 anti-AM and anti-GL antibodies, and SH1000 treated with 1:100 PIA antibody grown for 24 hrs at 37°C on hydrophobic 96-well polystyrene. Results of at least three independent experiments are shown. Percentage decrease in biofilm formation relative to SH1000 treated with 1:100 IgG is shown. Standard deviations are indicated. Statistical significance denoted as NS for $P > 0.05$, as * for $P \leq 0.05$, as ** for $P \leq 0.01$ and as *** for $P \leq 0.001$.

### 3.2.3 Contribution of Atl to CA-MRSA biofilm formation and lytic activity

CA-MRSA infection rates in people with no pre-disposing risk factors are an increasing concern. CA-MRSA strains are traditionally associated with skin and soft tissue infections. However, CA-MRSA is emerging as a causative agent of biofilm-associated infections (258, 369). The most prominent CA-MRSA strain is USA300. For this work the strain USA300 JE2 was used, a strain that was cured of all plasmids and is the genetic background for the Nebraska Transposon Mutant Library (NTML) (347). To determine if Atl contributes to CA-MRSA biofilm formation as well as biofilm formation by HA-MRSA strains, JE2 biofilm formation was assessed by semi-quantitative biofilm assay. Optimal biofilm levels were exhibited by JE2 when grown on hydrophilic polystyrene. The *atl* mutant from the NTML exhibited a significant biofilm defect when grown in BHI 1% glucose on hydrophilic polystyrene ($P \leq 0.001$), the same conditions required to induce Atl-mediated biofilm formation by HA-MRSA strains (Fig. 3.5A). The multicopy plasmid pLI50-*tet* expressing the *atl* gene was introduced into the *atl* mutant. Possession of the empty vector pLI50-*tet* by JE2 Δ*atl* did not significantly affect the reduced biofilm levels expressed by the mutant. When the *atl* gene was introduced into the mutant, biofilm levels were significantly restored to levels comparable to the parent JE2 ($P \leq 0.001$, Fig 3.5A). Overexpression of *atl* also significantly improved biofilm formation by the parent strain ($P \leq 0.001$). All of this data implicates an important role for *atl* in CA-MRSA biofilm formation *in vitro*.

The JE2 Δ*atlR* mutant exhibited biofilm levels similar to the parent strain (Fig. 3.5B). The effect of multicopy atlR was also examined in JE2 and the JE2 atlR mutant. Control strains were also constructed carrying the empty pLI50 vector. Overall the biofilm data with JE2 strains carrying p*atlR* was not consistent with AtlR acting as a negative regulator of biofilm in this strain (Fig. 3.5B) in contrast to data obtained with the HA-MRSA strain BH1CC (38). Perhaps AtlR regulates other factors influencing the biofilm phenotype in JE2 and these would need to be clarified, although it is interesting to note that biofilm production by JE2 under these growth

conditions is significantly less than in BH1CC, which may mask the role of negative biofilm regulators in general.

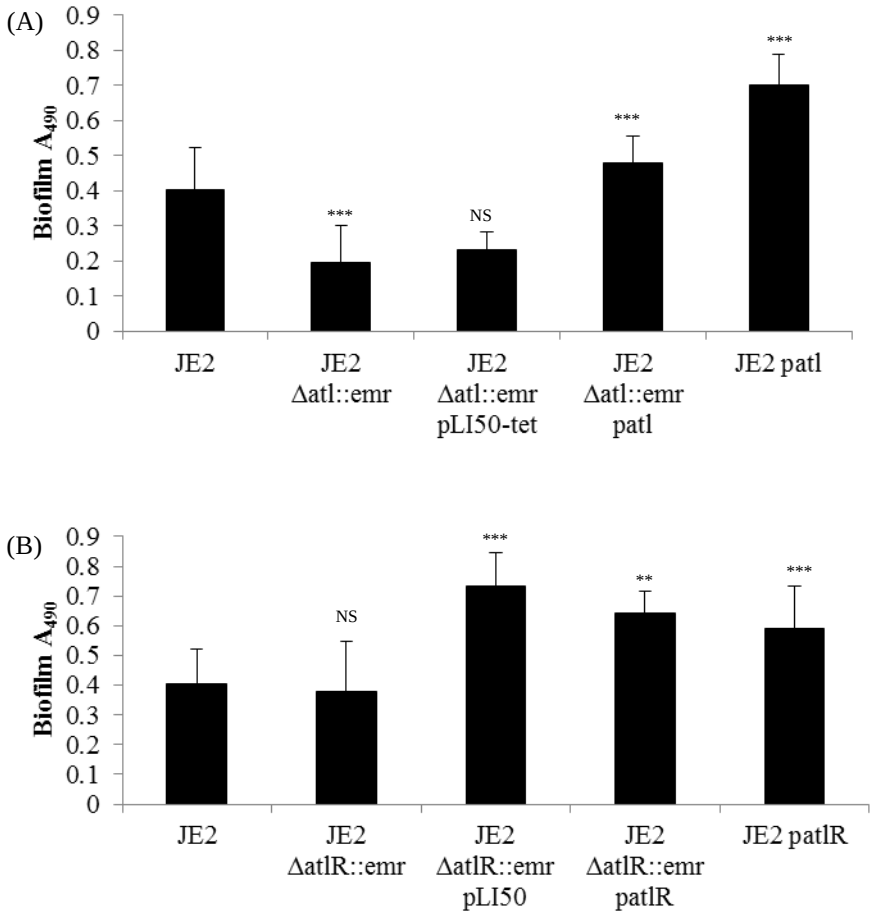


**Fig. 3.5. Contribution of Atl and AtlR to JE2 biofilm formation.** (A) Biofilm phenotypes of strains JE2, JE2 Δ*atl*::em$^r$, JE2 Δ*atl*::em$^r$ pLI50-*tet*, JE2 Δ*atl*::em$^r$ p*atl* and JE2 p*atl* grown for 24 hrs at 37°C in BHI 1% glucose on hydrophilic 96-well polystyrene plates. (B) Biofilm phenotypes of strains JE2, JE2 Δ*atlR*::em$^r$, JE2 Δ*atlR*::em$^r$ pLI50, JE2 Δ*atlR*::em$^r$ p*atlR* and JE2 p*atlR* grown for 24 hrs at 37°C in BHI 1% glucose on hydrophilic 96-well polystyrene plates. Results of at least three independent experiments are shown. Comparisons made between: 1) JE2 and the isogenic *atl* and *atlR* mutants without plasmids, 2) the *atl* and *atlR* mutants and the *atl* and *atlR* mutants carrying plasmids, 3) the *atl* and *atlR* mutants carrying plasmids and the complemented strains and 4) the *atl* and *atlR* mutants carrying the plasmids and JE2 overexpressing *atl* and *atlR*. Standard deviations are indicated. Statistical significance denoted as NS for $P > 0.05$, as * for $P \leq 0.05$, as ** for $P \leq 0.01$ and as *** for $P \leq 0.001$.

To further examine the role for Atl in CA-MRSA biofilm formation, JE2 mutants expressing active site mutations in the AM and GL regions of Atl were assessed for biofilm formation. These mutants were a kind gift from Dr Jeffery Bose of the University of Nebraska Medical Centre who, as discussed, had characterised the contribution of these mutations to biofilm formation by the MSSA strain UAMS-1 (57). The mutations in the active sties of the AM and GL regions rendered the proteins enzymatically inactive as assessed by zymograph analysis but did not affect expression of the Atl protein (Fig. 3.6). Mutation in the GL active site significantly reduced levels of JE2 biofilm formation whereas mutation of the AM active site did not significantly impact on JE2 biofilm (Fig. 3.7). This indicates that the GL region may have a more significant role in the JE2 biofilm phenotype. Of note, the GL mutation appears to partially reduce the AM activity of JE2 as observed by zymograph analysis in figure 3.6. When the AM region is catalytically inactive, the GL region may compensate to maintain biofilm production.

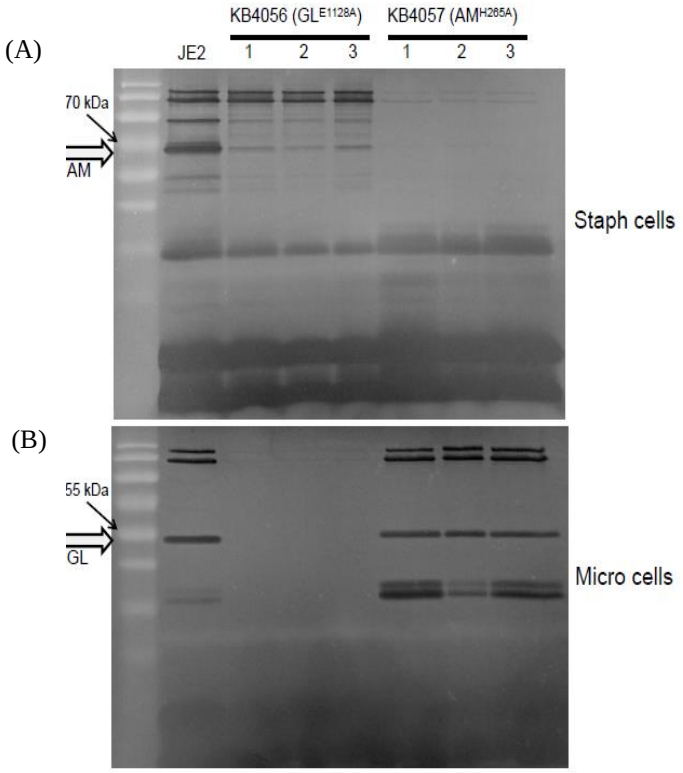


**Fig. 3.6. Zymograph analysis of JE2 ΔAM and ΔGL mutants.** Analysis of murein hydrolase activity of 3µg total extracellular protein from wild type JE2, three JE2 ΔGL (KB4056 $GL_{E1128A}$) candidates and three JE2 ΔAM (KB4057 $AM_{H265A}$) candidates. Protein samples were electrophoresed on a 12% SDS-PAGE acrylamide gel containing (A) 2.5 x $10^9$ CFU/ml heat-killed mid-exponential phase *S. aureus* UAMS-1 cells to detect *N*-acetylmuramyl-L-alanine amidase activity and (B) 1 mg/ml *Micrococcus lysodeikticus* ATCC No 4698 cells (Sigma Aldrich, St. Louis, MO) to detect endo-β-*N*-acetylglucosaminidase activity. Electrophoresis was conducted at 100 V for 2 hrs with a Mini-PROTEAN Tetra Electrophoresis System (Bio-Rad). Following electrophoresis, the gels were washed with 25 mM Tris-HCl (pH 8.0) with 1% Triton X-100 reaction buffer for 30 minutes followed by static incubation in reaction buffer overnight at 37$^{o}$C. Gels were rinsed three times with water and stained with 1% methylene blue in 0.01% KOH to detect clear zones of murein hydrolase activity. Molecular weight ladder is shown and arrows indicate designated molecular weights for the AM enzyme (63.3 kDa) and the GL enzyme (53.6 kDa). Image courtesy of Dr. Jeffrey Bose.

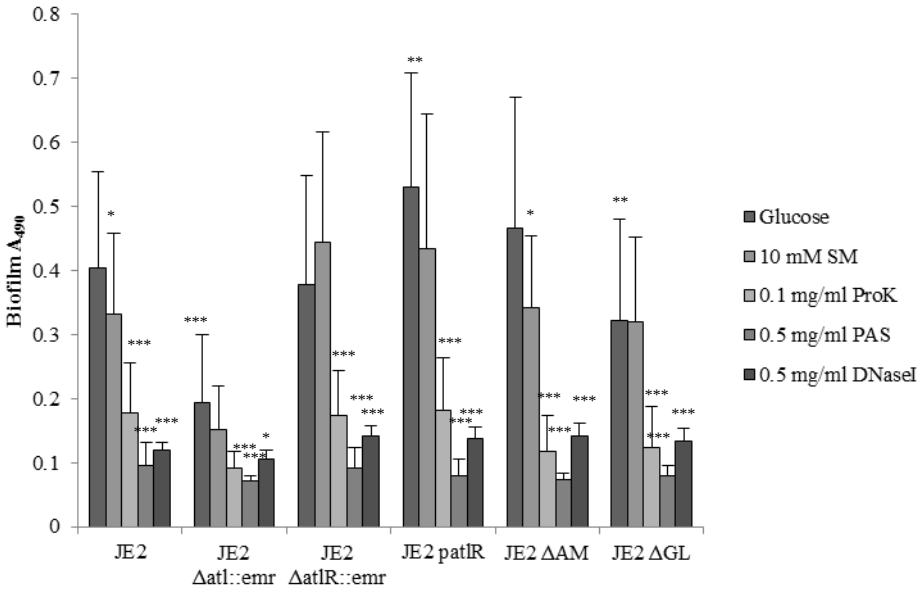


**Fig. 3.7. Contribution of Atl, protein adhesins, autolytic activity and eDNA to JE2 biofilm formation.** Biofilm phenotypes of strains JE2, JE2 Δ*atl*::em$^r$, JE2 Δ*atlR*::em$^r$, JE2 p*atlR*, JE2 ΔAM and JE2 ΔGL grown for 24 hrs at 37°C on hydrophilic 96-well polystyrene plates in BHI 1% glucose, BHI 1% glucose with 0.1mg/ml ProK, BHI 1% glucose with 0.5 mg/ml PAS, BHI 1% glucose with 0.5 mg/ml DNaseI and BHI 1% glucose with 10 mM SM. Results of at least three independent experiments are shown. Comparisons made between: 1) JE2 and the untreated isogenic mutants and 2) untreated controls and each treatment. Standard deviations are indicated. Statistical significance denoted as NS for $P > 0.05$, as * for $P \leq 0.05$, as ** for $P \leq 0.01$ and as *** for $P \leq 0.001$.

Correlating with the impact of the *atl* mutation on JE2 biofilm formation, PAS, Proteinase K (ProK) and DNaseI, which impair autolysis, degrade protein adhesins and degrade eDNA respectively, significantly impaired biofilm formation by JE2 and the JE2 *atl* and *atlR* mutants (Fig. 3.7). While sodium metaperiodate (SM) had some inhibitory effect on JE2 and JE2 ΔAM biofilm formation, the effects were not as pronounced as those seen with PAS, DNaseI and ProK (Fig. 3.7). Overall these data reveal that, as with HA-MRSA, the CA-MRSA strain JE2 requires protein adhesins (specifically Atl), autolytic activity and eDNA release mediated by the major autolysin for biofilm formation.

The JE2 *atl* mutant exhibited an over 40% reduction in triton X-100 induced autolysis compared to the parent strain (Fig. 3.8A). However, this defect in autolysis was not complemented by re-introduction of the *atl* gene on pLI50-*tet* (Fig. 3.8A). This plasmid was sufficient to restore some autolytic activity in the SH1000 background (Fig. 3.3) but was unable to restore any triton-induced autolysis by JE2 Δ*atl* (Fig. 3.8A). The reason for this failure

to complement the autolytic defect of JE2 Δ*atl* remains to be determined but perhaps expression of *atl* from the plasmid is not optimal in the JE2 background. The fact that the biofilm defect could be restored by introduction of p*atl* into JE2 Δ*atl* (Fig. 3.5A) but the defect in autolysis could not be complemented may indicate that the biofilm of JE2 is mediated more by non-specific interactions between the Atl protein and the polystyrene surface than by autolytic activity.

The *atlR* mutant exhibited levels of triton X-100 induced autolysis comparable to the parent JE2 (Fig. 3.8B). Complementation of the *atlR* mutant with p*atlR* had no impact on autolytic activity of this strain (Fig. 3.8B). Furthermore overexpression of *atlR* in the parent JE2 strain did not reduce levels of autolysis (Fig. 3.8B), which correlates with the biofilm phenotype of this strain illustrated in figures 3.5B and 3.7.

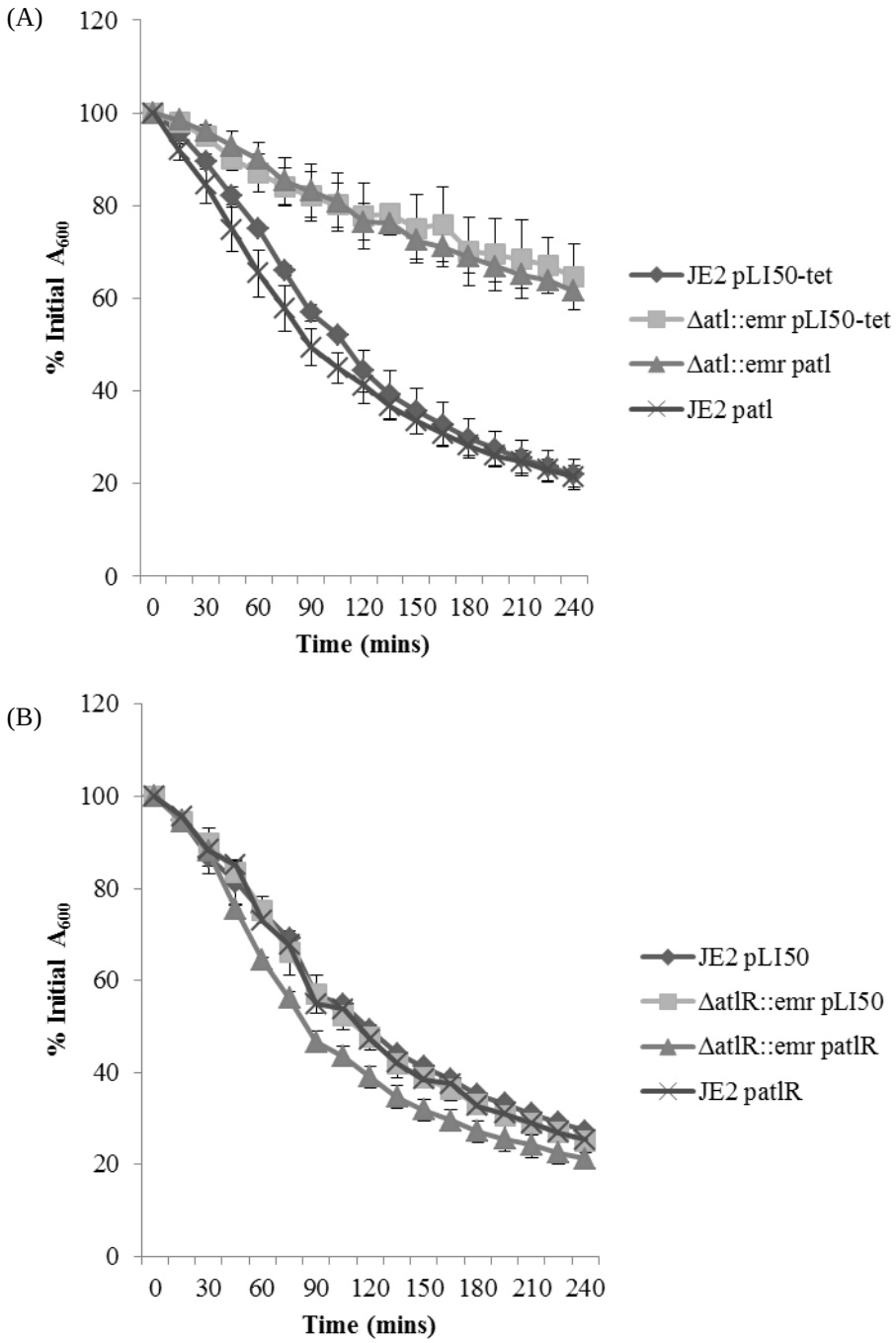


**Fig. 3.8. Contribution of Atl and AtlR to JE2 autolytic activity.** Comparison of Triton X-100-induced autolysis of (A) JE2 pLI50-*tet*, JE2 Δ*atl*::em$^r$ pLI50-*tet*, JE2 Δ*atl*::em$^r$ p*atl* and JE2 p*atl*, and (B) JE2 pLI50, JE2 Δ*atlR*::em$^r$ pLI50, JE2 Δ*atlR*::em$^r$ p*atlR* and JE2 p*atlR*. Cells were grown to early exponential phase in BHI at 37°C and washed in PBS and adjusted to $A_{600}$ = 1.0 in 0.01% TRX-100. The $A_{600}$ was measured and for 15 min intervals thereafter with shaking incubation at 37°C. Autolytic activity was expressed as a percentage of the initial $A_{600}$. Standard deviations are indicated. Results are representative of three independent experiments.

The contribution of each enzymatic region of Atl to JE2 autolysis was also assessed. The AM region significantly contributed to autolysis in JE2 compared to the GL region (Fig. 3.9). This data correlated with studies conducted in the UAMS-1 background (57), but contrasted with the significant contribution of the GL region to biofilm formation by JE2 (Fig. 3.7). This may be due to a more significant role for non-specific interactions between regions of the Atl protein and the polystyrene surface in JE2 biofilm formation than autolytic activity mediated by the AM and GL domains.

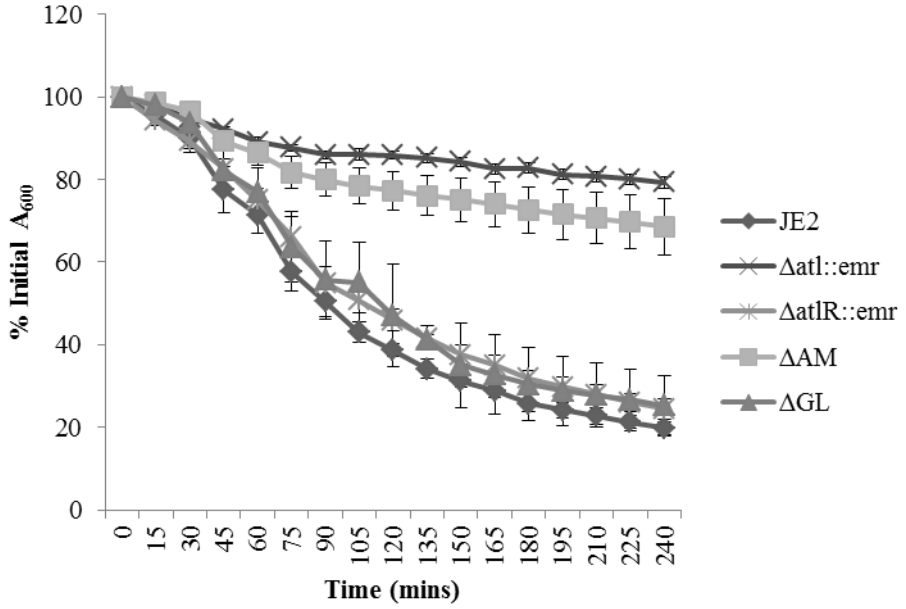


**Fig. 3.9. Contribution of the amidase and glucosaminidase enzymatic regions to JE2 autolytic activity.** JE2, JE2 Δ*atl*::em$^r$, JE2 Δ*atlR*::em$^r$, JE2 ΔAM and JE2 ΔGL. Cells were grown to early exponential phase in BHI at 37°C and washed in PBS and adjusted to $A_{600}$ = 1.0 in 0.01% TRX-100. The $A_{600}$ was measured and for 15 min intervals thereafter with shaking incubation at 37°C. Autolytic activity was expressed as a percentage of the initial $A_{600}$. Standard deviations are indicated. Results are representative of three independent experiments.

Next, AM and GL antibodies were assessed for their ability to inhibit triton X-100 induced autolysis. Both antibodies had an inhibitory effect on JE2 autolysis compared to control IgG (Fig. 3.10).

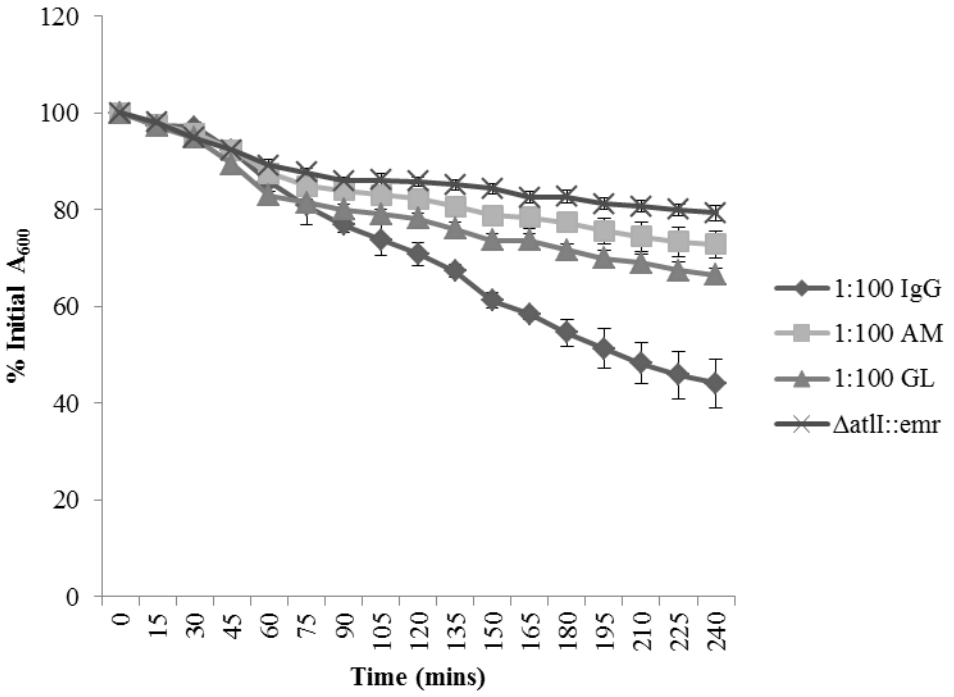


**Fig. 3.10. Inhibition of autolysis of JE2 with Atl antibodies.** Comparison of Triton X-100-induced autolysis of (A) JE2 incubated with 1:100 IgG, JE2 incubated with 1:100 AM, JE2 incubated with 1:100 GL and JE2 Δ*atl*::em$^{r}$. Cells were grown to early exponential phase in BHI at 37°C and washed in PBS and adjusted to $A_{600}$ = 1.0 in 0.01% TRX-100. The $A_{600}$ was measured and for 15 min intervals thereafter with shaking incubation at 37°C. Autolytic activity was expressed as a percentage of the initial $A_{600}$. Standard deviations are indicated. Results are representative of three independent experiments.

Atl antibodies were also assessed for inhibitory effects on JE2 biofilm formation. Incubation of JE2 with each Atl antibody at 1:100 concentration significantly reduced biofilm levels to those similar to the *atl* mutant ($P \leq 0.01$ for JE2 incubated with AM antibody and $P \leq 0.001$ for JE2 incubated with GL antibody, Fig. 3.11). Further reduction in biofilm formation beyond those exhibited by the *atl* mutant could be achieved by incubation of JE2 with both the AM and GL antibodies in combination ($P \leq 0.001$, Fig. 3.11). The 76% reduction in biofilm formation achieved by incubation of JE2 with both Atl antibodies attained levels that rendered the strain biofilm negative as determined by the semi-quantitative biofilm assay protocol described in chapter 2 (absorbance value below an $A_{490}$ of 0.17). This data, combined with the results for SH1000 above, indicate that Atl antibodies can successfully inhibit Atl-mediated biofilm phenotypes *in vitro* and further implicate Atl as an important factor for *in vitro* biofilm formation by JE2.

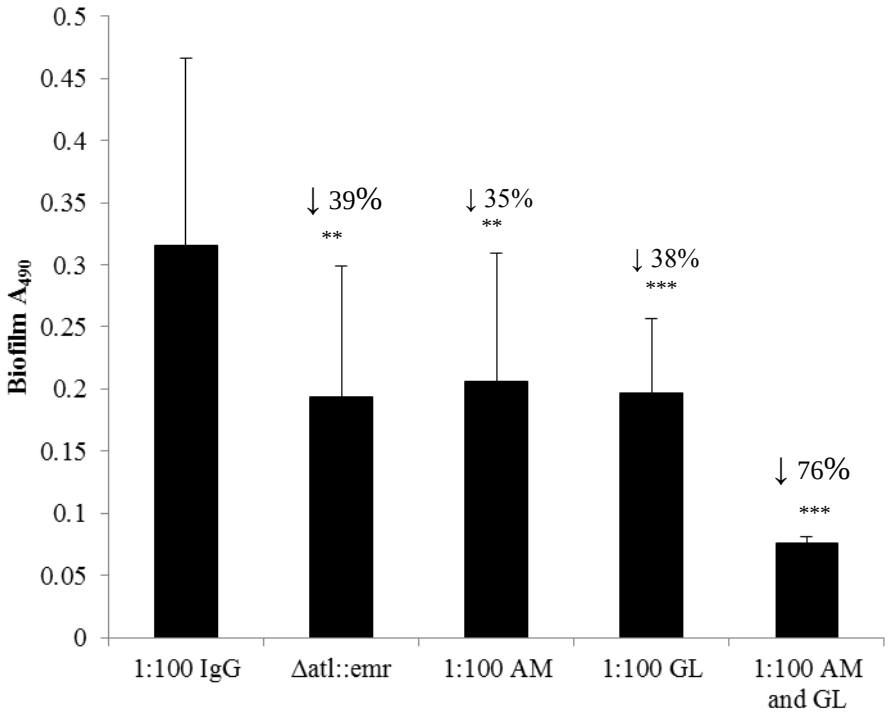


**Fig. 3.11. Inhibition of biofilm formation by JE2 by Atl antibodies.** Biofilm phenotypes of strains JE2 treated with 1:100 anti-IgG antibody, JE2 Δ*atl*::em$^{r}$, JE2 treated with 1:100 anti-AM antibody, JE2 treated with 1:100 anti-GL antibody and JE2 treated with a combination of 1:100 anti-AM and anti-GL antibodies grown for 24 hrs at 37°C on hydrophobic 96-well polystyrene. Results of at least three independent experiments are shown. Percentage decrease in biofilm formation relative to JE2 treated with 1:100 IgG shown. Standard deviations are indicated. Statistical significance denoted as NS for $P > 0.05$, as * for $P \leq 0.05$, as ** for $P \leq 0.01$ and as *** for $P \leq 0.001$.

### 3.2.4 Contribution of Atl to cytotoxin production by MRSA

Beyond a role in biofilm formation, Atl is involved in the secretion of cytoplasmic proteins via a nonclassical protein secretion system (368). Some of the cytoplasmic proteins known to be excreted via Atl-mediated cell lysis include virulence factors such as the alpha haemolysin precursor protein (Hla) and the Spa protein. In this section, experiments were conducted to determine how an *atl* mutations impact on MRSA cytotoxin production *in vitro*. Hla, β-toxin and δ-toxin are all reported to contribute to *S. aureus* biofilm formation under different conditions (370). Therefore, any impact of an *atl* mutation on the production of cytolytic toxins could potentially be an additional mechanism by which mutation of *atl* contributes to the biofilm negative phenotype of *S. aureus*. Cytolytic toxin production by the HA-MRSA strain BH1CC and its isogenic *atl* and *atlR* mutants was

examined by growth on horse and sheep blood plates. Zones of haemolysis on horse blood which indicates α-toxin activity were evident for the parent BH1CC strain and the isogenic *atlR* mutant (Fig. 3.12A). Consistent with the data from L. Pasztor, *et al*. (368), BH1CC Δ*atl* exhibited a smaller zone of haemolysis than the parent strain (Fig. 3.12A). Overexpression of *atlR* on pLI50 also reduced the α-haemolysis levels produced by BH1CC, indicating that Atl-mediated production of α-toxin is in part regulated by AtlR (Fig. 3.12A). A similar result was obtained when the strains were grown on sheep blood agar with a lawn of RN4220 cells which induces production of the phenol-soluble modulin delta toxin (245). A reduction in δ-toxin production was associated with the *atl* mutation and overexpression of *atlR* in BH1CC (Fig. 3.12B). This defect in δ-toxin production exhibited by BH1CC Δ*atl* could be restored with the *atlR* mutation (Fig. 3.12B). To further confirm that *atl* is involved in production of α-toxin, Western blot analysis of α-toxin expression by BH1CC and the isogenic *atl* mutant was assessed. As illustrated in figure 3.12C the *atl* mutation decreased the level of α-toxin production by BH1CC.

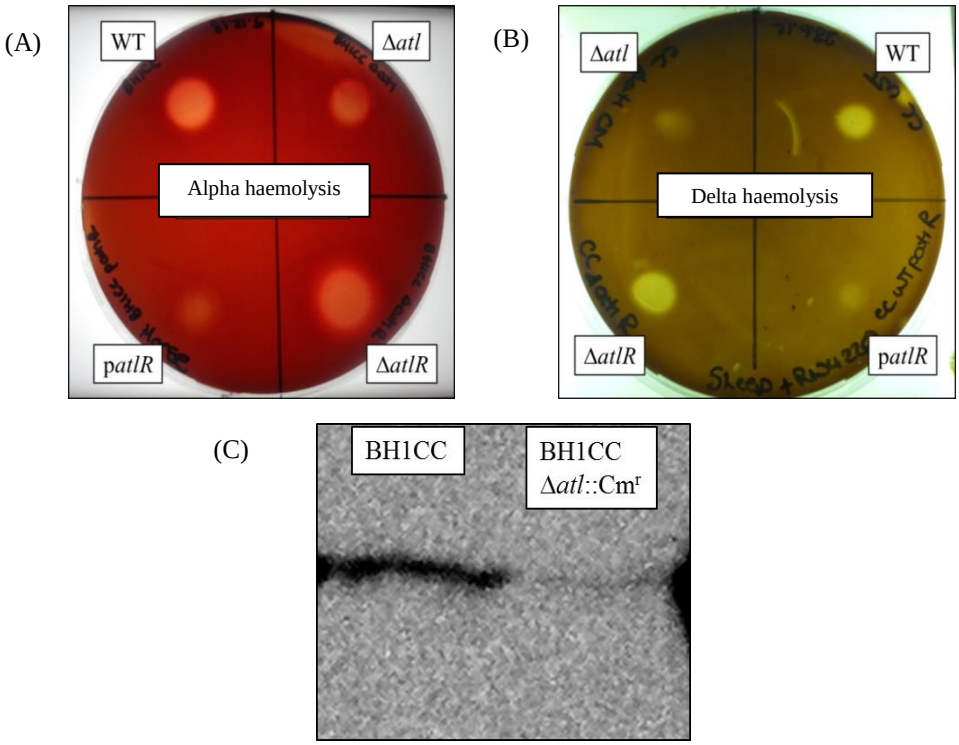


**Fig. 3.12. Contribution of Atl and AtlR to cytotoxin release by BH1CC.** (A) Contribution of *atl* and *atlR* to alpha haemolysin production. Adjusted cell suspensions of BH1CC, BH1CC Δ*atl*::Cm$^r$, BH1CC Δ*atlR*::Tc$^r$ and BH1CC p*atlR* were spotted onto a horse blood plate and incubated overnight at 37$^o$C. (B) Contribution of *atl* and *atlR* to delta haemolysin production. Adjusted cell suspensions of BH1CC, BH1CC Δ*atl*::Cm$^r$, BH1CC Δ*atlR*::Tc$^r$ and BH1CC p*atlR* were spotted onto a sheep blood plate with 100µl of RN4220 spread on the plate and incubated overnight at 37$^o$C. (C) Contribution of *atl* to alpha haemolysin release by BH1CC and BH1CC Δ*atl*::Cm$^r$ as determined by Western blot analysis with anti-alpha haemolysin antibody. Results shown are representative of at least three independent experiments.

Liquid haemolysis assays were used to further evaluate the roles of Atl and AtlR in alpha and beta haemolysin activity as described in chapter 2. Alpha haemolysis was significantly reduced in the BH1CC Δ*atl* strain and similar levels of reduced α-toxin activity were observed for the BH1CC p*atlR* strain ($P \leq 0.01$, Fig. 3.13A). Mutation of *atlR* also significantly reduced α-toxin activity but levels of α-haemolysis remained higher than those of BH1CC Δ*atl* or BH1CC p*atlR* ($P \leq 0.01$, Fig. 3.13A). In contrast to this data, the *atl* and *atlR* mutations did not significantly impair beta haemolysin activity by BH1CC (Fig. 3.13B).

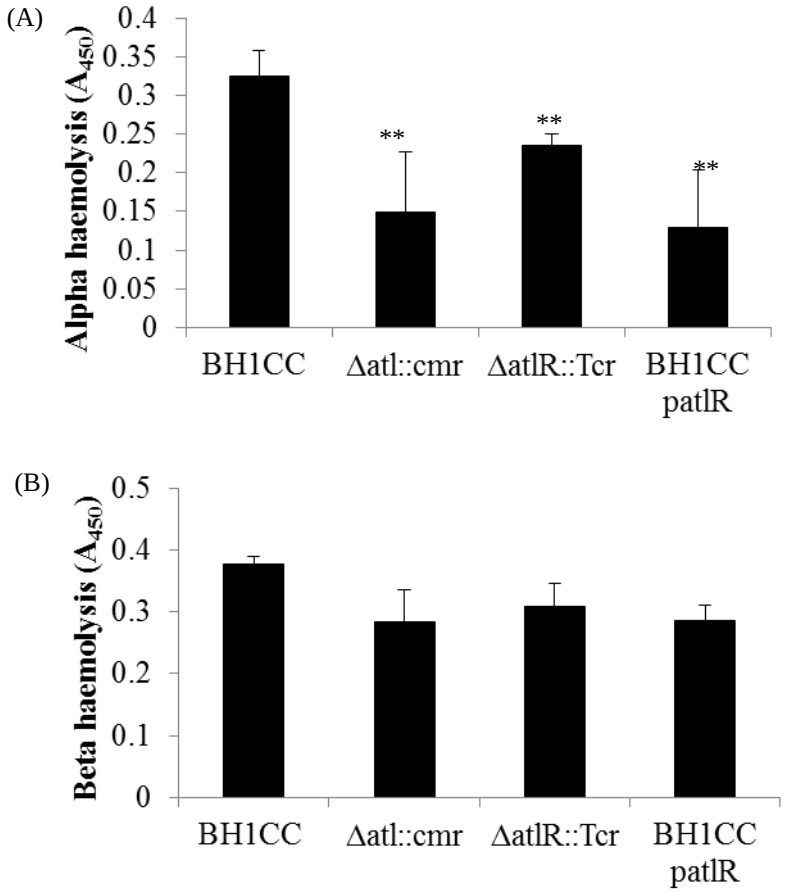


**Fig. 3.13. Contribution of Atl and AtlR to haemolysin activity of BH1CC.** (A) Alpha haemolysin activity of supernatants of BH1CC, BH1CC Δ*atl*::Cm$^r$, BH1CC Δ*atlR*::Tc$^r$ and BH1CC p*atlR*. (B) Beta haemolysin activity of supernatants of BH1CC, BH1CC Δ*atl*::Cm$^r$, BH1CC Δ*atlR*::Tc$^r$ and BH1CC p*atlR*. Supernatants from strains grown to 18hrs (stationary phase) were incubated with 1% sheep (beta haemolysis) or horse (alpha haemolysis) blood for 2 hours at 37$^o$C and $A_{450}$ of the blood was measured. Results shown are representative of at least three independent experiments. Comparisons made between parent BH1CC strain and the isogenic *atl* and *atlR* mutants. Standard deviations are indicated. Statistical significance denoted as NS for P > 0.05, as * for P ≤ 0.05, as ** for P ≤ 0.01 and as *** for P ≤ 0.001.

The effect of an *atl* mutation on haemolysin activity was also assessed for the CA-MRSA strain JE2. CA-MRSA strains carry smaller SCC*mec* elements than HA-MRSA strains associated with high level production of virulence factors while maintaining resistance to β-lactam antibiotics (279). Indeed the high level toxin production by JE2 made it difficult to visualise any differences in haemolysin production by growth on blood agar (data not shown). Using liquid haemolysis assays, a significant reduction in β-haemolysis was observed for the *atl* mutant, a defect that was complemented by introduction of the *atl* gene into the *atl* mutant (P ≤ 0.01, Fig. 3.14A). Overexpression of *atl* on the pLI50-*tet* plasmid restored high

levels of β-haemolysin activity. In contrast to the trend observed in the BH1CC background, the *atlR* mutation significantly reduced the level of β-haemolysin activity by JE2, although not to levels as low as the *atl* mutant ($P \leq 0.01$). Some of the β-haemolysin activity of JE2 Δ*atlR* could be restored by complementation of the mutation with p*atlR*. Overexpression of *atlR* in the JE2 background reduced levels of β-haemolysin activity although this reduction did not reach statistical significance. An increase in β-haemolysin activity was observed for the JE2 ΔAM and JE2 ΔGL strains with only the JE2 ΔAM reaching a statistically significant increase in activity. This may indicate compensatory roles for each enzymatic region of Atl in controlling β-haemolysin activity. A similar trend toward reduced activity for the *atl* mutant was observed for α-haemolysin activity by JE2 which could be complemented (Fig. 3.14B). Some differences were observed for α-haemolysin activity compared to β-haemolysin activity. The *atlR* mutation did not impair α-haemolysis and levels of α-haemolysis for JE2 Δ*atlR* remained at levels similar to wild type JE2. Overexpression of *atlR* was found to reduce α-haemolysis by JE2, a trend that matched the observations for the BH1CC strains grown on horse blood agar (Fig. 3.12A). Unlike the results for the β-haemolysin assay, the JE2 ΔGL mutant exhibited a reduction in α-haemolysis (Fig. 3.14B). The level of α-haemolysis exhibited by JE2 ΔAM was just above the wild type level of α-haemolysis. This indicates that the GL region of Atl may be more important for CA-MRSA virulence with respect to levels of α-toxin production.

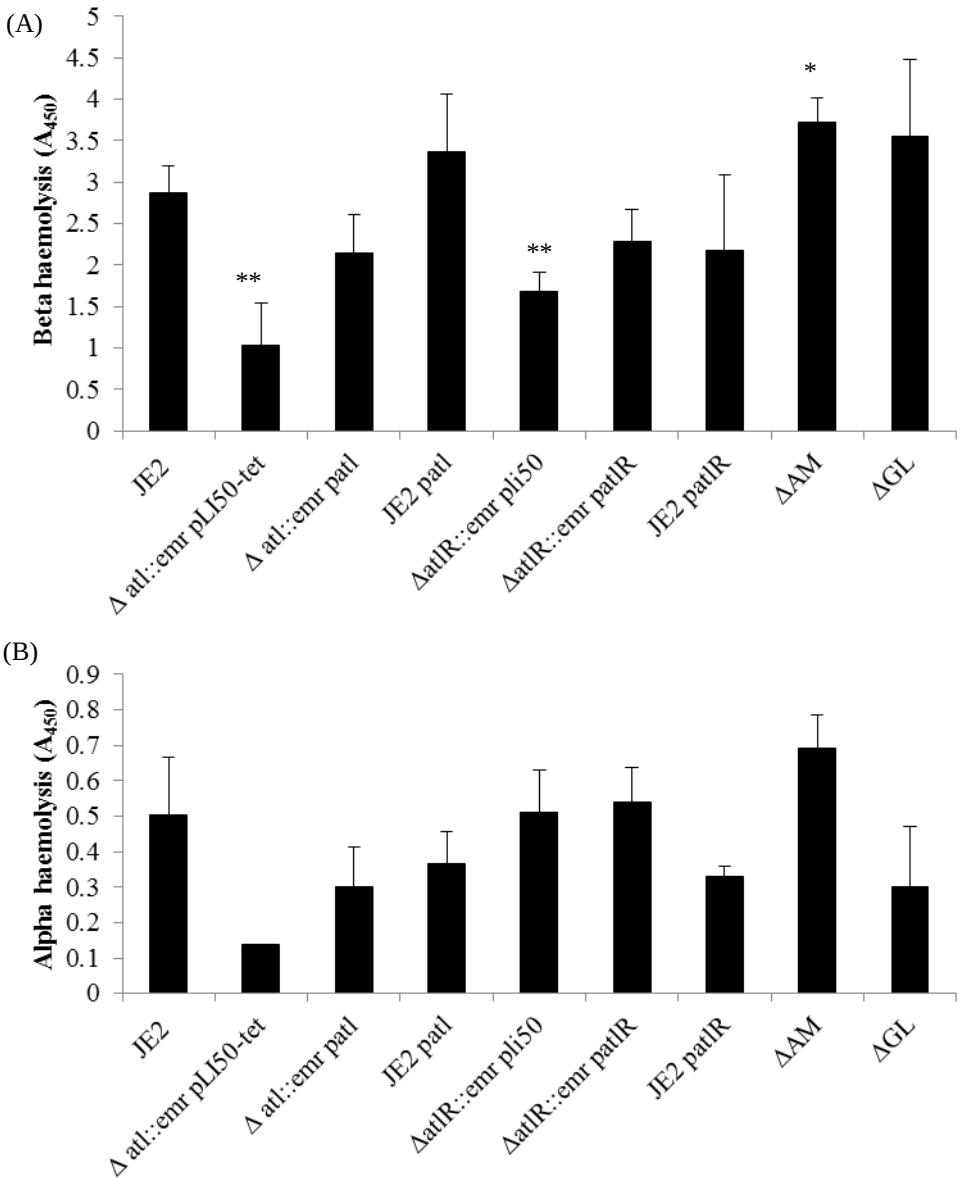


**Fig. 3.14. Contribution of Atl, AtlR and the enzymatic regions of *alt* to haemolysin activity of JE2**. (A) Beta haemolysin activity of supernatants of JE2, JE2 Δ*atl*::em$^r$ pLI50-*tet*, JE2 Δ*atl*::em$^r$ p*atl*, JE2 p*atl*, JE2 Δ*atlR*::em$^r$ pLI50, JE2 Δ*atlR*::em$^r$ p*atlR*, JE2 p*atlR*, JE2 ΔAM, JE2 ΔGL (B) Alpha haemolysin activity of supernatants of JE2, JE2 Δ*atl*::em$^r$ pLI50-*tet*, JE2 Δ*atl*::em$^r$ p*atl*, JE2 p*atl*, JE2 Δ*atlR*::em$^r$ pLI50, JE2 Δ*atlR*::em$^r$ p*atlR*, JE2 p*atlR*, JE2 ΔAM, JE2 ΔGL. Supernatants from strains grown to 18hrs (stationary phase) were incubated with 1% sheep (beta haemolysis) or horse (alpha haemolysis) blood for 2 hrs at 37$^o$C and $A_{450}$ of the blood was measured. Results are representative of at least two independent experiments. Comparisons made between parent JE2 and the isogenic *atl* and *atlR* mutants. Standard deviations are indicated. Statistical significance denoted as NS for $P > 0.05$, as * for $P \leq 0.05$, as ** for $P \leq 0.01$ and as *** for $P \leq 0.001$.

Despite observing trends of reduced haemolysis for the JE2 *atl* mutants with the liquid assays, the high level of toxin production by JE2 made the assays challenging. In an effort to obtain more conclusive data on the role of Atl in CA-MRSA toxin production expression of *atl* and *hla* was assessed in the JE2 Δ*atl* and Δ*atlR* strains by RT-PCR as described in chapter 2. Strains were grown to 20 hours at which point RNA was extracted and processed. As anticipated, there was a significant 17.35-fold decrease in *atl* transcription by JE2 Δ*atl* ($P \leq 0.05$), a defect that could be complemented by the p*atl* plasmid (Fig. 3.15A). Introduction of *atl* into JE2 Δ*atl* significantly increased expression of *atl* by over 15-fold ($P \leq 0.001$) and overexpression of *atl* in the parent strain increased *atl* transcription by nearly 11-fold ($P \leq 0.05$, Fig. 3.15A). The JE2 Δ*atl* strain exhibited a significant 3.21-fold reduction in *hla* transcription ($P \leq 0.05$) compared to JE2, a phenotype that was complemented by p*atl* (Fig. 3.15B). Expression of *atl* was not significantly different between any of the *atlR* mutants (Fig. 3.16A). However, significant increases in *hla* transcription were observed when JE2 Δ*atlR* and JE2 carried the p*atlR* plasmid ($P \leq 0.001$), a finding which contradicted the liquid haemolysis data for JE2 and the blood plate data for BH1CC (Fig. 3.16B). Correlating with the findings of Dr Bose during the construction of the JE2 AM and GL mutations, the active site mutations in the AM and GL regions did not significantly impact on *atl* transcription by JE2 (Fig. 3.17A). Correlating with the observed trend for the liquid haemolysis assays (Fig. 3.14B), a significant reduction in *hla* expression was seen for the GL mutant which exhibited a 4.66-fold decrease in *hla* expression ($P \leq 0.01$, Fig. 3.17B). The transcription of *hla* was not affected by the AM mutation, a finding that also correlated with the liquid haemolysis assays (Fig 3.14B). Overall this data shows that *hla* expression is regulated by Atl at the transcriptional level in JE2, with a predominant role for the GL domain of Atl. The downregulation of Hla activity by *atlR* expression appears to be a strain dependent phenotype that is observed in BH1CC and not in JE2, whereas the correlation between reduced Hla activity and mutation of *atl* is observed in both strains. Therefore, *atl* appears to be an important modulator of *hla* expression, a phenotype which could contribute to *S. aureus* virulence *in vivo*.

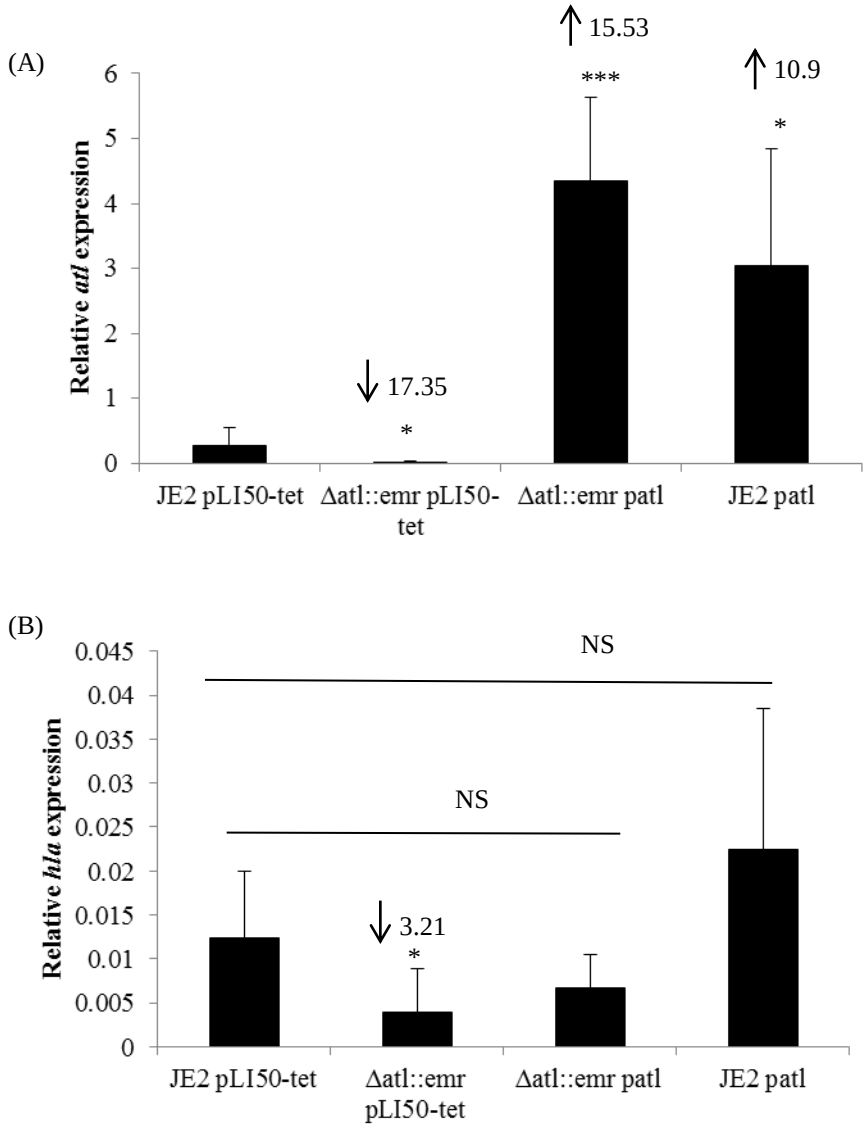


**Fig. 3.15. Contribution of *atl* mutations to JE2 *atl* and *hla* transcription. (A)** Comparison of relative *atl* transcription by RT-PCR by JE2 pLI50-*tet*, JE2 Δ*atl*::em$^r$ pLI50-*tet*, JE2 Δ*atl*::em$^r$ p*atl*, JE2 p*atl*. (B) Comparison of relative *hla* transcription by JE2 pLI50-*tet*, JE2 Δ*atl*::em$^r$ pLI50-*tet*, JE2 Δ*atl*::em$^r$ p*atl*, JE2 p*atl*. Total RNA was extracted from cells grown at 37$^o$C for 20 hrs (stationary phase) in BHI. Results shown are representative of at least three independent experiments. Fold increase/decrease in *atl* and *hla* expression relative to parent strain indicated by arrows. Standard deviations are indicated. Statistical significance denoted as NS for $P > 0.05$, as * for $P \leq 0.05$, as ** for $P \leq 0.01$ and as *** for $P \leq 0.001$.

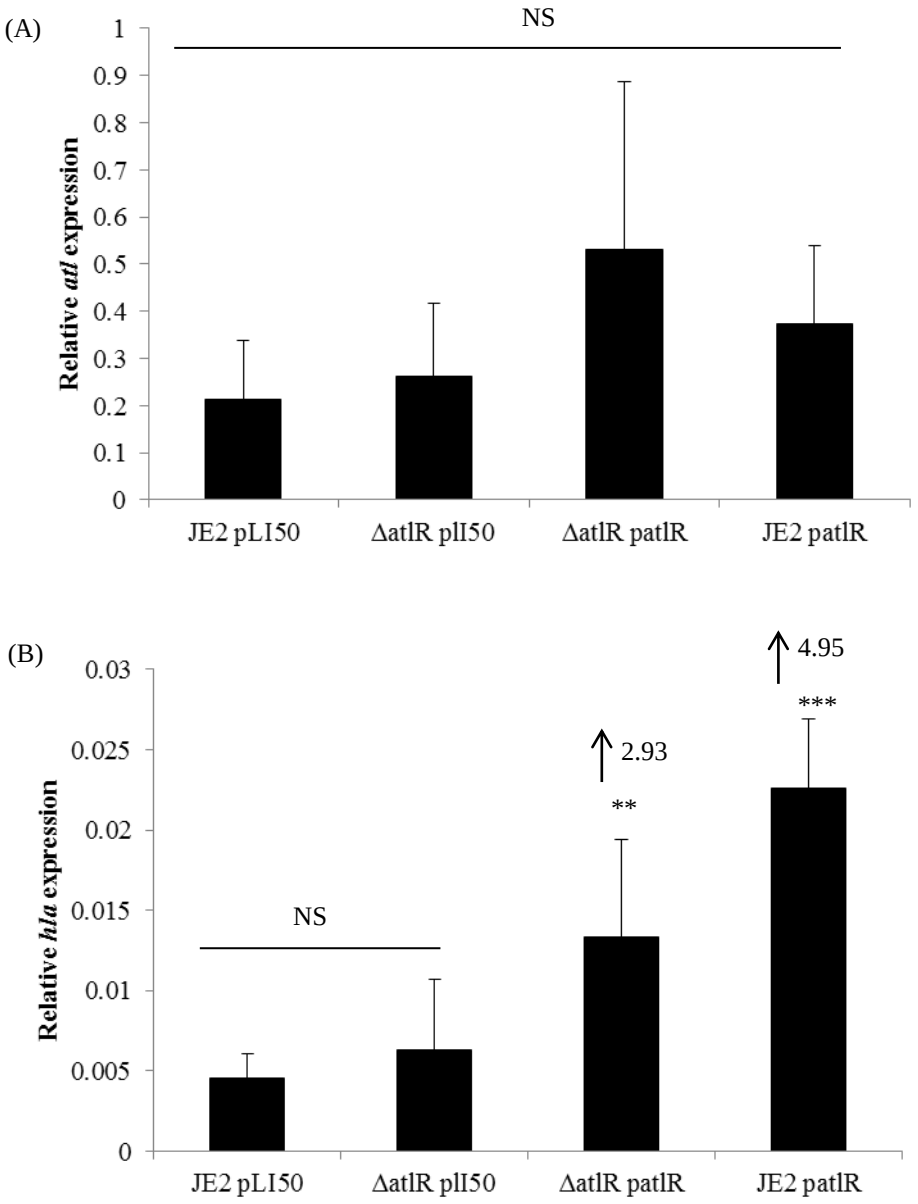


**Fig. 3.16. Contribution of *atlR* mutations to JE2 *atl* and *hla* transcription. (A)** Comparison of relative *atl* transcription by RT-PCR by JE2 pLI50, JE2 Δ*atlR*::em$^r$ pLI50, JE2 Δ*atlR*::em$^r$ p*atlR*, JE2 p*atlR*. (B) Comparison of relative *hla* transcription by JE2 pLI50, JE2 Δ*atlR*::em$^r$ pLI50, JE2 Δ*atlR*::em$^r$ p*atlR*, JE2 p*atlR*. Total RNA was extracted from cells grown at 37$^o$C for 20 hrs (stationary phase) in BHI. Results shown are representative of at least three independent experiments. Fold increase/decrease in *atl* and *hla* expression relative to parent strain indicated by arrows. Standard deviations are indicated. Statistical significance denoted as NS for $P > 0.05$, as * for $P \leq 0.05$, as ** for $P \leq 0.01$ and as *** for $P \leq 0.001$.

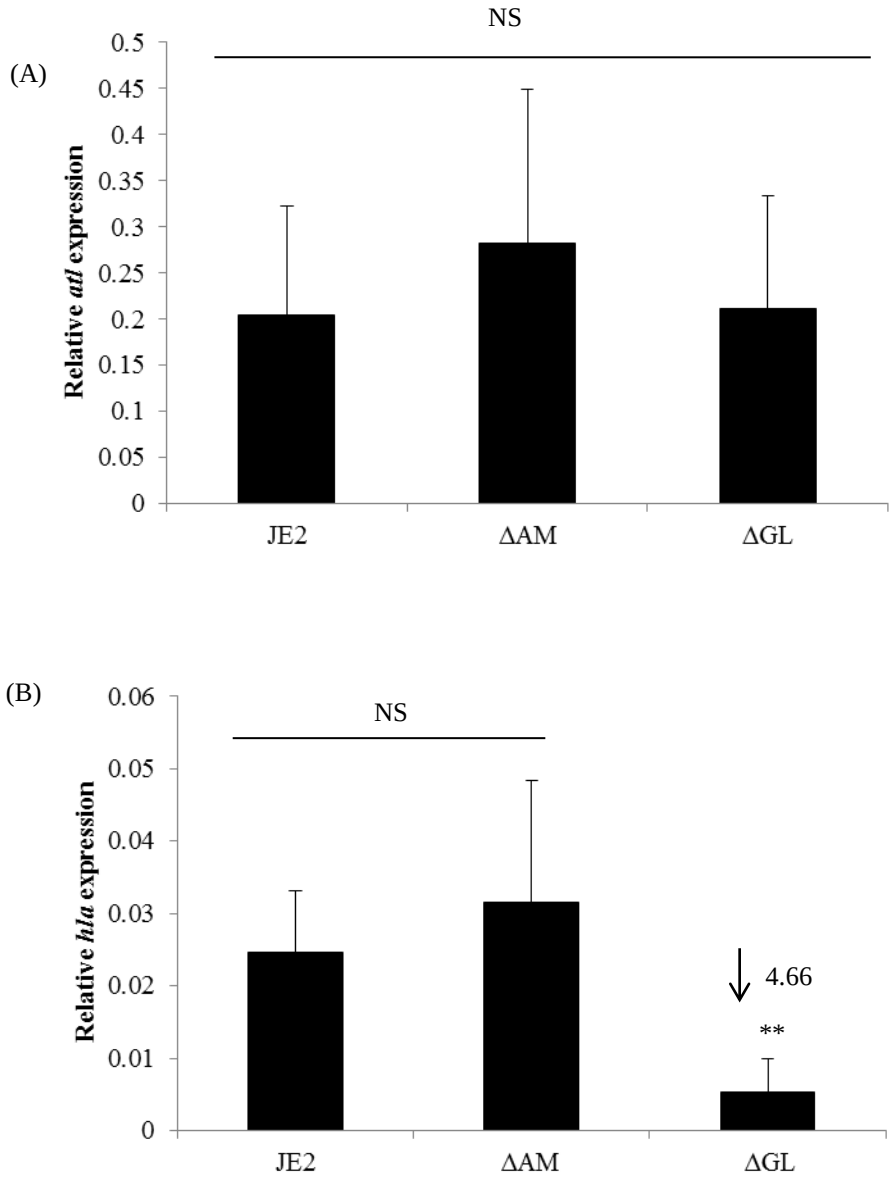


**Fig. 3.17. Contribution of AM and GL mutations to JE2 *atl* and *hla* transcription.** **(A)** Comparison of relative *atl* transcription by RT-PCR by JE2, JE2 ΔAM and JE2 ΔGL. (B) Comparison of relative *hla* transcription by JE2, JE2 ΔAM and JE2 ΔGL. Total RNA was extracted from cells grown at 37$^{o}$C for 20 hrs (stationary phase) in BHI. Results shown are representative of at least three independent experiments. Fold increase/decrease in *atl* and *hla* expression relative to parent strain indicated by arrows. Standard deviations are indicated. Statistical significance denoted as NS for $P > 0.05$, as * for $P \leq 0.05$, as ** for $P \leq 0.01$ and as *** for $P \leq 0.001$.

### 3.2.5 Investigation into the *in vivo* relevance of Atl for DRIs

A mouse model of device-related infections was used to assess the contribution of Atl to biofilm formation and virulence as described in chapter 2. These experiments were carried out in the laboratory of Prof Paul Fey. An inoculum of $5x10^5$ CFU/ml was used to infect 1 cm catheter segments surgically implanted into the flank of the mice. Two experiments were set up, a three day infection to determine any contribution of Atl to the early stages of infection and a seven day infection to examine how Atl contributes to the later stages of device-related infections (DRIs). After the experimental time course was finished, the animals were sacrificed and the catheter, surrounding peri-catheter tissue, liver, spleen and one kidney were harvested and assessed for CFU counts. The following strains were tested in the infection model, JE2, JE2 Δ*atl*, JE2 Δ*atlR*, JE2 p*atlR*, JE2 ΔAM and JE2 ΔGL. After the three day infection course, no significant differences were observed in colonisation of any of the organs by any of the six strains (Fig. 3.18). Bacterial burdens remained high for all organs showing that all mutants were capable of colonising the implanted catheters and disseminating well from the site of infection up to day three.

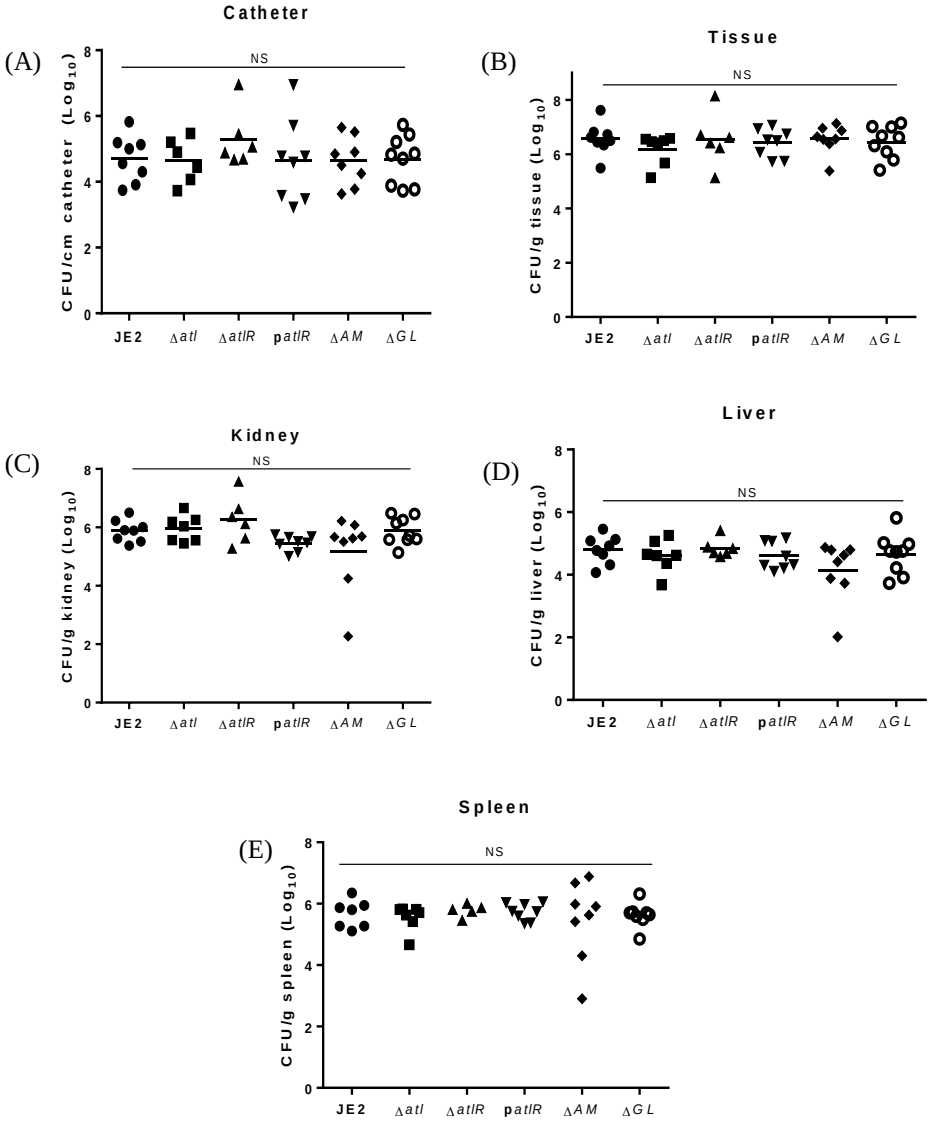


**Fig. 3.18. Three day infection model.** Catheter colonisation and dissemination of JE2 and JE2 *atl* and *atlR* mutants in a mouse device-related infection model. Implanted catheter segments were infected with $5x10^5$ CFU of JE2, JE2 Δ*atl*::em$^r$, JE2 Δ*atlR*::em$^r$, JE2 p*atlR*, JE2 ΔAM and JE2 ΔGL . Mice were sacrificed after three days and CFU per centimetre segment of catheter (A), per gram of tissue (B), per gram of kidney (C) per gram of liver (D) and per gram of spleen (E) were recovered and counted. Comparisons made between JE2 and the isogenic *atl* and *atlR* mutants. Statistical significance/not significant (NS) indicated. *n* ranges from 6-9 mice per group.

However, statistically significant differences in colonisation levels were observed between the strains after seven days of infection. Colonisation of the peri-catheter tissue by JE2 Δ*atl*, JE2 p*atlR* and JE2 ΔGL was significantly decreased compared to JE2 ($P < 0.01$, Fig. 3.19A). Statistically significant differences were also obtained in the levels of kidney colonisation (Fig. 3.19B). All mutants except JE2 ΔAM colonised the kidney at significantly reduced rates compared to JE2 ($P < 0.05$, Fig. 3.19B). Only JE2 Δ*atl* colonised the spleen at a significantly reduced rate compared to the parent strain ($P < 0.05$, Fig. 3.19C) and no significant differences were observed between the six strains for colonisation of the liver (Fig. 3.19D). Despite the significant differences observed, the bacterial burden remained high in all organs for all strains (Fig. 3.19). Additionally, by day seven all of the mice had developed severe abscesses at the sites of infection that facilitated loss of the implanted catheters for almost all of the animals by the end of the experimental time course. Consequently we were unable to obtain enough data from the few remaining implanted catheters to conclusively determine if there was a colonisation defect of the implanted catheters associated with mutations in *atl* and if this might be contributing to the significant decreases in colonisation of the peri-catheter tissue and organs. These data indicate that *S. aureus* retains the capacity to cause robust DRIs even in the absence of the major autolysin Atl.

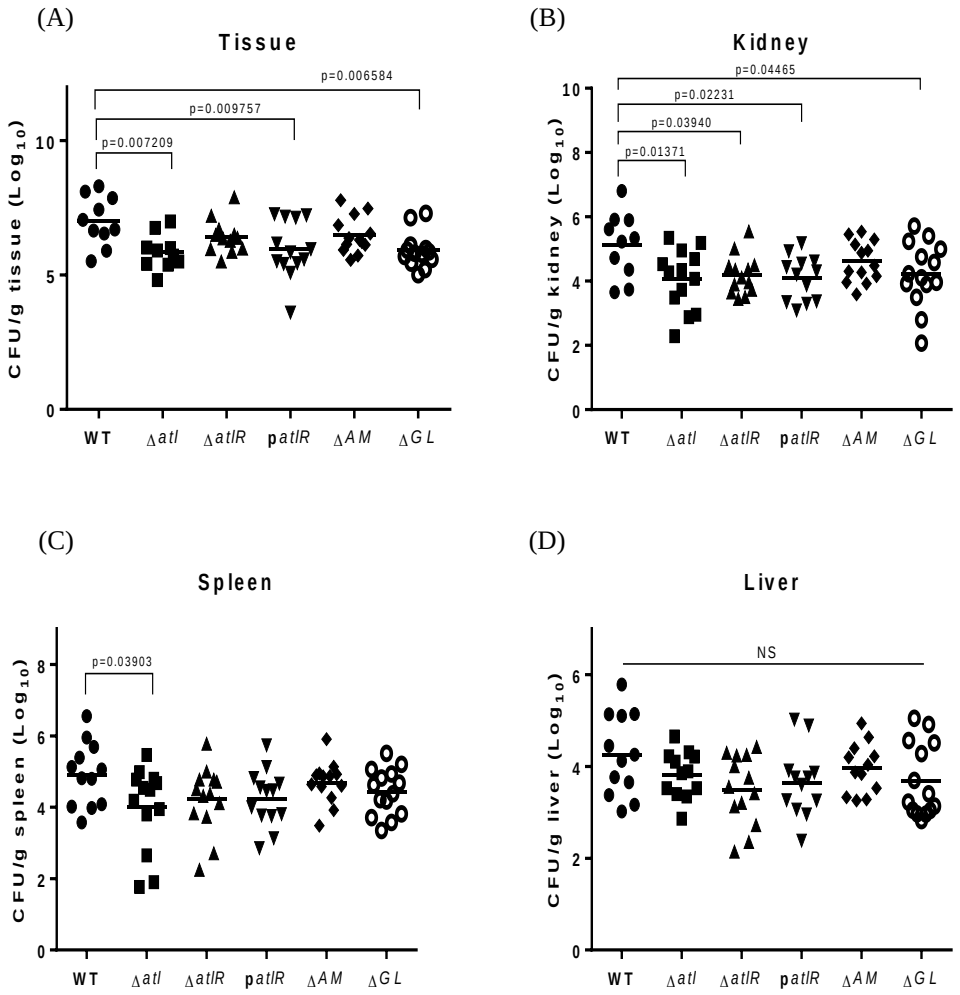


**Fig. 3.19. Seven day infection model.** Catheter colonisation and dissemination of JE2 and JE2 *atl* and *atlR* mutants in a mouse device-related infection model. Implanted catheter segments were infected with $5x10^5$ CFU of JE2 wild type (WT), JE2 Δ*atl*::em$^r$, JE2 Δ*atlR*::em$^r$, JE2 p*atlR*, JE2 ΔAM and JE2 ΔGL . Mice were sacrificed after seven days and CFU per centimetre segment of catheter (A), per gram of tissue (B), per gram of kidney (C) per gram of liver (D) and per gram of spleen (E) were recovered and counted. Comparisons made between JE2 and the isogenic *atl* and *atlR* mutants. Statistical significance/not significant (NS) indicated. *n* ranges from 10-14 mice per group.

A significant reduction in colonisation of the kidney by the *atlR* mutant was observed by day seven ($P < 0.05$, Fig. 3.19B). As shown in figure 3.20 there was no difference in growth rates between the parent JE2 strain and JE2 Δ*atlR*, perhaps suggesting that reduced colonisation by the *atlR* mutant may be due to de-regulated autolytic activity.

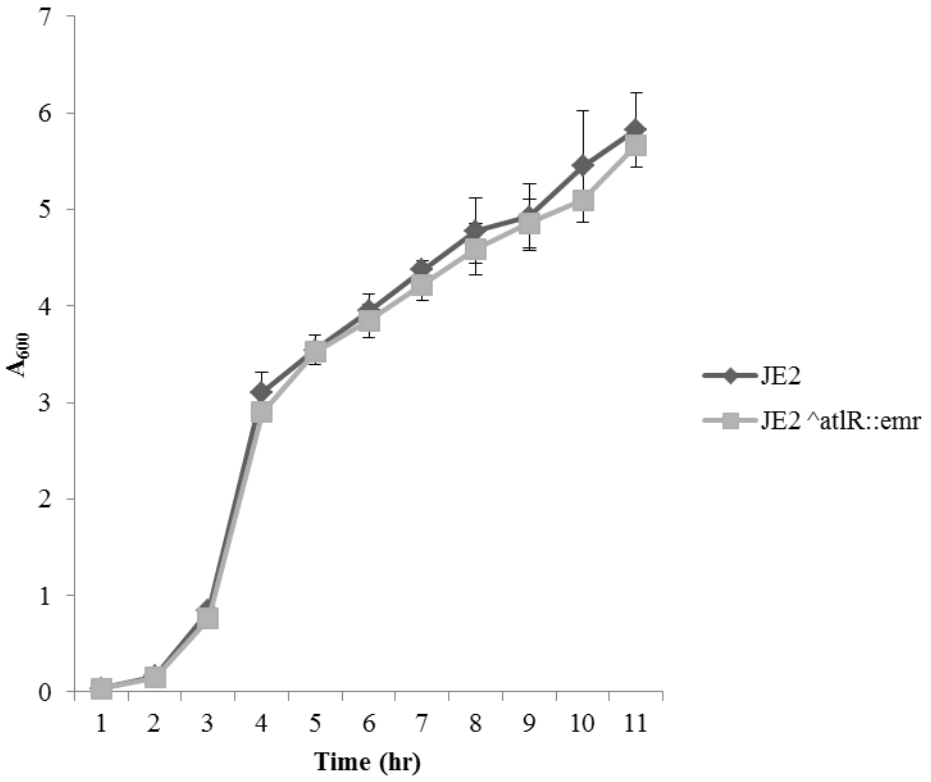


**Fig. 3.20. Growth curve of JE2 and JE2 Δ*atlR*::em$^{r}$.** Strains were grown in BHI at 37ºC at 200rpm. A600 of cultures were measured every hour for eleven hours. Data presented are representative of two independent experiments and standard deviations are indicated.

In an effort to try to explain the mechanisms behind these observed differences in CFU counts between the wild type and Δ*atl* mutant after seven days of infection, the inflammatory response was examined using the Proteome Profiler™ Array Mouse Cytokine Array Panel A kit (R&D Systems). This assay enables rapid analysis of the relative expression of 40 different mouse cytokines in one experiment. Infection with the *atl* mutant was associated with a somewhat reduced pro-inflammatory response in the peri-catheter tissue than with the wild type strain (Fig. 3.21). Cytokines that were upregulated in the peri-catheter tissue by infection with JE2 and JE2 Δ*atl* are shown (Fig. 3.21). For example, tumor necrosis factor alpha levels were 5.6-fold lower in tissue infected by the *atl* mutant compared to the wild type and interleukins associated with the pro-inflammatory response were also lower in tissue infected by the *atl* mutant (Table 3.1A). RANTES was the only chemokine expressed at a 5-fold higher concentration in peri-catheter tissue infected with the *atl* mutant than JE2 (Fig. 3.21, Table 3.1A), perhaps indicating a higher level of leukocyte recruitment to tissue infected

with JE2 Δ*atl* compared to JE2. Although these data may indicate that the atl mutant is somewhat less virulent, overall cytokine levels in tissue infected with JE2 and its isogenic *atl* mutant were not significantly different and may reflect the similarities in virulence observed between the two strains.

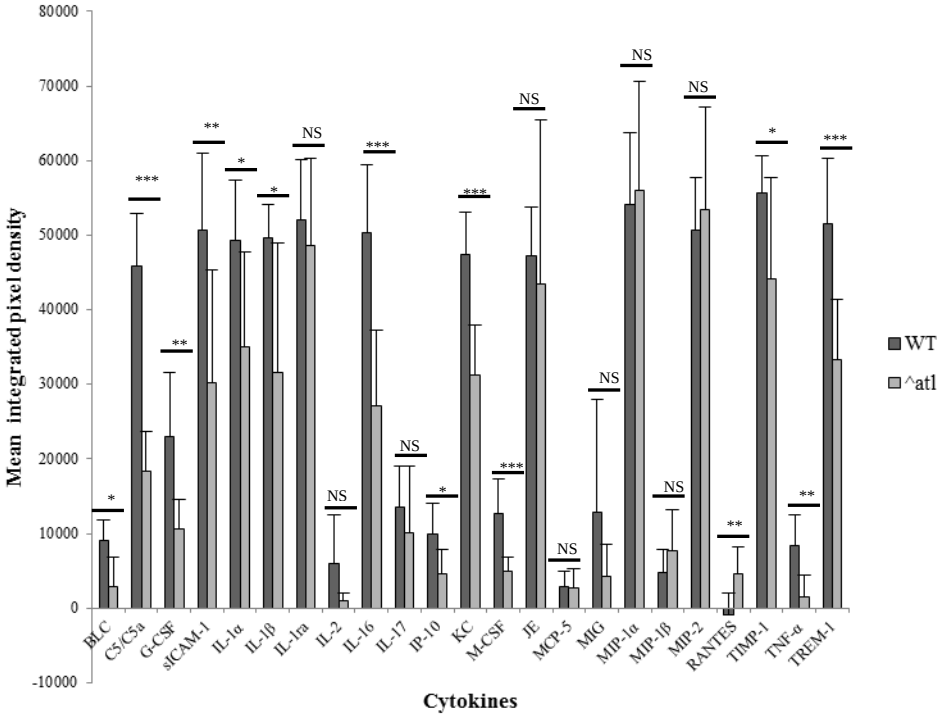


**Fig. 3.21. Cytokine response in peri-catheter tissue recovered from mice infected for 7 days with JE2 and JE2 Δ*atl*::em$^{r}$.** Immune response measured in four samples from mice infected each with JE2 wild type (WT) and JE2 Δ*atl*::em$^{r}$ with the Proteome Profiler Array Mouse Cytokine Array Panel A by R&D Systems by following the manufacturer's instructions. Statistical significance denoted as NS for $P > 0.05$, as * for $P \leq 0.05$, as ** for $P \leq 0.01$ and as *** for $P \leq 0.001$.

**Table 3.1A**
**Cytokines expressed at significantly different levels in peri-catheter tissue infected with JE2 Δ*atl* compared to tissue infected with JE2**

| Cytokine | Fold Change compared to JE2 | Significance |
|---|---|---|
| BLC | ↓ 3.188696 | * |
| C5/C5a | ↓ 2.506696917 | *** |
| G-CSF | ↓ 2.170831 | ** |
| sICAM-1 | ↓ 1.679864633 | ** |
| IL-1α | ↓ 1.41319 | * |
| IL-1β | ↓ 1.570301527 | * |
| IL-16 | ↓ 1.859711 | *** |
| IP-10 | ↓ 2.164194 | * |
| KC | ↓ 1.512398 | *** |
| M-CSF | ↓ 2.607979 | *** |
| RANTES | ↑ 5.12971 | ** |
| TIMP-1 | ↓ 1.25868 | * |
| TNF-α | ↓ 5.601932 | ** |
| TREM-1 | ↓ 1.547691 | *** |

| Table 3.1B<br>Cytokines not expressed at significantly different levels in peri-catheter tissue infected with JE2 and JE2 Δ*atl* | | | |
|---|---|---|---|
| **Cytokine** | **WT** | **Δ*atl*::em$^r$** | **Significance** |
| **Mean integrated pixel density** | | | |
| IL-1ra | 52077.375 | 48568.5 | NS |
| IL-2 | 5900.75 | 987.75 | NS |
| IL-17 | 13567 | 10069.13 | NS |
| JE | 47223.88 | 43380.75 | NS |
| MCP-5 | 2798.75 | 2627.375 | NS |
| MIG | 12862.25 | 4310.375 | NS |
| MIP-1α | 54041.13 | 56066.13 | NS |
| MIP-1β | 4798.875 | 7736.875 | NS |
| MIP-2 | 50717.25 | 53434.38 | NS |

**Table 3.1: Summary of results of cytokine analysis.** (A) Cytokines that are produced at significantly different levels in the surrounding peri-catheter tissue infected with the JE2 wild type (WT) strain versus the *atl*::em$^r$ mutant. Fold change for cytokines produced in tissue infected with JE2 Δ*atl*::em$^r$ compared to tissue from strains infected with WT JE2. Red indicates a decrease level of cytokine production from tissue infected with JE2 Δ*atl*::em$^r$ compared to tissue infected with WT JE2 and black indicates an increase level compared to the WT as indicated by the arrows. Statistical significance denoted as NS for $P > 0.05$, as * for $P \leq 0.05$, as ** for $P \leq 0.01$ and as *** for $P \leq 0.001$. (B) Table summarising cytokines that do not reach statistically significant differences in expression in tissue infected with WT versus *atl*::em$^r$.

### 3.3. Discussion

Our laboratory has previously characterised an essential role for Atl in biofilm formation by a collection of clinical HA-MRSA isolates (38). Atl was found to be essential for the primary attachment stage of biofilm formation by HA-MRSA while the FnBPs were required for the accumulation phase of biofilm formation. MRSA strains formed biofilm independent of PIA production whereas clinical MSSA strains required PIA for biofilm formation on hydrophilic polystyrene. It was reported that the laboratory MSSA strain 8325-4 could form biofilm dependent on both PIA and Atl on hydrophobic polystyrene, indicating that Atl has a role in MSSA biofilm formation that is influenced by surface hydrophobicity. Data presented in this chapter expands on this finding. The laboratory MSSA strain RN4220 exhibited the same biofilm phenotype as that reported for 8325-4, namely a biofilm that was solely PIA dependent on hydrophilic polystyrene and a biofilm on hydrophobic polystyrene that could be mediated by both PIA and Atl. Additional experiments with the *rsbU* repaired derivative of 8325-4, strain SH1000, provided further evidence for a role for Atl in MSSA biofilm formation that was influenced by surface hydrophobicity. SH1000 formed biofilm independent of Atl on hydrophilic polystyrene but required Atl for biofilm formation on hydrophobic polystyrene. Biofilm formation could be restored in the SH1000 Δ*atl* strain by re-introduction of the *atl* gene on pLI50-*tet* thereby directly correlating Atl with SH1000 biofilm formation on hydrophobic surfaces.

Atl can mediate biofilm formation through non-specific interactions with inert surfaces but also mediates biofilm formation through tightly regulated autolytic activity and eDNA release through the activity of the AM and GL domains. Previous work from our laboratory demonstrated that the activity of the AM region of Atl was vital for clinical HA-MRSA biofilm formation (38). Data presented in this chapter demonstrates that the AM region also needs to be enzymatically active for SH1000 to form biofilm on hydrophobic surfaces. Furthermore, the SH1000 biofilm formed on hydrophobic polystyrene was susceptible to treatment with PAS, ProK and DNaseI. This data combined demonstrates that the SH1000 biofilm formed

on hydrophobic polystyrene is dependent on expression of and the activity of Atl, specifically the AM region, for eDNA release and mediating interactions between the cells and the inert surface to initiate biofilm formation. Further correlating a role for Atl-mediated autolytic activity in biofilm formation was the finding that SH1000 Δ*atl* was impaired in triton X-100 induced autolysis, a defect that could be complemented by the *atl* gene. Additionally, the active site mutation of AM on plasmid p*atl*H265A could not substantially restore triton X-100 induced autolysis by SH1000 Δ*atl*. This data suggests that the biofilm defect of this strain is due to the reduced autolytic activity of the AM region. Further evidence for a prominent role for Atl in SH1000 biofilm formation was demonstrated by the ability of antibodies to the AM and GL regions of Atl and not PIA antibodies to significantly inhibit SH1000 biofilm formation on hydrophobic polystyrene.

CA-MRSA strains are emerging as causative agents of DRIs and data presented in this chapter demonstrates an essential role for Atl in CA-MRSA *in vitro* biofilm formation. The CA-MRSA stain JE2 Δ*atl* exhibited reduced biofilm forming capacity on hydrophilic polystyrene which could be complemented by expression of *atl* on pLI50-*tet*. Mutation of the negative regulator of *atl*, *atlR*, retained biofilm levels at those comparable to JE2 wild type. Further implicating a role for Atl in CA-MRSA biofilm formation was the finding that similar to the SH1000 biofilm phenotype, PAS, ProK and DNaseI had inhibitory effects on JE2 biofilm formation. The triton X-100 induced autolysis defect of JE2 Δ*atl* correlated with the defect in biofilm formation exhibited by the strain. JE2 Δ*atlR* exhibited autolytic activity at levels comparable to JE2, correlating with the similar levels of biofilm formation by the two strains. However, overexpression of *atlR* on the pLI50 plasmid could not impair biofilm formation or autolytic activity by JE2. The reason for this might be associated with the observation by Houston *et al* (2011) (38) that the activity of the *atlR* gene is upregulated at 30$^{o}$C. The experiments presented in this chapter were all carried out at 37$^{o}$C for *in vivo* relevance. Therefore the *atlR* gene on pLI50 may not be optimally expressed under the conditions used here. The upregulation of *atlR* at the lower temperature of 30$^{o}$C suggests that this regulator may have

a limited role *in vivo* for regulating *atl*-dependent phenotypes. It may only have a relevant role during colonisation of the skin or anterior nares which are sites where *S. aureus* would encounter temperatures lower than 37$^{o}$C. Alternatively, when *atlR* is overexpressed, other surface proteins may be contributing to biofilm formation. Further investigations are required to determine if AtlR regulates any genes other than *atl*.

In an effort to expand on the work by Bose *et al* (2012) showing a role for the AM and GL regions of Atl in MSSA biofilm formation, active site mutations were constructed in the AM and GL regions of JE2 Atl by Dr Bose. Analysis of biofilm formation by these strains demonstrated that only the GL region significantly contributed to JE2 biofilm formation *in vitro*. This was in contrast to the work conducted with these mutations in the UAMS-1 background, in which both regions were found to significantly contribute to biofilm formation. The AM region was found to contribute more to the triton X-100 induced autolysis of JE2 with the GL mutant exhibiting levels of autolysis comparable to wild type JE2. Similarly, antibodies to the AM region had a more inhibitory effect on JE2 autolysis than GL antibodies. This data indicates that the biofilm defect of the GL mutant may not necessarily be attributed to a loss of GL-mediated autolysis by this strain and may indicate a more important role for non-specific interactions with the polystyrene surface mediated by the GL region in contributing to the JE2 biofilm formation. However, the GL mutation did appear to reduce the level of AM activity expressed by JE2 when assessed by zymograph analysis which could also be a mechanism for the reduced biofilm forming capacity of JE2 ΔGL. Atl antibodies were capable of impairing JE2 biofilm formation, with GL antibodies having a great effect than AM antibodies, further implicating a significant role for Atl in CA-MRSA biofilm formation *in vitro*.

Atl also contributes to the secretion of cytolytic toxins by HA and CA-MRSA strains. As described before by Pasztor *et al* (2010), α-toxin production by BH1CC and JE2 was impaired by mutation in *atl*. Likewise, secretion of δ and β-toxin was affected by mutation of *atl*. This Atl-dependent secretion of cytolytic toxins was found to be directly affected by mutation in *atlR* and could be complemented by overexpression of p*atlR* in

a strain-dependent manner. Atl was shown to affect *hla* expression at the transcriptional level. All of this data combined indicate important roles for Atl in *in vitro* biofilm formation and virulence by clinically relevant *S. aureus* strains. The ability of antibodies to Atl to abolish biofilm formation by both MSSA and CA-MRSA *in vitro* would indicate that targeting Atl-dependent biofilms may have therapeutic potential. However, when assessed *in vivo* using a mouse model of DRIs, *S. aureus* was found to be able to mount a successful infection in the absence of *atl*. A mutation in *atl* did result in some significant differences in colonisation and dissemination of JE2 *in vivo* with significantly reduced numbers of JE2 Δ*atl* able to colonise the surrounding peri-catheter tissue and disseminate to the kidney and the spleen by day seven. Additionally there were some significant differences in the pro-inflammatory response to infection with JE2 Δ*atl* compared to JE2 which most likely correlates with reduced cytolytic α-toxin expression by the *atl* mutant. For example, α-toxin is known to induce expression of the highly pro-inflammatory cytokine IL-1β (371) which was one of the cytokines that was expressed at significantly reduced levels in tissue infected with JE2 Δ*atl* ($P \leq 0.05$, Fig. 3.21 and Table 3.1A). This finding correlates with the downregulated *hla* expression associated with mutation in *atl*. Additionally this result also suggests that altered autolytic activity and rates of cell wall turnover due to the *atl* mutation are contributing to the reduced levels of pro-inflammatory cytokine induction. Cell wall degradation and upregulation of autolysis have previously been shown to induce a pro-inflammatory cytokine response (372, 373). However, some cytokines associated with the pro-inflammatory response were not differentially upregulated between inflammatory responses to infections with the *atl* mutant and JE2. Additionally, bacterial burdens remained high in all organs harvested and by day three there were no significant differences in colonisation and dissemination between any of the *atl* mutants. The loss of the majority of the catheters from the animals by day seven of the longer infection course highlighted the severity of the skin abscesses that formed by infection with all strains. Combined, this data demonstrates that *S. aureus* can develop severe skin abscesses and disseminate and colonise organs at a high rate from the site of infection in

the absence of *atl*. Therefore, despite the *in vitro* relevance for Atl in *S. aureus* biofilm formation and virulence, the findings of the infection model studies indicate that Atl does not contribute to the success of *S. aureus* during a DRI.

The data presented in this chapter highlights the importance of animal models for confirming *in vitro* phenotypes. The *in vitro* role for Atl in *S. aureus* biofilm formation and virulence did not translate to a contributory role during infection of the mice. Work presented in the next chapter was undertaken to try to elucidate the contributory factors to *S. aureus* DRIs and *in vivo* biofilm formation. Alternative protocols for *in vitro* studies of biofilm formation that are more physiologically relevant are described in the next chapter.

# Chapter 4:

# Atl does not contribute to biofilm formation under physiologically relevant conditions

## 4.1 Introduction

The findings presented in chapter three demonstrate how *in vitro* data may not necessarily correlate with *in vivo* phenotypes. The *in vitro* findings of chapter 3, and that of previous publications attribute an essential role to Atl in *S. aureus in vitro* biofilm formation and virulence (38, 57, 368). However, the results of the infection model presented in chapter 3 demonstrated that despite the *in vitro* data, *S. aureus* is capable of developing a successful DRI in the absence of Atl.

Research into biofilm formation by staphylococci has generally involved assessment of the phenotype on artificial surfaces such as glass, polystyrene and other abiotic surfaces without the involvement of any host glycoproteins. Implanted medical devices are rapidly coated with host plasma components that act as receptors for a number of *S. aureus* surface proteins (244). As described in chapter one, the MSCRAMM proteins FnBPA and FnBPB can mediate attachment to surfaces coated with fibronectin, elastin and fibrinogen (187, 189, 190, 192-194, 201), Spa has binding affinity for von Willebrand factor and platelets (209, 210) and the ClfA and B proteins mediate attachment to fibrinogen (85, 117, 120, 121). Likewise, the secreted proteins Eap and Emp can mediate attachment to a variety of host ligands (129, 136-139, 147). Moreover, *in vitro* biofilm assays generally include the use of nutrient rich bacteriological growth media which provides bacteria with nutrients that may otherwise be depleted in the *in vivo* milieu. Recent advances in methodologies have led to the development of sophisticated microfluidic flow cell systems that can add shear stress conditions to *in vitro* biofilm assays, another important stress factor encountered by invading staphylococci that is not generally incorporated into the traditionally static semi-quantitative biofilm assay (374).

To address the issues with conventional *in vitro* biofilm assays and to determine what factors are likely to be critical for biofilm formation *in vivo*, we re-evaluated the semi-quantitative biofilm assay protocol described in chapter 2. Re-design of the biofilm assays was done in collaboration with Dr Marta Zapotoczna and Dr Eoghan O'Neill at RCSI in Dublin. Human

plasma from healthy volunteers was incorporated into the semi-quantitative biofilm assays and the Bioflux 1000Z microfluidic system was used to add biologically-relevant shear stress conditions to the assays as described previously (374). Furthermore, nutrient rich media used for the biofilm assays was replaced with the iron free tissue culture media RPMI-1640 to reflect iron-limitation stress encountered by bacteria *in vivo* (375).

A collection of mutants from the NTML were assessed for biofilm formation under the more physiologically relevant conditions described above. This included mutants of regulators and secreted and surface proteins known to contribute to *in vitro* and/or *in vivo* biofilm formation. Experiments conducted by our collaborators at RCSI revealed that *S. aureus* biofilm formation on surfaces conditioned with platelet-rich and platelet-poor plasma (PRP and PPP respectively) were similar (Zapotoczna, McCarthy *et al.*, submitted) (447) and all subsequent experiments were conducted with PPP. Additionally, optimal biofilm levels in static assays were achieved by growth on 20% v/v plasma in carbonate buffer (Zapotoczna, McCarthy *et al.*, submitted) (447).

## 4.2 Results

### 4.2.1 Atl is not required for *S. aureus* biofilm formation on plasma-coated surfaces

When tested for biofilm formation on human plasma-conditioned surfaces under static conditions in BHI, JE2 and the isogenic *atl* and *atlR* mutants tested in the mouse infection model formed similar levels of biofilm (Fig. 4.1). The defects in biofilm formation exhibited by the *atl* and GL mutants grown in BHI glucose on uncoated plates was restored by growth on 20% v/v PPP and significant increases in biofilm formation were achieved by all strains when grown on plasma ($P < 0.001$, Fig. 4.1). The data demonstrate that JE2 is capable of forming biofilm on plasma in the absence of Atl.

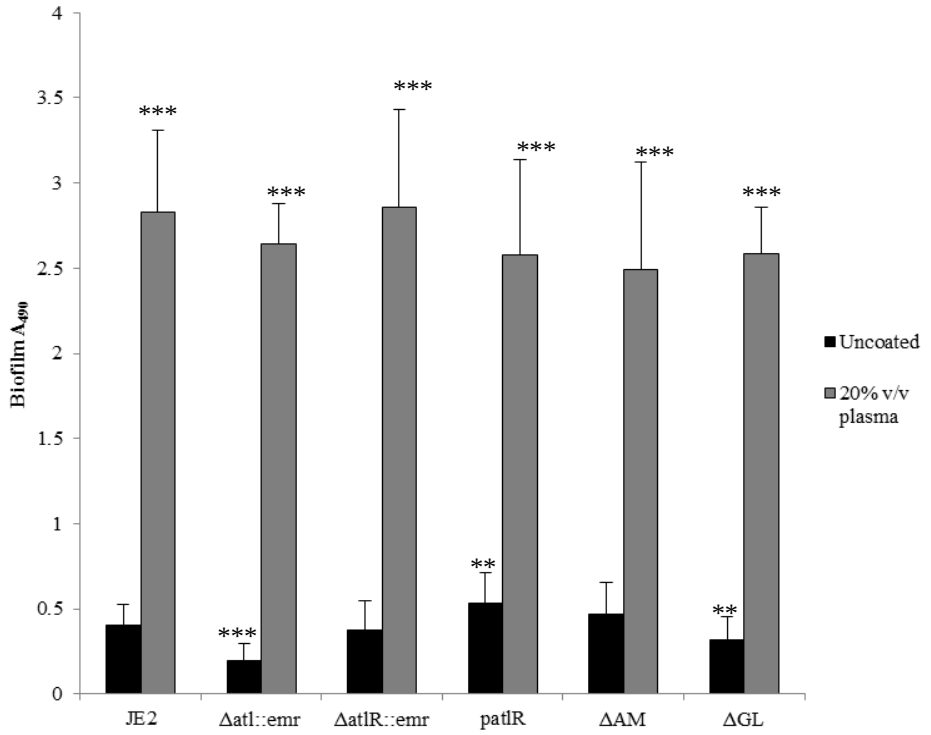


**Fig. 4.1. Biofilm phenotypes of JE2 and JE2 *atl* mutants with and without 20% plasma coating.** Semi-quantitative measurements of biofilm formation under static conditions were performed on hydrophilic 96-well polystyrene plates. Biofilms were grown in BHI 1% glucose on uncoated surfaces and on a plate coated for 1 hr prior to set-up with 20% v/v plasma in the presence of BHI only. Strains were grown for 24 hrs at 37°C in BHI. Results are shown of at least three independent experiments. Comparisons made between: 1) JE2 grown on uncoated plates and the isogenic mutants grown in the same conditions and 2) strains grown on uncoated plates and the same strains grown on 20% plasma. Standard deviations are indicated. Statistical significance denoted as NS for $P > 0.05$, as * for $P < 0.05$, as ** for $P < 0.01$ and as *** for $P < 0.001$.

Biofilm assays were also conducted with human serum. Undiluted serum and serum diluted to 20% v/v in carbonate buffer were used to pre-condition tissue-culture treated plates. As seen in figure 4.2 the six JE2 strains were unable to form substantial levels of biofilm on either 100% or 20% v/v serum-coated polystyrene whereas significant increases in biofilm formation were achieved by all strains when grown on surfaces conditioned with 20% v/v PPP ($P < 0.001$). This finding indicates that the increase in biofilm formation observed on surfaces pre-treated with 20% v/v PPP is specifically dependent on proteins present in plasma and not in serum.

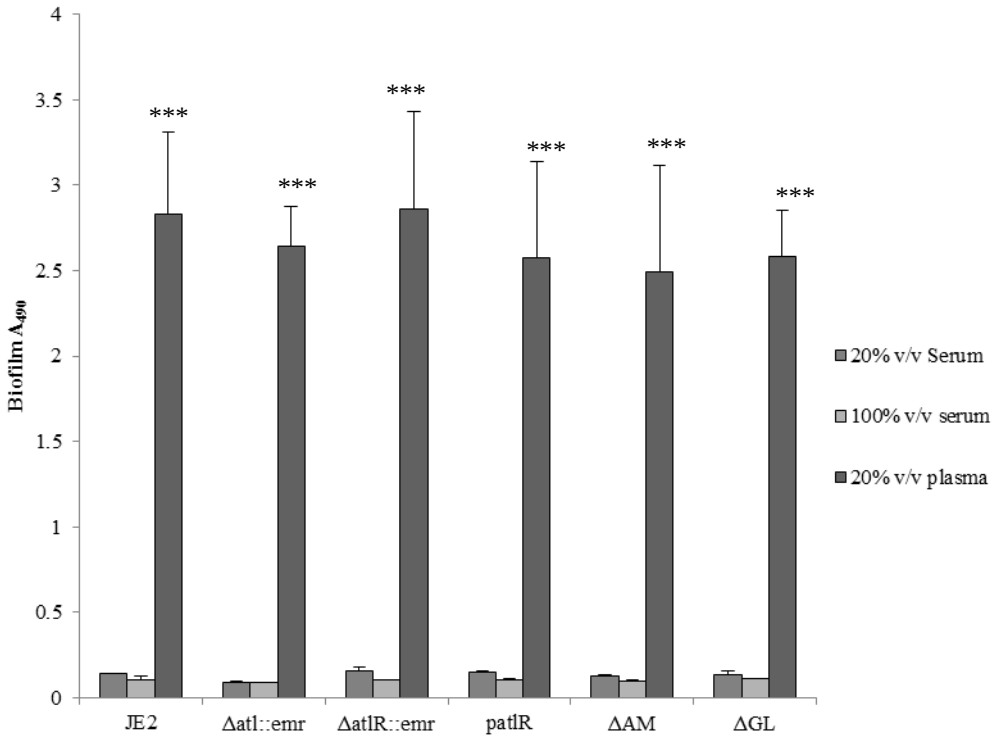


**Fig. 4.2. Biofilm phenotypes of JE2 and JE2 *atl* mutants with 100% serum coating, 20% serum coating and 20% plasma coating.** Semi-quantitative measurements of biofilm formation under static conditions were performed in Nunclon tissue culture treated 96-well polystyrene plates. Biofilms were grown in BHI on a plate coated for 1 hr prior to set up with either 10% serum, 20% serum or 20% v/v plasma in the presence of BHI only. Strains were grown for 24 hrs at 37°C in BHI. Results are shown of at least three independent experiments, except for those carried out with serum, which are from a single data set. Comparisons made between strains grown on 20% serum and isogenic strains grown on 20% plasma. Standard deviations are indicated. Statistical significance denoted as NS for $P > 0.05$, as * for $P < 0.05$, as ** for $P < 0.01$ and as *** for $P < 0.001$.

The findings of chapter 3 and those of P. Houston, *et al*. (38) demonstrate a critical role for Atl in *in vitro* biofilm formation by the HA-MRSA strain BH1CC. To determine if the restoration of biofilm formation by the JE2 Δ*atl* strain is strain specific, the collection of BH1CC *atl* and *atlR* mutants from chapter 3 were assessed for static biofilm formation on 20% v/v PPP. Additionally, the fibronectin binding proteins have been shown to contribute to the accumulation stage of BH1CC biofilm formation (38, 90). These proteins are known to bind to the extracellular matrix proteins fibronectin, elastin and fibrinogen (187, 189, 190, 192-194, 201). Therefore the BH1CC Δ*fnbpAB* mutant was also assessed for biofilm formation on 20% v/v PPP. As seen in figure 4.3, and correlating with the data in figure 4.1, the defect in biofilm formation by the BH1CC Δ*atl* strain grown on uncoated plates was restored by growth on 20% v/v PPP. All BH1CC strains grown on 20% v/v PPP exhibited a significant increase in biofilm formation. The biofilm formed by BH1CC on 20% v/v PPP appears to be independent of the FnBPs as biofilm formation by the double FnBP mutant is restored to significantly increased levels by growth on plasma (Fig. 4.3).

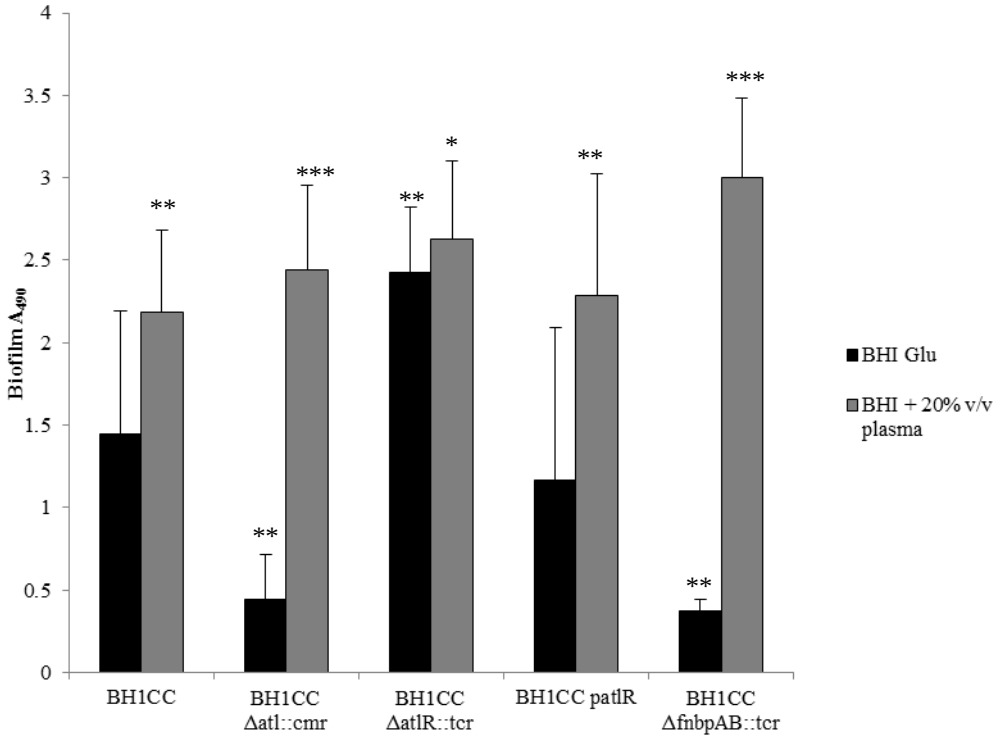


**Fig. 4.3. Biofilm formation of BH1CC with and without 20% plasma coating.** Semi-quantitative measurements of biofilm formation under static conditions were performed in Nunclon tissue culture treated 96-well polystyrene plates coated for 1 hr prior to set-up with 20% v/v plasma. Strains were grown for 24 hrs at 37°C in BHI. Results are shown of at least three independent experiments. Comparisons made between: 1) BH1CC and isogenic mutants grown on uncoated plates and 2) strains grown on uncoated plates and the strains grown on 20% plasma. Standard deviations are indicated. Statistical significance denoted as NS for $P > 0.05$, as * for $P < 0.05$, as ** for $P < 0.01$ and as *** for $P < 0.001$.

In order to determine what factors may be contributing to biofilm formation on plasma, biofilm inhibition and dispersal assays were conducted as described in chapter 2. DNaseI, ProK and PAS all inhibited JE2 biofilm formation on 20% v/v PPP (Fig. 4.4). Because eDNA and autolysis were found to significantly contribute ($P<0.001$), this data would indicate an important role for autolytic activity in the JE2 biofilm phenotype on plasma. However, the data from figure 4.1 shows that JE2 is capable of biofilm formation on plasma in the absence of *atl*. Therefore, it appears that there may be compensatory mechanisms of biofilm formation on plasma-conditioned surfaces and/or other factors that regulate autolysis beyond Atl which could be vital for biofilm formation under these conditions. ProK also dispersed JE2 biofilm formation on 20% v/v PPP indicating a vital role for protein adhesins in this biofilm phenotype (Fig. 4.4). Impairment of biofilm formation on plasma by ProK would not be specific to a role for Atl in the

biofilm and may indicate a role for other proteins or the protein components of the plasma. SM was unable to abolish biofilm formation by any of the JE2 strains, suggesting that the biofilm formation on plasma is independent of PIA production (Fig. 4.4).

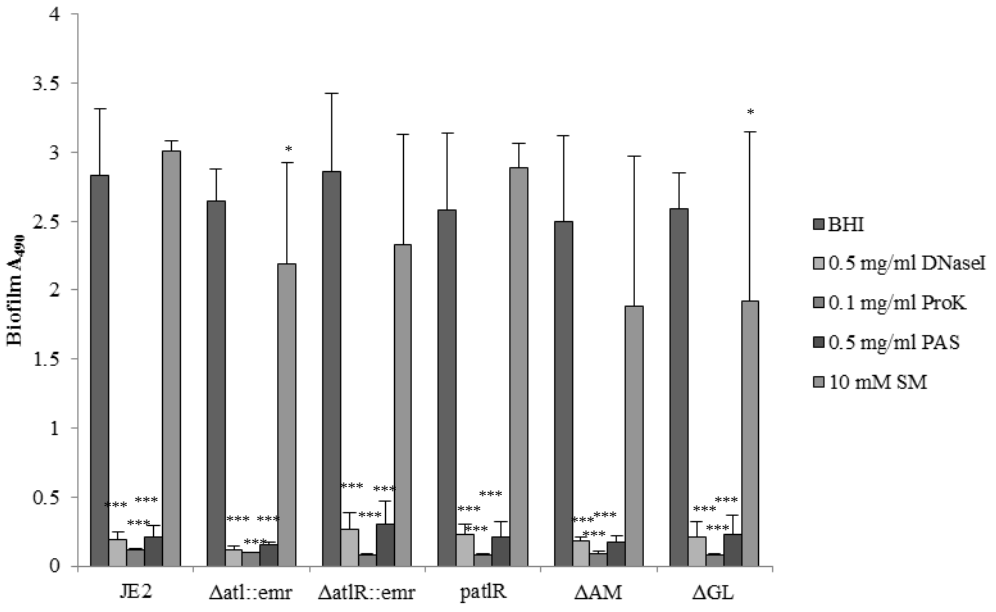


**Fig. 4.4. Biofilm phenotypes of JE2 and JE2 *atl* mutants with 20% plasma coating.** Semi-quantitative measurements of biofilm formation under static conditions were performed in Nunclon tissue culture treated 96-well polystyrene plates. Biofilms were grown in BHI supplemented with 0.5 mg/ml DNaseI, 0.1 mg/ml ProK, 0.5 mg/ml PAS and 10 mM SM where indicated on a plate coated for 1 hr prior to set-up with 20% v/v plasma in the presence of BHI only. Strains were grown for 24 hrs at 37°C in BHI. Results are shown of at least three independent experiments. Comparisons made between: 1) untreated controls and the untreated parent JE2 strain and 2) untreated controls and the different treatments. Standard deviations are indicated. Statistical significance denoted as NS for $P > 0.05$, as * for $P < 0.05$, as ** for $P < 0.01$ and as *** for $P < 0.001$.

Further evidence that the biofilm formed on plasma is independent of Atl came from antibody inhibition assays. As noted in Chapter 3, JE2 biofilms grown on uncoated plates were inhibited up to 76% using a combination of both AM and GL antibodies (Fig. 3.10). However, Atl antibodies had no inhibitory effect on JE2 biofilms grown on plates conditioned with 20% v/v PPP (Fig. 4.5).

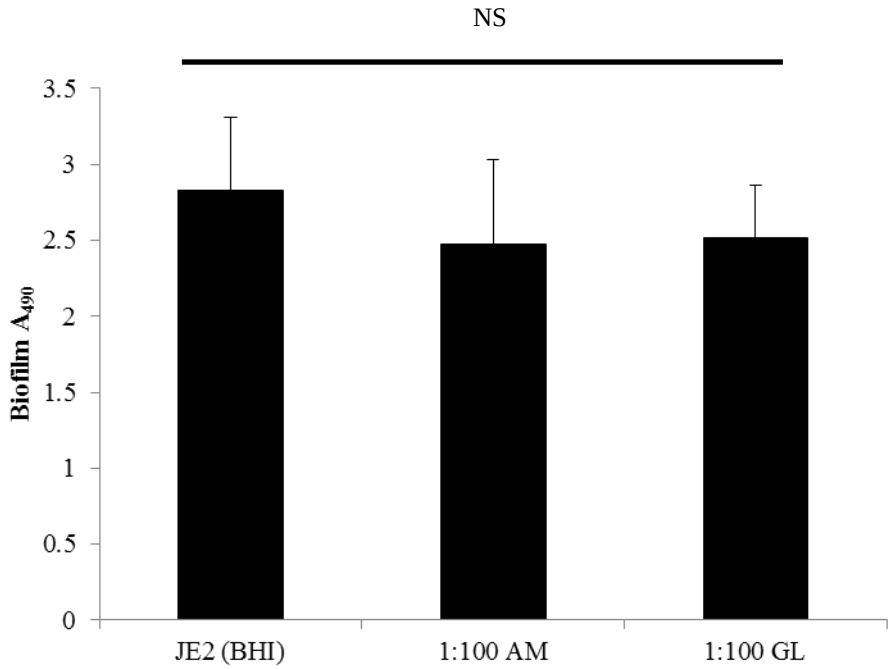


**Fig. 4.5. Biofilm phenotypes of JE2 in the presence of Atl antibodies with 20% plasma coating.** Semi-quantitative measurements of biofilm formation under static conditions were performed in Nunclon tissue culture treated 96-well polystyrene plates. Biofilms were grown in BHI supplemented with 1:100 anti-AM and 1:100 anti-GL antibodies where indicated on a plate coated for 1 hr prior to set-up with 20% v/v plasma in the presence of BHI only. Strains were grown for 24 hrs at 37°C in BHI. Results are shown of at least three independent experiments. Standard deviations are indicated. Statistical significance denoted as NS for $P > 0.05$, as * for $P < 0.05$, as ** for $P < 0.01$ and as *** for $P < 0.001$.

### 4.2.2 A double *atl srtA* mutation reduces biofilm forming capacity of JE2 on plasma under physiologically relevant conditions but does not completely abolish biofilm formation

In an attempt to elucidate the critical factors for biofilm formation under physiologically relevant conditions a double *atl srtA* mutant was constructed in JE2 using phage 80α as described in chapter 2. Biofilm formation under shear flow conditions was assessed using the BioFlux 1000Z microfluidic system. A shear flow rate of 0.6 dy/cm$^2$ was applied to the system which enabled experimental run times of 18 hours. Plates were pre-treated with undiluted human plasma and RPMI-1640 media was used as an alternative to BHI to create iron limited conditions. Under these physiologically relevant conditions JE2 Δ*atl srtA* exhibited reduced biofilm forming capacity compared to JE2 wild type (Fig. 4.6). The mutant was not defective in primary attachment to the plasma-coated BioFlux plate and could sustain this attachment throughout the 18 hour run. However, cellular aggregation and accumulation were visibly reduced in the double mutant compared to

the wild type JE2. Attempts to create a triple *atl srtA ica* mutant by phage transduction were unsuccessful, perhaps because phage infection of the *atl srtA* mutant was affected.

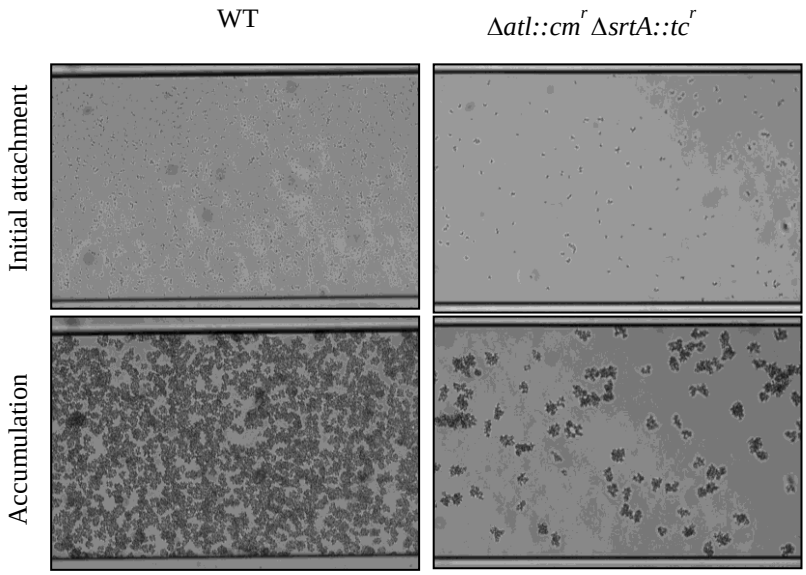


**Fig. 4.6. Biofilm formation by JE2 and JE2 Δ*atl::cm*$^r$ Δ*srtA::tc*$^r$ under physiologically relevant conditions.** Strains were grown in RPMI-1640 media and exposed to a shear flow rate of 0.6 dynes/cm$^2$ for 18 hours (equivalent to 64µl/hour) at 37$^o$C in the BioFlux 1000Z instrument. Plates were coated with undiluted human plasma. Brightfield images captured at 10X magnification are representative of at least two independent experiments.

### 4.2.3 The two component regulatory system SaeRS is essential for biofilm formation on plasma-coated surfaces

To reveal what factors may be critical for biofilm formation on plasma-coated surfaces, a collection of mutants from the NTML were assessed for biofilm formation under physiologically relevant conditions. These mutants are listed in table 4.1 and include mutants in global virulence regulators and individual proteins that are known to be involved in biofilm formation.

**Table 4.1:**

**Transposon mutants from the NTML screened for biofilm formation under physiologically relevant conditions**

| | Gene name | Protein name | Reference |
|---|---|---|---|
| **1.** | *atl* | Major autolysin | (38, 57) |
| **2.** | *icaA* | Intercellular adhesin protein A of the *icaADBC* operon | (154-156) |
| **3.** | *fnbpA* | Fibronectin binding protein A | (90) |
| **4.** | *fnbpB* | Fibronectin binding protein B | (90) |
| **5.** | *clfA* | Clumping factor A | (117, 126) |
| **6.** | *clfB* | Clumping factor B | (85) |
| **7.** | *eap* | Extracellular adherence protein | (136, 140, 141) |
| **8.** | *emp* | Extracellular matrix binding protein | (141) |
| **9.** | *srtA* | Sortase A | (90) |
| **10.** | *srtB* | Sortase B | (108, 110) |
| **11.** | *spa* | Protein A | (91) |
| **12.** | *nuc* | Thermonuclease | (59) |
| **13.** | *sarA* | Staphylococcal accessory regulator A | (28, 251, 254, 274) |
| **14.** | *fur* | Ferrick uptake regulator protein | (141, 270) |
| **15.** | *saeS* | *S. aureus* exoprotein expression histidine kinase | (141) |
| **16.** | *agrC* | Accessory gene regulator sensor kinase | (61, 148, 239) |

As part of a collaboration with Dr Zapotoczna and Dr O'Neill of RCSI, screening of the NTML mutants by static biofilm assays was conducted with TSB media (as an alternative to BHI) and the iron-free RPMI-1640 media on 20% v/v PPP. In TSB the factors found to most significantly contribute to biofilm formation on plasma ($P < 0.001$) were ClfA, SrtA and SarA (Fig. 4.7A). These results support previous findings regarding roles for ClfA (126), SrtA (90) and SarA (251, 252, 274) in biofilm formation in nutrient rich media. However, as with the screens of various *atl* mutants in section 4.2.1, other factors that were previously reported as being critical for biofilm were not found to be vital for JE2 biofilm formation on plasma when grown in TSB (Fig. 4.7A). In contrast, growth in RPMI-1640 was associated with lower levels of biofilm production by the NTML strains compared to growth in TSB and no defect in biofilm formation under static conditions was identified for the collection of mutants grown in RPMI-1640 (Fig. 4.7B). RPMI-1640 medium is commonly used during tissue culture and is more representative than TSB or BHI for reflecting the *in vivo* nutrient environment that is encountered by invading staphylococci. When grown in RPMI-1640, all of the mutants produced higher levels of biofilm than the parent JE2. This may indicate that there are multiple mechanisms of biofilm formation operating under these growth conditions.

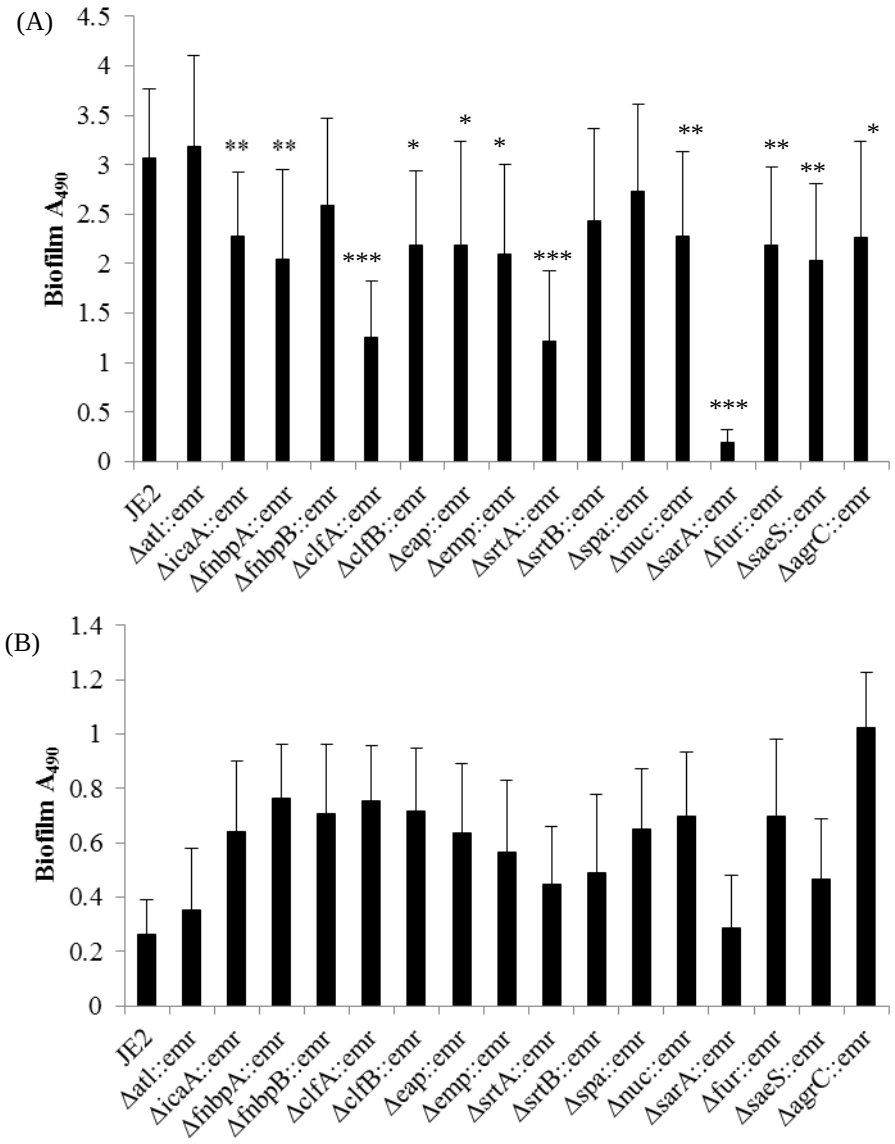


**Fig. 4.7. Biofilm phenotypes of JE2 transposon mutants on plasma-coated plate.** Strains were grown on hydrophilic polystyrene Nunc 96-well plates in (A) TSB and (B) RPMI-1640 at 37°C for 24 hours. Plates were coated with 20% v/v/ plasma for 1 hour prior to experimental set-up. Results are shown of at least three independent experiments. Standard deviations indicated. Statistical significance denoted as NS for $P > 0.05$, as * for $P < 0.05$, as ** for $P < 0.01$ and as *** for $P < 0.001$.

As mentioned in section 4.2.2, the BioFlux 1000Z microfluidic system was used to incorporate shear flow conditions into the experimental design and make the *in vitro* assays as physiologically relevant as possible. Screening of the mutants listed in table 4.1 on plasma coated surfaces in RPMI-1640 media using the BioFlux system revealed some differences in the biofilm phenotypes compared to nutrient rich media but none were biofilm negative (Fig. 4.8). The *atl* mutant for example produced large clumps during biofilm

formation under these conditions, a trait commonly reported for *atl* mutants (45, 57).

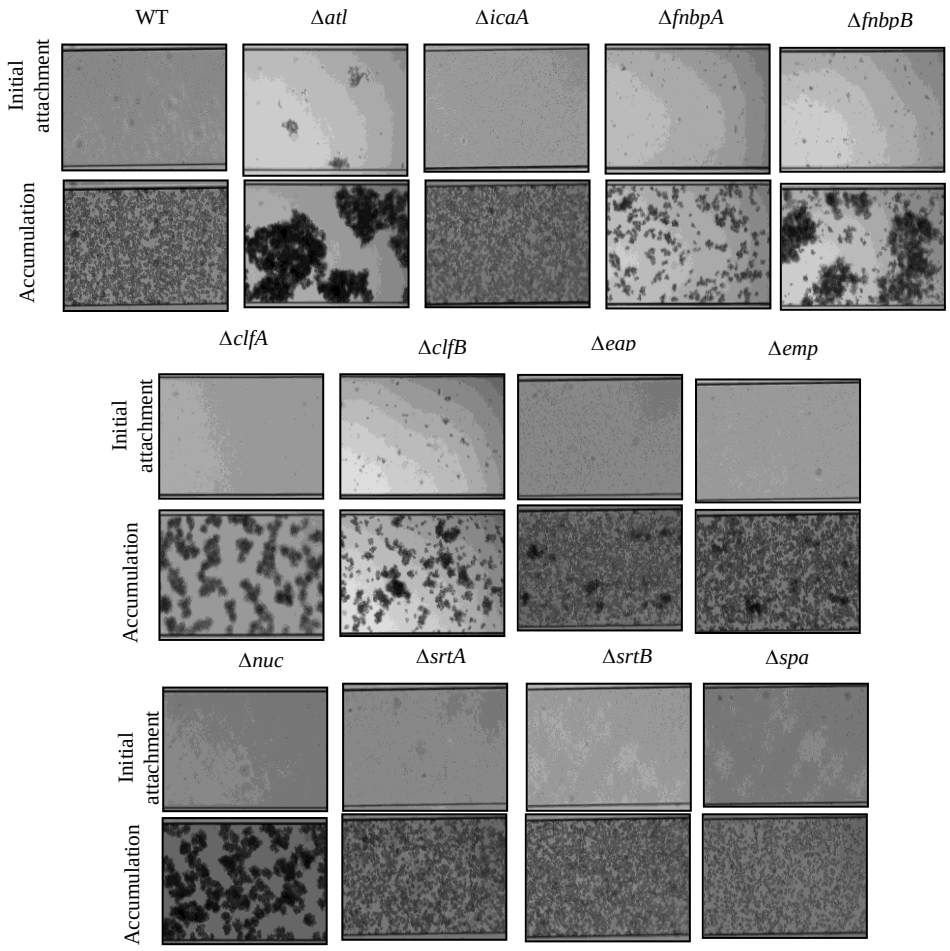


**Fig. 4.8. Attachment and accumulation of JE2 biofilm on human plasma under physiologically relevant conditions**. Strains from the Nebraska Transposon Mutant Library were grown in RPMI-1640 media and exposed to a shear flow rate of 0.6 dynes/cm$^2$ for 18 hrs (equivalent to 64µl/hr) at 37$^o$C in the BioFlux 1000Z instrument. Plates were coated with undiluted human plasma. Brightfield images captured at 10X magnification are representative of at least two independent experiments.

A subsequent screen of the global virulence regulators known to be involved in biofilm formation revealed the *saeS* mutant to be defective in biofilm formation (Fig. 4.9). SaeS was found to be the only factor absolutely critical for attachment and biofilm formation in RPMI-1640 media on plasma-coated surfaces under physiologically relevant shear. Only towards the end of the 18 hour experiments was JE2 Δ*saeS* able to sustain a low level of attachment to the edges of the chambers of the BioFlux plates. This may be due to the plasma conditioning film deteriorating over the 18 hour period at

37°C. All other regulator mutants were capable of biofilm formation under these conditions (Fig. 4.9).

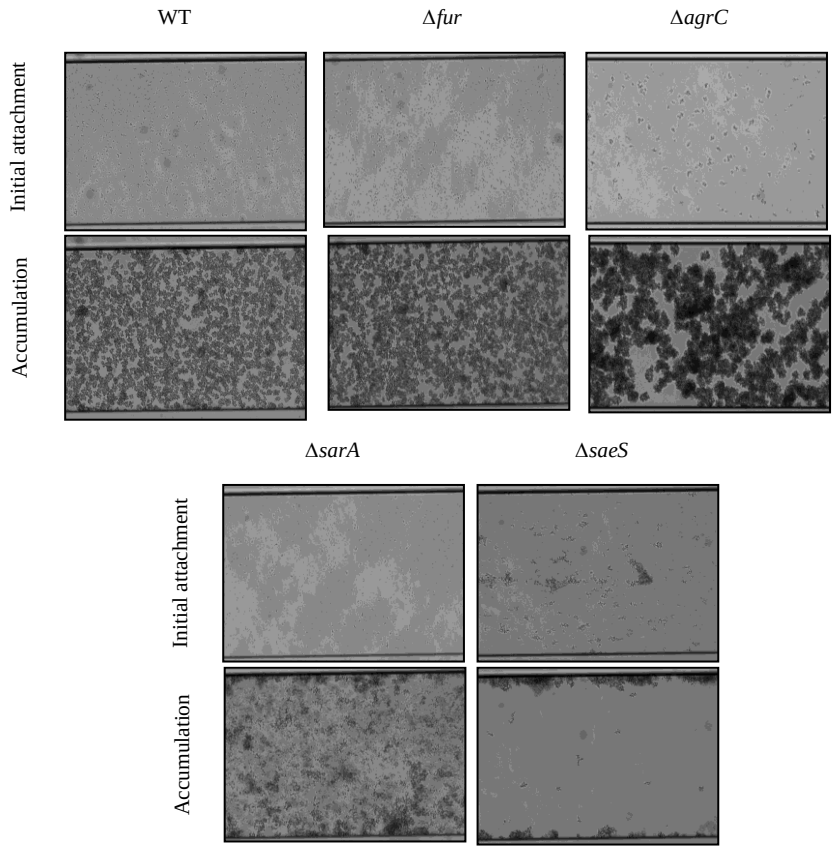


**Fig. 4.9. Initial attachment and subsequent biofilm formation by JE2 transposon mutants of global regulators under physiologically relevant conditions**. Strains from the Nebraska Transposon Mutant Library were grown in RPMI-1640 media and exposed to a shear flow rate of 0.6 dynes/cm$^2$ for 18 hrs (equivalent to 64µl/hr) at 37°C in the BioFlux 1000Z instrument. Plates were coated with undiluted human plasma. Brightfield images captured at 10X magnification are representative of at least two independent experiments.

Next *saePQRS* mutants in various genetic backgrounds were tested for biofilm formation on plasma-coated surfaces. No significant differences in biofilm formation were observed between the clinical MSSA isolate UAMS-1 and the CA-MRSA strains USA300 LAC and MW2 and their isogenic *saePQRS* mutants grown statically in TSB on 20% v/v PPP (Fig. 4.10A). This was consistent with the initial screen of the NTML strains under these conditions where ClfA, SrtA and SarA were found to be most important for biofilm formation (Fig. 4.7A). Static growth in RPMI-1640 media on 20% v/v PPP did yield some significant differences between the various *saePQRS* mutants (Fig. 4.10B). There was a significant decrease in biofilm formation by the UAMS-1 Δ*saePQRS* strain compared to the parent

strain (P < 0.01, Fig. 4.10B). Likewise, the MW2 Δ*saePQRS* strain produced significantly less biofilm in RPMI-1640 than the parent MW2 strain (P < 0.01, Fig. 4.10B). However, biofilm formation was not completely impaired in these strains under these conditions and JE2 and USA300 LAC had no statistically significant differences in biofilm forming capacity with their isogenic *saePQRS* mutants, which was consistent with the initial screen of the NTML strains (Fig. 4.10B and 4.7B). The complemented strain of MW2 Δ*saePQRS* exhibited reduced levels of biofilm formation that reached statistical significance in RPMI-1640 (P < 0.001, Fig. 4.10B), however this strain, as with the other *saePQRS* mutants that showed reduced biofilm forming capacity, was not defective in biofilm production and remained biofilm positive under these conditions.

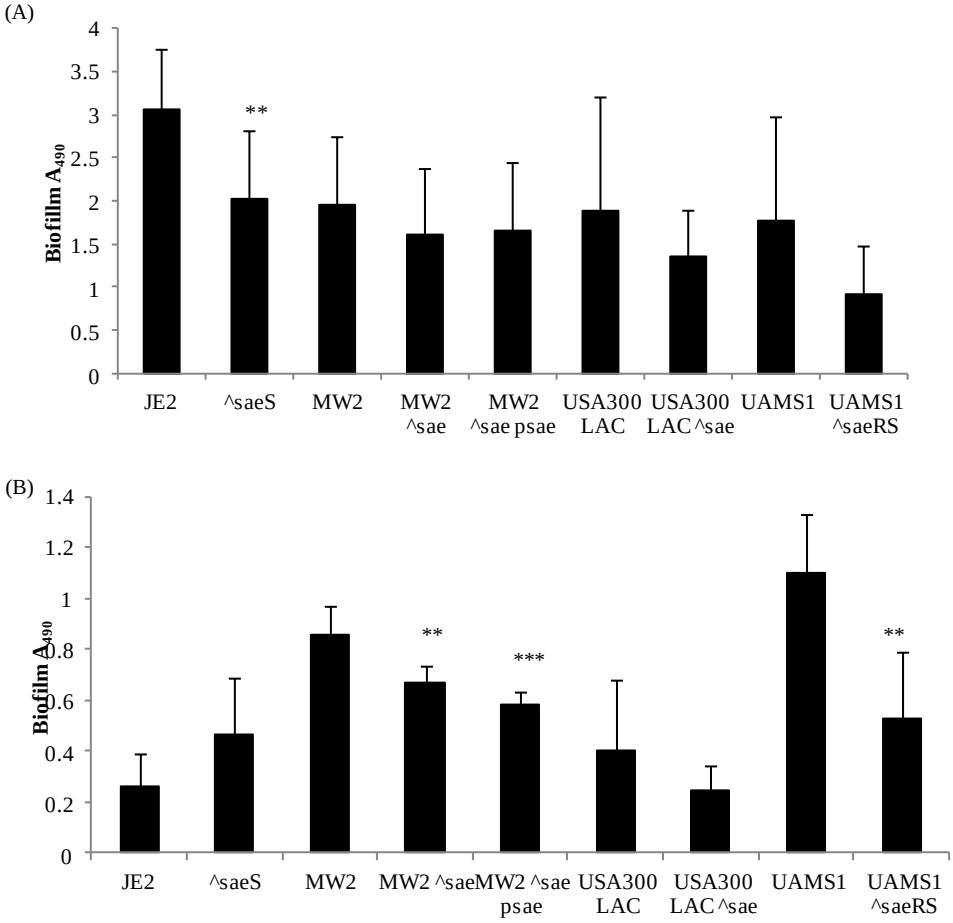


**Fig. 4.10. Biofilm phenotypes of *saePQRS* mutants in various genetic backgrounds on plasma-coated plate.** Strains were grown on hydrophilic polystyrene Nunc 96-well plates in (A) TSB and (B) RPMI-1640 at 37°C for 24 hrs. Plates were coated with 20% v/v plasma for 1 hr prior to experimental set-up. Results are shown of at least two independent experiments. Comparisons made between wild type strains and their isogenic *sae* mutants. Standard deviations indicated. Statistical significance denoted as NS for P > 0.05, as * for P < 0.05, as ** for P < 0.01 and as *** for P < 0.001.

Next the UAMS-1, USA300 LAC and MW2 strains and their isogenic *saePQRS* mutants were tested for biofilm formation under shear flow in the BioFlux instrument on plasma-conditioned surfaces in RPMI-1640 media. Consistent with the JE2 Δ*saeS* biofilm defect (Fig. 4.9), all of the *saePQRS* mutants exhibited a biofilm defect and were found to be defective in primary attachment and subsequent biofilm formation on the plasma-coated surface (Fig. 4.11). Further evidence for a direct role for *saePQRS* in *S. aureus* biofilm formation under these physiologically relevant conditions was the successful complementation of the biofilm defect of the MW2 Δ*saePQRS* strain with p*sae* plasmid (Fig. 4.11C). As with the JE2 Δ*saeS* phenotype (Fig. 4.9), all of the mutants were capable of attaching to the edges of the chambers of the BioFlux plates at low levels by the end of the 18 hour-long experiments, which may be due to the plasma conditioning film deteriorating towards the end of the experimental time course.

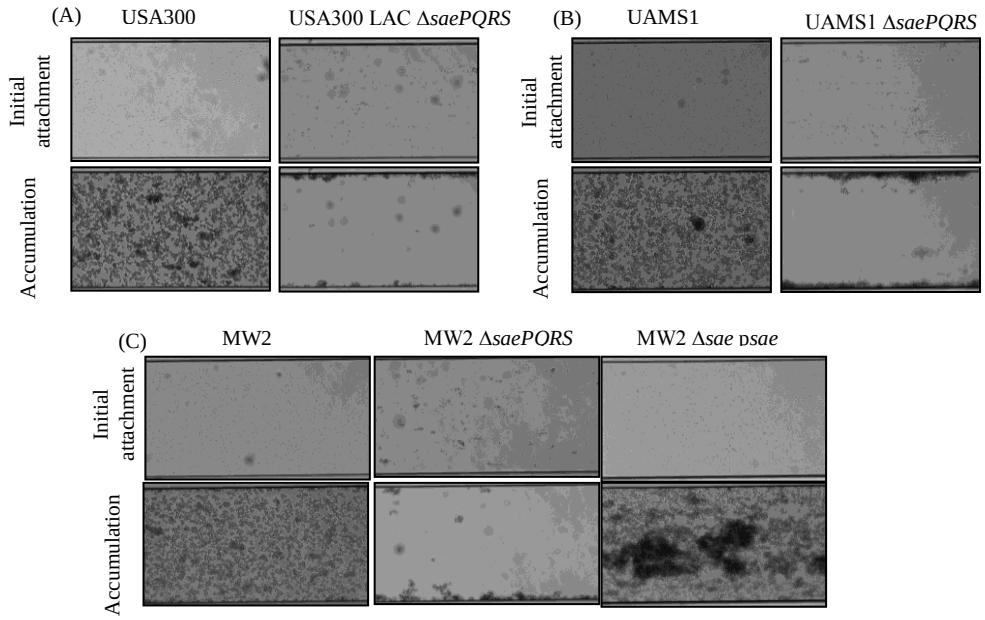


**Fig. 4.11. *saePQRS* contribution to biofilm formation in various *S. aureus* genetic backgrounds under physiologically relevant conditions**. Wild type and *sae* knock out strains of (A) USA300 LAC (B), UAMS1 (C) and MW2 were grown in RPMI-1640 media and exposed to a shear flow rate of 0.6 dynes/cm$^2$ for 18 hrs (equivalent to 64µl/hr) at 37$^o$C in the BioFlux 1000Z instrument. Plates were coated with undiluted human plasma. Brightfield images captured at 10X magnification are representative of at least two independent experiments.

### 4.2.4 Coagulase is the critical factor regulated by Sae for biofilm formation under physiologically relevant conditions

SaeRS is a two component system that is involved in global virulence gene regulation. One factor regulated by SaeRS that was not incorporated into the initial screen from the NTML was coagulase (Coa) (376). Coa is tightly regulated by SaeRS and is required for formation of the staphylothrombin complex which occurs through interaction between Coa and the host's prothrombin (377, 378). The staphylothrombin complex cleaves soluble fibrinogen to insoluble fibrin which aids clot formation and cellular aggregation during infection. Fibrinogen is a prominent factor present in plasma so the JE2 Δ*coa* mutant from the NTML was screened for biofilm formation under the physiologically relevant conditions. Another coagulase mutant was pulled from the library for screening, namely JE2 Δ*vwbp* which has a mutation in the von Willebrand factor-binding protein (vWbp). The recently identified vWbp also activates clot formation by activating host prothrombin and stimulating the formation of fibrin cables (377, 378). Both the *coa* and the *vwbp* mutants were assessed for biofilm formation under the physiologically relevant conditions of growth on plasma in RPMI-1640 and under shear flow. Under the physiologically relevant conditions only the *coa* mutant exhibited a biofilm defect similar to the *sae* mutants (Fig. 4.12). As with the *sae* mutations, Coa was critical for primary attachment to the plasma and JE2 Δ*coa* was unable to develop a biofilm under the physiologically relevant conditions (Fig. 4.12). In contrast to the critical role for Coa, the *vwbp* mutant was able to form biofilm under the physiologically relevant conditions. Coa therefore appears to be the sole critical factor that is regulated by SaeRS for biofilm formation under physiologically relevant conditions. This data indicates that the conversion of soluble fibrinogen to insoluble fibrin by Coa is essential for biofilm formation under the physiologically relevant conditions. Experiments to validate this finding by adding exogenous fibrin to the experiments conducted in the BioFlux system were unsuccessful and require further technical optimisation.

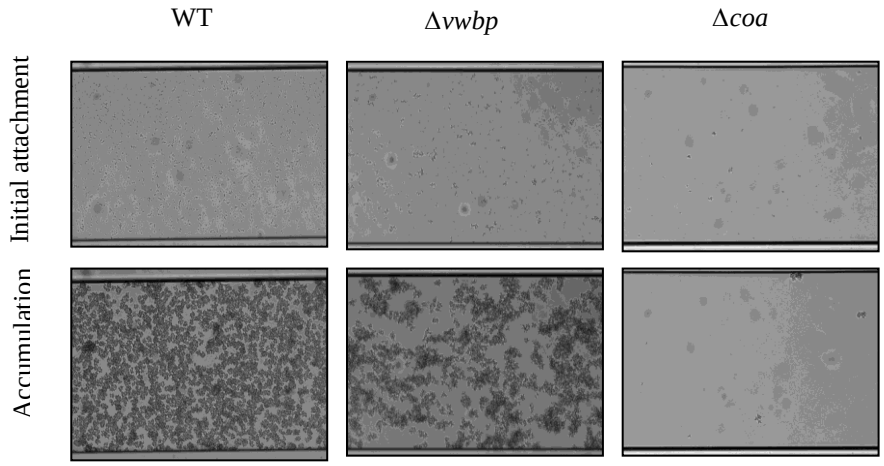


**Fig. 4.12. Biofilm formation by JE2 and JE2 Δ*vwbp::em*$^r$ and JE2 Δ*coa::em*$^r$ under physiologically relevant conditions.** Strains were grown in RPMI-1640 media and exposed to a shear flow rate of 0.6 dynes/cm$^2$ for 18 hrs (equivalent to 64µl/hr) at 37$^o$C in the BioFlux 1000Z instrument. Plates were coated with undiluted human plasma. Brightfield images captured at 10X magnification are representative of three independent experiments.

## 4.3 Discussion

Biofilm-associated infections are influenced by characteristics of the invading staphylococci and of the implanted biomaterial. Conventional *in vitro* assays for assessing essential factors for *S. aureus* biofilm formation typically involve inducing biofilm formation in nutrient rich broth with glucose or sodium chloride supplementation (90, 254). Additionally, *in vitro* biofilm assays are generally conducted on untreated or tissue-culture treated polystyrene without the incorporation of any host ligands (244). Implanted biomaterial is rapidly coated with host ligands with which *S. aureus* interacts during infection to establish biofilms (244). Therefore the *in vivo* relevance of these conventional *in vitro* assays is questionable. The findings presented in chapter three highlight how phenotypes characterised by *in vitro* biofilm assays may not always correlate with phenotypes from *in vivo* experiments. In an effort to elucidate the relevant mechanisms of *in vivo* biofilm formation by *S. aureus*, we re-designed the *in vitro* biofilm assay to be as relevant to the *in vivo* situation as possible. Our first step towards designing physiologically relevant *in vitro* assays involved coating 96-well plates with 20% v/v human plasma. When JE2 and the isogenic *atl* and *atlR* mutants examined in the mouse model of device-related infections in

chapter three were assessed for biofilm formation on 20% v/v plasma, all of the strains produced significantly increased levels of biofilm and the defects in biofilm formation by the *atl* and GL mutants on uncoated plates were restored. The data from this experiment and the experiment conducted with the characterised BH1CC *atl* and *atlR* mutants (38) demonstrated that Atl is not required for biofilm formation on plasma-coated surfaces. Additionally, a previously characterised BH1CC Δ*fnbpAB* mutant (38) had its biofilm forming capacity restored on 20% v/v plasma. This data questions the relevance of previous *in vitro* data that characterised certain factors as essential for *S. aureus* biofilm formation.

The biofilm phenotype on plasma was found to be specific to plasma proteins as growth on serum could not promote biofilm formation by the JE2 strains. Further characterisation of the JE2 biofilm phenotype on plasma demonstrated roles for autolysis, eDNA and protein adhesins but not PIA in the biofilm phenotype. The detrimental effects of DNaseI and PAS on JE2 biofilm formation and the restoration of biofilm formation by JE2 Δ*atl* on plasma indicate that perhaps JE2 can use multiple mechanisms of biofilm formation on plasma-coated surfaces that can compensate for each other upon inhibition. Other peptidoglycan hydrolases may be upregulated during growth on plasma in the absence of *atl* that could regulate autolysis and eDNA release to aid biofilm formation. For example LytM is a glycine-glycine endopeptidase that is overexpressed in an autolysis defective mutant and has affinity for a cleavage site in peptidoglycan similar to lysostaphin within the pentaglycine interpeptide bridge (43, 379). LytN is another peptidoglycan hydrolase that possesses amidase and endopeptidase activities (49). It is possible that LytM and/or LytN may be upregulated during growth on plasma in the absence of *atl* and could be regulating autolysis and eDNA release to mediate biofilm formation. Further experiments would be required to determine if these possible compensatory mechanisms of autolysis and eDNA release are employed by *S. aureus* when grown on plasma in the absence of *atl*.

Optimisation of the physiologically relevant assay led to the design of an assay that incorporated low-iron and shear stress conditions. RPMI-1640 was used as an alternative to nutrient rich BHI or TSB media. RPMI-1640 is

free of iron but contains amino acids, vitamins, inorganic salts and glucose at concentrations that are akin to *in vivo* conditions. Low iron conditions created by growth in RPMI-1640 would induce upregulation of siderophores and the Isd proteins which would be more reflective of the *in vivo* situation encountered by invading staphylococci (380-382). Conducting experiments in the BioFlux 1000Z microfluidic system enabled experiments to be carried out under biologically relevant continuous-flow conditions (374). Coating of the BioFlux plates with undiluted human plasma was the final modification that made these assays physiologically relevant.

Initial attempts to clarify the mechanisms for biofilm formation on plasma involved constructing a double *atl srtA* mutant in JE2. This mutant had reduced biofilm forming capacity under physiologically relevant conditions in RPMI-1640 media and under shear flow conditions. JE2 Δ*atl srtA* was defective in the accumulation phase of biofilm formation but was capable of attaching to the plasma-coated surface and maintaining this attachment throughout the experiment. This finding, similar to the inhibitory effects of PAS and DNaseI on the JE2 biofilm grown on plasma-coated plates highlights the complexity of the biofilm phenotype on plasma-coated surfaces and additional work is required to fully elucidate possible roles for autolysis and extracellular DNA in this biofilm phenotype. To address the concept that multiple mechanisms of biofilm formation may be employed during growth on plasma, attempts were made to construct a triple *atl srtA icaADBC* mutant. However, these transductions were unsuccessful, which may be due to the altered cell wall structure of the double *atl srtA* mutant that might render the cells less susceptible to infection by phage 80α. It would be interesting to see if introduction of Δ*icaADBC* into the double mutant would be sufficient to abolish attachment and accumulation under the physiologically relevant conditions.

As part of a collaboration with Dr Zapotoczna and Dr O'Neill at RCSI, a collection of transposon mutants from the NTML were assessed for biofilm formation under the physiologically relevant conditions. Assessment of biofilm formation by the collection of mutants with static assays performed on plasma coating in TSB validated previous findings and attributed biofilm formation to ClfA (126) and SrtA (90) with SarA (251, 252, 274) found to

be essential for this biofilm phenotype. However, some previously described factors essential for biofilm formation were not found to be required for biofilm formation on plasma in TSB. Similarly, no defects in biofilm formation were found when the collection of NTML strains was grown statically in RPMI-1640 on plasma. Only when growth was performed in RPMI-1640 media under shear flow was a critical factor for biofilm formation found, namely the histidine kinase SaeS of the SaeRS two component system (TCS). A possible explanation for the absence of a role for Sae for biofilm formation on plasma-coated surfaces in the TSB medium may be the inhibitory effect of glucose and mildly acidic conditions on *sae* expression (383, 384). The role for the SaeRS TCS in *S. aureus* biofilm formation on plasma was validated using *saePQRS* mutants in other strain backgrounds under the same physiologically relevant conditions. The *saePQRS* system is a global regulator of virulence *in vivo* and controls expression of virulence factors such as of α and β-haemolysin, Spa, FnBPA and Coa (385-387). The *sae* regulatory system consists of a histidine kinase (SaeS), a response regulator (SaeR), a membrane protein (SaeQ) and a lipoprotein (SaeP) (388). The Sae system has previously been shown to positively regulate biofilm formation *in vitro* via upregulation of the secreted proteins Eap and Emp under iron-restricted conditions (141, 271, 383). However, no critical role for Eap or Emp was found under the conditions used in this study. Previous studies describing a Sae-dependent role for Eap and Emp during biofilm formation were conducted in the Newman background. Newman expresses truncated forms of both the FnBP proteins that interfere with correct LPXTG-anchorage of the proteins to the cell surface and disrupts FnPB-dependent functions by this strain (142). Therefore, in our system a critical role for either Eap or Emp could be masked by expression of either or both of the FnBPs. It would be interesting to construct triple *fnbpAB eap* and *fnbpAB emp* mutants or a mutant in all four proteins and assess biofilm forming capacity under the physiologically relevant conditions. Alternatively, a triple *srtA eap emp* mutant could be assessed for biofilm formation as the LPXTG-anchored FnBPs would not be properly expressed in this strain.

Coa was found to be the essential factor regulated by Sae involved in biofilm formation under the physiologically relevant conditions. Coa expression is tightly regulated by Sae (376). Coa binds to host prothrombin in a 1:1 ratio which forms a staphylothrombin complex. This complex formation promotes non-proteolytic activation of the host's prothrombin and the subsequent conversion of soluble fibrinogen into insoluble fibrin (377, 389). It appears that this Coa-mediated conversion of fibrinogen to fibrin is the mechanism by which *S. aureus* is forming biofilm under the physiologically relevant conditions. Experiments attempting to supplement fibrin into the BioFlux experiments were unsuccessful and would require further technical optimisation. However, complementary experiments carried out by our collaborators demonstrated that biofilms grown on plasma-coated surfaces were dispersed by plasmin, which degrades fibrin clots, and coagulation of human plasma was found to be induced by supernatants from wild type *S. aureus* strains but not the isogenic *saePQRS* mutant (Zapotoczna, McCarthy *et al.*, submitted) (447). Additionally, the finding that biofilm formation was specific to plasma and not serum further supports a role for Coa-mediated conversion of fibrinogen to fibrin as the mechanisms for biofilm formation as serum lacks fibrinogen. Collectively this data supports the finding of a critical role for Sae-regulated Coa in *S. aureus* biofilm formation on plasma under physiologically relevant conditions.

Recent studies support our finding of an essential role for Coa in *S. aureus* biofilm formation. The work of T. Vanassche, *et al*. (390) demonstrates that Coa is vital for *in vitro* biofilm formation on plates coated with human plasma and that loss of coagulation and the formation of fibrin clots by a *coa* mutant attenuates virulence of *S. aureus* in a murine subcutaneous abscess model. Coa enables persistence and aggregation of *S. aureus in vivo* within the fibrin network through clotting of plasma (391). Antibodies to Coa have been shown to provide protective immunity to mice with a renal abscess model (392). Recent publications on the therapeutic benefits of dabigatran against *S. aureus* DRIs further support our finding of an essential role for Coa in biofilm formation under the physiologically relevant conditions (389, 390, 393, 394). Dabigatran is a small molecule

anticoagulant that binds with high affinity to the catalytic site of thrombin (390). This subsequently prevents interaction between the host thrombin and Coa and the formation of the staphylothrombin complex. A very recent study further supports a role for fibrin formation in mediating biofilm-associated infections and, similar to our findings, MRSA biofilms formed on human synovial fluid were susceptible to plasmin treatment (395).

The vWbp is another coagulase that can promote fibrin formation through formation of the staphylothrombin complex with host prothrombin and has been shown to contribute to *S. aureus* virulence through the formation of fibrin clots (377, 390, 392). However, mutation vWbp was not found to abolish biofilm formation under our physiologically relevant assay. A comparative study on *coa* and *vwbp* mutants has shown that Coa contributes more to static biofilm formation on plasma-coated surfaces than vWbp which may explain why we failed to observe a significant contribution for the *vwbp* mutation in our experiment (390). vWbp has two mechanisms by which it mediates vascular adhesion, namely through the formation of the staphylothrombin complex and fibrin aggregates and through shear-mediated binding to von Willebrand factor (396). In our model, vWbp may also have a shear-dependent role for biofilm formation. Intriguingly, no contribution for ClfA was observed in the static assays or during experiments conducted at a shear flow rate of 0.6 dy/cm$^2$ in the BioFlux system. However, a role for ClfA in biofilm formation on plasma was reported at a higher shear flow rate of 6.25 dy/cm$^2$ (Zapotoczna, McCarthy *et al.*, submitted) (447). Therefore it is feasible that at a higher flow rate the vWbp may also contribute to biofilm formation on plasma-coated surfaces. Additionally, *coa* expression in the *vwbp* mutant may be sufficient to sustain biofilm formation on plasma under the physiologically relevant conditions. It is also interesting to note that only *coa* is significantly regulated by Sae and *vwbp* is not, therefore the *vwbp* gene may not be upregulated under the experimental conditions used (387). Further experiments are required to determine if vWbp is being upregulated in our model and if it has shear-dependent role for biofilm formation on plasma.

The findings presented in this chapter help to explain why the *atl* mutant was not attenuated in the mouse infection model (chapter 3). By creating a

more physiologically relevant *in vitro* biofilm assay we showed that Sae-regulated Coa is the critical factor under these conditions for *S. aureus* biofilm formation. The physiologically relevant assay demonstrated that previously identified biofilm contributors, including Atl, are in fact redundant for *S. aureus* biofilm formation in the physiologically relevant assay. This highlights the important differences between *in vitro* and *in vivo* experiments and warrants re-assessment of conclusions that are drawn from conventional *in vitro* assays.

# Chapter 5:

# Atl and high-level homogeneous methicillin resistance

## 5.1 Introduction

Beyond its role in *in vitro* biofilm formation, Atl is involved in penicillin-induced cell lysis (289, 291, 397). Penicillin and other β-lactams inhibit the activity of the penicillin-binding proteins (PBPs) and prevent the PBPs from producing sufficient cross wall during transpeptidation (289). Correctly synthesised cross wall material normally protects the cells from murosome-induced perforations of the peripheral wall. The fatal effect of β-lactams on staphylococci is due to puncturing of the cell wall by autolysins within the splitting system, which in the absence of a properly formed cross wall results in a loss of cytoplasmic material from high internal turgor pressure. As described in chapter one, methicillin resistance is acquired upon acquisition of the *mecA* gene which encodes for PBP2A, an alternative penicillin-binding protein that can maintain transpeptidase activity in the presence of β-lactams due to its low affinity for β-lactam antibiotics. A characteristic of methicillin resistance of clinical MRSA strains is heterogeneity (305-307). The majority of cells within a clinical MRSA population express low-level resistance (an MIC of 1-10 μg/ml) and are classified as heterogeneously resistant (HeR) MRSA (306, 307). Within HeR populations exists a small subpopulation that occurs at a frequency of ≥1% containing cells capable of expressing high level resistance called homogeneous resistance (HoR) (306, 307). The mechanisms behind this switch from HeR to HoR resistance have not yet been fully elucidated and this is an intensely investigated area of staphylococcal biology.

Alterations in the activity of autolysins have been linked with the switch from a HeR to a HoR phenotype (397). However, there are conflicting reports on the influence of resistance levels on autolysis. Homogeneous resistance and growth in the presence of β-lactams have been associated with low levels of autolysis (398, 399). For example, growth of *S. aureus* in the presence of sub-inhibitory concentrations (half the MIC) of various β-lactam antibiotics provoked reduced transcription of multiple autolytic enzyme genes, including the major autolysin (399). A. Antignac, *et al*. (399) proposed that this reduction in autolysin gene transcription was a protective measure taken to prevent damage to the cell wall by autolysis. In contrast to

these findings, there are multiple reports that high-level methicillin resistance and growth in the presence of β-lactams has the opposite effect and upregulates autolysis (400-402). It has been proposed that an increased rate of autolysis associated with high-level methicillin resistance could be a repair mechanism employed by staphylococci, enabling excision and disposal of abnormal and potentially lethal cell wall material produced during growth in the presence of methicillin (400). It therefore appears that regulation of autolysis and cell wall turnover influence methicillin resistance via one or more mechanisms that remain to be elucidated.

Expression of *mecA* and HoR resistance by a HA-MRSA reduces the ability of HA-MRSA to detect AIP, which impacts on Agr-mediated toxin production and attenuates the virulence of HA-MRSA in a murine infection model (226). The authors proposed that expression of *mecA* was either directly or indirectly inducing changes in the cell wall which interfered with Agr-mediated detection of AIP (226). CA-MRSA strains, on the other hand, which generally express lower levels of *mecA* and a HeR phenotype, typically produce higher levels of toxins (279). Alterations in cell wall structure have further been implicated in decreased susceptibility to β-lactams (318). An increase in peptidoglycan cross-linking was related to increased resistance to β-lactams which correlated with increased autolysin production (318). Based on these findings and the conflicting reports on the influence of methicillin resistance on autolysis, experiments were undertaken to further investigate the relationship between methicillin resistance, cell wall biosynthesis and autolytic activity in the CA-MRSA strain USA300 LAC. Oxacillin was used as a substitute for methicillin in the following experiments as it is the clinically used derivative of methicillin.

## 5.2 Results

### 5.2.1 High-level homogeneous oxacillin resistance and growth in sub-inhibitory oxacillin increase autolytic activity

Initial experiments assessing the influence of homogeneous oxacillin resistance on autolysis were undertaken with a laboratory MSSA and its isogenic heterogeneous and homogeneously oxacillin resistant derivatives, namely 8325-4, 8325-4 p*mecA* HeR and 8325-4 *pmecA* HoR strains (316). The 8325-4 HoR strain was created by introduction of p*mecA* into the MSSA 8325-4 strain which produced a heterogeneously oxacillin resistant 8325-4 HeR strain. The 8325-4 HeR strain was grown on 100 μg/ml oxacillin to isolate 8325-4 HoR (316). Introduction of p*mecA* into 8325-4 and the expression of heterogeneous oxacillin resistance were accompanied by a modest increase in the rate of triton X-100-induced autolysis, while high-level homogeneous oxacillin resistance correlated with substantially increased autolytic activity (Fig. 5.1).

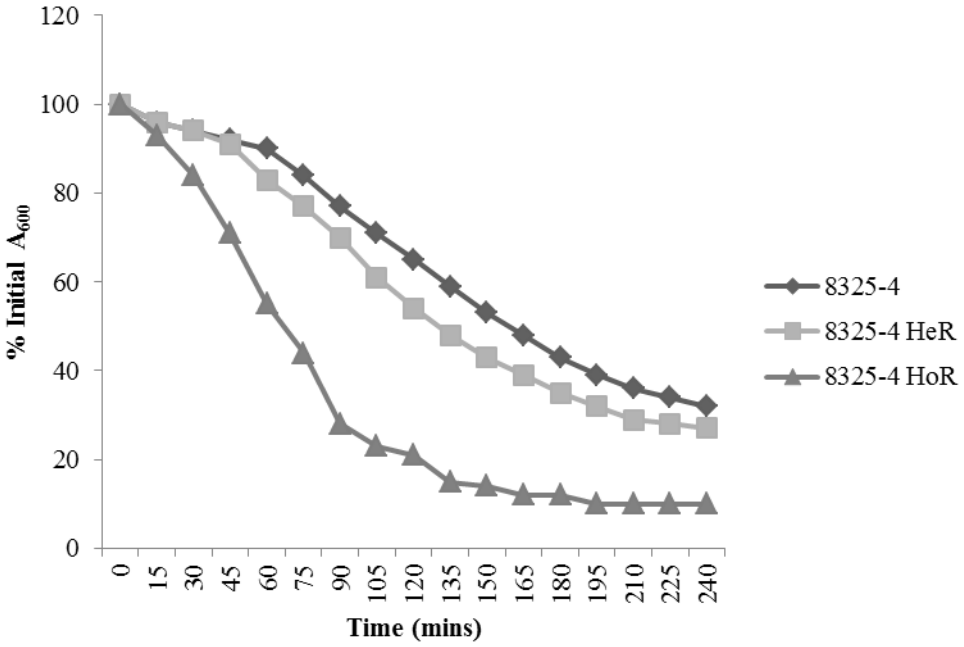


**Fig. 5.1. Contribution of HeR and HoR methicillin resistance levels to autolytic activity of 8325-4.** Comparison of Triton X-100-induced autolysis of 8325-4, 8325-4 p*mecA* HeR and 8325-4 p*mecA* HoR. Cells were grown to early exponential phase in BHI at 37°C and washed in PBS and adjusted to $A_{600}$ = 1.0 in 0.01% Triton X-100. The $A_{600}$ was measured for 15 min intervals thereafter with shaking incubation at 37°C. Autolytic activity is expressed as a percentage of the initial $A_{600}$.

Based on these findings with 8325-4, further experiments examining the influence of high-level methicillin resistance on autolysis were conducted in the naturally HeR methicillin resistant USA300 LAC strain (403). Extensive research is currently being conducted on USA300 LAC HeR strain and its HoR derivatives in our laboratory. DNA and RNA genome sequencing is under way to identify the mechanisms of the switch from heterogeneous to homogeneous resistance in this genetic background. Therefore, these strains were chosen for further experiments assessing the influence of the HoR phenotype on autolysis as any significant findings could be subsequently investigated through sequencing analysis. As with the 8325-4 strain set described above, a homogeneously resistant derivative of USA300 LAC was isolated on oxacillin 100 μg/ml plates (316).

Consistent with the 8325-4 strain set data, induction of high-level homogeneous oxacillin resistance in LAC was also associated with a substantial increase in the rate of autolysis (Fig. 5.2).

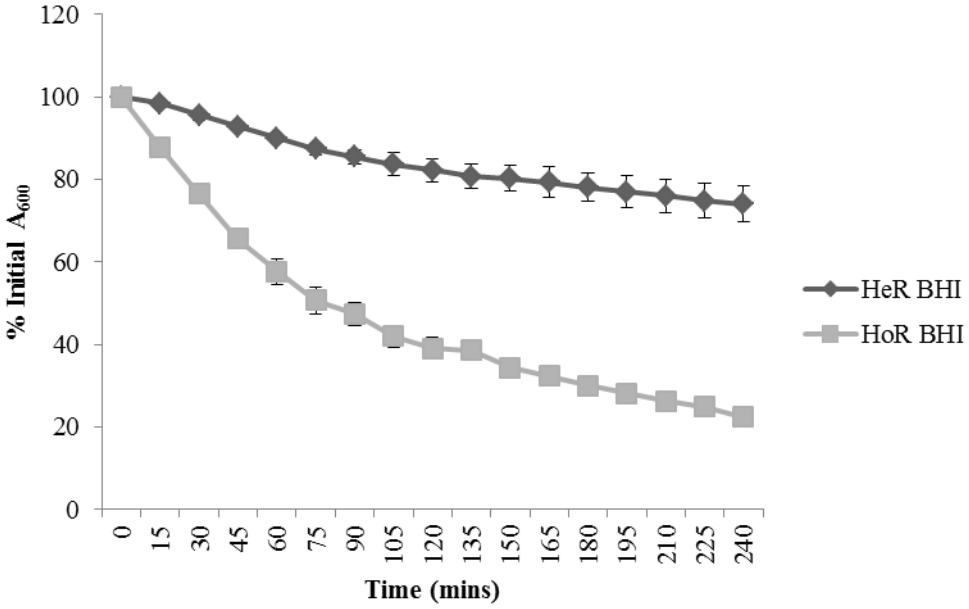


**Fig. 5.2. Contribution of HeR and HoR methicillin resistance levels to autolytic activity of USA300 LAC.** Comparison of Triton X-100-induced autolysis of USA300 LAC HeR and USA300 LAC HoR. Cells were grown to early exponential phase in BHI at 37°C and washed in PBS and adjusted to $A_{600}$ = 1.0 in 0.01% Triton X-100. The $A_{600}$ was measured for 15 min intervals thereafter with shaking incubation at 37°C. Autolytic activity is expressed as a percentage of the initial $A_{600}$. Results are representative of three independent experiments and standard deviations are indicated.

The triton X-100-induced autolytic assays from figure 5.2 were repeated with the strains grown in BHI and BHI supplemented with 0.5 μg/ml Ox to determine if growth in oxacillin could further increase the level of triton X-100-induced autolysis of LAC HeR and LAC HoR. A sub-inhibitory concentration of 0.5 μg/ml oxacillin (Ox) was chosen for these assays as previous work from our laboratory had determined that growth by LAC at this concentration of oxacillin was not affected (330). As Figure 5.3 illustrates, growth in sub-inhibitory oxacillin enhanced triton X-100-induced autolysis of both LAC HeR and HoR. Growth in sub-inhibitory oxacillin had the greatest impact on the autolytic activity of LAC HeR with growth in 0.5 μg/ml Ox resulting in a 62% higher level of autolysis at the final time point compared to growth in BHI (Fig. 5.3A). Following this trend, growth in sub-inhibitory oxacillin also increased the rate of autolysis by the LAC HoR strain and on the final time point LAC HoR grown in 0.5 μg/ml Ox exhibited an increase in autolysis of 12.8% compared to growth in BHI (Fig. 5.3B). This data confirms that growth in sub-inhibitory oxacillin can further increase autolytic activity in of LAC HeR and HoR.

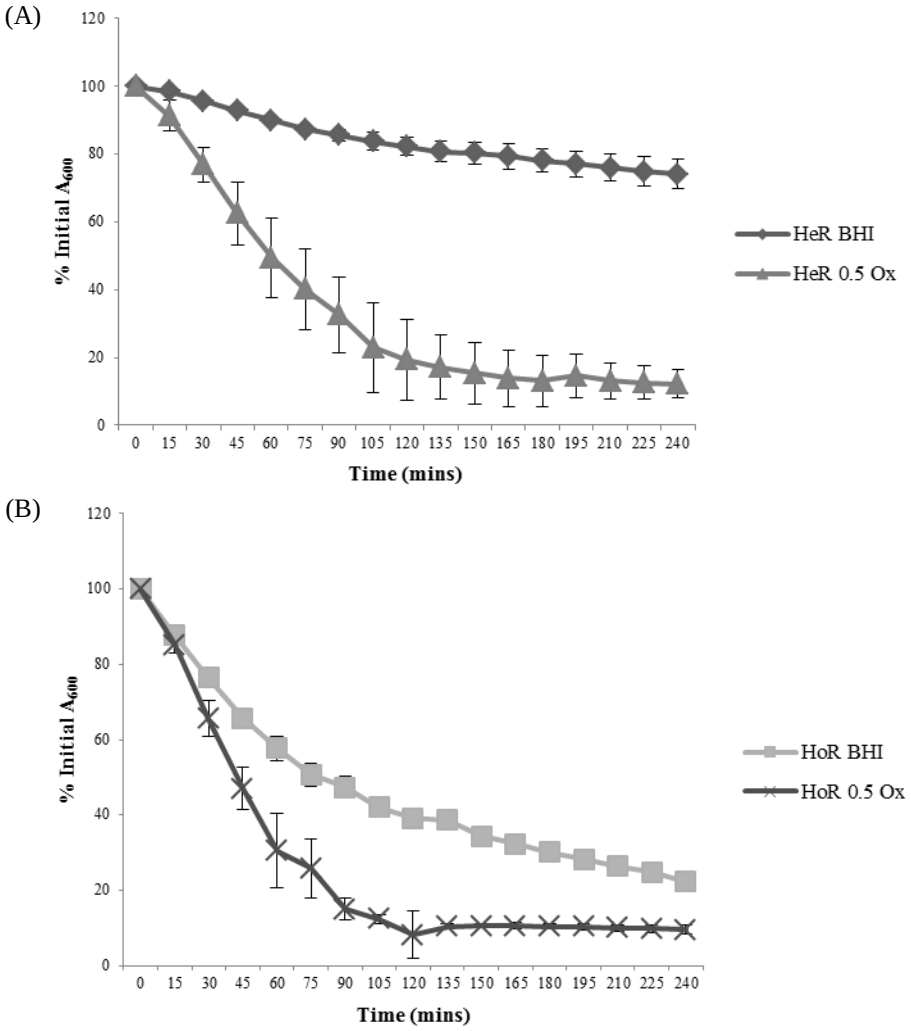


**Fig. 5.3. Contribution of sub-inhibitory oxacillin to autolytic activity of USA300 LAC HeR and HoR.** (A) Comparison of Triton X-100-induced autolysis of USA300 LAC HeR grown in BHI and LAC HeR grown in 0.5 µg/ml oxacillin (Ox). (B) Comparison of Triton X-100-induced autolysis of USA300 LAC HoR grown in BHI and LAC HoR grown in 0.5 µg/ml Ox. Cells were grown to early exponential phase in either BHI or BHI supplemented with 0.5 µg/ml Ox at 37°C, washed in PBS and adjusted to $A_{600}$ = 1.0 in 0.01% Triton X-100. The $A_{600}$ was measured and for 15 min intervals thereafter with shaking incubation at 37°C. Autolytic activity is expressed as a percentage of the initial $A_{600}$. Results are representative of three independent experiments and standard deviations are indicated.

To determine the relative contributions of the amidase (AM) and glucosaminidase (GL) regions of Atl to this phenotype, LAC HeR and HoR cell suspensions were incubated in PBS and triton X-100 supplemented with either 1:100 AM or 1:100 GL antibody. 1:100 IgG was used as a control. Both Atl antibodies reduced LAC HeR autolytic activity, particularly the AM antibody (Fig. 5.4A), perhaps suggesting a more important role for *N*-acetylmuramyl-L-alanine amidase activity in LAC HeR triton X-100-

induced autolysis than endo-β-*N*-acetylglucosaminidase activity and possible upregulated biosynthesis of the stem pentapeptide of peptidoglycan (404). However, neither Atl antibody had a significant inhibitory effect on the already very high levels of autolytic activity of LAC HoR (Fig. 5.4B), perhaps suggesting that the HoR phenotype may be associated with the upregulation of other autolysins not inhibited by the AM or GL antibodies.

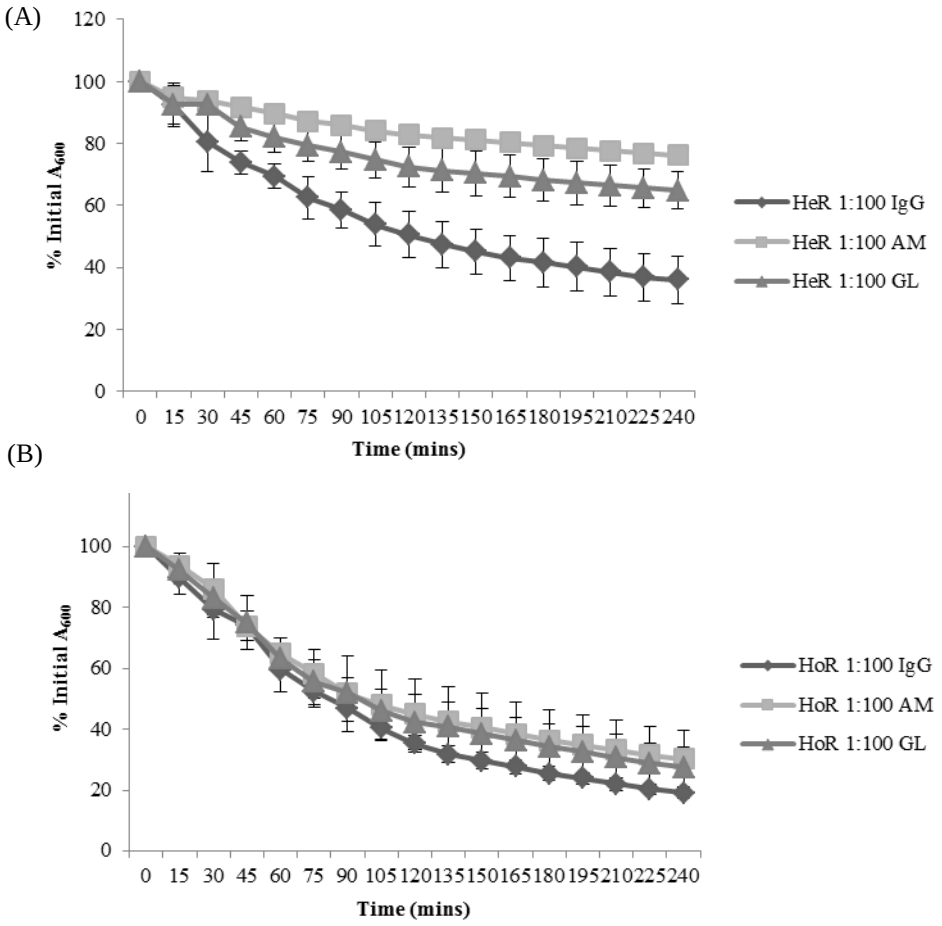


**Fig. 5.4. Inhibition of triton X-100-induced autolysis of LAC HeR and LAC HoR by Atl antibodies.** (A) Comparison of Triton X-100-induced autolysis of USA300 LAC HeR grown in BHI supplemented with either 1:100 IgG, 1:100 AM or 1:100 GL antibody. (B) Comparison of Triton X-100-induced autolysis of USA300 LAC HoR grown in BHI supplemented with either with 1:100 IgG, 1:100 AM or 1:100 GL antibody. Cells were grown to early exponential phase in BHI at 37°C and washed in PBS and adjusted to $A_{600}$ = 1.0 in 0.01% Triton X-100. The $A_{600}$ was measured and for 15 min intervals thereafter with shaking incubation at 37°C. Autolytic activity is expressed as a percentage of the initial $A_{600}$. Results are representative of three independent experiments and standard deviations are indicated.

RT-PCR analysis to examine the relationship between homogeneous resistance and increased autolysis revealed a significant 5.4-fold increase in *atl* expression in LAC HoR compared to LAC HeR grown in BHI ($P \leq 0.001$, Fig. 5.5). Interestingly even though growth in sub-inhibitory oxacillin increased autolytic activity in LAC HeR, no significant difference in *atl* expression was measured (Fig. 5.5 and 5.3). Similarly sub-inhibitory oxacillin had no effect on *atl* transcription in LAC HoR (Fig. 5.5 and 5.3). These findings indicate that significantly increased *atl* transcription may directly correlate with increased autolytic activity in HoR strains. However, because growth in sub-inhibitory oxacillin did not increase *atl* transcription, it seems possible that other peptidoglycan hydrolases, which may influence the cell wall structure, are responsible for increased triton X-100-induced autolysis under these conditions.

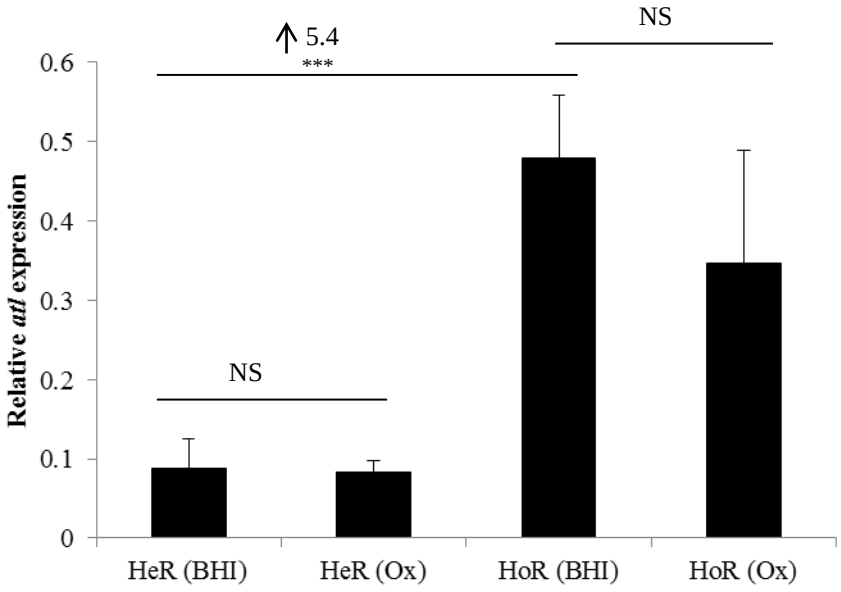


**Fig. 5.5. Contribution of heterogeneous and homogeneous oxacillin resistance and growth in sub-inhibitory oxacillin to *atl* transcription.** Comparison of relative *atl* transcription in LAC HeR and LAC HoR grown in BHI and in BHI supplemented with 0.5 µg/ml Ox. Total RNA was extracted from cells grown at 37$^{o}$C for 20 hrs in BHI. Results shown are representative of at least three independent experiments. Fold increase/decrease in *atl* expression relative to parent strains indicated by arrows. Standard deviations are indicated. Statistical significance denoted as NS for $P > 0.05$, as * for $P \leq 0.05$, as ** for $P \leq 0.01$ and as *** for $P \leq 0.001$.

### 5.2.2 Impact of homogeneous oxacillin resistance and growth in sub-inhibitory oxacillin on biofilm formation by LAC

Previous work has shown that growth in sub-inhibitory concentrations of β-lactams can induce biofilm formation in *S. aureus* and other bacteria as a global stress response is induced (405-407). High-level homogeneous methicillin resistance expressed by 8325-4 HoR has also been associated with a switch from a PIA to a protein-dependent biofilm phenotype and deletion of *mecA* in the HA-MRSA strain BH1CC resulted in a lower level of biofilm formation (316). Therefore, experiments were undertaken to examine if increased autolysis in LAC HoR was associated with altered biofilm formation. Levels of biofilm formation by LAC HeR were significantly increased by growth in sub-inhibitory oxacillin and by the switch from the HeR to the HoR phenotype ($P \leq 0.001$, Fig. 5.6) in BHI supplemented with 1% glucose on both hydrophilic and hydrophobic plates but not in BHI or BHI 4% NaCl media. This glucose-induced biofilm phenotype expressed by LAC HeR and HoR is consistent with a proteinaceous biofilm phenotype and correlates with the work of C. Pozzi, *et al*. (316) and E. O'Neill, *et al*. (254). Furthermore, increased autolytic activity and biofilm production exhibited by LAC HoR and HeR grown in 0.5 μg/ml Ox (Fig. 5.2 and 5.3A) correlate with previous work in our laboratory reporting an association between autolytic activity and glucose-induced biofilm formation by 8325-4 HoR (Pozzi *et al*., 2012).

Interestingly, sub-inhibitory oxacillin significantly reduced biofilm production by LAC HoR (Fig. 5.6) even though autolytic activity in this strain was increased under these growth conditions (Fig. 5.3B). However, *atl* transcription was not upregulated in LAC HoR grown in 0.5 μg/ml Ox and in any event sub-inhibitory oxacillin may negatively influence the activity of other biofilm mediators.

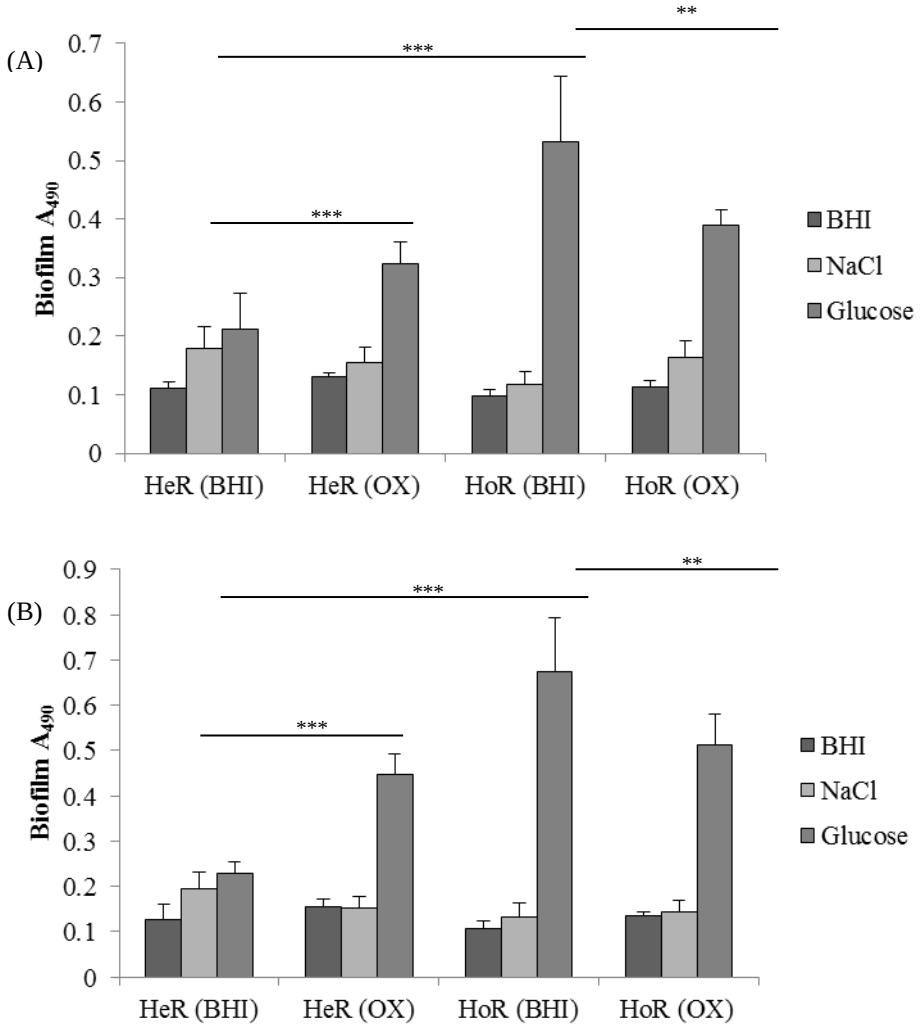


**Fig. 5.6. Impact of heterogeneous and homogeneous oxacillin resistance and growth in sub-inhibitory oxacillin on biofilm phenotypes of LAC.** Biofilm phenotypes of LAC HeR and LAC HoR grown at 37ºC for 24hrs in BHI and BHI supplemented with 0.5 µg/ml Ox prior to experimental biofilm assay set-up in either BHI, BHI 4% NaCl or BHI 1% glucose on (A) hydrophilic 96-well plates and (B) hydrophobic 96-well plates. Results shown are representative of at least three independent experiments. Comparisons made between strains grown in BHI 1% glucose. Standard deviations are indicated. Statistical significance denoted as NS for $P > 0.05$, as * for $P \leq 0.05$, as ** for $P \leq 0.01$ and as *** for $P \leq 0.001$.

ProK and DNaseI significantly inhibited biofilm formation by both LAC HeR and HoR in the presence and absence of 0.5 µg/ml Ox on both hydrophilic and hydrophobic polystyrene (Fig. 5.7A and B). This indicates that protein adhesins are required for the early stages of this biofilm phenotype and correlates with the reported biofilm phenotypes of other clinical MRSA isolates (254, 316). Furthermore, the inhibitory effects of DNaseI on all biofilms indicate that eDNA is a component of the biofilm matrix of LAC that is required under all test conditions. Since autolytic

activity is required for eDNA release, this correlates with the increase in triton X-100-induced autolysis exhibited by LAC with the switch from the HeR to the HoR phenotype and by growth in 0.5 µg/ml Ox (Fig. 5.2 and 5.3) (38, 57).

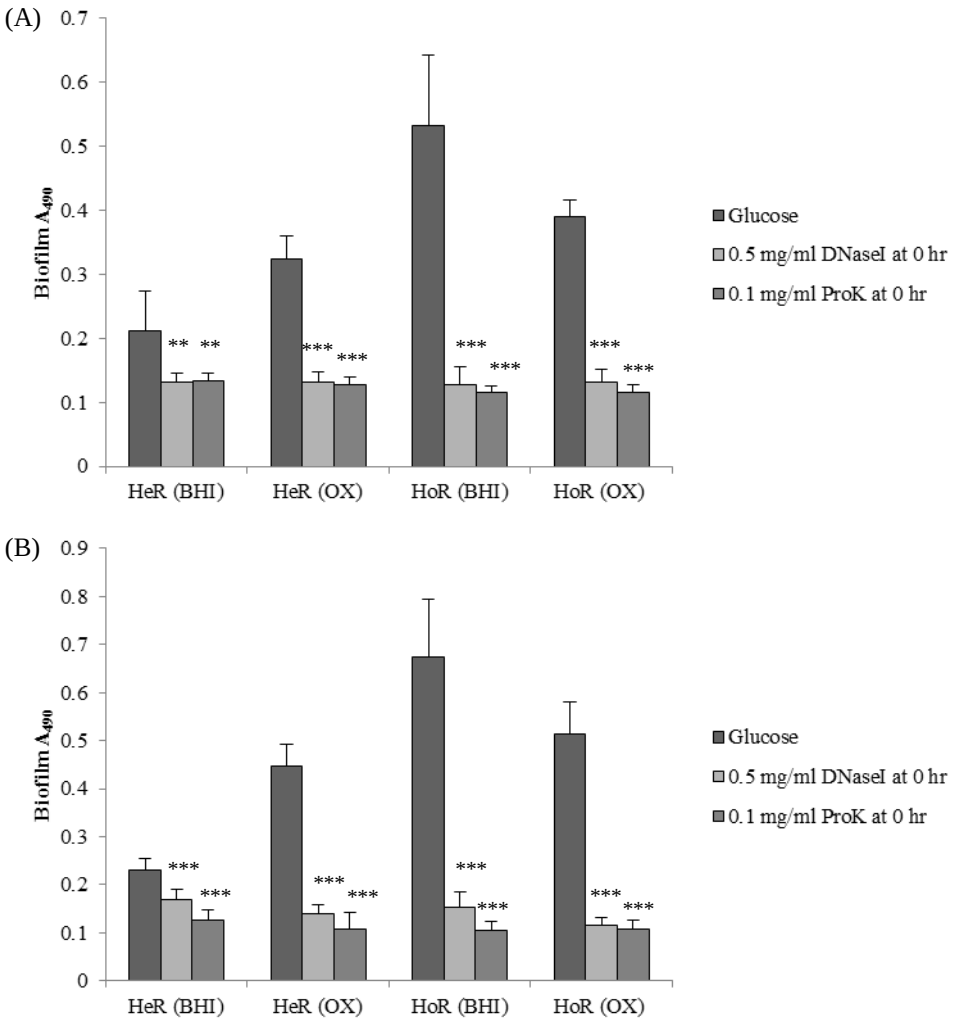


**Fig. 5.7. Impact of heterogeneous and homogeneous oxacillin resistance and growth in sub-inhibitory oxacillin on biofilm phenotypes of LAC.** Biofilm phenotypes of LAC HeR and LAC HoR grown in BHI and BHI supplemented with 0.5 µg/ml Ox prior to experimental biofilm assay set up in BHI 1% glucose. Biofilm phenotype of strains grown on (A) hydrophilic 96-well plates and (B) hydrophobic 96-well plates in BHI 1% glucose supplemented with 0.5 mg/ml DNaseI and 0.1 mg/ml ProK at experimental set up (0 hr). Biofilms are grown for 24 hrs at 37$^{o}$C. Results shown are representative of at least three independent experiments. Standard deviations are indicated. Statistical significance denoted as NS for $P > 0.05$, as * for $P \leq 0.05$, as ** for $P \leq 0.01$ and as *** for $P \leq 0.001$.

Proteinase K, DNaseI and sodium metaperiodate significantly dispersed mature LAC HeR and HoR biofilms grown with and without 0.5 µg/ml Ox ($P \leq 0.001$, Fig. 5.8A and B). The inhibitory effect of SM on the biofilms suggests that LAC can use PIA as well as protein adhesins and eDNA to aid biofilm formation.

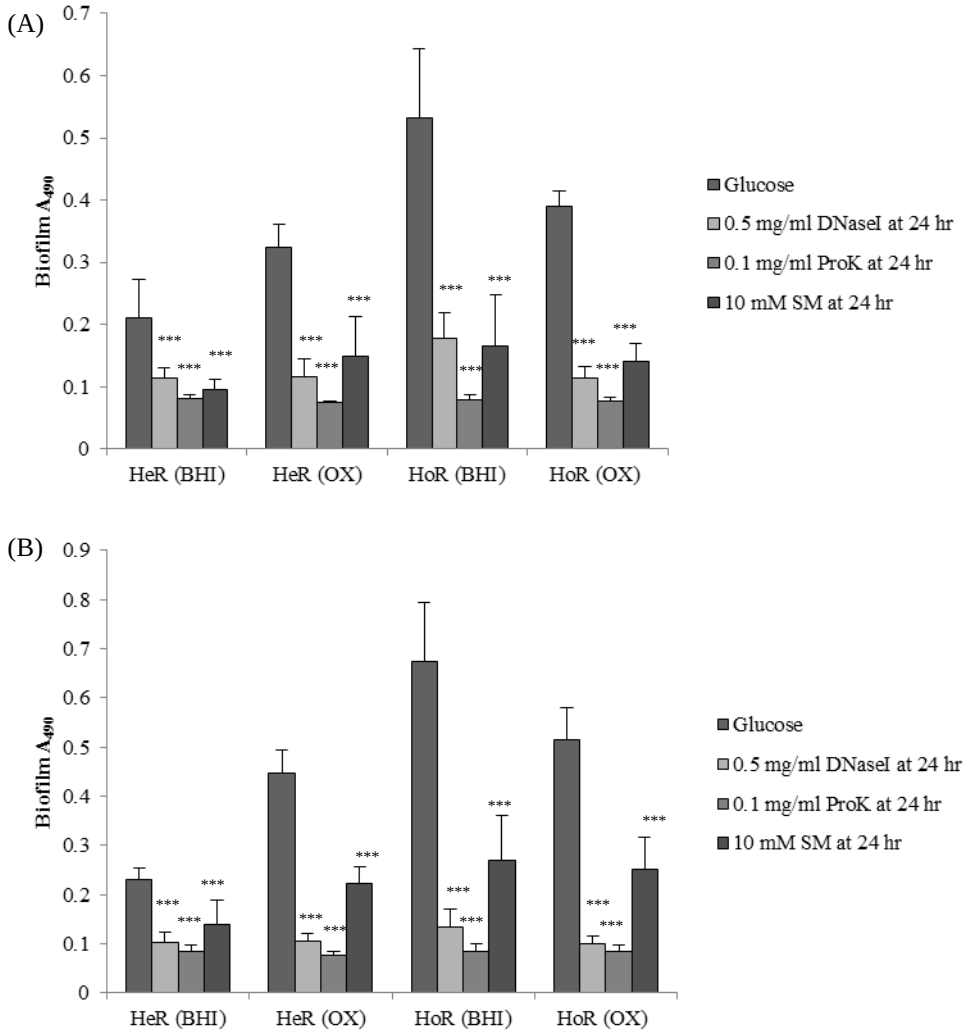


**Fig. 5.8. Impact of heterogeneous and homogeneous oxacillin resistance and growth in sub-inhibitory oxacillin on mature biofilm phenotypes of LAC.** Mature biofilm phenotypes of LAC HeR and LAC HoR grown in BHI and BHI supplemented with 0.5 µg/ml Ox prior to experimental biofilm assay set up in BHI 1% glucose. Phenotype of mature biofilms of LAC HeR and HoR grown for 24 hrs at 37°C on (A) hydrophilic 96-well plates and (B) hydrophobic 96-well plates in BHI 1% glucose and treated with 0.5 mg/ml DNaseI, 0.1 mg/ml ProK and 10 mM of SM for a further 2 hrs at 37°C. Results shown are representative of at least three independent experiments. Standard deviations are indicated. Statistical significance denoted as NS for $P > 0.05$, as * for $P \leq 0.05$, as ** for $P \leq 0.01$ and as *** for $P \leq 0.001$.

### 5.2.3. Assessment of the influence of the HoR phenotype and oxacillin growth pressure on cell wall metabolism

Previous studies have reported that the association between increased autolysis and increased levels of methicillin resistance is related to altered cell wall structure (400, 408). Oxacillin can induce the cell wall stress stimulon and in addition to expression of PBP2a, auxiliary genes involved in cell wall metabolism and stress response are required for high level homogeneous resistance to β-lactams (409, 410). Some of these auxiliary factors are known to influence methicillin resistance levels through altered cell wall metabolism which has a direct effect on autolysis (411). Here RT-PCR analysis of some of the factors and regulators involved in cell wall turnover and autolysis was undertaken to determine if cell wall metabolism was affected by the switch from HeR to HoR resistance or growth in sub-inhibitory oxacillin.

Transcription of *fmtA* was assessed in LAC HeR and HoR grown with and without sub-inhibitory oxacillin. FmtA was initially identified as a factor contributing to methicillin resistance that influences autolysis by H. Komatsuzawa, *et al*. (412). *fmtA* expression is associated with increased methicillin resistance and the gene is a member of the core cell wall stimulon responsible for increased peptidoglycan cross-linking in the presence of β-lactam antibiotics (413, 414). Inactivation of *fmtA* is accompanied by increased rates of triton X-100-induced autolysis (412). However, low concentrations of exogenous FmtA has been shown to enhance autolysis and biofilm formation by *S. aureus* in a manner dependent on WTA (413). *fmtA* expression has been shown to be dose-dependently increased by growth in the presence of β-lactam antibiotics (415). While no statistically significant differences were seen, there was a trend towards increased *fmtA* expression in the HoR strains and by growth in 0.5 µg/ml Ox (Fig. 5.9). This could indicate increased peptidoglycan cross-linking in LAC upon acquisition of the HoR phenotype and growth in oxacillin and may be a contributory factor to the observed increase in autolysis.

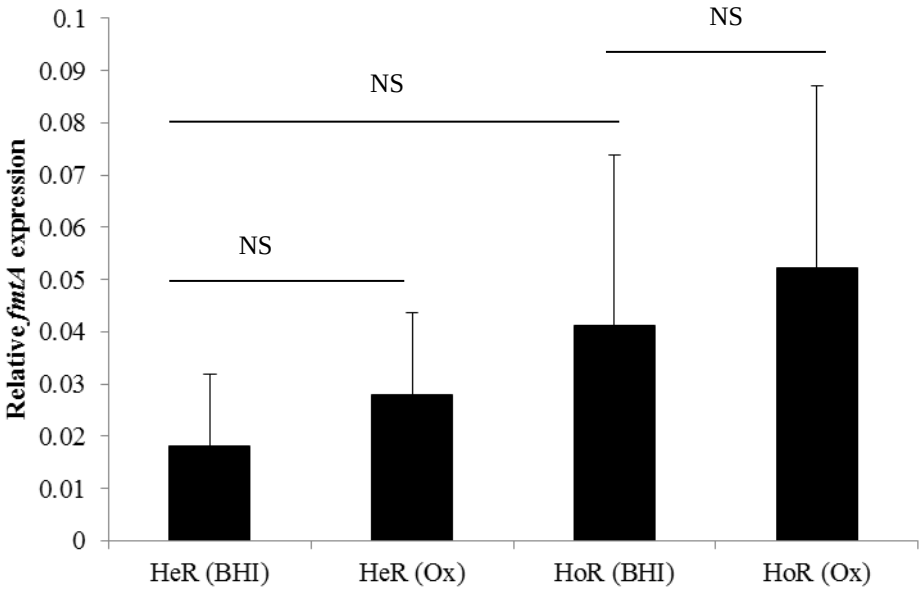


**Fig. 5.9. Contribution of heterogeneous and homogeneous oxacillin resistance and growth in sub-inhibitory oxacillin to *fmtA* transcription.** Comparison of relative *fmtA* transcription by LAC HeR and LAC HoR grown in BHI and in BHI supplemented with 0.5 µg/ml Ox. Total RNA was extracted from cells grown at 37°C for 20 hrs in BHI. Results shown are representative of at least three independent experiments. Standard deviations are indicated. Statistical significance denoted as NS for $P > 0.05$, as * for $P \leq 0.05$, as ** for $P \leq 0.01$ and as *** for $P \leq 0.001$.

Another factor examined was *murZ*, a UDP-*N*-acetylglucosamine-1-carboxyvinyltransferase which catalyses the first step in peptidoglycan precursor synthesis (410). *murZ* is reported to be upregulated in the presence of oxacillin and this has been postulated to be in response to increased rates of peptidoglycan biosynthesis (410). Transcription of *murZ* was upregulated in LAC HoR compared to LAC HeR and in both the HeR and HoR strains when grown in sub-inhibitory oxacillin (Fig. 5.10). As with *fmtA* expression no statistically significant differences were seen. However, the trend for increased *murZ* transcription would suggest that peptidoglycan biosynthesis overall is upregulated following the induction of the HoR phenotype or in HeR strains subjected to sub-inhibitory oxacillin stress.

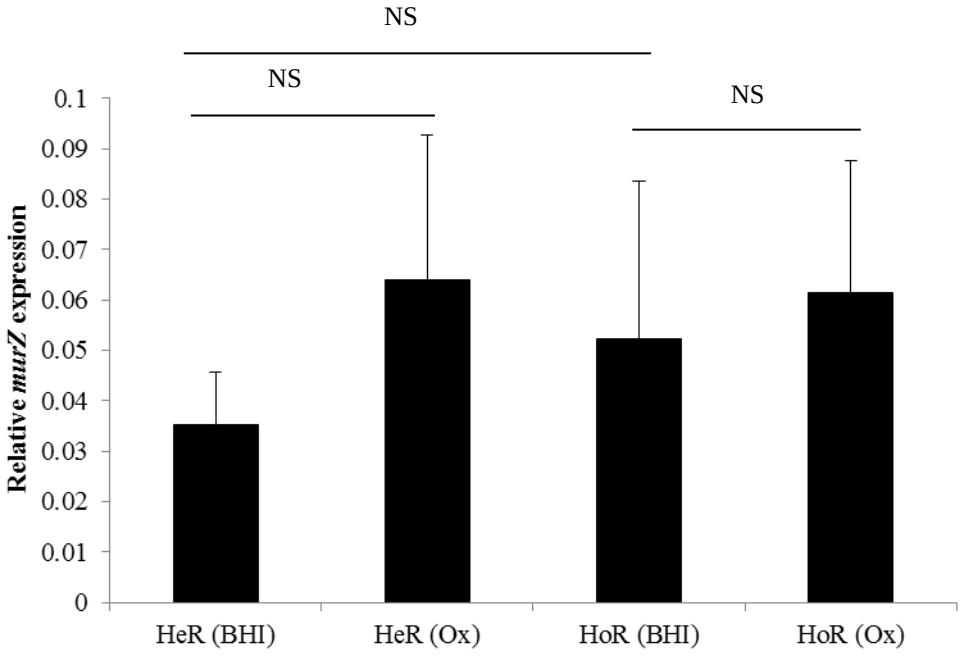


**Fig. 5.10. Contribution of heterogeneous and homogeneous oxacillin resistance and growth in sub-inhibitory oxacillin to *murZ* transcription.** Comparison of relative *murZ* transcription by LAC HeR and LAC HoR grown in BHI and in BHI supplemented with 0.5 µg/ml Ox. Total RNA was extracted from cells grown at 37°C for 20 hrs in BHI. Results shown are representative of at least three independent experiments. Standard deviations are indicated. Statistical significance denoted as NS for $P > 0.05$, as * for $P \leq 0.05$, as ** for $P \leq 0.01$ and as *** for $P \leq 0.001$.

The LytSR two component system (TCS) modulates autolysis and levels of murein hydrolase activity in *S. aureus* (416). The LytSR system consists of the sensor histidine kinase (LytS) and a response regulator (LytR) which function in part via modulating expression of the antiholin encoded by the *lrgAB* operon (417). Disruption of the LytSR TCS results in upregulated autolysis and increased biofilm formation (417, 418). Expression of the LytSR-regulated *lrgAB* operon is required to inhibit penicillin-induced killing of *S. aureus* (419). As observed in figures 5.11A and B there was a trend of upregulated transcription of the *lytSR* TCS upon transition by LAC from a HeR to a HoR phenotype and during growth of both strains in sub-inhibitory oxacillin. Significantly, *lytS* was induced 5.4-fold in LAC HeR grown in 0.5 µg/ml Ox and *lytR* was induced 6.9-fold ($P \leq 0.001$, Fig. 5.11A and B). Transcription levels of the TCS are highest in LAC HeR when grown in sub-inhibitory oxacillin and levels of transcription are also upregulated upon transition to a HoR phenotype. Upregulation of the LytSR TCS may be acting as a survival mechanism for growth in sub-inhibitory

oxacillin and suggests upregulated antiholin activity associated with the switch from a HeR to a HoR phenotype (419).

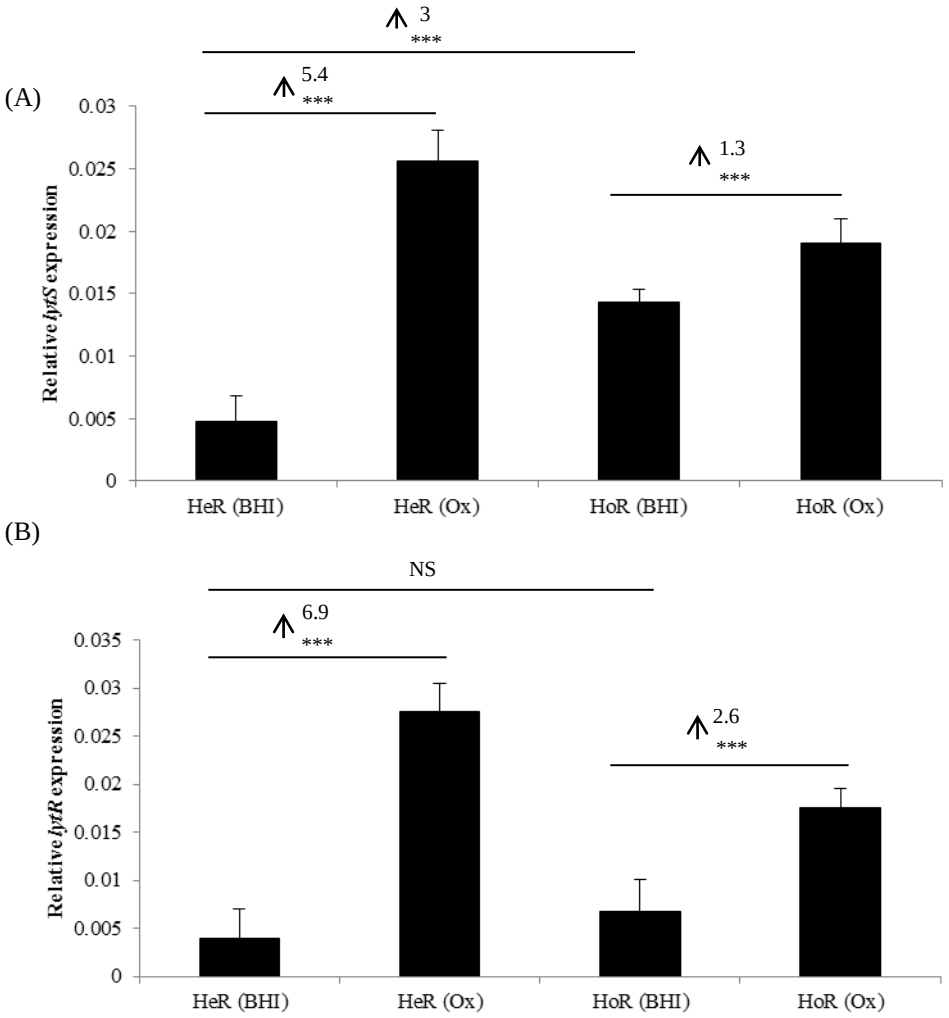


**Fig. 5.11. Contribution of heterogeneous and homogeneous oxacillin resistance and growth in sub-inhibitory oxacillin to *lytSR* transcription.** Comparison of relative transcription by LAC HeR and LAC HoR grown in BHI and in BHI supplemented with 0.5 µg/ml Ox of (A) *lytS* and (B) *lytR*. Total RNA was extracted from cells grown at 37$^{o}$C for 20 hrs in BHI. Results shown are representative of at least three independent experiments. Fold increase/decrease in *atl* expression relative to parent strains indicated by arrows. Standard deviations are indicated. Statistical significance denoted as NS for $P > 0.05$, as * for $P \leq 0.05$, as ** for $P \leq 0.01$ and as *** for $P \leq 0.001$.

The WalKR TCS is essential for viability of *S. aureus* and is a global regulator of cell wall biosynthesis (420). WalKR, consisting of the WalR response regulator and the WalK sensor histidine kinase, positively regulates autolysis and biofilm formation (421). The TCS positively regulates a total of 13 genes involved in cell wall metabolism, including the two major autolysins *atl* and *lytM* (421, 422). *fmtA* and *fmtB*, which are both required for high level methicillin resistance are also positively regulated by WalKR (372). Correlating with the increased rates of autolysis and biofilm formation observed, growth of LAC HeR in sub-inhibitory oxacillin resulted in a significant 1.9-fold increase in expression of the sensor kinase gene *walK* ($P \leq 0.001$, Fig. 5.12A) and a 2.5-fold increase of the response regulator gene *walR* ($P \leq 0.001$, Fig. 5.12B). The switch from a HeR to a HoR phenotype also significantly upregulated expression of the WalKR TCS with *walK* upregulated 1.4-fold and *walR* upregulated 2-fold ($P \leq 0.001$, Fig. 5.12A and B). Intriguingly, there was no significant increase in transcription of either *walK* or *walR* between LAC HoR grown in BHI or in sub-inhibitory oxacillin. This does not correlate with the increase in autolysis observed when LAC HoR is grown in 0.5 µg/ml Ox compared to growth of the strain in BHI (Fig. 5.3B) and suggests that LAC HoR may have adapted in other ways to the presence of sub-inhibitory oxacillin.

Table 5.1 below summarises all of the phenotypic and transcriptional changes induced in LAC upon acquisition of the HoR phenotype and from growth of both the HeR and HoR strains in sub-inhibitory oxacillin.

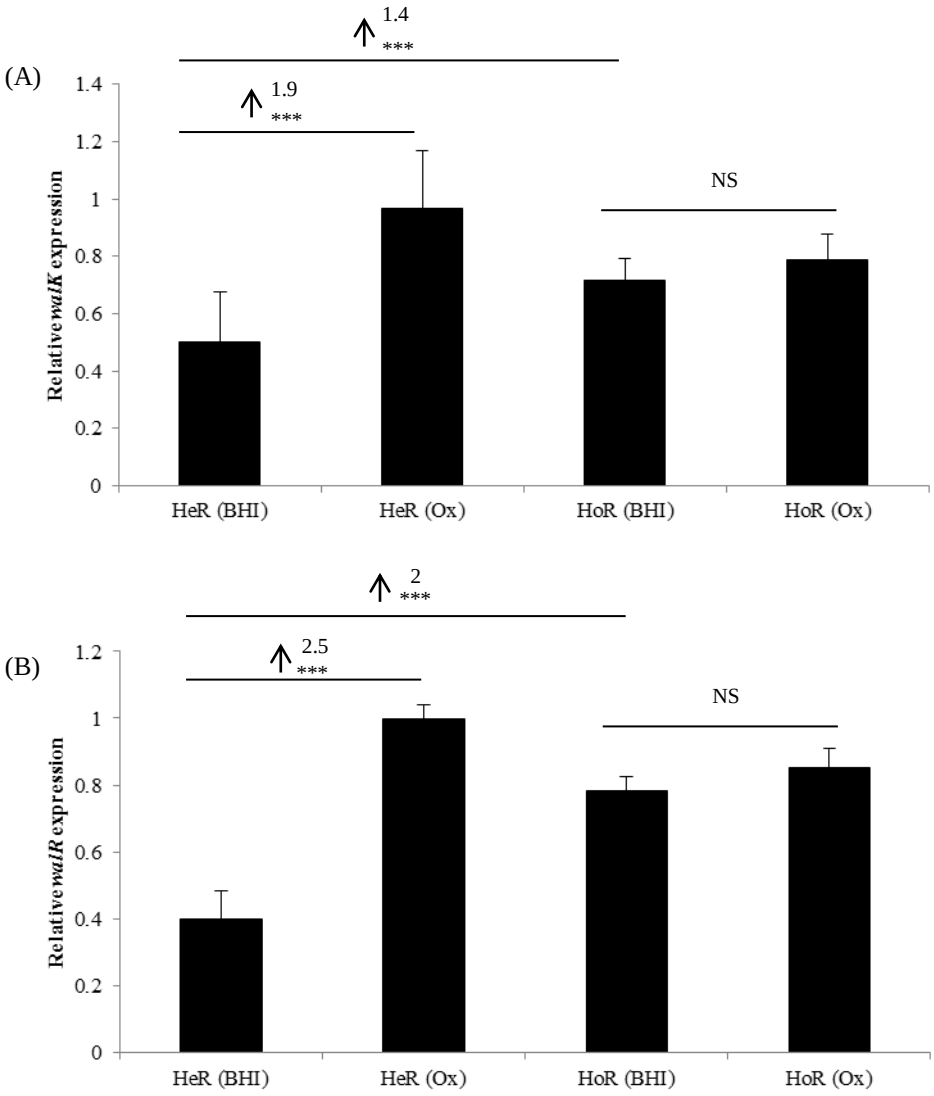


**Fig. 5.12. Contribution of heterogeneous and homogeneous oxacillin resistance and growth in sub-inhibitory oxacillin to *walKR* transcription.** Comparison of relative transcription by LAC HeR and LAC HoR grown in BHI and in BHI supplemented with 0.5 µg/ml Ox of (A) *walK* and (B) *walR*. Total RNA was extracted from cells grown at 37$^{o}$C for 20 hrs in BHI. Results shown are representative of at least three independent experiments. Fold increase/decrease in *atl* expression relative to parent strains indicated by arrows. Standard deviations are indicated. Statistical significance denoted as NS for $P > 0.05$, as * for $P \leq 0.05$, as ** for $P \leq 0.01$ and as *** for $P \leq 0.001$.

**Table 5.1:**

Summary of phenotypic and transcriptional changes in LAC associated with the HoR phenotype and with growth in sub-inhibitory oxacillin

| **Autolytic activity** | HeR (BHI) < HoR (BHI) < HeR (Ox) < HoR (Ox) | | |
|---|---|---|---|
| | **HeR (Ox) Vs HeR (BHI)** | **HoR (BHI) Vs HeR (BHI)** | **HoR (Ox) Vs HoR (BHI)** |
| **Biofilm formation in BHI 1% glucose (hydrophilic)** | ↑ 1.5-fold ($P \leq 0.001$) | ↑ 2.5-fold ($P \leq 0.001$) | ↓ 1.3-fold ($P \leq 0.01$) |
| **Biofilm formation in BHI 1% glucose (hydrophobic)** | ↑ 1.9-fold ($P \leq 0.001$) | ↑ 2.9-fold ($P \leq 0.001$) | ↓ 1.3-fold ($P \leq 0.01$) |
| **Transcriptional changes** | | | |
| ***atl*** | ↓ 0.9-fold ($P > 0.05$) | ↑ 5.4-fold ($P \leq 0.001$) | ↓ 0.7-fold ($P > 0.05$) |
| ***fmt*** | ↑ 1.5-fold ($P > 0.05$) | ↑ 2.3-fold ($P > 0.05$) | ↑ 1.3-fold ($P > 0.05$) |
| ***murZ*** | ↑ 1.8-fold ($P > 0.05$) | ↑ 1.5-fold ($P > 0.05$) | ↑ 1.2-fold ($P > 0.05$) |
| ***lytS*** | ↑ 5.4-fold ($P \leq 0.001$) | ↑ 3-fold ($P \leq 0.001$) | ↑ 1.3-fold ($P \leq 0.001$) |
| ***lytR*** | ↑ 6.9-fold ($P \leq 0.001$) | ↑ 1.7-fold ($P > 0.05$) | ↑ 2.6-fold ($P \leq 0.001$) |
| ***walK*** | ↑ 1.9-fold ($P \leq 0.001$) | ↑ 1.4-fold ($P \leq 0.001$) | ↑ 1.1-fold ($P > 0.05$) |
| ***walR*** | ↑ 2.5-fold ($P \leq 0.001$) | ↑ 2-fold ($P \leq 0.001$) | ↑ 1.1-fold ($P > 0.05$) |

## 5.3 Discussion

Data presented in this chapter provides evidence for an association between high level homogeneous oxacillin resistance and upregulated autolytic activity. The HoR phenotype of USA300 LAC was found to significantly upregulate *atl* transcription which correlates with increased rates of autolysis. While *atl* transcription was not significantly upregulated in either LAC HeR or HoR by growth in sub-inhibitory oxacillin, autolytic activity was increased in these strains under these same conditions. These findings are in agreement with other research on the influence of high level methicillin resistance and growth in the presence of β-lactams on autolysis (400-402) but also contradict some published work on the topic (398, 399). The conflicting data on the influences of high level methicillin resistance and growth in the presence of β-lactams on autolysis would suggest that there are multiple mechanisms through which *S. aureus* can obtain a HoR phenotype and cope with growth in the presence of β-lactams and that not all of these mechanisms have the same influence on autolysis. Recent work has shown that multiple mutations are acquired by *S. aureus* upon expression of high level methicillin resistance (423). In the USA300 LAC strain assessed here, there was a direct reproducible influence of the HoR phenotype or growth in sub-inhibitory oxacillin on autolysis, which may suggest that increased autolytic activity is a survival mechanism of LAC to cope with oxacillin-induced stress (400). As suggested by B. L. de Jonge, *et al*. (400), upregulated autolysis in LAC upon exposure to oxacillin may enhance excision and removal of anomalous and potentially lethal segments of the cell wall produced from altered rates of acylation by the different PBPs in the presence of oxacillin. Additionally, the upregulated rate of autolysis exhibited by LAC upon acquisition of the HoR phenotype could indicate that the structure and/or synthesis of the cell wall has changed to enable LAC to express HoR resistance to oxacillin (318). Alterations in cell wall composition mediated by the *femA* locus, for example, have previously been associated with reduced susceptibility to β-lactams and reduced rates of autolysis (411, 424).

The increased autolytic activity observed for LAC induced by sub-inhibitory oxacillin or upon acquisition of the HoR phenotype may suggest increased rates of peptidoglycan biosynthesis under these conditions. To investigate this, transcription of both the *fmtA* and *murZ* genes was assessed under these conditions. Expression of both of these genes is associated with increased peptidoglycan biosynthesis and increased levels of methicillin resistance (410, 413, 414). *fmtA* and *murZ* transcription were increased by acquisition of HoR resistance and by growth in sub-inhibitory oxacillin, albeit not significantly. This suggests that upregulated peptidoglycan biosynthesis is likely induced by the HoR phenotype and by growth in sub-inhibitory oxacillin. However, further work would be required to confirm if upregulated peptidoglycan biosynthesis is indeed associated with the observed increases in autolysis. HPLC analysis of mutanaolysin digested peptidoglycan would be an appropriate method for determining how peptidoglycan biosynthesis and composition are influenced in LAC upon acquisition of HoR resistance and by growth in sub-inhibitory oxacillin (318).

The striking upregulation of the LytSR TCS by LAC HeR grown in sub-inhibitory oxacillin indicates a stress response required for growth and survival in the presence of the β-lactam, a response that is not required to the same extent by the isogenic HoR which has adapted to antibiotic stress. The LytSR TCS is a known negative regulator of autolysis (417), therefore the increased expression of both *lytS* and *lytR* observed by transition of LAC from HeR to HoR resistance and by growth in sub-inhibitory oxacillin does not correlate with the observed increases in autolytic activity. However, it has been suggested that the antiholin *lrgAB*, which is regulated by LytSR may not play a major role in MRSA autolysis and only influences MSSA autolysis (425). The *lrgAB* operon is known to protect *S. aureus* from penicillin-induced killing in a manner independent of cell lysis (419). Therefore, the predominant effect of upregulated *lytSR* activity in LAC from oxacillin stress is likely to aid survival of LAC HeR in the presence of sub-inhibitory oxacillin and may not be acting directly on autolysis or biofilm formation (419). It is probable that the WalKR TCS, for example, has a

greater influence on the increased levels of autolysis and biofilm formation reported here (421).

Levels of transcription of both *walK* and *walR* in LAC HoR grown either with or without 0.5 µg/ml Ox were lower than the levels expressed by LAC HeR grown in 0.5 µg/ml Ox. This suggests that greater cell wall stress is exhibited in LAC HeR during growth in sub-inhibitory oxacillin than in the HoR strain and that peptidoglycan biosynthesis and turnover are upregulated in LAC HeR in response to the oxacillin pressure (421). This upregulation of *walK* and *walR* correlates with the increases in autolysis and biofilm formation (421). Increased *walK* and *walR* expression associated with the oxacillin pressure however contradicts previous work demonstrating that expression of the TCS is repressed by this antibiotic (420). It has been proposed that the oxidative stress exerted on cells by oxacillin affects WalK sensing and results in de-activation of WalR (420). It would be worth investigating the oxidative stress response in LAC to sub-inhibitory oxacillin to determine the reason for this observed difference.

While the HoR strain exhibited a significantly higher level of both *walK* and *walR* expression compared to the HeR strain grown in BHI, there was no significant difference in expression of the TCS between LAC HoR grown with and without oxacillin. This suggests that increased transcription of the WalKR TCS is a feature associated with the acquisition of HoR resistance and that oxacillin pressure does not affect this elevated basal level of expression in LAC HoR, which has successfully adapted to the pressure. Whole genome DNA and RNA sequencing of LAC HeR and HoR currently being conducted in our laboratory should reveal if there exists any SNP(s) in the WalKR TCS or a promoter of the system that is responsible for the increased basal level of expression exhibited by the HoR strain.

Production of the secondary messenger c-di-AMP has also been implicated in multiple phenotypic changes, including increased high level oxacillin resistance, upregulated autolysis and altered cell wall structure (318, 319). Previous sequencing analysis of LAC HoR revealed a SNP in the *gdpP* gene although levels of c-di-AMP have not been measured (316). It would be interesting to investigate if c-di-AMP levels are altered in LAC upon

acquisition of HoR resistance or during growth in sub-inhibitory oxacillin and if this is connected with altered cell wall biosynthesis and the SNP in *gdpP* associated with the HoR phenotype (316). The stringent response alarmone, ppGpp, has also been implicated in increased resistance to β-lactams and cell envelope stress and investigations into the effect of HoR resistance and sub-inhibitory oxacillin on the stringent response by LAC may also provide insights into the mechanisms of high level resistance (423, 426-428).

The increase in autolysis associated with the HoR phenotype and growth in sub-inhibitory oxacillin may also be influenced by alterations to WTA and/or LTA production. WTA and LTA are known to influence autolytic activity (53, 77, 429) and recently it has been shown that β-*O*-*N*-acetyl-D-glucosamine modification of WTA by the glycosyltransferase gene *tarS* is required for maintaining resistance to β-lactams (430). While deletion of *tarS* does not affect autolytic activity of MRSA strains, this finding reveals the importance of WTA for resistance to β-lactams. Additionally, inhibition of *tarO*, the gene encoding the first step of WTA synthesis, was recently shown to render MRSA sensitive to β-lactams (431). Compensatory mutations in *gdpP* have been linked to a LTA-deficient phenotype and were associated with expression of increased levels of β-lactam resistance (318). Therefore, it would be intriguing to examine in further detail if WTA and/or LTA synthesis and modification are altered in LAC upon acquisition of the HoR phenotype and during growth in sub-inhibitory oxacillin and if this is associated with the altered autolytic activities. Whole genome DNA and RNA sequencing analysis currently being performed in our laboratory of LAC HeR and HoR should yield insights into all of these proposed hypotheses.

The influence of sub-inhibitory oxacillin on biofilm formation by LAC HeR correlates with previous studies which demonstrated that sub-inhibitory concentrations of β-lactams can upregulate biofilm formation (405-407). Increased levels of biofilm formation by LAC HoR compared to LAC HeR correlate with increased *atl* transcription and autolytic activity. However, there was no significant difference in *atl* transcription between LAC HeR and HoR when grown in BHI compared to growth in sub-inhibitory

oxacillin and yet growth in sub-inhibitory oxacillin upregulated autolysis by these strains. This may suggest that growth in sub-inhibitory oxacillin also upregulates other peptidoglycan hydrolases which could induce autolysis in the presence of triton X-100. Growth in sub-inhibitory oxacillin was associated with upregulated expression of the *walKR* TCS in both LAC HeR and HoR when compared to LAC HeR grown in BHI. The WalKR system is known to positively regulate biofilm formation and expression of 13 genes involved in cell wall metabolism, some of which could contribute to upregulated autolytic activity (421, 422). Along with autolytic activity, upregulated expression of PBP2a has also been implicated in biofilm formation by 8325-4 HoR (316). Therefore, it would be interesting to investigate if PBP2a is also contributing to the increased biofilm levels exhibited by LAC HeR and HoR grown with and without sub-inhibitory oxacillin. The *in vivo* relevance of upregulated biofilm formation by LAC remains to be determined. In the 8325-4 background, *in vivo* biofilm formation and colonisation rates of implanted biomaterial was the same for both the MSSA and its isogenic HoR MRSA strain (316). However, it would be interesting to investigate the *in vivo* relevance of the upregulated *in vitro* biofilm formation of LAC upon acquisition of HoR resistance and growth in sub-inhibitory oxacillin and if increased *in vitro* biofilm formation correlates with greater colonisation rates *in vivo*. High level homogeneous methicillin resistance was previously shown to be associated with a downregulation of toxin production via repression of *agr* which is consistent with increased biofilm formation *in vitro* (148, 226). Therefore it is plausible that acquisition of HoR resistance and growth of MRSA in sub-inhibitory oxacillin could improve the ability of *S. aureus* to form biofilms *in vivo*.

# Chapter 6:

# Characterising the roles of surface proteins in *S. epidermidis* biofilm formation

## 6.1 Introduction

While PIA production is one of the best characterised mechanisms of *S. epidermidis* biofilm formation (150-153), PIA-independent mechanisms of biofilm formation are also important (37, 81, 87, 130, 432). Investigations into the contributions of surface proteins to *S. epidermidis* biofilm formation are important for the development of new therapeutics to combat biofilm-associated infection caused by this proficient opportunistic pathogen.

Work presented in this thesis describes discrepancies between *in vitro* and *in vivo* biofilm phenotypes in *S. aureus*. AtlE, the *S. epidermidis* homologue of Atl has previously been shown to contribute to *S. epidermidis in vitro* and *in vivo* biofilm formation and a *S. epidermidis* O-47 Δ*atlE* mutant was attenuated in a rat central venous catheter (CVC) model (37, 66). Previous work from our laboratory has characterised the biofilm phenotype and the contribution of AtlE to *in vitro* biofilm formation by the clinical isolate CSF41498 (79, 161, 433, 434). Unlike *in vitro* Atl-dependent biofilm formation by *S. aureus*, which requires Atl-mediated autolysis and eDNA release (38, 57), autolytic activity and eDNA were not found to significantly contribute to CSF41498 *in vitro* biofilm formation (433). In fact, growth of CSF41498 in the presence of PAS upregulated biofilm formation via a > 4-fold induction in expression of *icaA* (433). However, disruption of the *atlE* gene was sufficient to impair biofilm formation by CSF41498 (433). Further work demonstrated that a plasmid expressing an AtlE allele with an active site mutation in the AM domain retained the capacity to complement the biofilm defect of the CSF41498 Δ*atlE* mutant (433). Combined, these data suggest that biofilm formation by CSF41498 does not require AtlE-mediated peptidoglycan hydrolase/autolytic activity but is dependent on the unprocessed AtlE pro-protein, which may function as a cell wall anchored adhesin. The accumulation associated protein, Aap, has also been implicated in *S. epidermidis* biofilm formation (87, 113, 435). Proteolytic processing of this SrtA-anchored multidomain protein to expose the B domain is further implicated in Aap-mediated biofilm accumulation (113, 183). Recent research from our laboratory demonstrated that CSF41498 required Aap for primary attachment and that, unlike previously characterised *S. epidermidis*

strains, the CSF41498 Aap protein is not proteolytically processed and is expressed as an unprocessed 220 kDa protein (115). Antibodies to the A domain of Aap were able to inhibit CSF41498 *in vitro* primary attachment but not primary attachment in *S. epidermidis* 1457, in which Aap is proteolytically processed (115).

Taken together these studies suggest novel roles for unprocessed Atl and Aap proteins in the *S. epidermidis* CSF41498 biofilm phenotype and further suggest that extracellular protease activity in this strain may be different to other well characterised biofilm-forming *S. epidermidis* isolates. Investigations were undertaken to further elucidate the roles for AtlE, Aap and protease activity in *S. epidermidis* biofilm formation and the results are presented here.

## 6.2 Results

### 6.2.1 Autolytic activity contributes to RP62A biofilm formation but not to CSF41498 or 1457 biofilm formation

Previous work from our laboratory conducted by Dr Brian Conlon demonstrated an essential role for the AtlE protein in CSF41498 biofilm formation that was independent of autolytic activity (433). Biofilm assays conducted with CSF41498 and the clinical isolates 1457 and RP62A confirmed that the presence of PAS significantly increased levels of biofilm formation by CSF41498 but also by strain 1457 ($P \leq 0.001$, Fig. 6.1). However, growth in the presence of PAS had the opposite effect on the biofilm phenotype of RP62A and significantly reduced the levels of biofilm formation ($P \leq 0.001$, Fig. 6.1). This data reveals a strain dependent role for autolytic activity in *S. epidermidis* biofilm formation and indicates that RP62A employs different mechanisms of *in vitro* biofilm formation to CSF41498 and 1457.

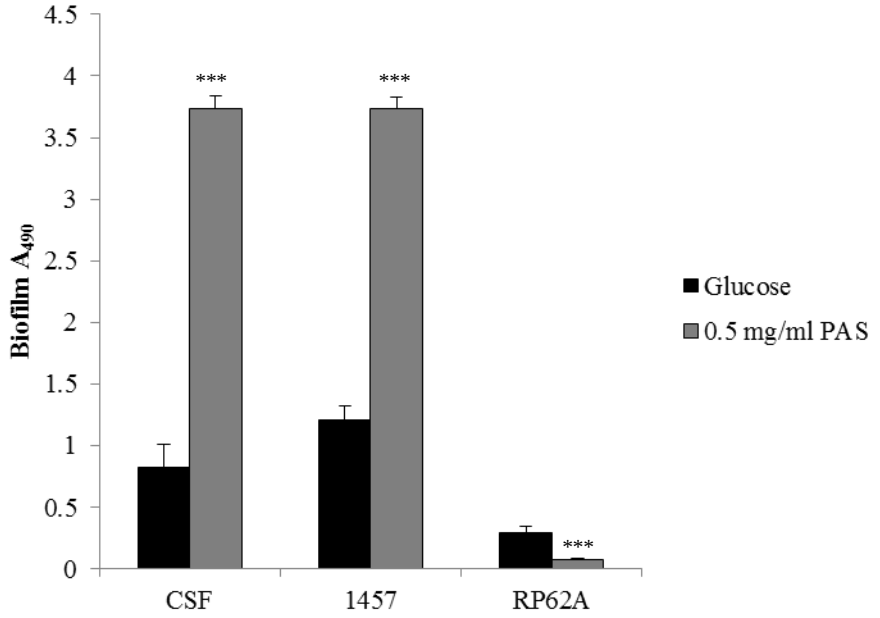


**Fig. 6.1. Contribution of autolytic activity to *S. epidermidis* biofilm formation.** Biofilm phenotypes of CSF41498, 1457 and RP62A grown for 24 hrs at 37°C on hydrophilic polystyrene in BHI 1% glucose and BHI 1% glucose supplemented with 0.5 mg/ml PAS. Results shown are of at least three independent experiments. Standard deviations are indicated. Statistical significance denoted as NS for $P > 0.05$, as * for $P \leq 0.05$, as ** for $P \leq 0.01$ and as *** for $P \leq 0.001$.

ProteinaseK significantly inhibited biofilm formation by RP62A ($P \leq 0.001$, Fig. 6.2A) and dispersed mature RP62A biofilms ($P \leq 0.001$, Fig. 6.2B). Growth in the presence of DNaseI significantly inhibited biofilm formation by RP62A and also dispersed the mature biofilm indicating that eDNA release is an important component of the RP62A biofilm matrix (Fig. 6.2A and B). These data are consistent with an important role for autolytic activity in the RP62A biofilm phenotype (Fig. 6.1). Of note, RP62A biofilms were also significantly dispersed by sodium metaperiodate (SM), indicating that RP62A uses autolytic activity, eDNA and PIA for *in vitro* biofilm formation ($P \leq 0.001$, Fig. 6.2B and 6.1).

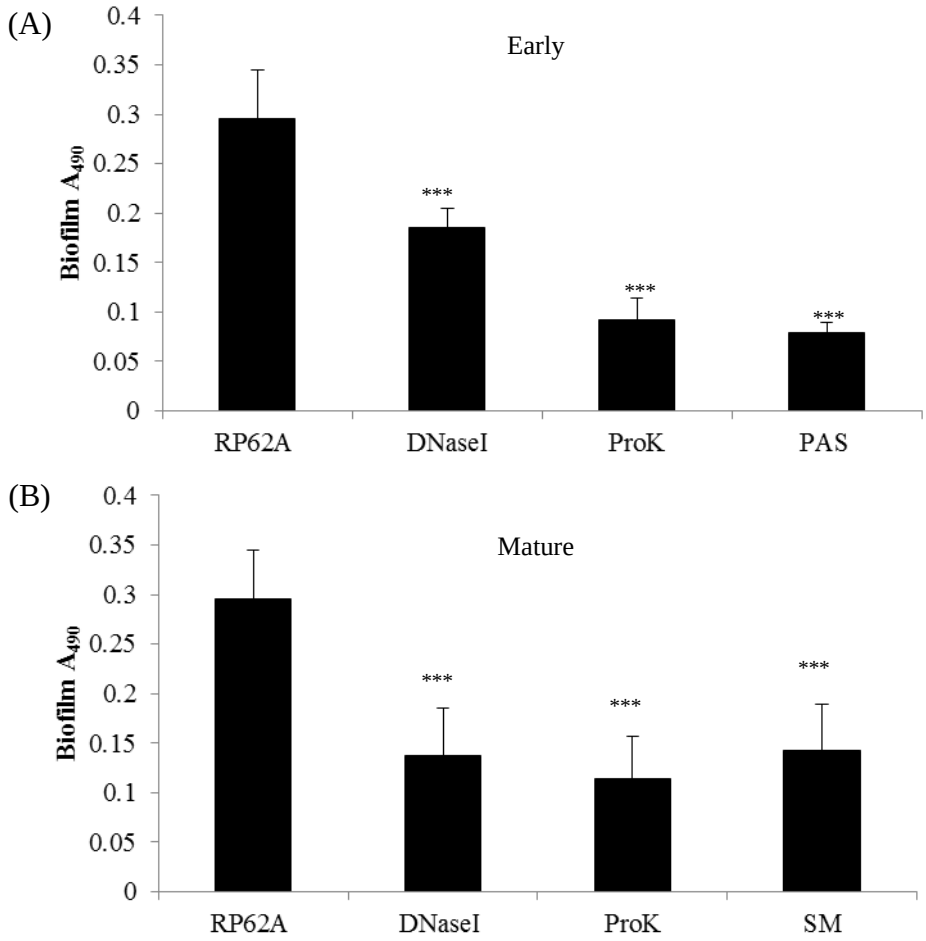


**Fig. 6.2. Characterisation of RP62A biofilm formation.** Biofilm phenotypes of RP62A grown for 24 hrs at 37$^{o}$C on hydrophilic polystyrene in (A) BHI 1% glucose, BHI 1% glucose supplemented with 0.5 mg/ml DNaseI at 0 hr, BHI 1% glucose supplemented with 0.1 mg/ml ProK at 0 hr and BHI 1% glucose supplemented with 0.5 mg/ml PAS at 0 hr, and (B) 24 hr old biofilms grown in BHI 1% glucose and treated for 2 hrs with 0.5 mg/ml DNaseI, 0.1 mg/ml ProK and 10 mM SM. Results shown are of at least three independent experiments. Standard deviations are indicated. Statistical significance denoted as NS for $P > 0.05$, as * for $P \leq 0.05$, as ** for $P \leq 0.01$ and as *** for $P \leq 0.001$.

### 6.2.2 Aap contributes to biofilm formation by CSF41498 but not by 1457

Previous work from our laboratory demonstrated that a *srtA* mutation impaired CSF41498 biofilm formation (115). Subsequent investigations found that the reduced biofilm formation was directly due to loss of anchoring of Aap to the cell wall (115). Unlike previously characterised *S. epidermidis* strains, Aap in CSF41498 was shown to be expressed as an unprocessed protein > 220 kDa. Antibodies to the A-domain of Aap inhibited CSF41498 primary attachment but were ineffective against 1457 primary attachment, in which the Aap protein is processed (115), suggesting different roles for Aap in the CSF41498 and 1457 biofilm phenotypes. Subsequent to this work, CSF41498 and 1457 *aap* mutants were constructed (115). Here, the biofilm phenotypes of CSF41498 and 1457 and their isogenic *aap* mutants were characterised in BHI, BHI 1% glucose and BHI 4% NaCl. Aap was found to be essential for CSF41498 biofilm formation in BHI and BHI 1% glucose ($P \leq 0.001$, Fig. 6.3). While there was a significant decrease in the level of biofilm formation produced by CSF41498 Δ*aap* in BHI 4% NaCl media, the strain still maintained a high level of biofilm formation in this growth media ($P \leq 0.001$, Fig. 6.3). Given that NaCl is known to activate the *icaADBC* operon, this data is consistent with a role for PIA in CSF41498 biofilm formation. In contrast to the biofilm phenotype for CSF41498 Δ*aap*, 1457 Δ*aap* was not defective in biofilm formation under any of the three growth conditions (Fig. 6.3). The mutation in *aap* actually significantly increased the levels of 1457 biofilm production in BHI 1% glucose ($P \leq 0.01$) and BHI 4% NaCl ($P \leq 0.05$), suggesting that other mechanisms of biofilm formation may be upregulated by 1457 in the absence of *aap* under these growth conditions.

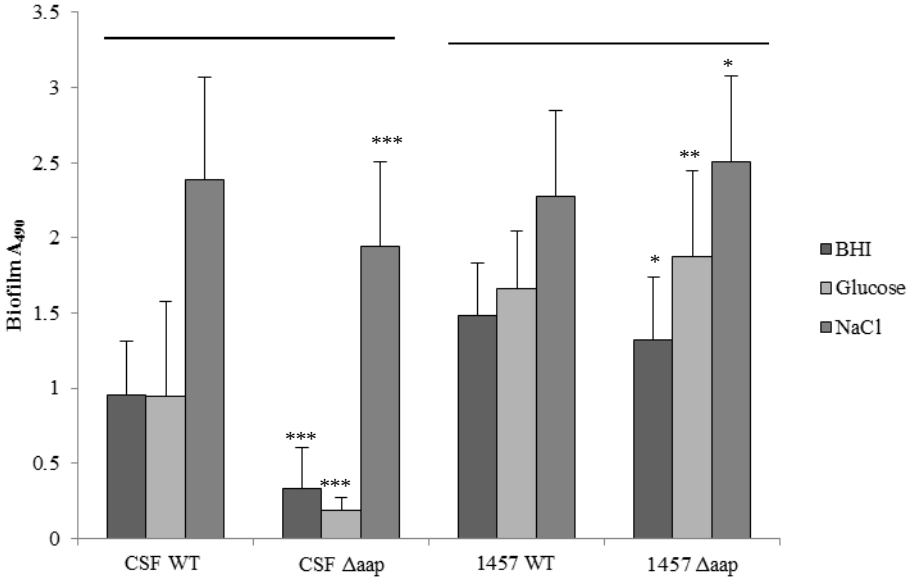


**Fig. 6.3. Biofilm phenotypes of *aap* mutants.** Strains CSF, CSF Δ*aap*::Tc$^r$ , 1457, 1457 Δ*aap*::Tc$^r$ were grown in BHI, BHI 1% glucose and BHI 4% NaCl for 24 hrs at 37$^o$C on hydrophilic 96-well polystyrene plates. Results shown are of at least three independent experiments. Standard deviations are indicated. Comparisons made between parent strains and their isogenic *aap* mutants in the various growth conditions. Statistical significance denoted as NS for $P > 0.05$, as * for $P \leq 0.05$, as ** for $P \leq 0.01$ and as *** for $P \leq 0.001$.

CSF41498 biofilms formed in BHI media were inhibited by DNaseI, ProK and SM ($P \leq 0.001$, Fig. 6.4). While the Δ*aap* mutation significantly impaired CSF41498 biofilm, growth in BHI supplemented with DNaseI, ProK and SM completely abolished the minimal levels of biofilm formation by the mutant ($P \leq 0.001$, Fig. 6.4). This indicates roles for both *aap*, eDNA and PIA in the CSF41498 biofilm formed in BHI. 1457 formed higher levels of biofilm in BHI compared to CSF41498 and, while DNaseI treatment did result in a statistically significant reduction in biofilm levels, the 1457 biofilm was most susceptible to SM treatment ($P \leq 0.001$, Fig. 6.4). Treatment of 1457 Δ*aap* biofilms grown in BHI with SM completely abolished biofilm formation ($P \leq 0.001$, Fig. 6.4). While ProK and DNaseI treatment significantly reduced the levels of 1457 Δ*aap* biofilm formation in BHI, the strain was still capable of producing substantial levels of biofilm in the presence of these enzymes ($P \leq 0.001$, Fig. 6.4). Therefore, this data would suggest that PIA production is the dominant mechanism by which 1457 produces biofilm in BHI whereas CSF41498 appears to be able to use both PIA and Aap for biofilm formation in BHI. This would explain the

findings of B. P. Conlon, *et al*. (115) who reported that antibodies to the A domain of Aap could inhibit CSF41498 primary attachment but not 1457 primary attachment.

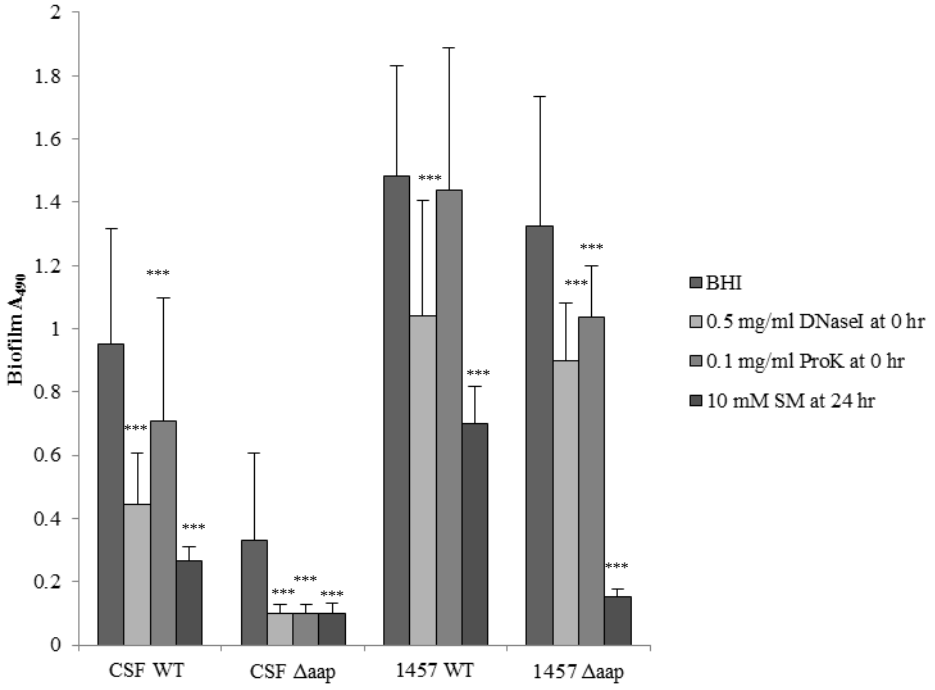


**Fig. 6.4. Biofilm phenotypes of CSF41498 and 1457 wild type and *aap* mutants in BHI.** Biofilm phenotypes of CSF41498, 1457 and their isogenic *aap* mutants grown on hydrophilic polystyrene in BHI. Biofilms treated at experimental set-up with BHI supplemented with 0.5 mg/ml DNaseI and 0.1 mg/ml ProK and grown for 24 hrs at 37$^{o}$C. Mature 24 hr old biofilms treated with 10 mM SM for a further 2 hrs. Results shown are representative of at least three independent experiments. Standard deviations are indicated. Statistical significance denoted as NS for $P > 0.05$, as * for $P \leq 0.05$, as ** for $P \leq 0.01$ and as *** for $P \leq 0.001$.

The biofilm phenotypes for CSF41498 and 1457 grown in BHI 1% glucose were similar to the phenotypes exhibited by growth in BHI (Fig. 6.5). CSF41498 appears to be able to use both protein adhesins and PIA for biofilm formation with *aap* also contributing significantly to biofilm formation in BHI 1% glucose (Fig. 6.5). In contrast, 1457 forms a biofilm in BHI 1% glucose that predominantly consists of PIA as evidenced by significant dispersal with SM ($P \leq 0.001$, Fig. 6.5). Interestingly, the residual biofilm produced by wild type 1457 in the presence of SM suggests that this strain may use *aap* for biofilm formation in the absence of PIA. However, in the absence of *aap*, PIA becomes the sole mechanism by which 1457 forms biofilm in BHI and BHI 1% glucose.

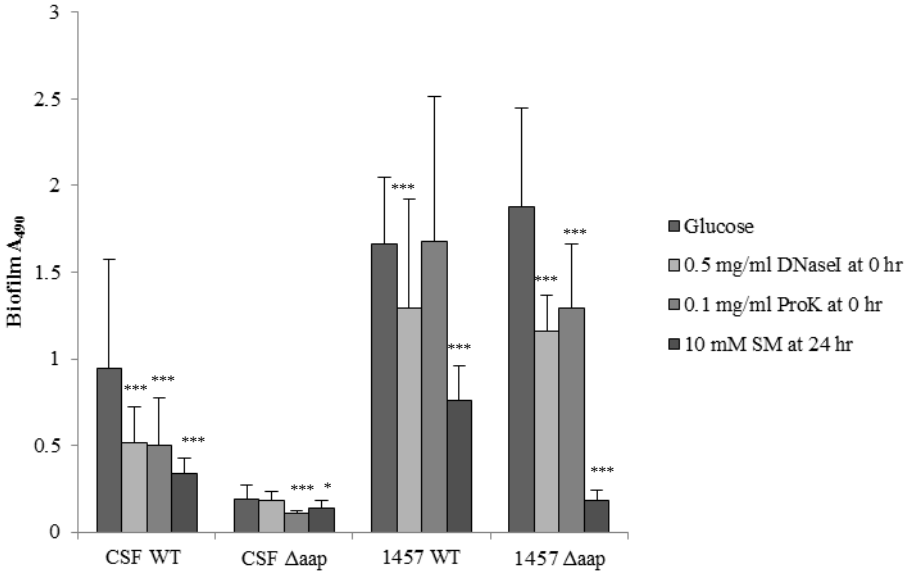


**Fig. 6.5. Biofilm phenotypes of CSF41498 and 1457 wild type and *aap* mutants in BHI 1% glucose.** Biofilm phenotypes of CSF41498, 1457 and their isogenic *aap* mutants grown on hydrophilic polystyrene in BHI 1% glucose. Biofilms treated at experimental set-up with BHI 1% glucose supplemented with 0.5 mg/ml DNaseI and 0.1 mg/ml ProK and grown for 24 hrs at 37°C. Mature 24 hr old biofilms treated with 10 mM SM for a further 2 hrs. Results shown are representative of at least three independent experiments. Standard deviations are indicated. Statistical significance denoted as NS for $P > 0.05$, as * for $P \leq 0.05$, as ** for $P \leq 0.01$ and as *** for $P \leq 0.001$.

Growth in BHI 4% NaCl alters the biofilm phenotype of CSF41498 and Aap is no longer required for biofilm formation in this growth medium (Fig. 6.6). Treatment of the CSF414198 biofilm grown in BHI NaCl with ProK and DNaseI demonstrated a minor role for protein adhesins and eDNA in the biofilm phenotype (Fig. 6.6), and the greatest level of biofilm dispersal was achieved by treatment with SM ($P \leq 0.001$, Fig. 6.6). While a similar level of reduction of the CSF41498 Δ*aap* biofilm is observed upon treatment with SM as for the parent strain, ProK and DNaseI treatment have a greater effect on the CSF41498 Δ*aap* biofilm ($P \leq 0.001$, Fig. 6.6). This finding suggests that in the absence of *aap*, PIA remains an important biofilm adhesin but that other protein adhesins and eDNA also become more important for CSF41498 biofilm production. In this context AtlE, which contributes to CSF41498 biofilm formation in BHI NaCl (433), may be an important biofilm mediator. In BHI 4% NaCl, the biofilm phenotype of 1457 remains similar to that induced by growth in BHI and BHI 1% glucose (Fig. 6.4 and 6.5), with a dominant role for PIA as demonstrated by SM dispersal of 1457 and 1457 Δ*aap* biofilms ($P \leq 0.001$, Fig. 6.6).

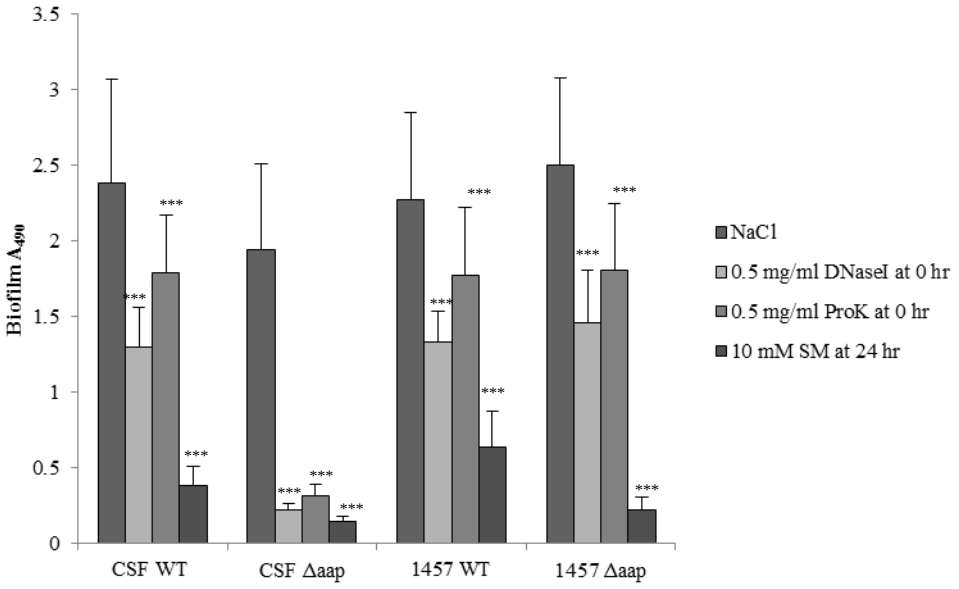


**Fig. 6.6. Biofilm phenotypes of CSF41498 and 1457 wild type and *aap* mutants in BHI 4% NaCl.** Biofilm phenotypes of CSF41498, 1457 and their isogenic *aap* mutants grown on hydrophilic polystyrene in BHI 4% NaCl. Biofilms treated at experimental set-up with BHI 1% glucose supplemented with 0.5 mg/ml DNaseI and 0.1 mg/ml ProK and grown for 24 hrs at 37$^{o}$C. Mature 24 hr old biofilms treated with 10 mM SM for a further 2 hrs. Results shown are representative of at least three independent experiments. Standard deviations are indicated. Statistical significance denoted as NS for $P > 0.05$, as * for $P \leq 0.05$, as ** for $P \leq 0.01$ and as *** for $P \leq 0.001$.

Biofilm formation by CSF41498 and 1457 and their isogenic *aap* mutants was also assessed in the Bioflux 1000Z instrument to assess the contribution of shear. When grown in BHI and BHI 1% glucose, similar biofilm phenotypes were observed for all strains. Representative results in which the strains were grown in BHI demonstrated that CSF41498 Δ*aap* is unable to form biofilm under flow conditions whereas1457 and its isogenic Δ*aap* mutant are both able to form biofilm (Fig. 6.7). These phenotypes are consistent with data from the static assays (Fig. 6.3, 6.4 and 6.5). In BHI and BHI 1% glucose, CSF41498 Δ*aap* mutant cells attached to the surface of the flow chamber at the beginning of the experiments but were defective in intercellular accumulation. In contrast, 1457 and its isogenic *aap* mutant accumulate strongly throughout the experiment leading to the periodic detachment of large cell aggregates. We conclude that mutation of *aap* is not significantly affecting biofilm forming capacity of 1457 under shear flow conditions but does impair CSF41498 biofilm formation. Unexpectedly both CSF41498 and 1457 failed to form biofilm when grown in BHI 4% NaCl in the Bioflux instrument. Further work will be required to investigate

this observation, but it appears that excess PIA production induced by NaCl interferes with *S. epidermidis* attachment to the BioFlux flow cells under flow conditions

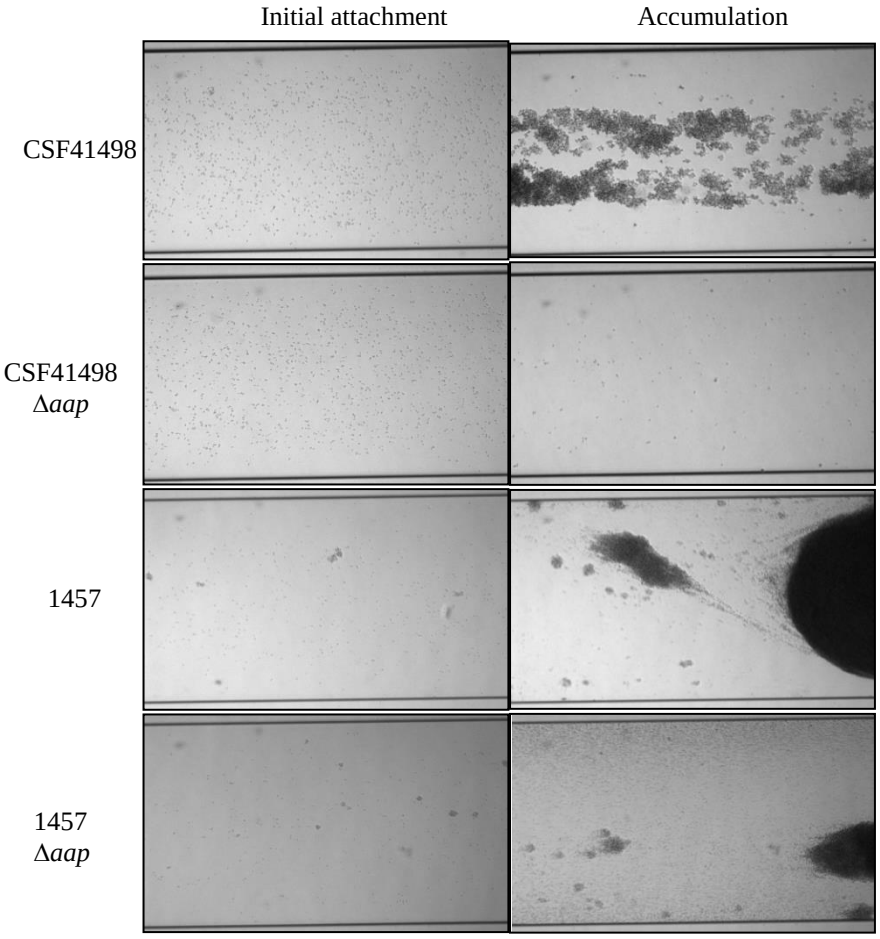


**Fig. 6.7. Attachment and accumulation of *aap* mutants under shear flow conditions**. Strains CSF41498, CSF Δ*aap*::Tc$^r$ , 1457, 1457 Δ*aap*::Tc$^r$ were grown in BHI and exposed to a shear flow rate of 0.6 dynes/cm$^2$ for 18 hrs (equivalent to 64µl/hr) at 37$^o$C in the Bioflux 1000Z instrument. Images shown here are of initial attachment and of accumulation after 18 hours. Brightfield images captured at 10X magnification are representative of at least two independent experiments.

### 6.2.3 Protease activity differs between CSF41498 and 1457

The Aap protein consists of an N-terminal A domain that is predicted to fold into an all β-structure and has previously been reported to contribute to skin colonisation and adherence to desquamated epithelial cells (Fig. 6.8) (180, 181). Aap also consists of a B region which is composed of variable numbers of G5 and E domains (Fig. 6.8) (183). Cleavage of the B region from the A domain has been implicated in the accumulation phase of biofilm formation by *S. epidermidis* (113, 183). Analysis of the expression of Aap by CSF41498 and 1457 revealed that the proteins are processed differently between the strains (115). Western blot analysis showed that the 220 kDa Aap is unprocessed in CSF41498 cell wall fractions (115). In contrast, the protein is processed in 1457. This may account for the differences in the contribution of Aap to biofilm formation by the two strains.


**Fig. 6.8. Schematic diagram of the domain arrangement of the unprocessed Aap protein.** The unprocessed Aap protein consists of a N-terminal signal sequence (S) and A domain and C-terminal wall (W) and membrane (M) spanning domains. The B domain consists of numbers of repeated G5 and E domains, the number of which differs between strains. Adapted from Conlon *et al*., 2014 (114).

To determine why the Aap protein is processed differently in CSF41498 compared to 1457, protease activity by the two strains was assessed on skimmed milk agar plates. As shown in figure 6.9, CSF41498 has a greater level of protease activity on skimmed milk agar compared to 1457. This was surprising given that Aap is processed by 1457 and not processed by CSF41498 (115). However, the cleavage of Aap may be conducted by a specific protease of 1457 which is absent or differentially expressed by CSF41498, a subtle difference which may not be detectable by comparison of growth on skimmed milk agar.

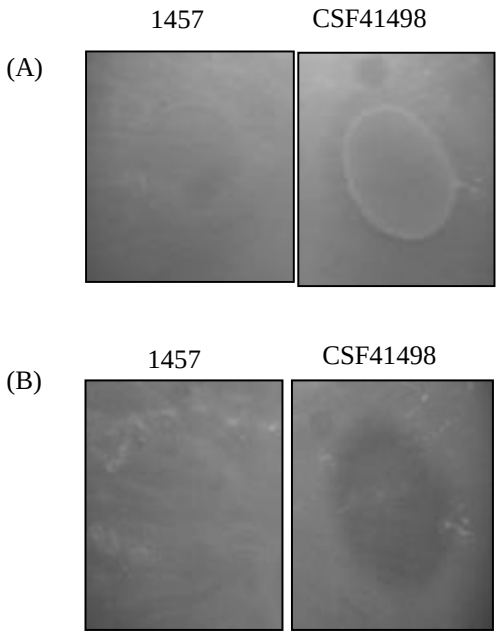


**Fig. 6.9. Protease activity of 1457 and CSF41498.** Protease activity of 1457 and CSF41498 cells grown on skimmed milk agar plates overnight at 37$^{o}$C. (A) Presence/absence of protease halo around colonies. (B) Zones/absence of protease activity on skimmed milk agar after colonies are removed. Results shown are representative of three independent experiments.

The *S. epidermidis* serine protease Esp contributes to promoting growth of *S. epidermidis* in the presence of *S. aureus* by aiding inhibition of *S. aureus* biofilm formation and nasal colonisation (436). Esp is known to degrade Atl and other proteins involved in *S. aureus* biofilm formation and levels of expression of Esp can vary among *S. epidermidis* isolates (437-439). Therefore we set out to determine if carriage of the *esp* gene differed between CSF41498 and 1457 and if this was perhaps the reason for the different processing of Aap between the two strains. However PCR analysis of genomic DNA from CSF41498 and 1457 revealed that *esp* is carried by both strains (Fig. 6.10). *S. aureus* JE2 DNA was included as a control as the gene is absent in *S. aureus*. This finding makes it difficult to attribute differential *esp* expression to the differential processing of Aap between CSF41498 and 1457. A recent communication from Alexander Horswill's group reported that the SepA and Ecp proteases of *S. epidermidis* are required for full Aap processing and Aap-dependent biofilm formation (Paharik *et al.*, Poster Presentation, International Symposium on Staphylococci and Staphylococcal Infections, Chicago, August 2014). Using

1457 in which Aap processing promotes biofilm, Paharik *et al* showed that the activity of SepA and Ecp increased biofilm production. Future studies to compare the activity of SepA and Ecp in CSF41498 and 1457 will be important in elucidating the role of Aap in CSF41498 biofilm formation.

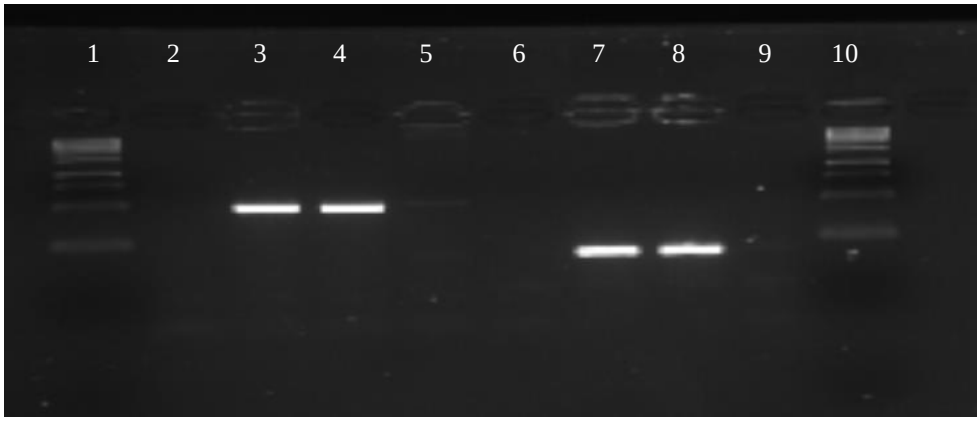


**Fig. 6.10. PCR to detect the presence of the ESP serine protease gene in CSF41498 and 1457.** PCR of the Esp serine protease gene on DNA from CSF41498, 1457 and JE2 with Esp1 and Esp2 primer sets run with a 1kb ladder on a 2% agarose gel. Lane 1: 1kb ladder, lane 2: negative control, lane 3: CSF DNA amplified with Esp1 primer set (200bp product), lane 4: 1457 DNA amplified with Esp1 primer set (200bp product), lane 5: JE2 DNA amplified with Esp1 primer set (200bp product), lane 6: negative control, lane 7: CSF DNA amplified with Esp2 primer set (500bp product), lane 8: 1457 DNA amplified with Esp2 primer set (500bp product), lane 9: JE2 DNA DNA amplified with Esp2 primer set (500bp product) and lane 10: 1kb ladder.

### 6.2.4 Incubation of CSF41498 in supernatant from 1457 cultures improves biofilm formation

Next we investigated the possibility that proteases present in *S. epidermidis* culture supernatants may influence biofilm by processing Aap. Biofilm assays were performed on CSF41498 pre-incubated in filter-sterilised culture supernatants from 1457, 1457 Δ*aap* and 1457 Δ*ica* (Fig. 6.11). Pre-incubation of CSF41498 with culture supernatants from all three 1457 strains for one hour at 37$^{o}$C prior to the start of the biofilm assay significantly increased biofilm forming capacity in BHI 1% glucose ($P \leq 0.001$, Fig. 6.11). In contrast, pre-incubation of the CSF41498 Δ*aap* mutant with supernatants from the three 1457 strains failed to restore biofilm forming capacity by this strain (Fig. 6.11) suggesting that a factor present in

the 1457 supernatant (perhaps a protease that processes Aap) promotes CSF41498 biofilm in a Aap-dependent manner. Incubation of the CSF41498 Δ*ica* mutant with 1457 supernatants also significantly enhanced biofilm formation by this strain ($P \leq 0.05$, Fig. 6.11).

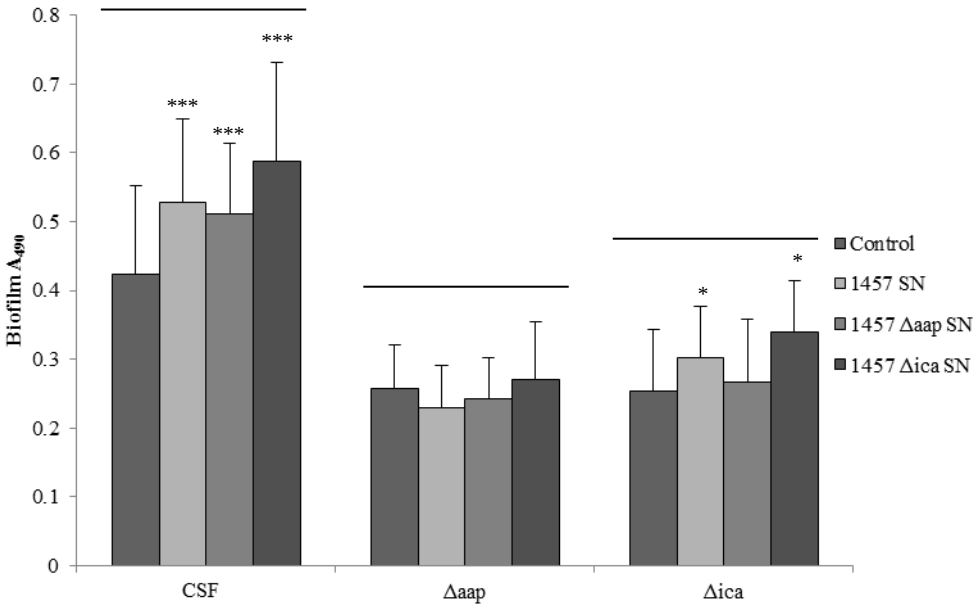


**Fig. 6.11. Biofilm phenotypes of CSF41498 and isogenic *aap* and *ica* mutants grown in culture supernatants from 1457 and isogenic *aap* and *ica* mutants.** Strains CSF41498, CSF Δ*aap*::Tc$^r$ , CSF Δ*icaC*::IS*256*Δ*tnp* incubated in filter-sterilised 1457 overnight culture supernatant, filter-sterilised 1457 Δ*aap*::Tc$^r$ overnight culture supernatant and 1457 Δ*icaADBC*::Tmp$^r$ overnight culture supernatant for 1 hr at 37$^o$C. Cell suspensions were then diluted 1:200 in BHI 1% glucose and grown for 24 hrs at 37$^o$C on hydrophilic 96-well polystyrene plates. Results shown are of at least three independent experiments. Standard deviations are indicated. Statistical significance denoted as NS for $P > 0.05$, as * for $P \leq 0.05$, as ** for $P \leq 0.01$ and as *** for $P \leq 0.001$.

To determine if the enhanced biofilm formation was specific to a component of 1457 supernatant and not due to removal of an inhibitor of biofilm formation, control experiments were performed in which CSF41498 cells were pre-incubated in filter-sterilised BHI media or washed in PBS prior to pre-incubation in filter-sterilised BHI media before the biofilm assays were performed. CSF41498 cells washed in PBS followed by pre-incubation for one hour at 37ºC in BHI significantly enhanced biofilm formation ($P \leq 0.001$, Fig. 6.12). The enhanced biofilm forming capacity exhibited by CSF41498 cells pre-washed in PBS did not correlate with increased cell density (Fig. 6.12 and 6.13). Unlike CSF41498, incubation of 1457 in either

CSF41498 supernatant, its own filter-sterilised supernatant or sterile BHI did not enhance biofilm formation (Fig. 6.14). Taken together these data suggest that the enhanced biofilm formation observed following pre-incubation of CSF41498 in 1457 supernatant or pre-washing with PBS may be due to removal of an inhibitor of CSF41498 biofilm formation. However, the mechanism(s) underlying this phenomenon are likely to be complex and further experiments are needed.

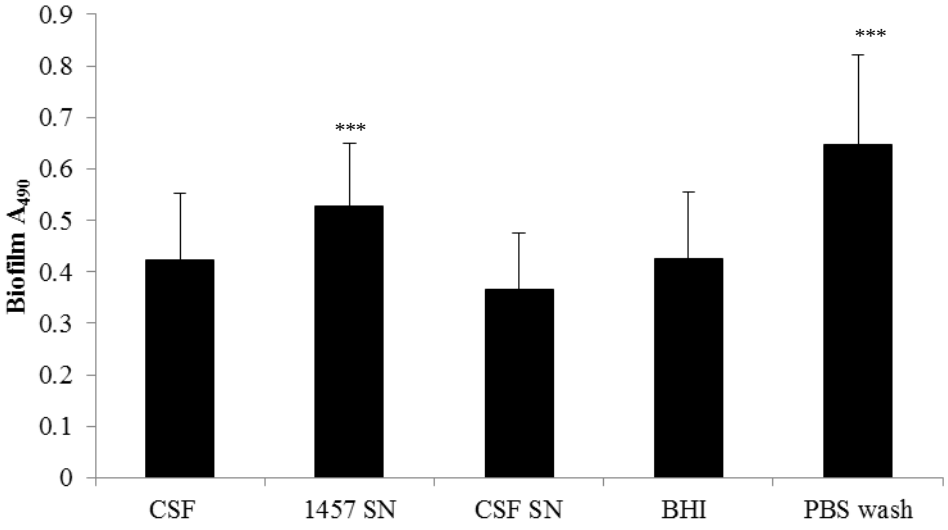


**Fig. 6.12. Effect of culture supernatants, fresh BHI and PBS washing of cells on CSF41498 biofilm formation.** Strain CSF41498 cells were incubated in BHI, filter-sterilised 1457 overnight culture supernatant, filter-sterilised CSF overnight culture supernatant, fresh BHI and fresh BHI after cells were washed in PBS for 1 hr at 37$^{o}$C. Cell suspensions were then diluted 1:200 in BHI 1% glucose and grown for 24 hrs at 37$^{o}$C on hydrophilic 96-well polystyrene plates. Results shown are of at least three independent experiments. Standard deviations are indicated. Statistical significance denoted as NS for $P > 0.05$, as * for $P \leq 0.05$, as ** for $P \leq 0.01$ and as *** for $P \leq 0.001$.

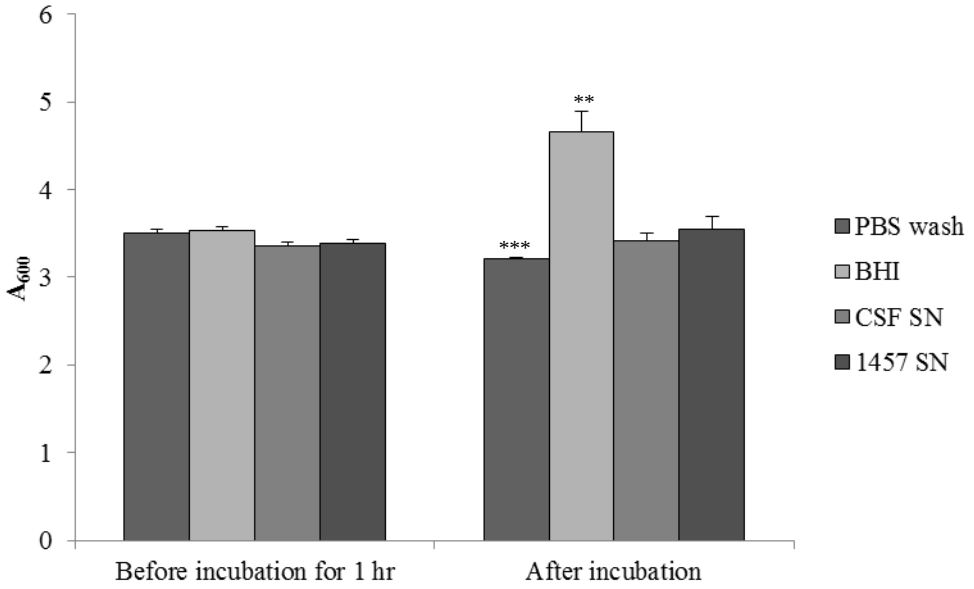


**Fig. 6.13. Comparison of the effect of different treatments on the *A600* values of CSF41498 cultures recorded before and after one hour incubation in varied media.** *A600* readings of CSF41498 cultures were taken prior to 1 hr incubation at 37°C. CSF41498 cells were treated as follows prior to the 1 hr incubation and $A_{600}$ values recorded; 1) cells were washed in PBS and resuspended in BHI media, 2) cells were resuspended in fresh BHI, 3) cells were resuspended in filter-sterilised CSF41498 culture supernatant and 4) cells were resuspended in filter-sterilised 1457 culture supernatant. After the 1 hr incubation at 37°C, the $A_{600}$ value was recorded for all CSF41498 samples. Results presented are average of three independent experiments. Standard deviations are indicated. Statistical significance denoted as NS for $P > 0.05$, as * for $P \leq 0.05$, as ** for $P \leq 0.01$ and as *** for $P \leq 0.001$.

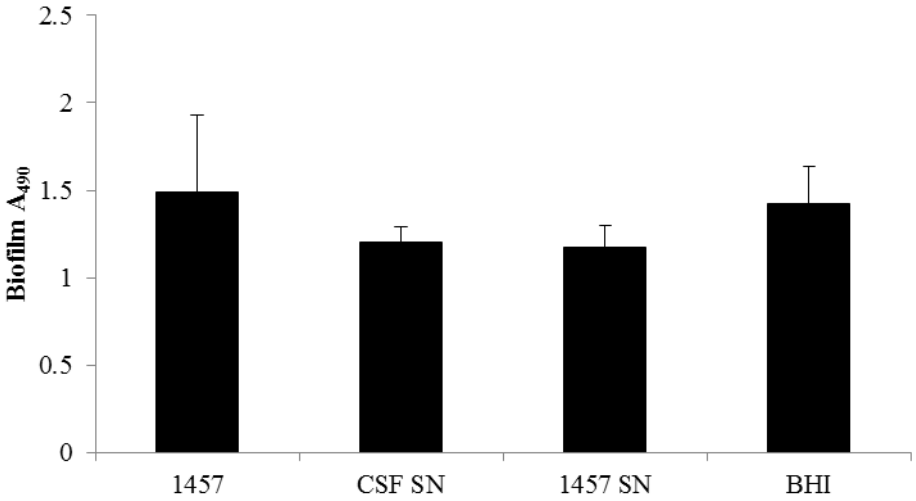


**Fig. 6.14. Effect of culture supernatants on 1457 biofilm formation.** Strain 1457 cells were incubated for 1 hr at 37°C in filter-sterilised CSF41498 overnight culture supernatant, filter-sterilised 1457 overnight culture supernatant and fresh BHI. Cells suspensions were diluted 1:200 in BHI 1% glucose and grown for 24 hrs at 37°C on hydrophilic 96-well polystyrene plates. Results shown are of at least three independent experiments. Standard deviations are indicated. Statistical significance denoted as NS for $P > 0.05$, as * for $P \leq 0.05$, as ** for $P \leq 0.01$ and as *** for $P \leq 0.001$.

## 6.3 Discussion

Data presented in this chapter reveal roles for surface proteins in *S. epidermidis* biofilm formation that function in a strain dependent manner. The contributions of two surface proteins, AtlE and Aap to *S. epidermidis in vitro* biofilm formation were assessed. Building on previous findings from our laboratory (433), the relationship between autolytic activity and biofilm formation varied between strains. CSF41498 and 1457 biofilm formation was enhanced by inhibition of autolysis whereas RP62A biofilm formation was dependent on autolytic activity. Increased biofilm formation by 1457 grown in the presence of PAS is due to upregulated *icaADBC* transcription (433). Differential proteolytic processing of AtlE may account for the different roles for autolysis in biofilm formation among the clinical isolates. It is known that Atl and AtlE must undergo proteolytic processing to generate the lytic enzymes AM and GL (37, 46). As with Aap, AtlE may not be fully processed by CSF41498, whereas it may be fully processed by RP62A, which could account for the different roles for autolysis in biofilm formation by the two strains. It appears that PIA production plays a dominant role in 1457 and surface protein adhesins are less important for *in vitro* biofilm formation by 1457 than in CSF41498 and RP62A. Western blot analysis of the AtlE protein from RP62A and CSF41498 should reveal any differences in proteolytic processing that may be attributed to alternating roles in biofilm formation. As Esp is known to cleave Atl of *S. aureus* it would also be interesting to determine if this gene is differentially expressed between CSF41498 and RP62A and if this serine protease can process AtlE (437-439).

Further assessment revealed that the RP62A biofilm was susceptible to ProK and DNaseI treatment as well as SM treatment. This suggests an important role for AtlE-mediated autolysis and eDNA release in RP62A biofilm formation and that RP62A can also use PIA for *in vitro* biofilm formation. Previous research from our laboratory demonstrated that a *srtA* mutation impaired CSF41498 biofilm formation due to loss of anchoring of Aap to the cell wall (115). Antibodies to the A domain of Aap inhibited CSF41498 but not 1457 primary attachment (115). Western blot analysis

revealed that 1457 processed the protein whereas Aap remained unprocessed and was expressed as a 220 kDa protein by CSF414198 (115). Contrary to previous publications on a role for the B domain of Aap in biofilm formation (113, 183), it appears that CSF41498 biofilm formation is mediated by the A domain of unprocessed Aap (115). Here, the contribution of Aap to both CSF41498 and 1457 biofilm formation was investigated and it was found that Aap has a strain-dependent role in *S. epidermidis* biofilm formation that varied depending on the growth conditions. Aap was found to contribute to CSF41498 biofilm formation in BHI and BHI glucose under static and flow conditions but was redundant for 1457 biofilm formation under all growth conditions. In BHI NaCl however, CSF41498 Δ*aap* was capable of wild type levels of biofilm formation. This finding, combined with the susceptibility of CSF41498 biofilm to SM treatment, would suggest that CSF4148 is capable of using both PIA and Aap for biofilm formation and that under conditions of osmotic stress PIA becomes the main mechanism for biofilm formation and Aap is not required. The findings presented here show that CSF41498 can use multiple mechanisms for *in vitro* biofilm formation, including AtlE, Aap and PIA; whereas 1457 appears to predominantly use PIA for *in vitro* biofilm formation.

It remains unclear why Aap is processed differently between CSF41498 and 1457. However, it appears that this difference in processing of Aap might be the reason for different roles for the protein in biofilm formation. Aap shares a high level of sequence homology with the SasG protein of *S. aureus* (180) which mediates PIA-independent biofilm formation via the B region following proteolytic processing (89). Investigations using inhibitors and mutants failed to identify a protease that cleaves SasG and it has been suggested that the protein may spontaneously cleave at labile peptide bonds within the G5 and E domains (89). This could apply to Aap of *S. epidermidis*. However, B. P. Conlon, *et al*. (115) have reported that the *aap* gene sequences corresponding to the A domain and cleavage site in strains 1457 and CSF41498 are identical. Biofilm assays with CSF41498 pre-treated with 1457 filter-sterilised supernatant suggest that a specific protease in the supernatant of 1457 may cleave Aap of CSF41498 to promote biofilm formation (113, 183). However pre-washing CSF41498 cells in PBS also

promoted CSF41498 biofilm, suggesting that removal of a biofilm inhibitor may also explain this phenotype. Such an inhibitor may affect the activity of a protease active against Aap, and the corresponding protease in 1457 is not sensitive to this inhibitor. Clearly this phenomenon is complex and further investigations are required, particularly given that overall protease activity as indicated on skimmed milk agar is higher in CSF41498 than 1457.Comparative analysis of the CSF41498 and 1457 genomes and in particular protease genes will be helpful.

# Chapter 7:

# Conclusions and future directions

Biofilm-associated infections caused by staphylococci are a serious medical concern. Staphylococci encased within a biofilm are protected from factors of the host's immune system and from the actions of antibiotics, making biofilm-associated infections notoriously difficult to treat and eradicate (17). Device-related infections (DRIs) associated with biofilms formed by staphylococci are life-threatening and are associated with high rates of morbidity and metastatic infections (440). The failure of conventional chemotherapeutics to eradicate biofilm-associated infections formed by staphylococci often results in the surgical removal of the infected medical devices being the only viable treatment option (440). This solution presents risks to the patient and has a vast financial impact on the healthcare sector. Antibiotic resistance is currently exacerbating staphylococcal biofilm-associated infections and complicating the treatment courses for such infections (441). A greater understanding of how staphylococci cause biofilm-associated infections and express varying levels of antibiotic resistance is urgently needed to advance medical care and improve the prognosis for patients infected by this opportunistic pathogen.

In this thesis, investigations were undertaken to advance recent findings from our laboratory in which a key role was reported for the major autolysin Atl in biofilm formation by *S. aureus* (38). The contribution of Atl to *S. aureus* biofilm formation and virulence both *in vitro* and *in vivo* was assessed and the therapeutic potential of Atl as a novel target for treating *S. aureus* DRIs was investigated. The relationship between autolytic activity and antibiotic resistance was also investigated in an attempt to elucidate the mechanisms underpinning expression of high-level methicillin resistance. Expanding on the theme of this thesis focusing on the role of surface proteins in the staphylococcal biofilm phenotype, the contribution of AtlE and Aap in *S. epidermidis* biofilm formation was also assessed. The principal findings and conclusions of this work are discussed here.

### 7.1 Atl does not contribute to *S. aureus* virulence *in vivo*

Previous research from our laboratory reported an essential role for Atl in MRSA biofilm formation whereas MSSA Atl-dependent biofilm formation was influenced by surface hydrophobicity (38). Here, using other MSSA strains, the surface hydrophobicity-dependent role of Atl in MSSA biofilm formation was verified. Atl-dependent biofilm formation was also shown to be used by the CA-MRSA strain USA300 JE2. Antibodies raised against the AM and GL domains of Atl inhibited both MRSA and MSSA biofilm formation. Furthermore Atl was also shown to contribute to the secretion of cytolytic toxins via a mechanism in part dependent on the negative regulator AtlR. Point mutations in the AM and GL active sites revealed a more important role for the GL domain of Atl for CA-MRSA biofilm formation and cytolytic toxin release compared to the AM domain. It remains to be determined why the GL region plays a more important role in *in vitro* biofilm formation but a recent study raises the possibility that the GL domain protein can bind DNA (442), which in turn may influence gene regulation and cell physiology. Alternatively, following cell lysis induced by Atl, the GL domain protein may bind to eDNA and augment the biofilm matrix.

Based on the *in vitro* studies presented in this thesis, we proposed that Atl and possibly the GL region alone would be important contributors to *S. aureus* virulence in a murine model of device-related infections. However, the *in vitro* data did not correlate with the phenotypes exhibited *in vivo* in the mouse model of device-related infection. Despite some statistically significant differences in colonisation rates and inflammatory response of the mice to infections with the wild type and *atl* mutants, the bacterial burdens in all organs remained high in mice infected with all strains. Furthermore, the severity of the DRIs caused by all strains was similar, as shown by the development of severe skin abscesses at the infection site in almost all mice and the loss of the majority of the implanted catheters by the end of the seven day infection course. On the basis of these *in vivo* data we can conclude that the pathogenesis of *S. aureus* DRIs is largely independent of Atl.

The absence of an *in vivo* role for Atl in device-related infection prompted us to re-evaluate the relevance of *in vitro* biofilm assays. In particular the rapid coating of implanted biomaterials with host extracellular matrix proteins is known to affect bacterial cell interactions *in vivo* (443). However, interactions between the bacteria and host ligands would not influence persistence of *S. aureus* within the environment. Given that our *in vitro* data shows a prominent role for Atl in biofilm formation by MRSA and MSSA on uncoated polystyrene, Atl may contribute to persistence and transmission of *S. aureus* within the environment. MRSA is reported to persist within hospital environments for up to a year when mixed with dust particles (444), which are likely to be an important source of transmission (445). Additional studies are needed to determine if Atl contributes to persistence of *S. aureus* on inert surfaces. These findings highlight the importance of *in vivo* models for validating *in vitro* phenotypes. They also raise questions about the *in vivo* relevance of *in vitro* studies on Atl (38, 47, 57). Interestingly, the *in vivo* data presented in this thesis correlates with a report from J. Takahashi, *et al*. (45) who reported that an *atl* mutation did not significantly affect the ability of *S. aureus* to establish an acute infection in a murine sepsis model.

### 7.2 *sae*-regulated coagulase activity is the critical factor required for biofilm formation under *in vivo*-mimicking conditions.

Because of the discrepancies observed between our *in vitro* and *in vivo* data on Atl, we re-designed our *in vitro* assays to be more physiologically relevant. Our new conditions involved pre-coating polystyrene surfaces with extracellular matrix proteins (30), growing the bacteria under physiologically relevant shear and using cell culture media to reflect *in vivo* nutrient availability (375). The original *in vitro* 96-well plate biofilm assay protocol designed by G. D. Christensen, *et al*. (363) does not evaluate the contribution of shear stress, nutrient limitation or interaction with host extracellular matrix proteins to biofilm formation by *S. aureus*. Our new assays, developed in collaboration with Dr Zapotoczna and Dr O'Neill at RCSI, involve coating 96-well plates with platelet-poor plasma from healthy donors prior to experimental set-up, replacement of nutrient rich media with

iron-limited RPMI-1640 tissue culture media and the application of shear forces using BioFlux or Cellix microfluidics instruments. A screen of previously characterised biofilm mutants (Table 4.1) using this new model identified the *saeRS* two component system as a critical factor for biofilm formation. In contrast, Atl, PIA and the FnBPs along with other previously characterised biofilm factors were found to be less significant. The *saeRS* two component system regulates a wide variety of biofilm and virulence factors (383, 385-387), including coagulase gene expression, and the *coa* gene was subsequently implicated in the biofilm phenotype. These data highlight the shortcomings of conventional *in vitro* biofilm assays and suggest redundancies between different mechanisms of biofilm formation used by *S. aureus*. Future investigation of factors potentially critical for biofilm formation should be assessed in similar physiologically relevant models and followed up with relevant *in vivo* models of DRIs to avoid discrepancies between *in vitro* and *in vivo* biofilm phenotypes.

The finding that coagulase was critical for biofilm formation on human plasma-coated surfaces was consistent with reports from the laboratory of Peter Verhamme and colleagues who reported a vital role for coagulase in *S. aureus* catheter-related infections (389, 390, 446). Coa is required for clot formation during infections, which results from the activity of coagulase on prothrombin in the host (377, 389) leading to the formation of the staphylothrombin complex and the conversion of soluble fibrinogen to insoluble fibrin, which becomes a scaffold for bacterial cell aggregation. Further experiments carried out by our collaborators at RCSI demonstrated that plasmin, which degrades fibrin clots, inhibited Coa-mediated biofilm on human plasma and support the conclusion that coagulase-mediated conversion of fibrinogen to fibrin is the mechanism of *S. aureus* biofilm formation on human plasma coated surfaces (447). Verhamme and colleagues have shown that chemical inactivation of coagulase activity by dabigatran has therapeutic potential in treating *S. aureus* DRIs *in vivo* (389, 390, 393). This finding that the conversion of fibrinogen to fibrin by Coa is required for biofilm formation under physiologically relevant conditions explains the observed inconsistencies between the *in vitro* and *in vivo* data on Atl presented here. Based on this data, a role for Coa in biofilm

formation would likely compensate for the *atl* defect in the murine model of DRIs.

The only discrepancy between the findings presented in this thesis and those of Verhamme and colleagues was our finding that the second *S. aureus* coagulase enzyme, von Willibrand binding protein vWbp, does not contribute to biofilm formation on human plasma-coated surfaces. Verhamme and colleagues reported that both vWbp and Coa were required for the pathogenesis of *S. aureus* catheter related infections (389). This discrepancy may be explained by the relatively low flow rate used in our BioFlux microfluidics experiments, 0.6 dynes/cm$^2$, compared to physiological shear forces in blood vessels which can be significantly higher (448). vWbp-mediated adhesion of *S. aureus* to blood vessels is shear-dependent (396), which may be masked under our experimental conditions. Furthermore, it has also been shown that binding of *S. aureus* to von Willebrand factor increases as shear force increases (449). Using a Cellix microfluidics system our collaborators in RCSI also identified a role for *clfA* in biofilm formation at 6.25 dynes/cm$^2$ (Zapotoczna, McCarthy *et al*., submitted) (447) that was not identified at the lower flow rate (0.6 dynes/cm$^2$) in the BioFlux system. Therefore, depending on the location of the implanted biomaterial within a patient, different adhesins/enzymes might contribute to *S. aureus* biofilm formation in a shear-dependent manner. However, the finding that the *sae*-regulated Coa is the critical factor for biofilm formation in both the BioFlux and the Cellix systems underline its importance in the *S. aureus* biofilm phenotype. Future studies are needed to further assess the contribution of vWbp to the biofilm phenotype, including experiments in rodent device-related infection models with *clfA*, *coa* and *vwbp* mutants. Further work should also be undertaken to examine *vwbp* regulation (at the transcriptional and protein levels) in our system. It is known that *coa* is tightly regulated by SaeRS but *vwbp* is not (387). Given the critical role for *saeRS* and *coa* in our system and the findings of Verhamme and co-workers, it will be important to determine if *vwbp* is expressed in our strains under the growth conditions used in our physiologically relevant biofilm assays.

### 7.3 High-level homogeneous oxacillin resistance upregulates autolysis in *S. aureus*

The primary physiological role for the major autolysin is to mediate daughter cell separation and cell wall turnover during normal growth and during growth in the presence of β-lactams (44, 45, 291). Conflicting reports in the literature indicate that high-level homogeneous methicillin resistance can be associated with down-regulation of Atl expression and autolysis (398, 399) or the upregulation of Atl activity (400-402). It appears that there may be multiple mechanisms for expression of HoR resistance and adaptation to growth in the presence of β-lactams. Most hospital MRSA strains express the HoR phenotype whereas CA-MRSA are typically heterogeneously resistant (279). Therefore the HeR and HoR phenotypes are clinically important. Recent studies show that high level homogeneous methicillin resistance is associated with a down regulation of virulence gene expression by *S. aureus* (226, 316, 323). It has now become important to identify mutations associated with the HoR phenotype which contribute to the balance between fitness, virulence and antibiotic resistance in MRSA strains (427, 450-452). Current research in our laboratory has revealed that some MRSA strains are able to maintain wild type levels of virulence gene expression while expressing homogeneous methicillin resistance (Gallagher, Black and O'Gara, unpublished data) and investigations into the mechanisms underpinning the switch from HeR to HoR resistance are underway. In this thesis a direct correlation is reported between the HoR phenotype and increased autolytic activity. Increased autolytic activity did not always correlate with increased *atl* mRNA levels as measured by RT-qPCR implicating post-transcriptional regulation of Atl in this phenotype. Alternatively, other peptidoglycan hydrolase genes may be upregulated in HoR strains to increase autolytic activity, or the effect of sub-inhibitory oxacillin on autolytic activity may be an artefact if the antibiotic is causing pleiotropic cell wall changes that render *S. aureus* more susceptible to triton X-100-induced autolysis.

Enhanced autolytic activity associated with HoR resistance and growth in sub-inhibitory oxacillin may be indicative of increased rates of cell wall

turnover and cell wall synthesis (410, 413, 414). Elevated expression of *murZ* and *fmtA* under these conditions, albeit not to a significant level, is also consistent with this possibility (410, 413, 414). Alterations in cell wall structure and increased peptidoglycan crosslinking have been associated with upregulated autolytic activity and increased resistance to β-lactams (318). The finding that the WalKR and LytSR two component systems (TCSs) are differentially regulated in the LAC HeR and HoR strains by sub-inhibitory oxacillin may indicate the existence of more than one mechanism for adaptation to cell wall stress. Consistent with previous reports (416, 420), the higher level of activation of both TCSs in LAC HeR grown in sub-inhibitory oxacillin compared to LAC HoR further demonstrates the presence of a distinct adaptive response to cell wall stress, possibly facilitated by secondary mutations, in the HoR strain (416, 420). Further experiments are required to determine if and how the cell wall composition and peptidoglycan synthesis differ between LAC HeR and HoR and how this impacts on virulence. Repression of the Agr system in HoR strains was attributed to an inability of the MRSA cell wall to detect AIP (226). Experiments to characterise cell wall differences in LAC HeR and HoR could include muropeptide analysis by HPLC and microscopic analysis of the cell wall by transmission electron microscopy. Further analysis could also involve studies of the synthesis and structure of WTA and LTA in LAC HeR and HoR. Both WTA and LTA are known to regulate Atl localisation at the cell wall and autolytic activity (53, 77, 429), and alterations in LTA and WTA production have been implicated in increased levels of autolytic activity associated with increased resistance to β-lactams (318, 430). On-going research in our laboratory to elucidate the mechanism(s) of homogeneous resistance includes whole genome DNA and RNA sequencing of LAC HeR and HoR.

Our data correlating increased autolytic activity in HoR strains and HeR strains grown in sub-inhibitory oxacillin with increased biofilm production are consistent with previous reports of biofilm induction by sub-inhibitory concentrations of antibiotics (405-407). However, the *in vivo* relevance of this phenotype remains to be determined. Recent work from our laboratory has shown therapeutic potential of using sub-inhibitory concentrations of

oxacillin to repress toxin production by CA-MRSA strains through induction of *mecA* expression (330). While sub-inhibitory oxacillin was associated with increased production of alpha-toxin and PVL, expression of *agr* and subsequent PSM production were repressed (330). This repression of *agr* correlates with the observed increase in biofilm formation by LAC when grown in sub-inhibitory oxacillin (148), a phenotype that needs to be considered when further evaluating the therapeutic potential of sub-inhibitory oxacillin for attenuating CA-MRSA *in vivo*. Increased biofilm formation induced by sub-inhibitory oxacillin may have the potential to enhance persistence of MRSA *in vivo* and lead to the formation of chronic infections. While repression of toxin production by sub-inhibitory oxacillin would likely reduce the severity of MRSA infections, the induction of biofilm formation would be a detrimental outcome and could complicate treatment of infections. However, additional research from our laboratory shows that the MSSA strain 8325-4 and its isogenic HoR strain are equally capable of colonising implanted catheter segments in mice and that the HoR strain is attenuated in overall virulence (316). Therefore, the increase in biofilm formation by LAC observed during growth in sub-inhibitory oxacillin and acquisition of HoR resistance may not enhance colonisation rates. Moreover, the *in vivo* data presented in this thesis suggest that upregulated *atl* expression and autolytic activity are unlikely to enhance MRSA colonisation rates *in vivo*.

### 7.4 The role for surface proteins in *S. epidermidis in vitro* biofilm formation is strain-dependent

The focus of this thesis on biofilm protein adhesins in *S. aureus* was extended to three *S. epidermidis* strains. Previous work from our laboratory revealed that AtlE was essential for CSF41498 *in vitro* biofilm formation and yet PAS treatment, which chemically blocks autolytic activity, upregulated biofilm production by this strain (433). In contrast, PAS treatment impaired RP62A biofilm formation. Clearly, AtlE and autolytic activity have different roles in the biofilm phenotype of these two strains. Proteolytic cleavage of AtlE is required for activation of the AM and GL cell wall hydrolysing enzymes (37). Different rates of AtlE processing in

CSF41498 and RP62A may account for the differing contribution of autolytic activity to *in vitro* biofilm formation. Further experiments with an AtlE knockout mutant of RP62A and analysis of AtlE and protease expression profiles between CSF41498 and RP62A are required to investigate this possibility. Additional experiments to determine the specificity and role of the extracellular serine protease (Esp) in AtlE processing are also needed, given that recent data shows that this protease cleaves Atl of *S. aureus* (438). Perhaps Esp is expressed differently in CSF41498 and RP62A (437) and different proteolytic processing may also be responsible for the different roles of Aap in CSF41498 and 1457 biofilm formation. Aap is processed by strain 1457 but remains unprocessed in CSF41498 (113, 115, 183). Data presented here revealed that CSF41498 biofilm formation was increased by incubation of CSF41498 cells in 1457 supernatant in an Aap-dependent manner. It is tempting to speculate that this may be due to processing of CSF41498 Aap by a protease present in the 1457 supernatant. Plans are underway to sequence the genomes of 1457 and CSF41498 which may provide clues to the identity of an Aap protease(s) present in 1457 but absent in the CSF41498. Overall analysis of the biofilm phenotypes of CSF41498, RP62A and 1457 suggest that extracellular protease activity plays an important role in PIA-independent biofilm formation by *S. epidermidis*. Further experiments using protease mutants are now needed to further investigate this observation.

Interestingly, while our data on the role of coagulase in the *S. aureus* biofilm phenotype on plasma coated surfaces help to explain why the *atl* mutant was not attenuated *in vivo*, Coa is evidently not relevant to biofilm formation by *S. epidermidis* and other coagulase-negative staphylococci. Atl homolog proteins may have contributory roles towards *in vivo* biofilm formation for coagulase-negative staphylococci. Recent work has shown that AtlL of *S. lugdunensis* is required for *in vitro* biofilm formation, mediates attachment to a range of host extracellular matrix and plasma proteins and is required for internalisation by eukaryotic cells (453). AtlL has also been shown to contribute to virulence in a *Caenorhabditis elegans* model (454). Additionally, AtlE of *S. epidermidis* exhibits vitronectin-binding activity and contributes to virulence in a rat CVC model (37, 66).

Therefore, while the findings presented in this thesis do not attribute a vital role for Atl in *in vivo* biofilm formation and suggest a dominant role for Coa in *S. aureus* biofilm formation under physiologically relevant conditions, Atl homolog proteins may be vital for DRIs caused by coagulase-negative staphylococci. *S. epidermidis* expresses multiple surface proteins in addition to AtlE that interact with host extracellular matrix proteins to mediate biofilm formation such as SdrG (128) and Embp (88, 130). It would be worth conducting a similar screen for biofilm formation under the physiologically relevant conditions described here with a collection of *S. epidermidis* mutants lacking these biofilm factors. Work is currently under way to develop a *bursa aurealis* transposon mutant library in the *S. epidermidis* strain 1457 of all non-essential genes, similar to the NTML in the USA300 JE2 background (455). Validation of previously characterised biofilm factors and regulators in *S. epidermidis* could be carried out using this model and the role of proteases and surface protein processing in *S. epidermidis* examined.

### 7.5 Final thoughts

Data presented in this thesis reveals important discrepancies between *in vitro* and *in vivo* biofilm phenotypes expressed by *S. aureus*. Multiple groups have reported an essential role for the major autolysin Atl in *S. aureus* biofilm formation (38, 47, 57) and yet overall a *S. aureus atl* mutant was not significantly attenuated in a murine model of device-related infection. Further experiments revealed that a number of previously characterised *S. aureus* biofilm determinants were redundant in a novel model for assessing biofilm formation under physiologically relevant conditions. Whilst autolytic activity and upregulated *atl* expression appear to be associated with the switch from heterogeneous to homogeneous resistance in MRSA, the *in vivo* significance of this phenotype remains to be determined. Additionally, the contribution of autolytic activity and surface proteins to *S. epidermidis* biofilm formation needs to be assessed in our plasma biofilm model.

The work presented here prompts a re-evaluation of *S. aureus* biofilm mechanisms and the experimental methods used to investigate factors

relevant for *in vivo* biofilm formation. Ultimately, *in vitro* assays that are more physiologically relevant should be adopted to augment traditional *in vitro* methods for studying biofilm formation and are likely to aid in the discovery of novel therapeutic targets for treating DRIs caused by *S. aureus*.

# Chapter 8:
# Bibliography

1. **Zoll S, Patzold B, Schlag M, Gotz F, Kalbacher H, Stehle T.** 2010. Structural basis of cell wall cleavage by a staphylococcal autolysin. PLoS Pathog **6:**e1000807.
2. **Kuehnert MJ, Kruszon-Moran D, Hill HA, McQuillan G, McAllister SK, Fosheim G, McDougal LK, Chaitram J, Jensen B, Fridkin SK, Killgore G, Tenover FC.** 2006. Prevalence of *Staphylococcus aureus* nasal colonization in the United States, 2001-2002. J Infect Dis **193:**172-179.
3. **Wertheim HF, Melles DC, Vos MC, van Leeuwen W, van Belkum A, Verbrugh HA, Nouwen JL.** 2005. The role of nasal carriage in *Staphylococcus aureus* infections. Lancet Infect Dis **5:**751-762.
4. **von Eiff C, Becker K, Machka K, Stammer H, Peters G.** 2001. Nasal carriage as a source of *Staphylococcus aureus* bacteremia. Study Group. N Engl J Med **344:**11-16.
5. **Wertheim HF, Vos MC, Ott A, van Belkum A, Voss A, Kluytmans JA, van Keulen PH, Vandenbroucke-Grauls CM, Meester MH, Verbrugh HA.** 2004. Risk and outcome of nosocomial *Staphylococcus aureus* bacteraemia in nasal carriers versus non-carriers. Lancet **364:**703-705.
6. **Gill SR, Fouts DE, Archer GL, Mongodin EF, Deboy RT, Ravel J, Paulsen IT, Kolonay JF, Brinkac L, Beanan M, Dodson RJ, Daugherty SC, Madupu R, Angiuoli SV, Durkin AS, Haft DH, Vamathevan J, Khouri H, Utterback T, Lee C, Dimitrov G, Jiang L, Qin H, Weidman J, Tran K, Kang K, Hance IR, Nelson KE, Fraser CM.** 2005. Insights on evolution of virulence and resistance from the complete genome analysis of an early methicillin-resistant *Staphylococcus aureus* strain and a biofilm-producing methicillin-resistant *Staphylococcus epidermidis* strain. J Bacteriol **187:**2426-2438.
7. **Baba T, Takeuchi F, Kuroda M, Yuzawa H, Aoki K, Oguchi A, Nagai Y, Iwama N, Asano K, Naimi T, Kuroda H, Cui L, Yamamoto K, Hiramatsu K.** 2002. Genome and virulence determinants of high virulence community-acquired MRSA. Lancet **359:**1819-1827.
8. **Ito T, Okuma K, Ma XX, Yuzawa H, Hiramatsu K.** 2003. Insights on antibiotic resistance of *Staphylococcus aureus* from its whole genome: genomic island SCC. Drug Resist Updat **6:**41-52.
9. **Lowy FD.** 1998. *Staphylococcus aureus* infections. N Engl J Med **339:**520-532.
10. **Boucher HW, Corey GR.** 2008. Epidemiology of methicillin-resistant *Staphylococcus aureus*. Clin Infect Dis **46 Suppl 5:**S344-349.
11. **Otto M.** 2013. Coagulase-negative staphylococci as reservoirs of genes facilitating MRSA infection: Staphylococcal commensal species such as *Staphylococcus epidermidis* are being recognized as important sources of genes promoting MRSA colonization and virulence. Bioessays **35:**4-11.
12. **Hiramatsu K, Katayama Y, Matsuo M, Sasaki T, Morimoto Y, Sekiguchi A, Baba T.** 2014. Multi-drug-resistant *Staphylococcus aureus* and future chemotherapy. J Infect Chemother **20:**593-601.
13. **Otto M.** 2012. Molecular basis of *Staphylococcus epidermidis* infections. Semin Immunopathol **34:**201-214.
14. **Vuong C, Otto M.** 2002. *Staphylococcus epidermidis* infections. Microbes Infect **4:**481–489.
15. **Davies D.** 2003. Understanding biofilm resistance to antibacterial agents. Nat Rev Drug Discov **2:**114-122.
16. **Otto M.** 2013. Staphylococcal infections: mechanisms of biofilm maturation and detachment as critical determinants of pathogenicity. Annu Rev Med **64:**175-188.

17. **O'Gara JP, Humphreys H.** 2001. *Staphylococcus epidermidis* biofilms: importance and implications. Journal of Medical Microbiology **50:**582-587.
18. **Hammond AA, Miller KG, Kruczek CJ, Dertien J, Colmer-Hamood JA, Griswold JA, Horswill AR, Hamood AN.** 2011. An in vitro biofilm model to examine the effect of antibiotic ointments on biofilms produced by burn wound bacterial isolates. Burns **37:**312-321.
19. **Moreillon P, Entenza JM, Francioli P, McDevitt D, Foster TJ, François P, Vaudaux P.** 1995. Role of *Staphylococcus aureus* coagulase and clumping factor in pathogenesis of experimental endocarditis. Infect Immun **63:**4738-4743.
20. **Nethercott C, Mabbett AN, Totsika M, Peters P, Ortiz JC, Nimmo GR, Coombs GW, Walker MJ, Schembri MA.** 2013. Molecular characterization of endocarditis-associated *Staphylococcus aureus*. J Clin Microbiol **51:**2131-2138.
21. **Donlan RM, Costerton JW.** 2002. Biofilms: Survival Mechanisms of Clinically Relevant Microorganisms. Clinical Microbiology Reviews **15:**167-193.
22. **Hall-Stoodley L, Costerton JW, Stoodley P.** 2004. Bacterial biofilms: from the natural environment to infectious diseases. Nat Rev Microbiol **2:**95-108.
23. **Hogan S, Stevens NT, Humphreys H, O'Gara JP, O'Neill E.** 2014. Current and Future Approaches to the Prevention and Treatment of Staphylococcal Medical Device-Related Infections. Current Pharmaceutical Design **21**.
24. **de Lalla F.** 1999. Antimicrobial chemotherapy in the control of surgical infectious complications. J Chemother **11:**440-445.
25. **Høiby N, Bjarnsholt T, Givskov M, Molin S, Ciofu O.** 2010. Antibiotic resistance of bacterial biofilms. Int J Antimicrob Agents **35:**322-332.
26. **Conlon BP, Nakayasu ES, Fleck LE, LaFleur MD, Isabella VM, Coleman K, Leonard SN, Smith RD, Adkins JN, Lewis K.** 2013. Activated ClpP kills persisters and eradicates a chronic biofilm infection. Nature **503:**365-370.
27. **Luppens SB, Reij MW, van der Heijden RW, Rombouts FM, Abee T.** 2002. Development of a standard test to assess the resistance of *Staphylococcus aureus* biofilm cells to disinfectants. Appl Environ Microbiol **68:**4194-4200.
28. **Beenken KE, Dunman PM, McAleese F, Macapagal D, Murphy E, Projan SJ, Blevins JS, Smeltzer MS.** 2004. Global gene expression in *Staphylococcus aureus* biofilms. J Bacteriol **186:**4665-4684.
29. **Resch A, Rosenstein R, Nerz C, Götz F.** 2005. Differential gene expression profiling of *Staphylococcus aureus* cultivated under biofilm and planktonic conditions. Appl Environ Microbiol **71:**2663-2676.
30. **Foster TJ, Höök M.** 1998. Surface protein adhesins of *Staphylococcus aureus*. Trends Microbiol **6:**484-488.
31. **Vacheethasanee K, Temenoff JS, Higashi JM, Gary A, Anderson JM, Bayston R, Marchant RE.** 1998. Bacterial surface properties of clinically isolated *Staphylococcus epidermidis* strains determine adhesion on polyethylene. J Biomed Mater Res **42:**425-432.
32. **Götz F.** 2002. Staphylococcus and biofilms. Molecular Microbiology **43:**1367-1378.
33. **Dickinson GM, Bisno AL.** 1989. Infections associated with indwelling devices: concepts of pathogenesis; infections associated with intravascular devices. Antimicrob Agents Chemother **33:**597-601.

34. **Hogt AH, Dankert J, Hulstaert CE, Feijen J.** 1986. Cell surface characteristics of coagulase-negative staphylococci and their adherence to fluorinated poly(ethylenepropylene). Infect Immun **51:**294-301.
35. **Pascual A, Fleer A, Westerdaal NA, Verhoef J.** 1986. Modulation of adherence of coagulase-negative staphylococci to Teflon catheters in vitro. Eur J Clin Microbiol **5:**518-522.
36. **Timmerman CP, Fleer A, Besnier JM, De Graaf L, Cremers F, Verhoef J.** 1991. Characterization of a proteinaceous adhesin of *Staphylococcus epidermidis* which mediates attachment to polystyrene. Infect Immun **59:**4187-4192.
37. **Heilmann C, Hussain M, Peters G, Götz F.** 1997. Evidence for autolysin-mediated primary attachment of *Staphylococcus epidermidis* to a polystyrene surface. Mol Microbiol **24:**1013–1024.
38. **Houston P, Rowe SE, Pozzi C, Waters EM, O'Gara JP.** 2011. Essential role for the major autolysin in the fibronectin-binding protein-mediated *Staphylococcus aureus* biofilm phenotype. Infect Immun **79:**1153-1165.
39. **Chhatwal GS, Preissner KT, Müller-Berghaus G, Blobel H.** 1987. Specific binding of the human S protein (vitronectin) to streptococci, *Staphylococcus aureus*, and Escherichia coli. Infect Immun **55:**1878-1883.
40. **Herrmann M, Vaudaux PE, Pittet D, Auckenthaler R, Lew PD, Schumacher-Perdreau F, Peters G, Waldvogel FA.** 1988. Fibronectin, fibrinogen, and laminin act as mediators of adherence of clinical staphylococcal isolates to foreign material. J Infect Dis **158:**693-701.
41. **Herrmann M, Suchard SJ, Boxer LA, Waldvogel FA, Lew PD.** 1991. Thrombospondin binds to *Staphylococcus aureus* and promotes staphylococcal adherence to surfaces. Infect Immun **59:**279-288.
42. **Patti JM, Allen BL, McGavin MJ, Höök M.** 1994. MSCRAMM-mediated adherence of microorganisms to host tissues. Annu Rev Microbiol **48:**585-617.
43. **Götz F, Heilmann C, Stehle T.** 2014. Functional and structural analysis of the major amidase (Atl) in Staphylococcus. Int J Med Microbiol **304:**156-163.
44. **Yamada S, Sugai M, Komatsuzawa H, Nakashima S, Oshida T, Matsumoto A, Suginaka H.** 1996. An autolysin ring associated with cell separation of *Staphylococcus aureus*. J Bacteriol **178:**1565-1571.
45. **Takahashi J, Komatsuzawa H, Yamada S, Nishida T, Labischinski H, Fujiwara T, Ohara M, Yamagishi J, Sugai M.** 2002. Molecular characterization of an atl null mutant of *Staphylococcus aureus*. Microbiol Immunol **46:**601-612.
46. **Oshida T, Sugai M, Komatsuzawa H, Hong YM, Suginaka H, Tomasz A.** 1995. A *Staphylococcus aureus* autolysin that has an N-acetylmuramoyl-L-alanine amidase domain and an endo-beta-N-acetylglucosaminidase domain: cloning, sequence analysis, and characterization. Proc Natl Acad Sci U S A **92:**285-289.
47. **Biswas R, Voggu L, Simon UK, Hentschel P, Thumm G, Gotz F.** 2006. Activity of the major staphylococcal autolysin Atl. FEMS Microbiol Lett **259:**260-268.
48. **Kajimura J, Fujiwara T, Yamada S, Suzawa Y, Nishida T, Oyamada Y, Hayashi I, Yamagishi J, Komatsuzawa H, Sugai M.** 2005. Identification and molecular characterization of an N-acetylmuramyl-L-alanine amidase Sle1 involved in cell separation of *Staphylococcus aureus*. Mol Microbiol **58:**1087-1101.
49. **Frankel MB, Hendrickx AP, Missiakas DM, Schneewind O.** 2011. LytN, a murein hydrolase in the cross-wall compartment of *Staphylococcus aureus*, is involved in proper bacterial growth and envelope assembly. J Biol Chem **286:**32593-32605.

50. **Ramadurai L, Jayaswal RK.** 1997. Molecular cloning, sequencing, and expression of lytM, a unique autolytic gene of *Staphylococcus aureus*. J Bacteriol **179:**3625-3631.
51. **Delaune A, Poupel O, Mallet A, Coic YM, Msadek T, Dubrac S.** 2011. Peptidoglycan crosslinking relaxation plays an important role in *Staphylococcus aureus* WalKR-dependent cell viability. PLoS One **6:**e17054.
52. **Baba T, Schneewind O.** 1998. Targeting of muralytic enzymes to the cell division site of Gram-positive bacteria: repeat domains direct autolysin to the equatorial surface ring of *Staphylococcus aureus*. EMBO J **17:**4639-4646.
53. **Schlag M, Biswas R, Krismer B, Kohler T, Zoll S, Yu W, Schwarz H, Peschel A, Gotz F.** 2010. Role of staphylococcal wall teichoic acid in targeting the major autolysin Atl. Mol Microbiol **75:**864-873.
54. **Hirschhausen N, Schlesier T, Schmidt MA, Gotz F, Peters G, Heilmann C.** 2010. A novel staphylococcal internalization mechanism involves the major autolysin Atl and heat shock cognate protein Hsc70 as host cell receptor. Cell Microbiol **12:**1746-1764.
55. **Milohanic E, Pron B, Berche P, Gaillard JL.** 2000. Identification of new loci involved in adhesion of Listeria monocytogenes to eukaryotic cells. European Listeria Genome Consortium. Microbiology **146:**731-739.
56. **Milohanic E, Jonquières R, Cossart P, Berche P, Gaillard JL.** 2001. The autolysin Ami contributes to the adhesion of Listeria monocytogenes to eukaryotic cells via its cell wall anchor. Mol Microbiol **39:**1212-1224.
57. **Bose JL, Lehman MK, Fey PD, Bayles KW.** 2012. Contribution of the *Staphylococcus aureus* Atl AM and GL murein hydrolase activities in cell division, autolysis, and biofilm formation. PLoS One **7:**e42244.
58. **Qin Z, Ou Y, Yang L, Zhu Y, Tolker-Nielsen T, Molin S, Qu D.** 2007. Role of autolysin-mediated DNA release in biofilm formation of *Staphylococcus epidermidis*. Microbiology **153:**2083-2092.
59. **Kiedrowski MR, Kavanaugh JS, Malone CL, Mootz JM, Voyich JM, Smeltzer MS, Bayles KW, Horswill AR.** 2011. Nuclease modulates biofilm formation in community-associated methicillin-resistant *Staphylococcus aureus*. PLoS One **6:**e26714.
60. **Izano EA, Amarante MA, Kher WB, Kaplan JB.** 2008. Differential roles of poly-N-acetylglucosamine surface polysaccharide and extracellular DNA in *Staphylococcus aureus* and *Staphylococcus epidermidis* biofilms. Appl Environ Microbiol **74:**470-476.
61. **Lauderdale KJ, Malone CL, Boles BR, Morcuende J, Horswill AR.** 2010. Biofilm dispersal of community-associated methicillin-resistant *Staphylococcus aureus* on orthopedic implant material. J Orthop Res **28:**55-61.
62. **Rice KC, Mann EE, Endres JL, Weiss EC, Cassat JE, Smeltzer MS, Bayles KW.** 2007. The cidA murein hydrolase regulator contributes to DNA release and biofilm development in *Staphylococcus aureus*. Proc Natl Acad Sci U S A **104:**8113-8118.
63. **Gibson RL, Burns JL, Ramsey BW.** 2003. Pathophysiology and management of pulmonary infections in cystic fibrosis. Am J Respir Crit Care Med **168:**918-951.
64. **Mann EE, Rice KC, Boles BR, Endres JL, Ranjit D, Chandramohan L, Tsang LH, Smeltzer MS, Horswill AR, Bayles KW.** 2009. Modulation of eDNA release and degradation affects *Staphylococcus aureus* biofilm maturation. PLoS One **4:**e5822.
65. **Foulston L, Elsholz AK, DeFrancesco AS, Losick R.** 2014. The Extracellular Matrix of *Staphylococcus aureus* Biofilms Comprises

Cytoplasmic Proteins That Associate with the Cell Surface in Response to Decreasing pH. MBio **5:** e01667-01614.
66. **Rupp ME, Fey PD, Heilmann C, Götz F.** 2001. Characterization of the importance of *Staphylococcus epidermidis* autolysin and polysaccharide intercellular adhesin in the pathogenesis of intravascular catheter-associated infection in a rat model. J Infect Dis **183:**1038-1042.
67. **Pourmand MR, Clarke SR, Schuman RF, Mond JJ, Foster SJ.** 2006. Identification of antigenic components of *Staphylococcus epidermidis* expressed during human infection. Infect Immun **74:**4644-4654.
68. **Mani N, Baddour LM, Offutt DQ, Vijaranakul U, Nadakavukaren MJ, K. JR.** 1994. Autolysis-defective mutant of *Staphylococcus aureus*: pathological considerations, genetic mapping, and electron microscopic studies. Infect Immun **62:**1406-1409.
69. **Satta G, Varaldo PE, Grazi G, Fontana R.** 1977. Bacteriolytic activity in staphylococci. 16 **1**.
70. **Wuenscher MD, Köhler S, Bubert A, Gerike U, Goebel W.** 1993. The iap gene of Listeria monocytogenes is essential for cell viability, and its gene product, p60, has bacteriolytic activity. 175 **11**.
71. **Xia G, Kohler T, Peschel A.** 2010. The wall teichoic acid and lipoteichoic acid polymers of *Staphylococcus aureus*. Int J Med Microbiol **300:**148-154.
72. **Winstel V, Liang C, Sanchez-Carballo P, Steglich M, Munar M, Broker BM, Penades JR, Nubel U, Holst O, Dandekar T, Peschel A, Xia G.** 2013. Wall teichoic acid structure governs horizontal gene transfer between major bacterial pathogens. Nat Commun **4:**2345.
73. **Winstel V, Sanchez-Carballo P, Holst O, Xia G, Peschel A.** 2014. Biosynthesis of the unique wall teichoic acid of *Staphylococcus aureus* lineage ST395. MBio **5:**e00869.
74. **Endl J, Seidl HP, Fiedler F, Schleifer KH.** 1983. Chemical composition and structure of cell wall teichoic acids of staphylococci. Arch Microbiol **135:**215-223.
75. **Vinogradov E, Sadovskaya I, Li J, Jabbouri S.** 2006. Structural elucidation of the extracellular and cell-wall teichoic acids of *Staphylococcus aureus* MN8m, a biofilm forming strain. Carbohydr Res **341:**738-743.
76. **Gross M, Cramton SE, Gotz F, Peschel A.** 2001. Key role of teichoic acid net charge in *Staphylococcus aureus* colonization of artificial surfaces. Infect Immun **69:**3423-3426.
77. **Fedtke I, Mader D, Kohler T, Moll H, Nicholson G, Biswas R, Henseler K, Gotz F, Zahringer U, Peschel A.** 2007. A *Staphylococcus aureus* ypfP mutant with strongly reduced lipoteichoic acid (LTA) content: LTA governs bacterial surface properties and autolysin activity. Mol Microbiol **65:**1078-1091.
78. **Vergara-Irigaray M, Maira-Litrán T, Merino N, Pier GB, Penadés JR, Lasa I.** 2008. Wall teichoic acids are dispensable for anchoring the PNAG exopolysaccharide to the *Staphylococcus aureus* cell surface. Microbiology **154:**865-877.
79. **Holland LM, Conlon B, O'Gara JP.** 2011. Mutation of tagO reveals an essential role for wall teichoic acids in *Staphylococcus epidermidis* biofilm development. Microbiology **157:**408-418.
80. **Shahrooei M, Hira V, Stijlemans B, Merckx R, Hermans PW, Van Eldere J.** 2009. Inhibition of *Staphylococcus epidermidis* biofilm formation by rabbit polyclonal antibodies against the SesC protein. Infect Immun **77:**3670-3678.
81. **Davis SL, Gurusiddappa S, McCrea KW, Perkins S, Höök M.** 2001. SdrG, a fibrinogen-binding bacterial adhesin of the microbial surface

components recognizing adhesive matrix molecules subfamily from *Staphylococcus epidermidis*, targets the thrombin cleavage site in the Bbeta chain. J Biol Chem **276:**27799-27805.

82. **Lang S, Livesley MA, Lambert PA, Littler WA, Elliott TS.** 2000. Identification of a novel antigen from *Staphylococcus epidermidis*. FEMS Immunol Med Microbiol **29:**213-220.
83. **McCrea KW, Hartford O, Davis S, Eidhin DN, Lina G, Speziale P, Foster TJ, Höök M.** 2000. The serine-aspartate repeat (Sdr) protein family in *Staphylococcus epidermidis*. Microbiology **146:**1535-1546.
84. **McDevitt D, Francois P, Vaudaux P, Foster TJ.** 1995. Identification of the ligand-binding domain of the surface-located fibrinogen receptor (clumping factor) of *Staphylococcus aureus*. Mol Microbiol **16:**895-907.
85. **Ní Eidhin D, Perkins S, Francois P, Vaudaux P, Höök M, Foster TJ.** 1998. Clumping factor B (ClfB), a new surface-located fibrinogen-binding adhesin of *Staphylococcus aureus*. Mol Microbiol **30:**245-257.
86. **Ryding U, Flock JI, Flock M, Soderquist B, Christensson B.** 1997. Expression of collagen-binding protein and types 5 and 8 capsular polysaccharide in clinical isolates of *Staphylococcus aureus*. J Infect Dis **176:**1096-1099.
87. **Hussain M, Herrmann M, von Eiff C, Perdreau-Remington F, Peters G.** 1997. A 140-kilodalton extracellular protein is essential for the accumulation of *Staphylococcus epidermidis* strains on surfaces. Infection and Immunity **65:**519-524.
88. **Williams RJ, Henderson B, Sharp LJ, Nair SP.** 2002. Identification of a Fibronectin-Binding Protein from *Staphylococcus epidermidis*. Infection and Immunity **70:**6805-6810.
89. **Geoghegan JA, Corrigan RM, Gruszka DT, Speziale P, O'Gara JP, Potts JR, Foster TJ.** 2010. Role of surface protein SasG in biofilm formation by *Staphylococcus aureus*. J Bacteriol **192:**5663-5673.
90. **O'Neill E, Pozzi C, Houston P, Humphreys H, Robinson DA, Loughman A, Foster TJ, O'Gara JP.** 2008. A novel *Staphylococcus aureus* biofilm phenotype mediated by the fibronectin-binding proteins, FnBPA and FnBPB. J Bacteriol **190:**3835-3850.
91. **Merino N, Toledo-Arana A, Vergara-Irigaray M, Valle J, Solano C, Calvo E, Lopez JA, Foster TJ, Penadés JR, Lasa I.** 2009. Protein A-mediated multicellular behavior in *Staphylococcus aureus*. J Bacteriol **191:**832-843.
92. **Foster TJ, Geoghegan JA, Ganesh VK, Hook M.** 2014. Adhesion, invasion and evasion: the many functions of the surface proteins of *Staphylococcus aureus*. Nat Rev Microbiol **12:**49-62.
93. **Deivanayagam CC, Wann ER, Chen W, Carson M, Rajashankar KR, Höök M, Narayana SV.** 2002. A novel variant of the immunoglobulin fold in surface adhesins of *Staphylococcus aureus*: crystal structure of the fibrinogen-binding MSCRAMM, clumping factor A. EMBO J **21:**6660-6672.
94. **Mazmanian SK, Liu G, Ton-That H, Schneewind O.** 1999. *Staphylococcus aureus* sortase, an enzyme that anchors surface proteins to the cell wall. Science **285:**760-763.
95. **Mazmanian SK, Ton-That H, Schneewind O.** 2001. Sortase-catalysed anchoring of surface proteins to the cell wall of *Staphylococcus aureus*. Mol Microbiol **40:**1049-1057.
96. **Ton-That H, Mazmanian SK, Faull KF, Schneewind O.** 2000. Anchoring of surface proteins to the cell wall of *Staphylococcus aureus*. Sortase catalyzed in vitro transpeptidation reaction using LPXTG peptide and NH(2)-Gly(3) substrates. J Biol Chem **275:**9876-9881.

97. **Bowden MG, Chen W, Singvall J, Xu Y, Peacock SJ, Valtulina V, Speziale P, Höök M.** 2005. Identification and preliminary characterization of cell-wall-anchored proteins of *Staphylococcus epidermidis*. Microbiology **151:**1453-1464.
98. **Fischetti VA, Pancholi V, Schneewind O.** 1990. Conservation of a hexapeptide sequence in the anchor region of surface proteins from gram-positive cocci. Mol Microbiol **4:**1603-1605.
99. **Schneewind O, Mihaylova-Petkov D, Model P.** 1993. Cell wall sorting signals in surface proteins of gram-positive bacteria. EMBO J **12:**4803-4811.
100. **Schneewind O, Model P, Fischetti VA.** 1992. Sorting of protein A to the staphylococcal cell wall. Cell **70:**267-281.
101. **Navarre WW, Schneewind O.** 1994. Proteolytic cleavage and cell wall anchoring at the LPXTG motif of surface proteins in gram-positive bacteria. Mol Microbiol **14:**115-121.
102. **Schneewind O, Fowler A, Faull KF.** 1995. Structure of the cell wall anchor of surface proteins in *Staphylococcus aureus*. Science **268:**103-106.
103. **Ton-That H, Liu G, Mazmanian SK, Faull KF, Schneewind O.** 1999. Purification and characterization of sortase, the transpeptidase that cleaves surface proteins of *Staphylococcus aureus* at the LPXTG motif. Proc Natl Acad Sci U S A **96:**12424-12429.
104. **Ton-That H, Faull KF, Schneewind O.** 1997. Anchor structure of staphylococcal surface proteins. A branched peptide that links the carboxyl terminus of proteins to the cell wall. J Biol Chem **272:**22285-22292.
105. **Ton-That H, Schneewind O.** 1999. Anchor structure of staphylococcal surface proteins. IV. Inhibitors of the cell wall sorting reaction. J Biol Chem **274:**24316-24320.
106. **Mazmanian SK, Ton-That H, Su K, Schneewind O.** 2002. An iron-regulated sortase anchors a class of surface protein during *Staphylococcus aureus* pathogenesis. Proc Natl Acad Sci U S A **99:**2293-2298.
107. **Horsburgh MJ, Ingham E, Foster SJ.** 2001. In *Staphylococcus aureus*, fur is an interactive regulator with PerR, contributes to virulence, and Is necessary for oxidative stress resistance through positive regulation of catalase and iron homeostasis. J Bacteriol **183:**468-475.
108. **Jonsson IM, Mazmanian SK, Schneewind O, Bremell T, Tarkowski A.** 2003. The role of *Staphylococcus aureus* sortase A and sortase B in murine arthritis. Microbes Infect **5:**775-780.
109. **Jonsson I, M. , Mazmanian SK, Schneewind O, Verdrengh M, Bremell T, Tarkowski A.** 2002. On the role of *Staphylococcus aureus* sortase and sortase-catalyzed surface protein anchoring in murine septic arthritis. J Infect Dis **185:**1417-1424.
110. **Weiss WJ, Lenoy E, Murphy T, Tardio L, Burgio P, Projan SJ, Schneewind O, Alksne L.** 2004. Effect of srtA and srtB gene expression on the virulence of *Staphylococcus aureus* in animal models of infection. J Antimicrob Chemother **53:**480-486.
111. **Mazmanian SK, Liu G, Jensen ER, Lenoy E, Schneewind O.** 2000. *Staphylococcus aureus* sortase mutants defective in the display of surface proteins and in the pathogenesis of animal infections. Proc Natl Acad Sci U S A **97:**5510-5515.
112. **Roche FM, Massey R, Peacock SJ, Day NP, Visai L, Speziale P, Lam A, Pallen M, Foster TJ.** 2003. Characterization of novel LPXTG-containing proteins of *Staphylococcus aureus* identified from genome sequences. Microbiology **149:**643-654.
113. **Rohde H, Burdelski C, Bartscht K, Hussain M, Buck F, Horstkotte MA, Knobloch JK, Heilmann C, Herrmann M, Mack D.** 2005. Induction of *Staphylococcus epidermidis* biofilm formation via proteolytic

processing of the accumulation-associated protein by staphylococcal and host proteases. Mol Microbiol **55:**1883-1895.

114. **Signäs C, Raucci G, Jönsson K, Lindgren PE, Anantharamaiah GM, Höök M, Lindberg M.** 1989. Nucleotide sequence of the gene for a fibronectin-binding protein from *Staphylococcus aureus*: use of this peptide sequence in the synthesis of biologically active peptides. Proc Natl Acad Sci U S A **86:**699-703.
115. **Conlon BP, Geoghegan JA, Waters EM, McCarthy H, Rowe SE, Davies JR, Schaeffer CR, Foster TJ, Fey PD, O'Gara JP.** 2014. A role for the A-domain of unprocessed accumulation associated protein (Aap) in the attachment phase of the *Staphylococcus epidermidis* biofilm phenotype. J Bacteriol**:**JB.01946-01914.
116. **Herrick S, Blanc-Brude O, Gray A, Laurent G.** 1999. Fibrinogen. Int J Biochem Cell Biol **31:**741-746.
117. **McDevitt D, Nanavaty T, House-Pompeo K, Bell E, Turner N, McIntire L, Foster T, Höök M.** 1997. Characterization of the interaction between the *Staphylococcus aureus* clumping factor (ClfA) and fibrinogen. Eur J Biochem **247:**416-424.
118. **Ponnuraj K, Bowden MG, Davis S, Gurusiddappa S, Moore D, Choe D, Xu Y, Hook M, Narayana SV.** 2003. A "dock, lock, and latch" structural model for a staphylococcal adhesin binding to fibrinogen. Cell **115:**217-228.
119. **Walsh EJ, Miajlovic H, Gorkun OV, Foster TJ.** 2008. Identification of the *Staphylococcus aureus* MSCRAMM clumping factor B (ClfB) binding site in the alphaC-domain of human fibrinogen. Microbiology **154:**550-558.
120. **Ganesh VK, Rivera JJ, Smeds E, Ko YP, Bowden MG, Wann ER, Gurusiddappa S, Fitzgerald JR, Höök M.** 2008. A structural model of the *Staphylococcus aureus* ClfA-fibrinogen interaction opens new avenues for the design of anti-staphylococcal therapeutics. PLoS Pathog **4:**e1000226.
121. **Ganesh VK, Barbu EM, Deivanayagam CC, Le B, Anderson AS, Matsuka YV, Lin SL, Foster TJ, Narayana SV, Höök M.** 2011. Structural and biochemical characterization of *Staphylococcus aureus* clumping factor B/ligand interactions. J Biol Chem **286:**25963-25972.
122. **Farrell DH, Thiagarajan P, Chung DW, Davie EW.** 1992. Role of fibrinogen alpha and gamma chain sites in platelet aggregation. Proc Natl Acad Sci U S A **89:**10729-10732.
123. **Abraham NM, Jefferson KK.** 2012. *Staphylococcus aureus* clumping factor B mediates biofilm formation in the absence of calcium. Microbiology **158:**1504-1512.
124. **Abraham NM, Lamlertthon S, Fowler VG, Jefferson KK.** 2012. Chelating agents exert distinct effects on biofilm formation in *Staphylococcus aureus* depending on strain background: role for clumping factor B. J Med Microbiol **61:**1062-1070.
125. **Sullam PM, Bayer AS, Foss WM, Cheung AL.** 1996. Diminished platelet binding in vitro by *Staphylococcus aureus* is associated with reduced virulence in a rabbit model of infective endocarditis. Infect Immun **64:**4915-4921.
126. **Siboo IR, Cheung AL, Bayer AS, Sullam PM.** 2001. Clumping factor A mediates binding of *Staphylococcus aureus* to human platelets. Infect Immun **69:**3120-3127.
127. **Que YA, François P, Haefliger JA, Entenza JM, Vaudaux P, Moreillon P.** 2001. Reassessing the role of *Staphylococcus aureus* clumping factor and fibronectin-binding protein by expression in Lactococcus lactis. Infect Immun **69:**6296-6302.

128. **Hofmann CM, Anderson JM, Marchant RE.** 2012. Targeted delivery of vancomycin to *Staphylococcus epidermidis* biofilms using a fibrinogen-derived peptide. J Biomed Mater Res A **100:**2517-2525.
129. **Chavakis T, Wiechmann K, Preissner KT, Herrmann M.** 2005. *Staphylococcus aureus* interactions with the endothelium. The role of bacterial "Secretable Expanded Repertoire Adhesive Molecules" (SERAM) in disturbing host defense systems. Thrombosis and Haemostasis doi:10.1160/th05-05-0306.
130. **Christner M, Franke GC, Schommer NN, Wendt U, Wegert K, Pehle P, Kroll G, Schulze C, Buck F, Mack D, Aepfelbacher M, Rohde H.** 2010. The giant extracellular matrix-binding protein of *Staphylococcus epidermidis* mediates biofilm accumulation and attachment to fibronectin. Mol Microbiol **75:**187-207.
131. **Hussain M, Becker K, von Eiff C, Peters G, Herrmann M.** 2001. Analogs of Eap protein are conserved and prevalent in clinical *Staphylococcus aureus* isolates. Clin Diagn Lab Immunol **8:**1271-1276.
132. **Yousif Y, Mertz A, Batsford SR, Vogt A.** 1991. Cationic staphylococcal antigens have high affinity for glomerular structures. Possible pathogenic role in glomerulonephritis. Zentbl Bakteriol **21:**168–169.
133. **Bodén MK, Flock JI.** 1992. Evidence for three different fibrinogen-binding proteins with unique properties from *Staphylococcus aureus* strain Newman. Microb Pathog **12:**289-298.
134. **McGavin MH, Krajewska-Pietrasik D, Rydén C, Höök M.** 1993. Identification of a *Staphylococcus aureus* extracellular matrix-binding protein with broad specificity. Infect Immun **61:**2479-2485.
135. **Jönsson K, McDevitt D, McGavin MH, Patti JM, Höök M.** 1995. *Staphylococcus aureus* expresses a major histocompatibility complex class II analog. J Biol Chem **270:**21457-21460.
136. **Palma M, Haggar A, Flock JI.** 1999. Adherence of *Staphylococcus aureus* is enhanced by an endogenous secreted protein with broad binding activity. J Bacteriol **181:**2840-2845.
137. **Harraghy N, Hussain M, Haggar A, Chavakis T, Sinha B, Herrmann M, Flock JI.** 2003. The adhesive and immunomodulating properties of the multifunctional *Staphylococcus aureus* protein Eap. Microbiology **149:**2701-2707.
138. **Hansen U, Hussain M, Villone D, Herrmann M, Robenek H, Peters G, Sinha B, Bruckner P.** 2006. The anchorless adhesin Eap (extracellular adherence protein) from *Staphylococcus aureus* selectively recognizes extracellular matrix aggregates but binds promiscuously to monomeric matrix macromolecules. Matrix Biol **25:**252-260.
139. **Thompson KM, Abraham N, Jefferson KK.** 2010. *Staphylococcus aureus* extracellular adherence protein contributes to biofilm formation in the presence of serum. FEMS Microbiol Lett **305:**143-147.
140. **Kreikemeyer B, McDevitt D, Podbielski A.** 2002. The role of the map protein in *Staphylococcus aureus* matrix protein and eukaryotic cell adherence. Int J Med Microbiol **292:**283-295.
141. **Johnson M, Cockayne A, Morrissey JA.** 2008. Iron-regulated biofilm formation in *Staphylococcus aureus* Newman requires ica and the secreted protein Emp. Infect Immun **76:**1756-1765.
142. **Grundmeier M, Hussain M, Becker P, Heilmann C, Peters G, Sinha B.** 2004. Truncation of fibronectin-binding proteins in *Staphylococcus aureus* strain Newman leads to deficient adherence and host cell invasion due to loss of the cell wall anchor function. Infect Immun **72:**7155-7163.
143. **Bur S, Preissner KT, Herrmann M, Bischoff M.** 2013. The *Staphylococcus aureus* extracellular adherence protein promotes bacterial

internalization by keratinocytes independent of fibronectin-binding proteins. J Invest Dermatol **133:**2004-2012.
144. **Chavakis T, Hussain M, Kanse SM, Peters G, Bretzel RG, Flock JI, Herrmann M, Preissner KT.** 2002. *Staphylococcus aureus* extracellular adherence protein serves as anti-inflammatory factor by inhibiting the recruitment of host leukocytes. Nat Med **8:**687-693.
145. **Cheng AG, Kim HK, Burts ML, Krausz T, Schneewind O, Missiakas DM.** 2009. Genetic requirements for *Staphylococcus aureus* abscess formation and persistence in host tissues. FASEB J **23:**3393-3404.
146. **Stapels DA, Ramyar KX, Bischoff M, von Köckritz-Blickwede M, Milder FJ, Ruyken M, Eisenbeis J, McWhorter WJ, Herrmann M, van Kessel KP, Geisbrecht BV, Rooijakkers SH.** 2014. *Staphylococcus aureus* secretes a unique class of neutrophil serine protease inhibitors. Proc Natl Acad Sci U S A **111:**13187-13192.
147. **Hussain M, Becker K, von Eiff C, Schrenzel J, Peters G, Herrmann M.** 2001. Identification and characterization of a novel 38.5-kilodalton cell surface protein of *Staphylococcus aureus* with extended-spectrum binding activity for extracellular matrix and plasma proteins. J Bacteriol **183:**6778-6786.
148. **Boles BR, Horswill AR.** 2008. Agr-mediated dispersal of *Staphylococcus aureus* biofilms. PLoS Pathog **4:**e1000052.
149. **Rohde H, Frankenberger S, Zahringer U, Mack D.** 2010. Structure, function and contribution of polysaccharide intercellular adhesin (PIA) to *Staphylococcus epidermidis* biofilm formation and pathogenesis of biomaterial-associated infections. Eur J Cell Biol **89:**103-111.
150. **Mack D, Nedelmann M, Krokotsch A, Schwarzkopf A, Heesemann J, Laufs R.** 1994. Characterization of transposon mutants of biofilm-producing *Staphylococcus epidermidis* impaired in the accumulative phase of biofilm production: genetic identification of a hexosamine-containing polysaccharide intercellular adhesin. Infect Immun **62:**3244-3253.
151. **Heilmann C, Schweitzer O, Gerke C, Vanittanakom N, Mack D, Götz F.** 1996. Molecular basis of intercellular adhesion in the biofilm-forming *Staphylococcus epidermidis*. Molecular Microbiology **20:**1083-1091.
152. **Heilmann C, Gerke C, Perdreau-Remington F, Götz F.** 1996. Characterization of Tn917 insertion mutants of *Staphylococcus epidermidis* affected in biofilm formation. Infect Immun **64:**277-282.
153. **Heilmann C, Götz F.** 1998. Further characterization of *Staphylococcus epidermidis* transposon mutants deficient in primary attachment or intercellular adhesion. Zentralbl Bakteriol **287:**69-83.
154. **Cramton SE, Gerke C, Schnell NF, Nichols WW, Götz F.** 1999. The Intercellular Adhesion (ica) Locus Is Present in *Staphylococcus aureus* and Is Required for Biofilm Formation. Infection and Immunity **67:**5427-5433.
155. **Cramton SE, Ulrich M, Gotz F, Doring G.** 2001. Anaerobic conditions induce expression of polysaccharide intercellular adhesin in *Staphylococcus aureus* and *Staphylococcus epidermidis*. Infect Immun **69:**4079-4085.
156. **McKenney D, Pouliot KL, Wang Y, Murthy V, Ulrich M, Doring G, Lee JC, Goldmann DA, Pier GB.** 1999. Broadly protective vaccine for *Staphylococcus aureus* based on an in vivo-expressed antigen. Science **284:**1523–1527.
157. **Conlon KM, Humphreys H, O'Gara JP.** 2002. icaR Encodes a Transcriptional Repressor Involved in Environmental Regulation of ica Operon Expression and Biofilm Formation in *Staphylococcus epidermidis*. Journal of Bacteriology **184:**4400-4408.
158. **Gerke C, Kraft A, Süssmuth R, Schweitzer O, Götz F.** 1998. Characterization of the N-acetylglucosaminyltransferase activity involved

in the biosynthesis of the *Staphylococcus epidermidis* polysaccharide intercellular adhesin. J Biol Chem **273:**18586-18593.
159. **Otto M.** 2009. *Staphylococcus epidermidis*--the 'accidental' pathogen. Nat Rev Microbiol **7:**555-567.
160. **Vuong C, Kocianova S, Voyich JM, Yao Y, Fischer ER, DeLeo FR, Otto M.** 2004. A crucial role for exopolysaccharide modification in bacterial biofilm formation, immune evasion, and virulence. J Biol Chem **279:**54881-54886.
161. **Conlon KM, Humphreys H, O'Gara JP.** 2002. Regulation of icaR gene expression in *Staphylococcus epidermidis*. FEMS Microbiology Letters **216:**171-177.
162. **Fitzpatrick F, Humphreys H, O'Gara J P.** 2005. Evidence for low temperature regulation of biofilm formation in *Staphylococcus epidermidis*. J Med Microbiol **54:**509-510.
163. **Jefferson KK, Pier DB, Goldmann DA, Pier GB.** 2004. The teicoplanin-associated locus regulator (TcaR) and the intercellular adhesin locus regulator (IcaR) are transcriptional inhibitors of the ica locus in *Staphylococcus aureus*. J Bacteriol **186:**2449-2456.
164. **Christensen GD, Simpson WA, Bisno AL, Beachey EH.** 1983. Experimental foreign body infections in mice challenged with slime-producing *Staphylococcus epidermidis*. Infect Immun **40:**407-410.
165. **Christensen GD, Baddour LM, Simpson WA.** 1987. Phenotypic variation of *Staphylococcus epidermidis* slime production in vitro and in vivo. Infect Immun **55:**2870-2877.
166. **Rupp ME, Ulphani JS, Fey PD, Bartscht K, Mack D.** 1999. Characterization of the importance of polysaccharide intercellular adhesin/hemagglutinin of *Staphylococcus epidermidis* in the pathogenesis of biomaterial-based infection in a mouse foreign body infection model. Infect Immun **67:**2627-2632.
167. **Maira-Litran T, Kropec A, Goldmann D, Pier GB.** 2004. Biologic properties and vaccine potential of the staphylococcal poly-N-acetyl glucosamine surface polysaccharide. Vaccine **22:**872-879.
168. **Peacock SJ, Moore CE, Justice A, Kantzanou M, Story L, Mackie K, O'Neill G, Day NP.** 2002. Virulent combinations of adhesin and toxin genes in natural populations of *Staphylococcus aureus*. Infect Immun **70:**4987-4996.
169. **Muller E, Takeda S, Shiro H, Goldmann D, Pier GB.** 1993. Occurrence of capsular polysaccharide/adhesin among clinical isolates of coagulase-negative staphylococci. J Infect Dis **168:**1211-1218.
170. **Ziebuhr W, Heilmann C, Götz F, Meyer P, Wilms K, Straube E, Hacker J.** 1997. Detection of the intercellular adhesion gene cluster (ica) and phase variation in *Staphylococcus epidermidis* blood culture strains and mucosal isolates. Infect Immun **65:**890-896.
171. **Arciola CR, Baldassarri L, Montanaro L.** 2001. Presence of icaA and icaD genes and slime production in a collection of staphylococcal strains from catheter-associated infections. J Clin Microbiol **39:**2151-2156.
172. **Fowler VGJ, Fey PD, Reller LB, Chamis AL, Corey GR, Rupp ME.** 2001. The intercellular adhesin locus ica is present in clinical isolates of *Staphylococcus aureus* from bacteremic patients with infected and uninfected prosthetic joints. Med Microbiol Immunol **189:**127-131.
173. **Kojima Y, Tojo M, Goldmann DA, Tosteson TD, Pier GB.** 1990. Antibody to the capsular polysaccharide/adhesin protects rabbits against catheter-related bacteremia due to coagulase-negative staphylococci. J Infect Dis **162:**435-441.
174. **Takeda S, Pier GB, Kojima Y, Tojo M, Muller E, Tosteson T, Goldmann DA.** 1991. Protection against endocarditis due to

*Staphylococcus epidermidis* by immunization with capsular polysaccharide/adhesin. Circulation **84:**2539-2546.

175. **Maira-Litrán T, Kropec A, Abeygunawardana C, Joyce J, Mark Gr, Goldmann DA, Pier GB.** 2002. Immunochemical properties of the staphylococcal poly-N-acetylglucosamine surface polysaccharide. Infect Immun **70:**4433-4440.
176. **Francois P, Tu Quoc PH, Bisognano C, Kelley WL, Lew DP, Schrenzel J, Cramton SE, Götz F, Vaudaux P.** 2003. Lack of biofilm contribution to bacterial colonisation in an experimental model of foreign body infection by *Staphylococcus aureus* and *Staphylococcus epidermidis*. FEMS Immunol Med Microbiol **35:**135-140.
177. **Cucarella C, Solano C, Valle J, Amorena B, Lasa I, Penades JR.** 2001. Bap, a *Staphylococcus aureus* surface protein involved in biofilm formation. J Bacteriol **183:**2888-2896.
178. **Cucarella C, Tormo MA, Ubeda C, Trotonda MP, Monzón M, Peris C, Amorena B, Lasa I, Penadés JR.** 2004. Role of biofilm-associated protein bap in the pathogenesis of bovine *Staphylococcus aureus*. Infect Immun **72:**2177-2185.
179. **Vergara-Irigaray M, Valle J, Merino N, Latasa C, Garcia B, Ruiz de Los Mozos I, Solano C, Toledo-Arana A, Penades JR, Lasa I.** 2009. Relevant role of fibronectin-binding proteins in *Staphylococcus aureus* biofilm-associated foreign-body infections. Infect Immun **77:**3978-3991.
180. **Corrigan RM, Rigby D, Handley P, Foster TJ.** 2007. The role of *Staphylococcus aureus* surface protein SasG in adherence and biofilm formation. Microbiology **153:**2435-2446.
181. **Macintosh RL, Brittan JL, Bhattacharya R, Jenkinson HF, Derrick J, Upton M, Handley PS.** 2009. The terminal A domain of the fibrillar accumulation-associated protein (Aap) of *Staphylococcus epidermidis* mediates adhesion to human corneocytes. J Bacteriol **191:**7007-7016.
182. **Roche FM, Meehan M, Foster TJ.** 2003. The *Staphylococcus aureus* surface protein SasG and its homologues promote bacterial adherence to human desquamated nasal epithelial cells. Microbiology **149:**2759-2767.
183. **Conrady DG, Wilson JJ, Herr AB.** 2013. Structural basis for Zn2+-dependent intercellular adhesion in staphylococcal biofilms. Proc Natl Acad Sci U S A **110:**E202-211.
184. **Conrady DG, Brescia CC, Horii K, Weiss AA, Hassett DJ, Herr AB.** 2008. A zinc-dependent adhesion module is responsible for intercellular adhesion in staphylococcal biofilms. Proc Natl Acad Sci U S A **105:**19456-19461.
185. **Gruszka DT, Wojdyla JA, Bingham RJ, Turkenburg JP, Manfield IW, Steward A, Leech AP, Geoghegan JA, Foster TJ, Clarke J, Potts JR.** 2012. Staphylococcal biofilm-forming protein has a contiguous rod-like structure. Proc Natl Acad Sci U S A **109:**E1011-1018.
186. **Banner MA, Cunniffe JG, Macintosh RL, Foster TJ, Rohde H, Mack D, Hoyes E, Derrick J, Upton M, Handley PS.** 2007. Localized tufts of fibrils on *Staphylococcus epidermidis* NCTC 11047 are comprised of the accumulation-associated protein. J Bacteriol **189:**2793-2804.
187. **Jönsson K, Signäs C, Müller HP, Lindberg M.** 1991. Two different genes encode fibronectin binding proteins in *Staphylococcus aureus*. The complete nucleotide sequence and characterization of the second gene. Eur J Biochem **202:**1041-1048.
188. **Roche FM, Downer R, Keane F, Speziale P, Park PW, Foster TJ.** 2004. The N-terminal A domain of fibronectin-binding proteins A and B promotes adhesion of *Staphylococcus aureus* to elastin. J Biol Chem **279:**38433-38440.

189. **Wann ER, Gurusiddappa S, Hook M.** 2000. The fibronectin-binding MSCRAMM FnbpA of *Staphylococcus aureus* is a bifunctional protein that also binds to fibrinogen. J Biol Chem **275:**13863-13871.
190. **Greene C, McDevitt D, Francois P, Vaudaux PE, Lew DP, Foster TJ.** 1995. Adhesion properties of mutants of *Staphylococcus aureus* defective in fibronectin-binding proteins and studies on the expression of fnb genes. Mol Microbiol **17:**1143-1152.
191. **Schwarz-Linek U, Werner JM, Pickford AR, Gurusiddappa S, Kim JH, Pilka ES, Briggs JA, Gough TS, Höök M, Campbell ID, Potts JR.** 2003. Pathogenic bacteria attach to human fibronectin through a tandem beta-zipper. Nature **423:**177-181.
192. **Keane FM, Loughman A, Valtulina V, Brennan M, Speziale P, Foster TJ.** 2007. Fibrinogen and elastin bind to the same region within the A domain of fibronectin binding protein A, an MSCRAMM of *Staphylococcus aureus*. Mol Microbiol **63:**711-723.
193. **Burke FM, Di Poto A, Speziale P, Foster TJ.** 2011. The A domain of fibronectin-binding protein B of *Staphylococcus aureus* contains a novel fibronectin binding site. FEBS J **278:**2359-2371.
194. **Geoghegan JA, Monk IR, O'Gara JP, Foster TJ.** 2013. Subdomains N2N3 of fibronectin binding protein A mediate *Staphylococcus aureus* biofilm formation and adherence to fibrinogen using distinct mechanisms. J Bacteriol **195:**2675-2683.
195. **Sinha B, François PP, Nüsse O, Foti M, Hartford OM, Vaudaux P, Foster TJ, Lew DP, Herrmann M, Krause KH.** 1999. Fibronectin-binding protein acts as *Staphylococcus aureus* invasin via fibronectin bridging to integrin alpha5beta1. Cell Microbiol **1:**101-117.
196. **Peacock SJ, Foster TJ, Cameron BJ, Berendt AR.** 1999. Bacterial fibronectin-binding proteins and endothelial cell surface fibronectin mediate adherence of *Staphylococcus aureus* to resting human endothelial cells. Microbiology **145:**3477-3486.
197. **Peacock SJ, Day NP, Thomas MG, Berendt AR, Foster TJ.** 2000. Clinical isolates of *Staphylococcus aureus* exhibit diversity in fnb genes and adhesion to human fibronectin. J Infect **41:**23-31.
198. **Mongodin E, Bajolet O, Cutrona J, Bonnet N, Dupuit F, Puchelle E, de Bentzmann S.** 2002. Fibronectin-binding proteins of *Staphylococcus aureus* are involved in adherence to human airway epithelium. Infect Immun **70:**620-630.
199. **Dryla A, Prustomersky S, Gelbmann D, Hanner M, Bettinger E, Kocsis B, Kustos T, Henics T, Meinke A, Nagy E.** 2005. Comparison of antibody repertoires against *Staphylococcus aureus* in healthy individuals and in acutely infected patients. Clin Diagn Lab Immunol **12:**387-398.
200. **Rennermalm A, Li YH, Bohaufs L, Jarstrand C, Brauner A, Brennan FR, Flock JI.** 2001. Antibodies against a truncated *Staphylococcus aureus* fibronectin-binding protein protect against dissemination of infection in the rat. Vaccine **19:**3376-3383.
201. **McCourt J, O'Halloran DP, McCarthy H, O'Gara JP, Geoghegan JA.** 2014. Fibronectin-binding proteins are required for biofilm formation by community-associated methicillin-resistant *Staphylococcus aureus* strain LAC. FEMS Microbiol Lett **353:**157-164.
202. **Lower SK, Lamlertthon S, Casillas-Ituarte NN, Lins RD, Yongsunthon R, Taylor ES, DiBartola AC, Edmonson C, McIntyre LM, Reller LB, Que YA, Ros R, Lower BH, Fowler VGJ.** 2011. Polymorphisms in fibronectin binding protein A of *Staphylococcus aureus* are associated with infection of cardiovascular devices. Proc Natl Acad Sci U S A **108:**18372-18377.

203. **Sjodahl J.** 1977. Repetitive sequences in protein A from *Staphylococcus aureus*. Arrangement of five regions within the protein, four being highly homologous and Fc-binding. Eur J Biochem **73:**343-351.
204. **Moks T, Abrahmsén L, Nilsson B, Hellman U, Sjöquist J, Uhlén M.** 1986. Staphylococcal protein A consists of five IgG-binding domains. Eur J Biochem **156:**637-643.
205. **Uhlén M, Guss B, Nilsson B, Götz F, Lindberg M.** 1984. Expression of the gene encoding protein A in *Staphylococcus aureus* and coagulase-negative staphylococci. J Bacteriol **159:**713-719.
206. **Uhlén M, Guss B, Nilsson B, Gatenbeck S, Philipson L, Lindberg M.** 1984. Complete sequence of the staphylococcal gene encoding protein A. A gene evolved through multiple duplications. J Biol Chem **259:**1695-1702.
207. **Löfdahl S, Guss B, Uhlén M, Philipson L, Lindberg M.** 1983. Gene for staphylococcal protein A. Proc Natl Acad Sci U S A **80:**697-701.
208. **Foster TJ.** 2005. Immune evasion by staphylococci. Nat Rev Microbiol **3:**948-958.
209. **Hartleib J, Köhler N, Dickinson RB, Chhatwal GS, Sixma JJ, Hartford OM, Foster TJ, Peters G, Kehrel BE, Herrmann M.** 2000. Protein A is the von Willebrand factor binding protein on *Staphylococcus aureus*. Blood **96:**2149-2156.
210. **Nguyen T, Ghebrehiwet B, Peerschke EI.** 2000. *Staphylococcus aureus* protein A recognizes platelet gC1qR/p33: a novel mechanism for staphylococcal interactions with platelets. Infect Immun **68:**2061-2068.
211. **Goodyear CS, Silverman GJ.** 2004. Staphylococcal toxin induced preferential and prolonged in vivo deletion of innate-like B lymphocytes. Proc Natl Acad Sci U S A **101:**11392-11397.
212. **Gómez MI, Lee A, Reddy B, Muir A, Soong G, Pitt A, Cheung A, Prince A.** 2004. *Staphylococcus aureus* protein A induces airway epithelial inflammatory responses by activating TNFR1. Nat Med **10:**842-848.
213. **Gómez MI, Seaghdha MO, Prince AS.** 2007. *Staphylococcus aureus* protein A activates TACE through EGFR-dependent signaling. EMBO J **26:**701-709.
214. **O'Seaghdha M, van Schooten CJ, Kerrigan SW, Emsley J, Silverman GJ, Cox D, Lenting PJ, Foster TJ.** 2006. *Staphylococcus aureus* protein A binding to von Willebrand factor A1 domain is mediated by conserved IgG binding regions. FEBS J **273:**4831-4841.
215. **Martin FJ, Gomez MI, Wetzel DM, Memmi G, O'Seaghdha M, Soong G, Schindler C, Prince A.** 2009. *Staphylococcus aureus* activates type I IFN signaling in mice and humans through the Xr repeated sequences of protein A. J Clin Invest **119:**1931-1939.
216. **Palmqvist N, Foster T, Tarkowski A, Josefsson E.** 2002. Protein A is a virulence factor in *Staphylococcus aureus* arthritis and septic death. Microb Pathog **33:**239-249.
217. **Patel AH, Nowlan P, Weavers ED, Foster T.** 1987. Virulence of protein A-deficient and alpha-toxin-deficient mutants of *Staphylococcus aureus* isolated by allele replacement. Infect Immun **55:**3103-3110.
218. **Muthukrishnan G, Quinn GA, Lamers RP, Diaz C, Cole AL, Chen S, Cole AM.** 2011. Exoproteome of *Staphylococcus aureus* reveals putative determinants of nasal carriage. J Proteome Res **10:**2064-2078.
219. **Gil C, Solano C, Burgui S, Latasa C, García B, Toledo-Arana A, Lasa I, Valle J.** 2014. Biofilm matrix exoproteins induce a protective immune response against *Staphylococcus aureus* biofilm infection. Infect Immun **82:**1017-1029.

220. **Linnes JC, Ma H, Bryers JD.** 2013. Giant extracellular matrix binding protein expression in *Staphylococcus epidermidis* is regulated by biofilm formation and osmotic pressure. Curr Microbiol **66:**627-633.
221. **Rohde H, Kalitzky M, Kröger N, Scherpe S, Horstkotte MA, Knobloch JK, Zander AR, Mack D.** 2004. Detection of virulence-associated genes not useful for discriminating between invasive and commensal *Staphylococcus epidermidis* strains from a bone marrow transplant unit. J Clin Microbiol **42:**5614-5619.
222. **Rohde H, Burandt EC, Siemssen N, Frommelt L, Burdelski C, Wurster S, Scherpe S, Davies AP, Harris LG, Horstkotte MA, Knobloch JK, Ragunath C, Kaplan JB, Mack D.** 2007. Polysaccharide intercellular adhesin or protein factors in biofilm accumulation of *Staphylococcus epidermidis* and *Staphylococcus aureus* isolated from prosthetic hip and knee joint infections. Biomaterials **28:**1711-1720.
223. **Duggirala A, Kenchappa P, Sharma S, Peeters JK, Ahmed N, Garg P, Das T, Hasnain SE.** 2007. High-resolution genome profiling differentiated *Staphylococcus epidermidis* isolated from patients with ocular infections and normal individuals. Invest Ophthalmol Vis Sci **48:**3239-3245.
224. **Novick RP, Ross HF, Projan SJ, Kornblum J, Kreiswirth B, Moghazeh S.** 1993. Synthesis of staphylococcal virulence factors is controlled by a regulatory RNA molecule. EMBO J **12:**3967-3975.
225. **Kong KF, Vuong C, Otto M.** 2006. Staphylococcus quorum sensing in biofilm formation and infection. Int J Med Microbiol **296:**133-139.
226. **Rudkin JK, Edwards AM, Bowden MG, Brown EL, Pozzi C, Waters EM, Chan WC, Williams P, O'Gara JP, Massey RC.** 2012. Methicillin resistance reduces the virulence of healthcare-associated methicillin-resistant *Staphylococcus aureus* by interfering with the agr quorum sensing system. J Infect Dis **205:**798-806.
227. **Ji G, Beavis R, Novick RP.** 1997. Bacterial interference caused by autoinducing peptide variants. Science **276:**2027-2030.
228. **Ji G, Beavis RC, Novick RP.** 1995. Cell density control of staphylococcal virulence mediated by an octapeptide pheromone. Proc Natl Acad Sci U S A **92:**12055-12059.
229. **Saenz HL, Augsburger V, Vuong C, Jack RW, Götz F, Otto M.** 2000. Inducible expression and cellular location of AgrB, a protein involved in the maturation of the staphylococcal quorum-sensing pheromone. Arch Microbiol **174:**452-455.
230. **Zhang L, Lin J, Ji G.** 2004. Membrane anchoring of the AgrD N-terminal amphipathic region is required for its processing to produce a quorum-sensing pheromone in *Staphylococcus aureus*. J Biol Chem **279:**19448-19456.
231. **Novick RP.** 2003. Autoinduction and signal transduction in the regulation of staphylococcal virulence. Molecular Microbiology **48:**1429-1449.
232. **Zhang L, Gray L, Novick RP, Ji G.** 2002. Transmembrane topology of AgrB, the protein involved in the post-translational modification of AgrD in *Staphylococcus aureus*. J Biol Chem **277:**34736-34742.
233. **Queck SY, Jameson-Lee M, Villaruz AE, Bach TH, Khan BA, Sturdevant DE, Ricklefs SM, Li M, Otto M.** 2008. RNAIII-independent target gene control by the agr quorum-sensing system: insight into the evolution of virulence regulation in *Staphylococcus aureus*. Mol Cell **32:**150-158.
234. **Le KY, Dastgheyb S, Ho TV, Otto M.** 2014. Molecular determinants of staphylococcal biofilm dispersal and structuring. Front Cell Infect Microbiol **4:**eCollection 2014.

235. **Vuong C, Gerke C, Somerville GA, Fischer ER, Otto M.** 2003. Quorum-sensing control of biofilm factors in *Staphylococcus epidermidis*. J Infect Dis **188:**706-718.
236. **Vuong C, Saenz HL, Götz F, Otto M.** 2000. Impact of the agr quorum-sensing system on adherence to polystyrene in *Staphylococcus aureus*. J Infect Dis **182:**1688-1693.
237. **Yarwood JM, Bartels DJ, Volper EM, Greenberg EP.** 2004. Quorum sensing in *Staphylococcus aureus* biofilms. J Bacteriol **186:**1838-1850.
238. **Yao Y, Sturdevant DE, Otto M.** 2005. Genomewide analysis of gene expression in *Staphylococcus epidermidis* biofilms: insights into the pathophysiology of S. epidermidis biofilms and the role of phenol-soluble modulins in formation of biofilms. J Infect Dis **191:**289-298.
239. **Lauderdale KJ, Boles BR, Cheung AL, Horswill AR.** 2009. Interconnections between Sigma B, agr, and proteolytic activity in *Staphylococcus aureus* biofilm maturation. Infect Immun **77:**1623-1635.
240. **Vuong C, Kocianova S, Yao Y, Carmody AB, Otto M.** 2004. Increased colonization of indwelling medical devices by quorum-sensing mutants of *Staphylococcus epidermidis* in vivo. J Infect Dis **190:**1498-1505.
241. **Vuong C, Dürr M, Carmody AB, Peschel A, Klebanoff SJ, Otto M.** 2004. Regulated expression of pathogen-associated molecular pattern molecules in *Staphylococcus epidermidis*: quorum-sensing determines pro-inflammatory capacity and production of phenol-soluble modulins. Cell Microbiol **6:**753-759.
242. **Wang R, Braughton KR, Kretschmer D, Bach TH, Queck SY, Li M, Kennedy AD, Dorward DW, Klebanoff SJ, Peschel A, DeLeo FR, Otto M.** 2007. Identification of novel cytolytic peptides as key virulence determinants for community-associated MRSA. Nat Med **13:**1510-1514.
243. **Wang R, Khan BA, Cheung GY, Bach TH, Jameson-Lee M, Kong KF, Queck SY, Otto M.** 2011. *Staphylococcus epidermidis* surfactant peptides promote biofilm maturation and dissemination of biofilm-associated infection in mice. J Clin Invest **121:**238-248.
244. **Joo HS, Otto M.** 2012. Molecular basis of in vivo biofilm formation by bacterial pathogens. Chem Biol **19:**1503-1513.
245. **Traber KE, Lee E, Benson S, Corrigan R, Cantera M, Shopsin B, Novick RP.** 2008. agr function in clinical *Staphylococcus aureus* isolates. Microbiology **154:**2265-2274.
246. **Dunman PM, Murphy E, Haney S, Palacios D, Tucker-Kellogg G, Wu S, Brown EL, Zagursky RJ, Shlaes D, Projan SJ.** 2001. Transcription profiling-based identification of *Staphylococcus aureus* genes regulated by the agr and/or sarA loci. J Bacteriol **183:**7341-7353.
247. **Cheung AL, Koomey JM, Butler CA, Projan SJ, Fischetti VA.** 1992. Regulation of exoprotein expression in *Staphylococcus aureus* by a locus (sar) distinct from agr. Proc Natl Acad Sci U S A **89:**6462-6466.
248. **Fluckiger U, Wolz C, Cheung AL.** 1998. Characterization of a sar homolog of *Staphylococcus epidermidis*. Infect Immun **66:**2871-2878.
249. **Arya R, Princy SA.** 2013. An insight into pleiotropic regulators Agr and Sar: molecular probes paving the new way for antivirulent therapy. Future Microbiol **8:**1339-1353.
250. **Cheung AL, Nishina KA, Trotonda MP, Tamber S.** 2008. The SarA protein family of *Staphylococcus aureus*. Int J Biochem Cell Biol **40:**355-361.
251. **Valle J, Toledo-Arana A, Berasain C, Ghigo JM, Amorena B, Penades JR, Lasa I.** 2003. SarA and not sigmaB is essential for biofilm development by *Staphylococcus aureus*. Mol Microbiol **48:**1075–1087.

252. **Beenken KE, Blevins JS, Smeltzer MS.** 2003. Mutation of sarA in *Staphylococcus aureus* Limits Biofilm Formation. Infection and Immunity **71:**4206-4211.
253. **Tormo MA, Martí M, Valle J, Manna AC, Cheung AL, Lasa I, Penadés JR.** 2005. SarA is an essential positive regulator of *Staphylococcus epidermidis* biofilm development. J Bacteriol **187:**2348-2356.
254. **O'Neill E, Pozzi C, Houston P, Smyth D, Humphreys H, Robinson DA, O'Gara JP.** 2007. Association between methicillin susceptibility and biofilm regulation in *Staphylococcus aureus* isolates from device-related infections. J Clin Microbiol **45:**1379-1388.
255. **Karlsson A, Saravia-Otten P, Tegmark K, Morfeldt E, Arvidson S.** 2001. Decreased amounts of cell wall-associated protein A and fibronectin-binding proteins in *Staphylococcus aureus* sarA mutants due to up-regulation of extracellular proteases. Infect Immun **69:**4742-4748.
256. **Loughran AJ, Atwood DN, Anthony AC, Harik NS, Spencer HJ, Beenken KE, Smeltzer MS.** 2014. Impact of individual extracellular proteases on *Staphylococcus aureus* biofilm formation in diverse clinical isolates and their isogenic sarA mutants. Microbiologyopen **3:**897-909.
257. **Marti M, Trotonda MP, Tormo-Mas MA, Vergara-Irigaray M, Cheung AL, Lasa I, Penades JR.** 2010. Extracellular proteases inhibit protein-dependent biofilm formation in *Staphylococcus aureus*. Microbes Infect **12:**55-64.
258. **Zielinska AK, Beenken KE, Mrak LN, Spencer HJ, Post GR, Skinner RA, Tackett AJ, Horswill AR, Smeltzer MS.** 2012. sarA-mediated repression of protease production plays a key role in the pathogenesis of *Staphylococcus aureus* USA300 isolates. Mol Microbiol **86:**1183-1196.
259. **Weiss EC, Zielinska A, Beenken KE, Spencer HJ, Daily SJ, Smeltzer MS.** 2009. Impact of sarA on daptomycin susceptibility of *Staphylococcus aureus* biofilms in vivo. Antimicrob Agents Chemother **53:**4096-4102.
260. **Snowden JN, Beaver M, Beenken K, Smeltzer M, Horswill AR, Kielian T.** 2013. *Staphylococcus aureus* sarA regulates inflammation and colonization during central nervous system biofilm formation. PLoS One **8:**e84089.
261. **Bischoff M, Dunman P, Kormanec J, Macapagal D, Murphy E, Mounts W, Berger-Bächi B, Projan S.** 2004. Microarray-based analysis of the *Staphylococcus aureus* sigmaB regulon. J Bacteriol **186:**4085-4099.
262. **Horsburgh MJ, Aish JL, White IJ, Shaw L, Lithgow JK, Foster SJ.** 2002. sigmaB modulates virulence determinant expression and stress resistance: characterization of a functional rsbU strain derived from *Staphylococcus aureus* 8325-4. Journal of Bacteriology **184:**5457-5467.
263. **Senn MM, Giachino P, Homerova D, Steinhuber A, Strassner J, Kormanec J, Flückiger U, Berger-Bächi B, Bischoff M.** 2005. Molecular analysis and organization of the sigmaB operon in *Staphylococcus aureus*. J Bacteriol **187:**8006-8019.
264. **Cotter JJ, O'Gara JP, Mack D, Casey E.** 2009. Oxygen-mediated regulation of biofilm development is controlled by the alternative sigma factor sigma(B) in *Staphylococcus epidermidis*. Appl Environ Microbiol **75:**261-264.
265. **Mack D, Rohde H, Dobinsky S, Riedewald J, Nedelmann M, Knobloch JK, Elsner HA, Feucht HH.** 2000. Identification of three essential regulatory gene loci governing expression of *Staphylococcus epidermidis* polysaccharide intercellular adhesin and biofilm formation. Infect Immun **68:**3799-3807.
266. **Rachid S, Ohlsen K, Wallner U, Hacker J, Hecker M, Ziebuhr W.** 2000. Alternative transcription factor sigma(B) is involved in regulation of

biofilm expression in a *Staphylococcus aureus* mucosal isolate. J Bacteriol **182:**6824-6826.
267. **Cerca N, Brooks JL, Jefferson KK.** 2008. Regulation of the intercellular adhesin locus regulator (icaR) by SarA, sigmaB, and IcaR in *Staphylococcus aureus*. J Bacteriol **190:**6530-6533.
268. **Morrissey JA, Cockayne A, Brummell K, Williams P.** 2004. The staphylococcal ferritins are differentially regulated in response to iron and manganese and via PerR and Fur. Infect Immun **`72:**972-979.
269. **Litwin CM, Calderwood SB.** 1993. Role of iron in regulation of virulence genes. Clin Microbiol Rev **6:**137-149.
270. **Johnson M, Cockayne A, Williams PH, Morrissey JA.** 2005. Iron-responsive regulation of biofilm formation in *Staphylococcus aureus* involves fur-dependent and fur-independent mechanisms. J Bacteriol **187:**8211-8215.
271. **Johnson M, Sengupta M, Purves J, Tarrant E, Williams PH, Cockayne A, Muthaiyan A, Stephenson R, Ledala N, Wilkinson BJ, Jayaswal RK, Morrissey JA.** 2011. Fur is required for the activation of virulence gene expression through the induction of the sae regulatory system in *Staphylococcus aureus*. Int J Med Microbiol **301:**44-52.
272. **Novick RP, Jiang D.** 2003. The staphylococcal saeRS system coordinates environmental signals with agr quorum sensing. Microbiology **149:**2709-2717.
273. **Cassat JE, Hammer ND, Campbell JP, Benson MA, Perrien DS, Mrak LN, Smeltzer MS, Torres VJ, Skaar EP.** 2013. A secreted bacterial protease tailors the *Staphylococcus aureus* virulence repertoire to modulate bone remodeling during osteomyelitis. Cell Host Microbe **13:**759-772.
274. **Mrak LN, Zielinska AK, Beenken KE, Mrak IN, Atwood DN, Griffin LM, Lee CY, Smeltzer MS.** 2012. saeRS and sarA act synergistically to repress protease production and promote biofilm formation in *Staphylococcus aureus*. PLoS One **7:**e38453.
275. **Beenken KE, Mrak LN, Zielinska AK, Atwood DN, Loughran AJ, Griffin LM, Matthews KA, Anthony AM, Spencer HJ, Skinner RA, Post GR, Lee CY, Smeltzer MS.** 2014. Impact of the functional status of saeRS on in vivo phenotypes of *Staphylococcus aureus* sarA mutants. Mol Microbiol **92:**1299-1312.
276. **Olson ME, Nygaard TK, Ackermann L, Watkins RL, Zurek OW, Pallister KB, Griffith S, Kiedrowski MR, Flack CE, Kavanaugh JS, Kreiswirth BN, Horswill AR, Voyich JM.** 2013. *Staphylococcus aureus* nuclease is an SaeRS-dependent virulence factor. Infect Immun **81:**1316-1324.
277. **Lou Q, Zhu T, Hu J, Ben H, Yang J, Yu F, Liu J, Wu Y, Fischer A, Francois P, Schrenzel J, Qu D.** 2011. Role of the SaeRS two-component regulatory system in *Staphylococcus epidermidis* autolysis and biofilm formation. BMC Microbiol **11:**146.
278. **Jevons MP.** 1961. "Celbenin" - resistant Staphylococci. Br Med J **1:**124–125.
279. **Otto M.** 2013. Community-associated MRSA: what makes them special? Int J Med Microbiol **303:**324-330.
280. **von Eiff C, Reinert RR, Kresken M, Brauers J, Hafner D, Peters G.** 2000. Nationwide German multicenter study on prevalence of antibiotic resistance in staphylococcal bloodstream isolates and comparative in vitro activities of quinupristin-dalfopristin. J Clin Microbiol **38:**2819-2823.
281. **Schoenfelder SM, Lange C, Eckart M, Hennig S, Kozytska S, Ziebuhr W.** 2010. Success through diversity - how *Staphylococcus epidermidis* establishes as a nosocomial pathogen. Int J Med Microbiol **300:**380-386.

282. **Hanssen AM, Kjeldsen G, Sollid JU.** 2004. Local variants of Staphylococcal cassette chromosome mec in sporadic methicillin-resistant *Staphylococcus aureus* and methicillin-resistant coagulase-negative Staphylococci: evidence of horizontal gene transfer? Antimicrob Agents Chemother **48:**285-296.
283. **Jamaluddin TZ, Kuwahara-Arai K, Hisata K, Terasawa M, Cui L, Baba T, Sotozono C, Kinoshita S, Ito T, Hiramatsu K.** 2008. Extreme genetic diversity of methicillin-resistant *Staphylococcus epidermidis* strains disseminated among healthy Japanese children. J Clin Microbiol **46:**3778-3783.
284. **Shore AC, Rossney AS, O'Connell B, Herra CM, Sullivan DJ, Humphreys H, Coleman DC.** 2008. Detection of staphylococcal cassette chromosome mec-associated DNA segments in multiresistant methicillin-susceptible *Staphylococcus aureus* (MSSA) and identification of *Staphylococcus epidermidis* ccrAB4 in both methicillin-resistant S. aureus and MSSA. Antimicrob Agents Chemother **52:**4407-4419.
285. **Ruppé E, Barbier F, Mesli Y, Maiga A, Cojocaru R, Benkhalfat M, Benchouk S, Hassaine H, Maiga I, Diallo A, Koumaré AK, Ouattara K, Soumaré S, Dufourcq JB, Nareth C, Sarthou JL, Andremont A, Ruimy R.** 2009. Diversity of staphylococcal cassette chromosome mec structures in methicillin-resistant *Staphylococcus epidermidis* and Staphylococcus haemolyticus strains among outpatients from four countries. Antimicrob Agents Chemother **53:**442-449.
286. **Katayama Y, Ito T, Hiramatsu K.** 2000. A new class of genetic element, staphylococcus cassette chromosome mec, encodes methicillin resistance in *Staphylococcus aureus*. Antimicrob Agents Chemother **44:**1549-1555.
287. **Hiramatsu K, Ito T, Tsubakishita S, Sasaki T, Takeuchi F, Morimoto Y, Katayama Y, Matsuo M, Kuwahara-Arai K, Hishinuma T, Baba T.** 2013. Genomic Basis for Methicillin Resistance in *Staphylococcus aureus*. Infect Chemother **45:**117-136.
288. **Berger-Bachi B, Rohrer S.** 2002. Factors influencing methicillin resistance in staphylococci. Arch Microbiol **178:**165-171.
289. **Giesbrecht P, Kersten T, Maidhof H, Wecke J.** 1998. Staphylococcal cell wall: morphogenesis and fatal variations in the presence of penicillin. Microbiol Mol Biol Rev **62:**1371-1414.
290. **Tomasz A.** 1986. Penicillin-binding proteins and the antibacterial effectiveness of beta-lactam antibiotics. Rev Infect Dis **8:**S260-278.
291. **Sugai M, Yamada S, Nakashima S, Komatsuzawa H, Matsumoto A, Oshida T, Suginaka H.** 1997. Localized perforation of the cell wall by a major autolysin: atl gene products and the onset of penicillin-induced lysis of *Staphylococcus aureus*. J Bacteriol **179:**2958-2962.
292. **Pinho MG, Filipe SR, de Lencastre H, Tomasz A.** 2001. Complementation of the essential peptidoglycan transpeptidase function of penicillin-binding protein 2 (PBP2) by the drug resistance protein PBP2A in *Staphylococcus aureus*. J Bacteriol **183:**6525-6531.
293. **Lewis RA, Dyke KG.** 2000. MecI represses synthesis from the beta-lactamase operon of *Staphylococcus aureus*. J Antimicrob Chemother **45:**139-144.
294. **Clarke SR, Dyke KG.** 2001. The signal transducer (BlaRI) and the repressor (BlaI) of the *Staphylococcus aureus* beta-lactamase operon are inducible. Microbiology **147:**803-810.
295. **Zhang HZ, Hackbarth CJ, Chansky KM, Chambers HF.** 2001. A proteolytic transmembrane signaling pathway and resistance to beta-lactams in staphylococci. Science **291:**1962-1965.

296. **Ryffel C, Kayser FH, Berger-Bächi B.** 1992. Correlation between regulation of mecA transcription and expression of methicillin resistance in staphylococci. Antimicrob Agents Chemother **36:**25-31.
297. **McKinney TK, Sharma VK, Craig WA, Archer GL.** 2001. Transcription of the gene mediating methicillin resistance in *Staphylococcus aureus* (mecA) is corepressed but not coinduced by cognate mecA and beta-lactamase regulators. J Bacteriol **183:**6862-6868.
298. **(IWG-SCC). IWGotCoSCCE.** 2009. Classification of staphylococcal cassette chromosome mec (SCCmec): guidelines for reporting novel SCCmec elements. Antimicrob Agents Chemother **53:**4961-4967.
299. **Ito T, Katayama Y, Asada K, Mori N, Tsutsumimoto K, Tiensasitorn C, Hiramatsu K.** 2001. Structural comparison of three types of staphylococcal cassette chromosome mec integrated in the chromosome in methicillin-resistant *Staphylococcus aureus*. Antimicrob Agents Chemother **45:**1323-1336.
300. **Okuma K, Iwakawa K, Turnidge JD, Grubb WB, Bell JM, O'Brien FG, Coombs GW, Pearman JW, Tenover FC, Kapi M, Tiensasitorn C, Ito T, Hiramatsu K.** 2002. Dissemination of new methicillin-resistant *Staphylococcus aureus* clones in the community. J Clin Microbiol **40:**4289-4294.
301. **Ito T, Ma XX, Takeuchi F, Okuma K, Yuzawa H, Hiramatsu K.** 2004. Novel type V staphylococcal cassette chromosome mec driven by a novel cassette chromosome recombinase, ccrC. Antimicrob Agents Chemother **48:**2637-2651.
302. **Ma XX, Ito T, Tiensasitorn C, Jamklang M, Chongtrakool P, Boyle-Vavra S, Daum RS, Hiramatsu K.** 2002. Novel type of staphylococcal cassette chromosome mec identified in community-acquired methicillin-resistant *Staphylococcus aureus* strains. Antimicrob Agents Chemother **46:**1147-1152.
303. **Daum RS, Ito T, Hiramatsu K, Hussain F, Mongkolrattanothai K, Jamklang M, Boyle-Vavra S.** 2002. A novel methicillin-resistance cassette in community-acquired methicillin-resistant *Staphylococcus aureus* isolates of diverse genetic backgrounds. J Infect Dis **186:**1344-1347.
304. **Lee SM, Ender M, Adhikari R, Smith JM, Berger-Bächi B, Cook GM.** 2007. Fitness cost of staphylococcal cassette chromosome mec in methicillin-resistant *Staphylococcus aureus* by way of continuous culture. Antimicrob Agents Chemother **51:**1497-1499.
305. **Chambers HF, Hackbarth CJ.** 1987. Effect of NaCl and nafcillin on penicillin-binding protein 2a and heterogeneous expression of methicillin resistance in *Staphylococcus aureus*. Antimicrob Agents Chemother **31:**1982-1988.
306. **Chambers HF.** 1997. Methicillin resistance in staphylococci: molecular and biochemical basis and clinical implications. Clin Microbiol Rev **10:**781-791.
307. **Chambers HF.** 1999. Penicillin-binding protein-mediated resistance in pneumococci and staphylococci. J Infect Dis **179:**S353-359.
308. **Sabath LD, Wallace SJ.** 1971. The problems of drug-resistant pathogenic bacteria. Factors influencing methicillin resistance in staphylococci. Ann N Y Acad Sci **11:**258-266.
309. **Ryffel C, Strässle A, Kayser FH, Berger-Bächi B.** 1994. Mechanisms of heteroresistance in methicillin-resistant *Staphylococcus aureus*. Antimicrob Agents Chemother **38:**724-728.
310. **Píriz Durán S, Kayser FH, Berger-Bächi B.** 1996. Impact of sar and agr on methicillin resistance in *Staphylococcus aureus*. FEMS Microbiol Lett **141:**255-260.

311. **Nakao A, Imai S, Takano T.** 2000. Transposon-mediated insertional mutagenesis of the D-alanyl-lipoteichoic acid (dlt) operon raises methicillin resistance in *Staphylococcus aureus*. Res Microbiol **151:**823-829.
312. **Berger-Bächi B.** 1983. Insertional inactivation of staphylococcal methicillin resistance by Tn551. J Bacteriol **154:**479-487.
313. **Murakami K, Tomasz A.** 1989. Involvement of multiple genetic determinants in high-level methicillin resistance in *Staphylococcus aureus*. J Bacteriol **171:**874-879.
314. **Maki H, Yamaguchi T, Murakami K.** 1994. Cloning and characterization of a gene affecting the methicillin resistance level and the autolysis rate in *Staphylococcus aureus*. J Bacteriol **176:**4993-5000.
315. **Rohrer S, Berger-Bächi B.** 2003. FemABX peptidyl transferases: a link between branched-chain cell wall peptide formation and beta-lactam resistance in gram-positive cocci. Antimicrob Agents Chemother **47:**837-846.
316. **Pozzi C, Waters EM, Rudkin JK, Schaeffer CR, Lohan AJ, Tong P, Loftus BJ, Pier GB, Fey PD, Massey RC, O'Gara JP.** 2012. Methicillin resistance alters the biofilm phenotype and attenuates virulence in *Staphylococcus aureus* device-associated infections. PLoS Pathog **8:**e1002626.
317. **Griffiths JM, O'Neill AJ.** 2012. Loss of function of the gdpP protein leads to joint beta-lactam/glycopeptide tolerance in *Staphylococcus aureus*. Antimicrob Agents Chemother **56:**579-581.
318. **Corrigan RM, Abbott JC, Burhenne H, Kaever V, Grundling A.** 2011. c-di-AMP is a new second messenger in *Staphylococcus aureus* with a role in controlling cell size and envelope stress. PLoS Pathog **7:**e1002217.
319. **Dengler V, McCallum N, Kiefer P, Christen P, Patrignani A, Vorholt JA, Berger-Bachi B, Senn MM.** 2013. Mutation in the C-di-AMP cyclase dacA affects fitness and resistance of methicillin resistant *Staphylococcus aureus*. PLoS One **8:**e73512.
320. **Fitzpatrick F, Humphreys H, O'Gara JP.** 2005. Evidence for icaADBC-independent biofilm development mechanism in methicillin-resistant *Staphylococcus aureus* clinical isolates. J Clin Microbiol **43:**1973-1976.
321. **Fitzpatrick F, Humphreys H, O'Gara JP.** 2006. Environmental regulation of biofilm development in methicillin-resistant and methicillin-susceptible *Staphylococcus aureus* clinical isolates. J Hosp Infect **62:**120-122.
322. **Mizobuchi S, Minami J, Jin F, Matsushita O, Okabe A.** 1994. Comparison of the virulence of methicillin-resistant and methicillin-sensitive *Staphylococcus aureus*. Microbiol Immunol **38:**599-605.
323. **Collins J, Rudkin J, Recker M, Pozzi C, O'Gara JP, Massey RC.** 2010. Offsetting virulence and antibiotic resistance costs by MRSA. ISME J **4:**577-584.
324. **Abraham J, Mansour C, Veledar E, Khan B, Lerakis S.** 2004. *Staphylococcus aureus* bacteremia and endocarditis: the Grady Memorial Hospital experience with methicillin-sensitive S aureus and methicillin-resistant S aureus bacteremia. Am Heart J **147:**536-539.
325. **Wehrhahn MC, Robinson JO, Pascoe EM, Coombs GW, Pearson JC, O'Brien FG, Tan HL, New D, Salvaris P, Salvaris R, Murray RJ.** 2012. Illness severity in community-onset invasive *Staphylococcus aureus* infection and the presence of virulence genes. J Infect Dis **205:**1840-1848.
326. **Kaito C, Saito Y, Ikuo M, Omae Y, Mao H, Nagano G, Fujiyuki T, Numata S, Han X, Obata K, Hasegawa S, Yamaguchi H, Inokuchi K, Ito T, Hiramatsu K, Sekimizu K.** 2013. Mobile genetic element

SCCmec-encoded psm-mec RNA suppresses translation of agrA and attenuates MRSA virulence. PLoS Pathog **9:**e1003269.

327. **Queck SY, Khan BA, Wang R, Bach TH, Kretschmer D, Chen L, Kreiswirth BN, Peschel A, Deleo FR, Otto M.** 2009. Mobile genetic element-encoded cytolysin connects virulence to methicillin resistance in MRSA. PLoS Pathog **5:**e1000533.
328. **Kaito C, Omae Y, Matsumoto Y, Nagata M, Yamaguchi H, Aoto T, Ito T, Hiramatsu K, Sekimizu K.** 2008. A novel gene, fudoh, in the SCCmec region suppresses the colony spreading ability and virulence of *Staphylococcus aureus*. PLoS One **3:**e3921.
329. **Kaito C, Saito Y, Nagano G, Ikuo M, Omae Y, Hanada Y, Han X, Kuwahara-Arai K, Hishinuma T, Baba T, Ito T, Hiramatsu K, Sekimizu K.** 2011. Transcription and translation products of the cytolysin gene psm-mec on the mobile genetic element SCCmec regulate *Staphylococcus aureus* virulence. PLoS Pathog **7:**e1001267.
330. **Rudkin JK, Laabei M, Edwards AM, Joo HS, Otto M, Lennon KL, O'Gara JP, Waterfield NR, Massey RC.** 2014. Oxacillin alters the toxin expression profile of community-associated methicillin-resistant *Staphylococcus aureus*. Antimicrob Agents Chemother **58:**1100-1107.
331. **Zimmerli W, Waldvogel FA, Vaudaux P, Nydegger UE.** 1982. Pathogenesis of foreign body infection: description and characteristics of an animal model. J Infect Dis **146:**487-497.
332. **Kristian SA, Golda T, Ferracin F, Cramton SE, Neumeister B, Peschel A, Götz F, Landmann R.** 2004. The ability of biofilm formation does not influence virulence of *Staphylococcus aureus* and host response in a mouse tissue cage infection model. Microb Pathog **36:**237-245.
333. **Olson ME, Slater SR, Rupp ME, Fey PD.** 2010. Rifampicin enhances activity of daptomycin and vancomycin against both a polysaccharide intercellular adhesin (PIA)-dependent and -independent *Staphylococcus epidermidis* biofilm. J Antimicrob Chemother **65:**2164-2171.
334. **Vaudaux P, Grau GE, Huggler E, Schumacher-Perdreau F, Fiedler F, Waldvogel FA, Lew DP.** 1992. Contribution of tumor necrosis factor to host defense against staphylococci in a guinea pig model of foreign body infections. J Infect Dis **166:**58-64.
335. **Gallimore B, Gagnon RF, Subang R, Richards GK.** 1991. Natural history of chronic *Staphylococcus epidermidis* foreign body infection in a mouse model. J Infect Dis **164:**1220-1223.
336. **Carsenti-Etesse H, Entenza J, Durant J, Pradier C, Mondain V, Bernard E, Dellamonica P.** 1992. Efficacy of subinhibitory concentration of pefloxacin in preventing experimental *Staphylococcus aureus* foreign body infection in mice. Drugs Exp Clin Res **18:**415-422.
337. **Cavanagh JP, Granslo HN, Fredheim EA, Christophersen L, Jensen PØ, Thomsen K, Van Gennip M, Klingenberg C, Flaegstad T, Moser C.** 2013. Efficacy of a synthetic antimicrobial peptidomimetic versus vancomycin in a *Staphylococcus epidermidis* device-related murine peritonitis model. J Antimicrob Chemother **68:**2106-2110.
338. **Handke LD, Rogers KL, Olson ME, Somerville GA, Jerrells TJ, Rupp ME, Dunman PM, Fey PD.** 2008. *Staphylococcus epidermidis* saeR is an effector of anaerobic growth and a mediator of acute inflammation. Infect Immun **76:**141-152.
339. **Kadurugamuwa JL, Sin L, Albert E, Yu J, Francis K, DeBoer M, Rubin M, Bellinger-Kawahara C, Parr Jr TRJ, Contag PR.** 2003. Direct continuous method for monitoring biofilm infection in a mouse model. Infect Immun **71:**882-890.
340. **Kidd P.** 2003. Th1/Th2 balance: the hypothesis, its limitations, and implications for health and disease. Altern Med Rev **8:**223-246.

341. **Hume EB, Cole N, Khan S, Garthwaite LL, Aliwarga Y, Schubert TL, Willcox MD.** 2005. A *Staphylococcus aureus* mouse keratitis topical infection model: cytokine balance in different strains of mice. Immunol Cell Biol **83:**294-300.
342. **Prabhakara R, Harro JM, Leid JG, Keegan AD, Prior ML, Shirtliff ME.** 2011. Suppression of the inflammatory immune response prevents the development of chronic biofilm infection due to methicillin-resistant *Staphylococcus aureus*. Infect Immun **79:**5010-5018.
343. **Rupp ME, Ulphani JS, Fey PD, Mack D.** 1999. Characterization of *Staphylococcus epidermidis* polysaccharide intercellular adhesin/hemagglutinin in the pathogenesis of intravascular catheter-associated infection in a rat model. Infect Immun **67:**2656-2659.
344. **Rupp ME, Fey PD.** 2001. In vivo models to evaluate adhesion and biofilm formation by *Staphylococcus epidermidis*. Methods Enzymol **336:**206-215.
345. **Chauhan A, Lebeaux D, Decante B, Kriegel I, Escande MC, Ghigo JM, Beloin C.** 2012. A rat model of central venous catheter to study establishment of long-term bacterial biofilm and related acute and chronic infections. PLoS One **7:**e37281.
346. **Schaeffer CR, Woods KM, Longo GM, Kiedrowski MR, Paharik AE, Büttner H, Christner M, Boissy RJ, Horswill AR, Rohde H, Fey PD.** 2014. Accumulation-associated protein (Aap) enhances *Staphylococcus epidermidis* biofilm formation under dynamic conditions and is required for infection in a rat catheter model. Submitted.
347. **Fey PD, Endres JL, Yajjala VK, Widhelm TJ, Boissy RJ, Bose JL, Bayles KW.** 2013. A genetic resource for rapid and comprehensive phenotype screening of nonessential *Staphylococcus aureus* genes. MBio **4:**e00537-00512.
348. **Bae T, Banger AK, Wallace A, Glass EM, Aslund F, Schneewind O, Missiakas DM.** 2004. *Staphylococcus aureus* virulence genes identified by bursa aurealis mutagenesis and nematode killing. Proc Natl Acad Sci U S A **101:**12312-12317.
349. **Lampe DJ, Churchill ME, Robertson HM.** 1996. A purified mariner transposase is sufficient to mediate transposition in vitro. EMBO J **15:**5470-5479.
350. **Robertson HM, Lampe DJ.** 1995. Recent horizontal transfer of a mariner transposable element among and between Diptera and Neuroptera. Mol Biol Evol **12:**850-862.
351. **Kreiswirth BN, Löfdahl S, Betley MJ, O'Reilly M, Schlievert PM, Bergdoll MS, Novick RP.** 1983. The toxic shock syndrome exotoxin structural gene is not detectably transmitted by a prophage. Nature **305:**709-712.
352. **Foster SJ.** 1995. Molecular characterization and functional analysis of the major autolysin of *Staphylococcus aureus* 8325/4. J Bacteriol **177:**5723-5725.
353. **Voyich JM, Braughton KR, Sturdevant DE, Whitney AR, Said-Salim B, Porcella SF, Long RD, Dorward DW, Gardner DJ, Kreiswirth BN, Musser JM, DeLeo FR.** 2005. Insights into mechanisms used by *Staphylococcus aureus* to avoid destruction by human neutrophils. J Immunol **175:**3907-3919.
354. **Voyich JM, Vuong C, DeWald M, Nygaard TK, Kocianova S, Griffith S, Jones J, Iverson C, Sturdevant DE, Braughton KR, Whitney AR, Otto M, DeLeo FR.** 2009. The SaeR/S gene regulatory system is essential for innate immune evasion by *Staphylococcus aureus*. J Infect Dis **199:**1698-1706.

355. **Cassat JE, Dunman PM, McAleese F, Murphy E, Projan SJ, Smeltzer MS.** 2005. Comparative genomics of *Staphylococcus aureus* musculoskeletal isolates. J Bacteriol **187:**576-592.
356. **Martineau F, Picard FJ, Roy PH, Ouellette M, Bergeron MG.** 1996. Species-specific and ubiquitous DNA-based assays for rapid identification of *Staphylococcus epidermidis*. J Clin Microbiol **34:**2888-2893.
357. **Mack D, Bartscht K, Fischer C, Rohde H, de Grahl C, Dobinsky S, Horstkotte MA, Kiel K, Knobloch JK.** 2001. Genetic and biochemical analysis of *Staphylococcus epidermidis* biofilm accumulation. Methods Enzymol **336:**215-239.
358. **Christensen GD, Simpson WA, Bisno AL, Beachey EH.** 1982. Adherence of slime-producing strains of *Staphylococcus epidermidis* to smooth surfaces. Infect Immun **37:**318-326.
359. **Handke LD, Slater SR, Conlon KM, O'Donnell ST, Olson ME, Bryant KA, Rupp ME, O'Gara JP, Fey PD.** 2007. SigmaB and SarA independently regulate polysaccharide intercellular adhesin production in *Staphylococcus epidermidis*. Can J Microbiol **53:**82-91.
360. **Hennig S, Nyunt Wai S, Ziebuhr W.** 2007. Spontaneous switch to PIA-independent biofilm formation in an ica-positive *Staphylococcus epidermidis* isolate. Int J Med Microbiol **297:**117-122.
361. **Lee CY, Buranen SL, Ye ZH.** 1991. Construction of single-copy integration vectors for *Staphylococcus aureus*. Gene **103:**101-105.
362. **Moore GE, Glick JL.** 1967. Perspective of human cell culture. Surg Clin North Am **47:**1315-1324.
363. **Christensen GD, Simpson WA, Younger JJ, Baddour LM, Barrett FF, Melton DM, Beachey EH.** 1985. Adherence of coagulase-negative staphylococci to plastic tissue culture plates: a quantitative model for the adherence of staphylococci to medical devices. J Clin Microbiol Mol Biol Rev **22:**996–1006.
364. **Waters E, McCarthy H, Hogan S, Zapotoczna M, O'Neill E, O'Gara J.** 2014. Rapid Quantitative and Qualitative Analysis of Biofilm Production by *Staphylococcus epidermidis* Under Static Growth Conditions, p 157-166. *In* Fey PD (ed), *Staphylococcus epidermidis*, vol 1106. Humana Press.
365. **Moormeier D, Bayles K.** 2014. Examination of *Staphylococcus epidermidis* Biofilms Using Flow-Cell Technology, p 143-155. *In* Fey PD (ed), *Staphylococcus epidermidis*, vol 1106. Humana Press.
366. **Mani N, Tobin P, Jayaswal RK.** 1993. Isolation and characterization of autolysis-defective mutants of *Staphylococcus aureus* created by Tn917-lacZ mutagenesis. 175 **5**.
367. **Fournier B, Hooper DC.** 2000. A new two-component regulatory system involved in adhesion, autolysis, and extracellular proteolytic activity of *Staphylococcus aureus*. J Bacteriol **182:**3955-3964.
368. **Pasztor L, Ziebandt AK, Nega M, Schlag M, Haase S, Franz-Wachtel M, Madlung J, Nordheim A, Heinrichs DE, Gotz F.** 2010. Staphylococcal major autolysin (Atl) is involved in excretion of cytoplasmic proteins. J Biol Chem **285:**36794-36803.
369. **Thurlow LR, Hanke ML, Fritz T, Angle A, Aldrich A, Williams SH, Engebretsen IL, Bayles KW, Horswill AR, Kielian T.** 2011. *Staphylococcus aureus* biofilms prevent macrophage phagocytosis and attenuate inflammation in vivo. J Immunol **186:**6585-6596.
370. **Speziale P, Pietrocola G, Foster TJ, Geoghegan JA.** 2014. Protein-based biofilm matrices in Staphylococci. Front Cell Infect Microbiol **10:**171.
371. **Craven RR, Gao X, Allen IC, Gris D, Bubeck Wardenburg J, McElvania-Tekippe E, Ting JP, Duncan JA.** 2009. *Staphylococcus aureus* alpha-hemolysin activates the NLRP3-inflammasome in human and mouse monocytic cells. PLoS One **4:**e7446.

372. **Delauné A, Dubrac S, Blanchet C, Poupel O, Mäder U, Hiron A, Leduc A, Fitting C, Nicolas P, Cavaillon JM, Adib-Conquy M, Msadek T.** 2012. The WalKR system controls major staphylococcal virulence genes and is involved in triggering the host inflammatory response. Infect Immun **80:**3438-3453.
373. **Shimada T, Park BG, Wolf AJ, Brikos C, Goodridge HS, Becker CA, Reyes CN, Miao EA, Aderem A, Götz F, Liu GY, Underhill DM.** 2010. *Staphylococcus aureus* evades lysozyme-based peptidoglycan digestion that links phagocytosis, inflammasome activation, and IL-1beta secretion. Cell Host Microbe **7:**38-49.
374. **Moormeier DE, Endres JL, Mann EE, Sadykov MR, Horswill AR, Rice KC, Fey PD, Bayles KW.** 2013. Use of microfluidic technology to analyze gene expression during *Staphylococcus aureus* biofilm formation reveals distinct physiological niches. Appl Environ Microbiol **79:**3413-3424.
375. **Otto BR, Verweij-van Vught AM, MacLaren DM.** 1992. Blood substitutes and infection. Nature **358:**23-24.
376. **Mainiero M, Goerke C, Geiger T, Gonser C, Herbert S, Wolz C.** 2010. Differential target gene activation by the *Staphylococcus aureus* two-component system saeRS. J Bacteriol **192:**613-623.
377. **Cheng AG, McAdow M, Kim HK, Bae T, Missiakas DM, Schneewind O.** 2010. Contribution of coagulases towards *Staphylococcus aureus* disease and protective immunity. PLoS Pathog **6:**e1001036.
378. **Thomer L, Schneewind O, Missiakas D.** 2013. Multiple ligands of von Willebrand factor-binding protein (vWbp) promote *Staphylococcus aureus* clot formation in human plasma. J Biol Chem **288:**28283-28292.
379. **Ramadurai L, Lockwood KJ, Nadakavukaren MJ, Jayaswal RK.** 1999. Characterization of a chromosomally encoded glycylglycine endopeptidase of *Staphylococcus aureus*. Microbiology **145:**801-808.
380. **Cassat JE, Skaar EP.** 2012. Metal ion acquisition in *Staphylococcus aureus*: overcoming nutritional immunity. Semin Immunopathol **34:**215-235.
381. **Hood MI, Skaar EP.** 2012. Nutritional immunity: transition metals at the pathogen-host interface. Nat Rev Microbiol **10:**525-537.
382. **Skaar EP, Schneewind O.** 2004. Iron-regulated surface determinants (Isd) of *Staphylococcus aureus*: stealing iron from heme. Microbes Infect **6:**390-397.
383. **Harraghy N, Kormanec J, Wolz C, Homerova D, Goerke C, Ohlsen K, Qazi S, Hill P, Herrmann M.** 2005. sae is essential for expression of the staphylococcal adhesins Eap and Emp. Microbiology **151:**1789-1800.
384. **Weinrick B, Dunman PM, McAleese F, Murphy E, Projan SJ, Fang Y, Novick RP.** 2004. Effect of mild acid on gene expression in *Staphylococcus aureus*. J Bacteriol **186:**8407-8423.
385. **Giraudo AT, Raspanti CG, Calzolari A, Nagel R.** 1994. Characterization of a Tn551-mutant of *Staphylococcus aureus* defective in the production of several exoproteins. Can J Microbiol **40:**677-681.
386. **Date SV, Modrusan Z, Lawrence M, Morisaki JH, Toy K, Shah IM, Kim J, Park S, Xu M, Basuino L, Chan L, Zeitschel D, Chambers HF, Tan MW, Brown EJ, Diep BA, Hazenbos WL.** 2014. Global gene expression of methicillin-resistant *Staphylococcus aureus* USA300 during human and mouse infection. J Infect Dis **209:**1542-1550.
387. **Rogasch K, Rühmling V, Pané-Farré J, Höper D, Weinberg C, Fuchs S, Schmudde M, Bröker BM, Wolz C, Hecker M, Engelmann S.** 2006. Influence of the two-component system SaeRS on global gene expression in two different *Staphylococcus aureus* strains. J Bacteriol **188:**7742-7758.

388. **Steinhuber A, Goerke C, Bayer MG, Döring G, Wolz C.** 2003. Molecular architecture of the regulatory Locus sae of *Staphylococcus aureus* and its impact on expression of virulence factors. J Bacteriol **185:**6278-6286.
389. **Vanassche T, Peetermans M, Van Aelst LN, Peetermans WE, Verhaegen J, Missiakas DM, Schneewind O, Hoylaerts MF, Verhamme P.** 2013. The role of staphylothrombin-mediated fibrin deposition in catheter-related *Staphylococcus aureus* infections. 208 **1**.
390. **Vanassche T, Verhaegen J, Peetermans WE, VAN Ryn J, Cheng A, Schneewind O, Hoylaerts MF, Verhamme P.** 2011. Inhibition of staphylothrombin by dabigatran reduces *Staphylococcus aureus* virulence. J Thromb Haemost **9:**2436-2446.
391. **Loof T, Goldmann O, Naudin C, Mörgelin M, Neumann Y, Pils M, Foster S, Medina E, Herwald H.** 2014. *Staphylococcus aureus* induced clotting of plasma is an immune evasion mechanism to persist within the fibrin network. Microbiology **[Epub ahead of print]**.
392. **McAdow M, DeDent AC, Emolo C, Cheng AG, Kreiswirth BN, Missiakas DM, O. S.** 2012. Coagulases as determinants of protective immune responses against *Staphylococcus aureus*. Infect Immun **80:**3389-3398.
393. **Vanassche T, Verhaegen J, Peetermans WE, Hoylaerts MF, Verhamme P.** 2010. Dabigatran inhibits *Staphylococcus aureus* coagulase activity. J Clin Microbiol **48:**4248-4250.
394. **Veloso TR, Que YA, Chaouch A, Giddey M, Vouillamoz J, Rousson V, Moreillon P, Entenza JM.** 2014. Prophylaxis of Experimental Endocarditis With Antiplatelet and Antithrombin Agents: A Role for Long-term Prevention of Infective Endocarditis in Humans? J Infect Dis **pii:**[Epub ahead of print].
395. **Dastgheyb S, Parvizi J, Shapiro IM, Hickok NJ, Otto M.** 2014. Effect of Biofilms on Recalcitrance of Staphylococcal Joint Infection to Antibiotic Treatment. J Infect Dis **pii: jiu514**.
396. **Claes J, Vanassche T, Peetermans M, Liesenborghs L, Vandenbriele C, Vanhoorelbeke K, Missiakas D, Schneewind O, Hoylaerts MF, Heying R, Verhamme P.** 2014. Adhesion of *Staphylococcus aureus* to the vessel wall under flow is mediated by von Willebrand factor-binding protein. Blood **124:**1669-1676.
397. **Rohrer S, Maki H, Berger-Bächi B.** 2003. What makes resistance to methicillin heterogeneous? J Med Microbiol **52:**605-607.
398. **Gustafson JE, Wilkinson BJ.** 1989. Lower autolytic activity in a homogeneous methicillin-resistant *Staphylococcus aureus* strain compared to derived heterogeneous-resistant and susceptible strains. FEMS Microbiol Lett **50:**107-111.
399. **Antignac A, Sieradzki K, Tomasz A.** 2007. Perturbation of cell wall synthesis suppresses autolysis in *Staphylococcus aureus*: evidence for coregulation of cell wall synthetic and hydrolytic enzymes. J Bacteriol **189:**7573-7580.
400. **de Jonge BL, de Lencastre H, Tomasz A.** 1991. Suppression of autolysis and cell wall turnover in heterogeneous Tn551 mutants of a methicillin-resistant *Staphylococcus aureus* strain. J Bacteriol **173:**1105-1110.
401. **Qoronfleh MW, Wilkinson BJ.** 1986. Effects of growth of methicillin-resistant and -susceptible *Staphylococcus aureus* in the presence of beta-lactams on peptidoglycan structure and susceptibility to lytic enzymes. Antimicrob Agents Chemother **29:**250-257.
402. **Gustafson JE, Berger-Bachi B, Strassle A, Wilkinson BJ.** 1992. Autolysis of methicillin-resistant and -susceptible *Staphylococcus aureus*. Antimicrobial Agents and Chemotherapy **36:**566-572.

403. **Chung M, Antignac A, Kim C, Tomasz A.** 2008. Comparative study of the susceptibilities of major epidemic clones of methicillin-resistant *Staphylococcus aureus* to oxacillin and to the new broad-spectrum cephalosporin ceftobiprole. Antimicrob Agents Chemother **52:**2709-2717.
404. **Szweda P, Schielmann M, Kotlowski R, Gorczyca G, Zalewska M, Milewski S.** 2012. Peptidoglycan hydrolases-potential weapons against *Staphylococcus aureus*. Appl Microbiol Biotechnol **96:**1157-1174.
405. **Kaplan JB, Izano EA, Gopal P, Karwacki MT, Kim S, Bose JL, Bayles KW, Horswill AR.** 2012. Low levels of beta-lactam antibiotics induce extracellular DNA release and biofilm formation in *Staphylococcus aureus*. MBio **3:**e00198-00112.
406. **Rasigade JP, Moulay A, Lhoste Y, Tristan A, Bes M, Vandenesch F, Etienne J, Lina G, Laurent F, Dumitrescu O.** 2011. Impact of sub-inhibitory antibiotics on fibronectin-mediated host cell adhesion and invasion by *Staphylococcus aureus*. BMC Microbiol **11:**doi: 10.1186/1471-2180-1111-1263.
407. **Kaplan JB.** 2011. Antibiotic-induced biofilm formation. Int J Artif Organs **34:**737-751.
408. **Boneca IG, Xu N, Gage DA, de Jonge BLM, Tomasz A.** 1997. Structural Characterization of an Abnormally Cross-linked Muropeptide Dimer That Is Accumulated in the Peptidoglycan of Methicillin- and Cefotaxime-resistant Mutants of *Staphylococcus aureus*. Journal of Biological Chemistry **272:**29053-29059.
409. **De Lencastre H, Wu SW, Pinho MG, Ludovice AM, Filipe S, Gardete S, Sobral R, Gill S, Chung M, Tomasz A.** 1999. Antibiotic resistance as a stress response: complete sequencing of a large number of chromosomal loci in *Staphylococcus aureus* strain COL that impact on the expression of resistance to methicillin. Microb Drug Resist **5:**163-175.
410. **Utaida S, Dunman PM, Macapagal D, Murphy E, Projan SJ, Singh VK, Jayaswal RK, Wilkinson BJ.** 2003. Genome-wide transcriptional profiling of the response of *Staphylococcus aureus* to cell-wall-active antibiotics reveals a cell-wall-stress stimulon. Microbiology **149:**2719-2732.
411. **Maidhof H, Reinicke B, Blümel P, Berger-Bächi B, Labischinski H.** 1991. femA, which encodes a factor essential for expression of methicillin resistance, affects glycine content of peptidoglycan in methicillin-resistant and methicillin-susceptible *Staphylococcus aureus* strains. J Bacteriol **173:**3507-3513.
412. **Komatsuzawa H, Sugai M, Ohta K, Fujiwara T, Nakashima S, Suzuki J, Lee CY, Suginaka H.** 1997. Cloning and characterization of the fmt gene which affects the methicillin resistance level and autolysis in the presence of triton X-100 in methicillin-resistant *Staphylococcus aureus*. Antimicrob Agents Chemother **41:**2355-2361.
413. **Qamar A, Golemi-Kotra D.** 2012. Dual roles of FmtA in *Staphylococcus aureus* cell wall biosynthesis and autolysis. Antimicrob Agents Chemother **56:**3797-3805.
414. **McAleese F, Wu SW, Sieradzki K, Dunman P, Murphy E, Projan S, Tomasz A.** 2006. Overexpression of genes of the cell wall stimulon in clinical isolates of *Staphylococcus aureus* exhibiting vancomycin-intermediate- S. aureus-type resistance to vancomycin. J Bacteriol **188:**1120-1133.
415. **Komatsuzawa H, Ohta K, Labischinski H, Sugai M, Suginaka H.** 1999. Characterization of fmtA, a gene that modulates the expression of methicillin resistance in *Staphylococcus aureus*. Antimicrob Agents Chemother **43:**2121-2125.

416. **Brunskill EW, Bayles KW.** 1996. Identification and molecular characterization of a putative regulatory locus that affects autolysis in *Staphylococcus aureus*. J Bacteriol **178:**611-618.
417. **Sadykov MR, Bayles KW.** 2012. The control of death and lysis in staphylococcal biofilms: a coordination of physiological signals. Curr Opin Microbiol **15:**211-215.
418. **Sharma-Kuinkel BK, Mann EE, Ahn JS, Kuechenmeister LJ, Dunman PM, Bayles KW.** 2009. The *Staphylococcus aureus* LytSR two-component regulatory system affects biofilm formation. J Bacteriol **191:**4767-4775.
419. **Groicher KH, Firek BA, Fujimoto DF, Bayles KW.** 2000. The *Staphylococcus aureus* lrgAB operon modulates murein hydrolase activity and penicillin tolerance. J Bacteriol **182:**1794-1801.
420. **Dubrac S, Bisicchia P, Devine KM, Msadek T.** 2008. A matter of life and death: cell wall homeostasis and the WalKR (YycGF) essential signal transduction pathway. Mol Microbiol **70:**1307-1322.
421. **Dubrac S, Boneca IG, Poupel O, Msadek T.** 2007. New insights into the WalK/WalR (YycG/YycF) essential signal transduction pathway reveal a major role in controlling cell wall metabolism and biofilm formation in *Staphylococcus aureus*. J Bacteriol **189:**8257-8269.
422. **Cafiso V, Bertuccio T, Spina D, Purrello S, Campanile F, Di Pietro C, Purrello M, Stefani S.** 2012. Modulating activity of vancomycin and daptomycin on the expression of autolysis cell-wall turnover and membrane charge genes in hVISA and VISA strains. PLoS One **7:**e29573.
423. **Dordel J, Kim C, Chung M, Pardos de la Gándara M, Holden MT, Parkhill J, de Lencastre H, Bentley SD, Tomasz A.** 2014. Novel determinants of antibiotic resistance: identification of mutated loci in highly methicillin-resistant subpopulations of methicillin-resistant *Staphylococcus aureus*. MBio **5:**e01000.
424. **de Jonge BL, Sidow T, Chang YS, Labischinski H, Berger-Bachi B, Gage DA, Tomasz A.** 1993. Altered muropeptide composition in *Staphylococcus aureus* strains with an inactivated femA locus. J Bacteriol **175:**2779-2782.
425. **Memmi G, Nair DR, Cheung A.** 2012. Role of ArlRS in autolysis in methicillin-sensitive and methicillin-resistant *Staphylococcus aureus* strains. J Bacteriol **194:**759-767.
426. **Kim C, Mwangi M, Chung M, Milheirico C, de Lencastre H, Tomasz A.** 2013. The mechanism of heterogeneous beta-lactam resistance in MRSA: key role of the stringent stress response. PLoS One **8:**e82814.
427. **Mwangi MM, Kim C, Chung M, Tsai J, Vijayadamodar G, Benitez M, Jarvie TP, Du L, Tomasz A.** 2013. Whole-genome sequencing reveals a link between beta-lactam resistance and synthetases of the alarmone (p)ppGpp in *Staphylococcus aureus*. Microb Drug Resist **19:**153-159.
428. **Geiger T, Kästle B, Gratani FL, Goerke C, Wolz C.** 2014. Two small (p)ppGpp synthases in *Staphylococcus aureus* mediate tolerance against cell envelope stress conditions. J Bacteriol **196:**894-902.
429. **Biswas R, Martinez RE, Göhring N, Schlag M, Josten M, Xia G, Hegler F, Gekeler C, Gleske AK, Götz F, Sahl HG, Kappler A, Peschel A.** 2012. Proton-binding capacity of *Staphylococcus aureus* wall teichoic acid and its role in controlling autolysin activity. PLoS One **7:**e41415.
430. **Brown S, Xia G, Luhachack LG, Campbell J, Meredith TC, Chen C, Winstel V, Gekeler C, Irazoqui JE, Peschel A, Walker S.** 2012. Methicillin resistance in *Staphylococcus aureus* requires glycosylated wall teichoic acids. Proc Natl Acad Sci U S A **109:**18909-18914.
431. **Farha MA, Leung A, Sewell EW, D'Elia MA, Allison SE, Ejim L, Pereira PM, Pinho MG, Wright GD, Brown ED.** 2013. Inhibition of

WTA synthesis blocks the cooperative action of PBPs and sensitizes MRSA to β-lactams. ACS Chem Biol **8:**226-233.
432. **O'Gara JP.** 2007. ica and beyond: biofilm mechanisms and regulation in *Staphylococcus epidermidis* and *Staphylococcus aureus*. FEMS Microbiol Lett **270:**179-188.
433. **Conlon BP.** 2010. PhD thesis, University College Dublin.
434. **Holland LM, O'Donnell ST, Ryjenkov DA, Gomelsky L, Slater SR, Fey PD, Gomelsky M, O'Gara JP.** 2008. A staphylococcal GGDEF domain protein regulates biofilm formation independently of cyclic dimeric GMP. J Bacteriol **190:**5178-5189.
435. **Sun D, Accavitti MA, Bryers JD.** 2005. Inhibition of biofilm formation by monoclonal antibodies against *Staphylococcus epidermidis* RP62A accumulation-associated protein. Clin Diagn Lab Immunol **12:**93-100.
436. **Iwase T, Uehara Y, Shinji H, Tajima A, Seo H, Takada K, Agata T, Mizunoe Y.** 2010. *Staphylococcus epidermidis* Esp inhibits *Staphylococcus aureus* biofilm formation and nasal colonization. Nature **465:**346-349.
437. **Vandecandelaere I, Depuydt P, Nelis HJ, Coenye T.** 2014. Protease production by *Staphylococcus epidermidis* and its effect on *Staphylococcus aureus* biofilms. Pathog Dis **70:**321-331.
438. **Chen C, Krishnan V, Macon K, Manne K, Narayana SV, Schneewind O.** 2013. Secreted proteases control autolysin-mediated biofilm growth of *Staphylococcus aureus*. J Biol Chem **288:**29440-29452.
439. **Sugimoto S, Iwamoto T, Takada K, Okuda K, Tajima A, Iwase T, Mizunoe Y.** 2013. *Staphylococcus epidermidis* Esp degrades specific proteins associated with *Staphylococcus aureus* biofilm formation and host-pathogen interaction. J Bacteriol **195:**1645-1655.
440. **Fätkenheuer G, Cornely O, Seifert H.** 2002. Clinical management of catheter-related infections. Clin Microbiol Infect **8:**545-550.
441. **Wenzel RP.** 2007. Health care-associated infections: major issues in the early years of the 21st century. Clin Infect Dis **15:**Suppl 1:S85-88.
442. **Grilo IR, Ludovice AM, Tomasz A, de Lencastre H, Sobral RG.** 2014. The glucosaminidase domain of Atl - the major *Staphylococcus aureus* autolysin - has DNA-binding activity. Microbiologyopen **3:**247-256.
443. **Foster TJ.** 2009. Colonization and infection of the human host by staphylococci: adhesion, survival and immune evasion. Vet Dermatol **20:**456-470.
444. **Wagenvoort JH, Sluijsmans W, Penders RJ.** 2000. Better environmental survival of outbreak vs. sporadic MRSA isolates. J Hosp Infect **45:**231-234.
445. **Dancer SJ.** 2008. Importance of the environment in meticillin-resistant *Staphylococcus aureus* acquisition: the case for hospital cleaning. Lancet Infect Dis **8:**101-113.
446. **Vanassche T, Kauskot A, Verhaegen J, Peetermans WE, van Ryn J, Schneewind O, Hoylaerts MF, Verhamme P.** 2012. Fibrin formation by staphylothrombin facilitates *Staphylococcus aureus*-induced platelet aggregation. Thromb Haemost **107:**1107-1121.
447. **Zapotoczna M, McCarthy H, Rudkin JK, O'Gara JP, O'Neill E.** submitted. Early *Staphylococcus aureus* colonisation of human plasma coated biomaterials is characterised coagulase-dependent, drug-susceptible biofilm accumulation. Submitted.
448. **Mohamed N, Teeters MA, Patti JM, Höök M, Ross JM.** 1999. Inhibition of *Staphylococcus aureus* adherence to collagen under dynamic conditions. Infect Immun **67:**589-594.
449. **George NP, Wei Q, Shin PK, Konstantopoulos K, Ross JM.** 2006. *Staphylococcus aureus* adhesion via Spa, ClfA, and SdrCDE to

immobilized platelets demonstrates shear-dependent behavior. Arterioscler Thromb Vasc Biol **26:**2394-2400.

450. **Björkman J, Nagaev I, Berg OG, Hughes D, Andersson DI.** 2000. Effects of environment on compensatory mutations to ameliorate costs of antibiotic resistance. Science **287:**1479-1482.

451. **Nagaev I, Björkman J, Andersson DI, Hughes D.** 2001. Biological cost and compensatory evolution in fusidic acid-resistant *Staphylococcus aureus*. Mol Microbiol **40:**433-439.

452. **Dordel J, Kim C, Chung M, Pardos de la Gandara M, Holden MT, Parkhill J, de Lencastre H, Bentley SD, Tomasz A.** 2014. Novel determinants of antibiotic resistance: identification of mutated loci in highly methicillin-resistant subpopulations of methicillin-resistant *Staphylococcus aureus*. MBio **5:**e01000.

453. **Hussain M, Steinbacher T, Peters G, Heilmann C, Becker K.** 2014. The adhesive properties of the *Staphylococcus lugdunensis* multifunctional autolysin AtlL and its role in biofilm formation and internalization. Int J Med Microbiol **[Epub ahead of print]**.

454. **Gibert L, Didi J, Marlinghaus L, Lesouhaitier O, Legris S, Szabados F, Pons JL, Pestel-Caron M.** 2014. The major autolysin of *Staphylococcus lugdunensis*, AtlL, is involved in cell separation, stress-induced autolysis and contributes to bacterial pathogenesis. FEMS Microbiol Lett **352:**78-86.

455. **Widhelm TJ, Yajjala VK, Endres JL, Fey PD, Bayles KW.** 2014. Methods to generate a sequence-defined transposon mutant library in *Staphylococcus epidermidis* strain 1457. Methods Mol Biol **1106:**135-142.